JOHANNES GUTENBERG UNIVERSITÄT MAINZ

„Characterization of mesencephalic astrocyte-derived neurotrophic factor of *Suberites domuncula*“

Dissertation

zur Erlangung des Grades

Doktor der Naturwissenschaften

Am Fachbereich Biologie

der Johannes Gutenberg-Universität Mainz

Vorgelegt von

Dayane Sereno Baêta Rodrigues

Geb. am 20. May 1985 in Volta Redonda (Brasilien)

Mainz, 2018

Dekan:

1. Berichterstatter:

2. Berichterstatter:

Tag der mündlichen Prüfung: 5.12.2018

To my family

Publication

Some of the results within the thesis have been published in a peer-reviewed journal:

Sereno D, Müller WEG, Bausen M, Elkhooly TA, Markl JS, Wiens M (2017) An evolutionary perspective on the role of mesencephalic astrocyte-derived neurotrophic factor (MANF): At the crossroads of poriferan innate immune and apoptotic pathways. Biochem. Biophys. Rep. 11:161-173.
doi:10.1016/j.bbrep.2017.02

Appendice 2

INDEX

A. ABSTRACT

Sponges have been considered the earliest branching metazoan taxon, and therefore, are important in the reconstruction of early metazoan evolution. Besides, sponges lack a conventional nervous system, which provides an enticing opportunity to explore the evolutionary ancient role of neurotrophic factors and thus the understanding of specific Metazoan genetic toolkits and molecular signaling pathways. The mesencephalic astrocyte-derived neurotrophic factor (MANF) together with cerebral dopamine neurotrophic factor composes a family of evolutionarily conserved neurotrophic factors each selectively protects dopaminergic neurons. MANF is generally resident within the endoplasmic reticulum (ER) but can also be secreted. It is widely expressed in neurons and non-neuronal tissues. MANF is involved in the ER stress response and also has pro-survival effects. Here is reported the identification of the MANF homolog from the sponge *Suberites domuncula* (SDMANF). SDMANF possesses significant sequence similarity with its metazoan homologs. In *Suberites*, SDMANF is expressed in the vicinity of bacteriocytes and surrounding a eukaryotic sponge endobiont. In human embryonic kidney cells transfected with SDMANF, the protein was identified in the organelle protein fraction and also in the cell culture medium. The intracellular SDMANF level was up-regulated in response to a Golgi/ER transport inhibitor brefeldin A, and the apoptosis inducers cadmium and lipopolysaccharide (LPS). Upon LPS exposition, transfected cells present a reduced caspase 3 activity and enhanced cell viability with no increased expression of BCL-2-associated X (BAX) in comparison with not transfected cells/ wild-type cells. The aforementioned results suggest MANF has roles in cytoprotection with crossing functions on innate immunity and apoptosis pathways that were deeply evolutionary preserved, besides the neurotrophic function, which might have emerged later in metazoan evolution.

B. ZUSAMMENFASSUNG

Schwämme stellen eine der frühesten Verzweigungen der Metazoa dar und sind daher wichtig für die evolutionäre Rekonstruktion dieses Taxons im Speziellen und der Metazoa im Allgemeinen. Sie besitzen kein konventionelles Nervensystem, was die Erforschung alter evolutionärer Funktionen von neurotrophen Faktoren (NF) anhand von homologen Faktoren erleichtert und hierdurch das Verständnis von spezifischen genetischen Toolkits und molekularen Signalwegen der Metazoa fördert. Der mesenzephale astrozytenabgeleitete neurotrophe Faktor (MANF) bildet zusammen mit dem zerebralen dopaminergen neurotrophen Faktor eine Familie von evolutionär konservierten NF, die jeweils spezifisch dopaminerge Neuronen unterstützen. Hauptsächlich wird MANF im endoplasmatischen Retikulum (ER) von neuronalen und nicht-neuronalen Geweben exprimiert und zum Teil von den Zellen sekretiert. MANF ist an der ER-Stressreaktion beteiligt und stellt einen positiven Einflussfaktor für das Überleben der Zelle dar. Im Rahmen dieser Arbeit wurde in dem marinen Schwamm *Suberites domuncula,* der zu MANF homologe Faktor identifiziert, der im Folgenden als SDMANF bezeichnet wird. SDMANF zeigt eine signifikant ähnliche Sequenz zum metazoischen MANF auf. In *Suberites* wurde SDMANF in der Umgebung von Bakteriozyten und eukaryotischen Schwammendobionten festgestellt, nicht jedoch in anderen Teilen des Schwammes. Humane embryonale Nierenzellen (HEK), die mit SDMANF transfiziert wurden, zeigten eine Expression in der Organellenproteinfraktion des ER als auch eine Sekretion ins Zellkulturmedium. Der intrazelluläre SDMANF-Spiegel wurde als Reaktion auf den zugegebenen Golgi/ER-Transportinhibitor brefeldin A und den beiden apoptoseinduzierenden Substanzen Cadmium und LPS Lipopolysaccharid (LPS) hochreguliert. Nach der LPS-Exposition zeigten transfizierte HEK-Zellen eine reduzierte Caspase-3-Aktivität und im Vergleich zu Wildtyp-Zellen/nicht-transfizierten HEK-Zellen eine erhöhte Viabilität, ohne erhöhte BCL-2-associated X protein (BAX) Expression. Diese Ergebnisse legen nahe, dass das homologe MANF Protein der Schwämme eine Rolle bei der Zytoprotektion spielt, die sich auf das angeborene Immunsystem und die Signalwege der Apoptose auswirkt. Es scheint, dass diese Mechanismen im Laufe der Evolution stark konserviert wurden. Die neurotrophen Funktionen könnten demnach später in der metazoischen Evolution aufgetaucht sein.

C. INTRODUCTION

1. Neurotrophic factors

In general comprehension, Neurotrophic Factors (NTFs) can be secretion elements that support neurons (Lewin and Carter 2014). The NTFs work on the peripheral and central nervous system and can also be expressed on non-neuronal tissue (Reichardt 2006; Bothwell et al 2016). Neurotrophic factors have a pivotal regulatory role during development processes, providing guidance cues for developing neurons and also controlling the number of surviving neurons in order to ascertain an optimal density of neurons in a given target during cell differentiation (Reichardt 2006; Pardon 2010; Alsina et al 2012). Moreover, in adult neuronal function NTFs have also a significant role regulating the growth of neurons, synaptic function, differentiation, apoptosis and cellular plasticity (Reichardt 2006; Pardon 2010; Alsina et al 2012; Bothwell 2016; Vilar and Mira 2016). As well as, regulating metabolic functions such as protein synthesis and neurotransmission (Hefti et al 1993; Pirvola and Ylikoski 2003; Pardon 2010).

Several structurally and functionally related neurotrophic factors have been well characterized and can be grouped in families: The neurotrophin family comprises structurally related proteins such as nerve growth factor, brain-derived neurotrophic factor or neurotrophin three, four/five and six (Reichardt 2006; Bothwell 2014; Sampaio et al 2017). The family of glial cell-line derived neurotrophic factor and family ligands like neurturin, artemin or persephin (Airaksinen and Saarma 2002; Paratcha and Ledda 2008; Alsina et al 2012; Ibáñez and Andressoo 2017). The neurokine family with the ciliary neurotrophic factor, leukemia inhibitor, interleukine 6, cardiptrophin 1 or oncostatin M (Halvorsen and Kaur 2006; Gu 2017). A family of non-neuronal growth factors can be grouped together such as the epidermal growth factor, the bone morphogenetic protein, the acidic fibroblast growth factor, the basic fibroblast growth factor and the hepatocyte growth factor (Gu 2017). A novel family of NTFs is formed by the Mesencephalic Astrocyte-Derived Neurotrophic Factor (MANF) and Cerebral Dopamine Neurotrophic Factor (CDNF) (Lindahl et al 2017).

Neurotrophic factors have an important function on adult neurogenesis and normal physiology (Bothwell 2014; Lewin and Carter 2014). Changes in NTFs

expression itself, as well as their receptors expression and/or signaling can lead to neurodegenerative pathogenesis (Levy et al 2005; Lewin and Carter 2014; Vilar and Mira 20016). Due to those activities NTFs are therapeutic targets for several brain disorders, such as amyotrophic lateral sclerosis, Alzheimer's, Parkinson's, Huntington´s diseases and also psychiatric disorders such as anxiety-like behavior, rewarding and addictive behavior and neurodegenerative diseases (Pardon 2010; Brett et al 2014; Lewin and Carter 2014; Garea-Rodríguez et al 2016; Bartus and Johnson 2017; Gu 2017; Sampaio et al 2017).

Neurotrophins and their signaling system is evolutionary ancient and possess regulatory functions on many biological pathways (Bothwel 2016). Many invertebrates such as hemichordates, echinoderms, crustaceans, lophotrochozoan and annelids have neurotrophins (Bothwell 2006; 2016; Wilson 2009; Kassabov et al 2013; Lauri et al 2016). *Drosophila* (ecdysozoan) also has neurotrophins. In this case they have been referred to as neurotrophin-like cytokines because they communicate via toll-like receptors, rather than $p75^{NTR}$ or Trk-like receptors (DeLotto & DeLotto 1998; Zhu et al 2008; Ballard et al 2014; Bothwel 2016). Although cnidarians and ctenophores have a neuronal system, neurotrophin homologs have not been identified yet (Galli et al 2009; Moroz and Kohn 2016 Wenger et al 2016). The basal Metazoan genomics and metabolomics support an independent development of the neural signaling in ctenophores, cnidarians and bilaterians (Moroz and Kohn 2016). Poriferans and placozoans do not have a neural and muscular system but some molecular and anatomical analyses evidence the presence of a neuronal-like signaling and a (pre-) nervous system (Conaco et al 2012a; Smith et al 2014; Leys 2015).

2. The ER stress and unfold protein response

The Endoplasmic Reticulum (ER) is organized in a dynamic tubular network, responsible for several functions such as translocation, synthesis and folding of proteins (Fewell et al 2001; Voeltz et al 2002; Araki and Nagata 2011; Janssens et al 2014; Liu et al 2016a). Besides, the ER plays a role in post-translational modifications like glycosylation and disulfide bond formation (Ellgaard et al 2016). The ER lumen consists of several molecular chaperones and folding proteins with important functions on folding and sorting of proteins for example, glucose-related

protein 94, protein disulfide isomerase, calnexin and calreticulin (Mori 2000; Todd et al 2008; Hertz 2012; Ron and Harding 2012; Sarvani et al 2017).

Synthesized proteins that enter the ER pass through a sequence of modifications made by the combined work of chaperones and folding enzymes, this supports the proper folding and subsequent release of the proteins from the ER (Braakman and Hebert 2013). Cells require the ER to maintain cellular homeostasis, a balance between the demand for protein synthesis and its protein folding capacity, in terms of regulation of protein trafficking, synthesis, folding, and degradation (Ron 2002; Ron and Harding 2012; Perri et al 2016; Sarvani et al 2017). The processes of protein folding and maturation are carefully checked by the ER quality control system (Hetz 2012). In order to certify that only properly folded proteins leave the ER via the secretory pathway (i.e. ER, Golgi apparatus, lysosomes, endosomes, and secretory vesicles), while improper folded proteins exit the ER through ER-Associated Degradation (ERAD) or via autophagy (Smith et al 2011; Hetz 2012; Janssens et al 2014; Pluquet et al 2015). Protein folding mechanisms are sensitive of changes in the ER homeostasis, like aberrant calcium regulation, oxidative stress, hypoxia, nutrient/glucose deprivation, DNA damage, altered glycosylation or ER overload with unfolded aberrant/mutated proteins (Kaufman et al 2002; Chakrabati et al 2011; Hetz et al 2013; Cao et al 2016; Liu et al 2016a; Sarvani et al 2017).

The endoplasmic reticulum is involved in metabolic processes like gluconeogenesis and lipid synthesis (Hetz 2012; Bravo et al 2013; Sarvani et al 2017). In addition, it takes part in the formation of peroxisomes, lipid droplets, and omegasomes, which are the scaffolds of autophagosome production (Hetz 2012; Joshi et al 2017). Furthermore, the ER is the cell principal storage of calcium and plays a significant role in cell redox homeostasis (Araki and Nagata 2011; Appenzeller-Herzog and Simmen 2016; Chernorudskiy and Zito 2017).

The cellular mechanisms involved in ER stress response are part of the cellular basic physiology and probably played a role during the evolution of multicellular organisms (Kültz 2003; Moore and Hollien 2012; Hollien 2013). Furthermore, the stress response is possibly also involved in the development of cellular resilience mechanisms (Kültz 2003; Fulda et al 2010; Moore and Hollien 2012; Poljšak and Milisav 2012; Hollien 2013).

The ER is a highly dynamic organelle with an important role in coordinating signaling pathways that ensure cell adaptation, resilience and survival (Sano and Reed 2013). Endoplasmic reticulum stress can be very harmful for cells and sequences of adaptive and protective responses are triggered to manage and defeat the distress and/or improve the ER functions (Hetz 2012; Moore and Hollien 2012). This range of reactions is termed Unfolded Protein Response (UPR) (Hetz 2012; Moore and Hollien 2012). Unfold protein response is an adaptive mechanism, which aims to restore the protein protein-folding homeostasis and recover ER functions (Hetz et al 2015; Martins et al 2016).

Unfold protein response comprises three main mechanisms: 1) In order to control the excessive amount of unfolded/misfolded proteins accumulated in the ER, the global synthesis of the new protein is transiently suppressed. 2) To dissipate the accumulated proteins, many chaperone genes are induced at the transcriptional level, and the ER-associated degradation system is enhanced, which can translocate and remove misfolded proteins by proteasomal degradation. 3) When ER stress cannot be resolved, the ER induces apoptosis by a trigger system (Travers et al 2000; Meusser et al 2005; Hollien and Weissman 2006; Hollien et al 2009; Cao and Kaufman 2012; Lynch et al 2012; Janssens et al 2014; Zeng et al 2015; Liu et al 2016a).

Mechanisms of UPR are highly conserved across the kingdom of eukaryotes (Hollien 2013; Grootjans et al 2016). The UPR is mediated by three ER transmembrane receptor proteins: Inositol-Requiring Enzyme 1 (IRE1; earlier known as Ire1p; and also called ERN1); Double-Stranded RNA-Activated Protein Kinase (PKR)-Like Endoplasmic Reticulum Kinase (PERK also known as EIF2AK3); and Activating Transcription Factor 6 (ATF6) (Tood et al 2008; Promlek et al 2011; Teske et al 2011; Liu et al 2016a; Sarvani et al 2017). Proteins IRE1, PERK and ATF6 are ER stress sensors and their luminal domain responds to the level of unfolded/misfolded proteins in the ER (Cao and Kaufman 2012). Under homeostatic conditions the chaperon Immunoglobulin-Heavy-Chain-Binding Protein (BiP), also termed glucose-related protein 78 and Heat shock 70 kDa protein 5 is bound to the luminal domains of IRE1, PERK and ATF6 which thereby are kept in an inactive state (Fig. 1) (Bertolotti et al 2000; Shen et al 2005).

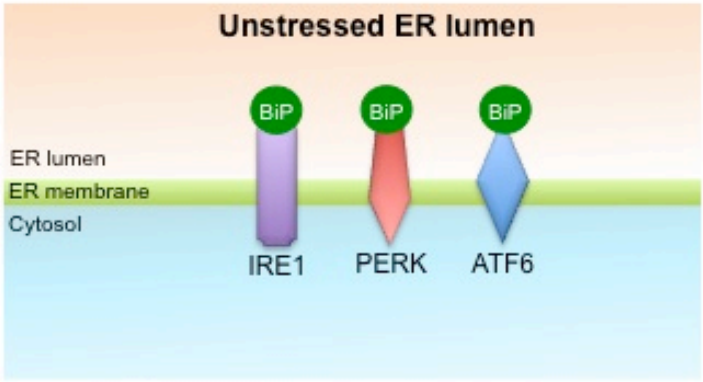

Figure 1: Endoplasmic reticulum lumen under unstressed conditions. During Endoplasmic Reticulum (ER) unstressed conditions the Immunoglobulin-Heavy-Chain-Binding Protein (BiP) binds and inhibits the ER stress sensors, the transmembrane proteins Activating Transcription Factor 6 (ATF 6), Inositol-Requiring Enzyme 1 (IRE1) and Double-Stranded RNA-Activated Protein Kinase (PKR)-Like Endoplasmic Reticulum Kinase (PERK).

When misfolded proteins accumulate in the ER lumen and the ER stress level increases, BiP dissociates from the sensing molecules IRE1, PERK and ATF6 in order to bind the unfolded proteins, caused by its high affinity to the latter (Hetz 2012). The released stress sensors then trigger downstream signaling (Fig. 2) (Tood et al 2008; Wang et al 2009; Pincus et al 2010; Grootjans et al 2016; Sarvani et al 2017).

Unfold protein response downstream transcriptional pathways are approaches to restore cell proteostasis (Grootjans et al 2016). Cells use different strategies coordinated by ER transmembrane stress sensors and the downstream transcription factors, which adjust gene expression to reduce stress or to induce pro-apoptotic activity (Chow et al 2015; Grootjans et al 2016; Hetz and Saxena 2017).

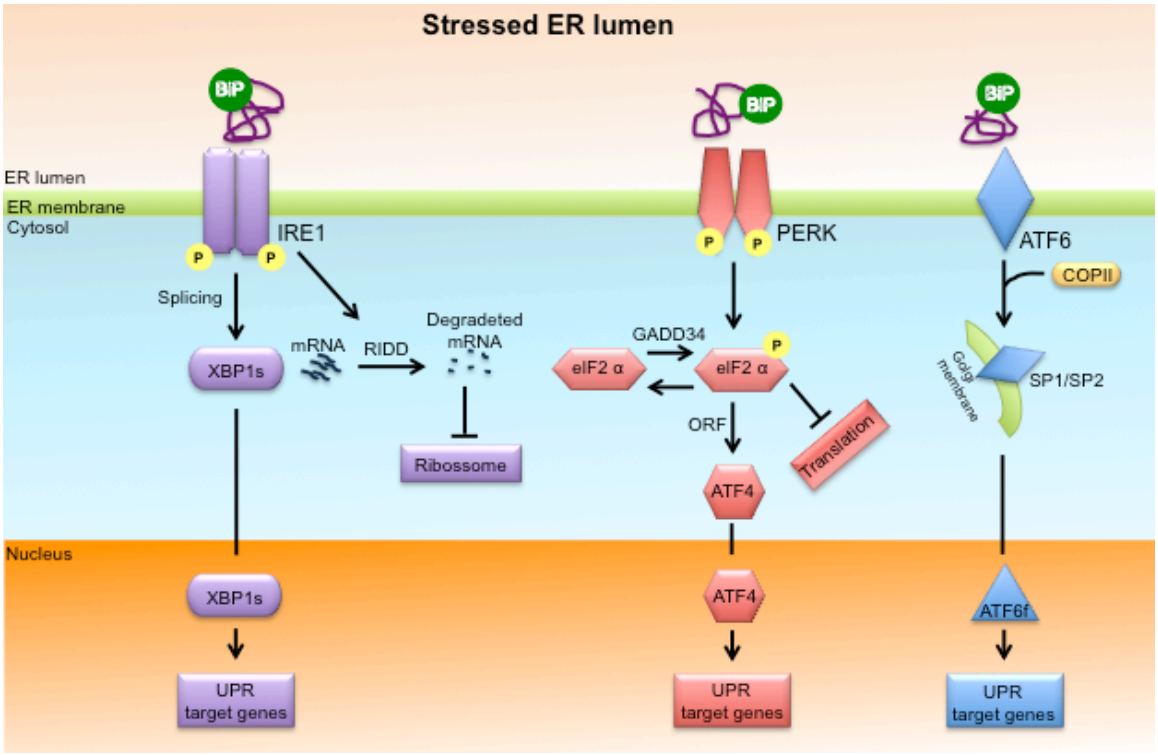

Figure 2: The three axes of the unfolded protein response. Immunoglobulin-Heavy-Chain-Binding Protein (BiP) binds to the misfolded proteins and dissociates from Inositol-Requiring Enzyme 1 (IRE1), Protein Kinase (PKR)-Like Endoplasmic Reticulum Kinase (PERK). When IRE1 is set free, it dimerizes and autophosphorylates (Tood et al 2008; Walter and Ron 2011; Cao and Kaufman 2012; Hetz 2012; Grootjans et al 2016). This triggers the endoribonuclease, induces the splicing of Xbox Binding Protein (XBP1) and its transformation in XBP1s (Calfon et al 2002; Tood et al 2008; Hetz 2012; Hetz et al 2013). The XBP1s translocates to the nucleus and binds to the unfolded protein response **(**UPR) target genes activating key genes for the secretory function (Hetz et al 2013; 2015). Another activity of the IRE1α is the Regulated IRE1-Dependent Decay of mRNA (RIDD) (Walter and Ron 2011). On RIDD the IRE1α RNase has an increase on its substrate activities and degrades ER-bound mRNAs, lessen the amount of newly translated proteins that enter the ER, reducing thereby ribosome functions (Harding et al 1999; 2000; Schenuer et al 2001; Walter and Ron 2011; Hertz et al 2013; Grootjans et al 2016; Niu et al 2017). A BiP release additionally activates the PERK autophosphorylation (Tood et al 2008). It subsequently phosphorylates Eukaryotic Translation-Initiation Factor 2α (eIF2α), which blocks the translation of most proteins (Walter and Ron 2011). The DNA Damage-Inducible Protein (GADD34) forms a complex with the catalytic subunit of protein phosphatase 1 promoting dephosphorylation of eIF2α, reinstating the mRNA translation (Novoa et al 2001; Connor et al 2001). Despite of the translation blocking, activating transcription factor (ATF4) mRNA is translated because of its upstream Open Reading Frame (ORF) (Tood et al 2008; Walter and Ron 2011). As XBP1s, ATF4 translocates to the nucleus, where it activates a set of UPR target genes (Tood et al 2008; Walter and Ron 2011). The BiP release reveals the ATF6 Golgi-localization sequence; Coat Protein II (COPII) transports ATF6 (Tood et al 2008; Schindler and Scheckman 2009). Inside the Golgi apparatus, the ATF6

is cleaved by the Site-1 and Site-2 Proteases (S1P, S2P) and the ATF6 fragment (ATF6f) is released (Ye et al 2000; Schindler and Scheckman 2009). ATF6f translocates to the nucleus and binds to a set of UPR target genes (Haze et al 1999; Tood et al 2008; Schindler and Scheckman 2009).

Inositol-requiring enzyme 1 axis is the most evolutionarily conserved of the UPR branches and includes X-box-binding protein 1 (XBP1), which is a homologue of *Saccharomyces cerevisiae* transcriptional activator HAC1 (Sidrauski and Walter 1997; Yoshida et al 2001; Calfon et al 2002; Lee et al 2002; Tood et al 2008; Grootjans et al 2016). The first description of IRE's atypical splicing was observed using the *S. cerevisiae* model (Sidrauski and Walter 1997).

Inositol-requiring enzyme 1 is a transmembrane protein that has two domains on the cytosolic region, a Ser/Thr kinase and an endoribonuclease (RNase) (Cao and Kaufman 2012; Cao et al 2016). When the IRE1 (see Fig. 2) is set free, it dimerizes and autophosphorylates (Tood et al 2008; Walter and Ron 2011; Cao and Kaufman 2012; Cao et al 2016). The possibility of unfolded proteins directly activate IRE1 has also be considered (Tood et al 2008; Cao et al 2016; Grootjans et al 2016).

The IRE1 endoribonuclease domain splices the mRNA that encodes XBP1 (Tood et al 2008). The intron of (26 base pair fragment) is cut out from mRNA, and the pieces are reconnected by a presumed tRNA ligase (Tood et al 2008). XBP1 mRNA is translated into an active form of the transcription factor (XBP1s) (see Fig. 2, Tood et al 2008). Then, XBP1s translocates to the nucleus and binds the ER Stress-Response Elements I (ERSE-I) and (ERSE-II) that are the promoter regions of unfold protein target genes (Tood et al 2008; Cao and Kaufamn 2012; Cao et al 2016; Grootjans et al 2016).

The active form of the Xbox binding protein (XBP1s) is a pivotal transcription regulator of a wide range of genes that encode chaperons, protein-folding enzymes, phospholipid synthesis as well as proteins related to ER trafficking and quality control (Yoshida et al 2001; Lee et al 2003; Cao and Kaufamn 2012; Hetz 2012; Hetz et al 2013). Additionally, XBP1s controls the ERAD, which is an elimination process of misfolded proteins accumulated at the ER through their retrotranslocation to the cytosol for subsequent ubiquitination and

further degradation by the 26S proteasome (Smith et al 2011; Cao and Kaufamn 2012; Hetz et al 2013).

Another activity of the IRE1α (see Fig. 2) is the regulated IRE1-dependent decay of mRNA (RIDD) (Walter and Ron 2011). Caused by the increased IRE1α RNase activity ER-bound mRNAs are degraded, which lessens the amount of newly translated proteins that enter the ER, reducing thereby ribosome functions (Harding et al 1999; 2000; Schenuer et al 2001; Walter and Ron 2011; Hertz et al 2013; Grootjans et al 2016; Niu et al 2017). The RIDD mechanisms have also been linked to the activation of retinoic acid-inducible gene 1 (RIG-1) causing a cell-autologous NF-κB mediated inflammatory response (Lencer et al 2015; Cao et al 2016). Furthermore, RIDD possibly has a role of pro-apoptotic mechanism by degrading mRNAs encoding for ER chaperons such as BiP (Hollien et al 2006; 2009; Urra et al 2013). Besides, the cleavage of microRNAs (miRNAs) significantly impact on regulation levels of caspase 2 and thioredoxin-interacting protein (Lerner et al 2012; Upton et al 2012; Urra et al 2013).

The activated IRE1α interacts with Tumor Necrosis Factor Receptor-Associated Factor 2 (TRAF2) to induce phosphorylation of Jun N-Terminal Kinase (JNK) and up-regulation of pro-inflammatory genes through activator protein 1 (Urano et al 2000; Grootjas et al 2016; Martins et al 2016). The IRE1α–TRAF2 complex also mediates the interaction between Mitogen-Activated Protein Kinase (MAPK), Apoptosis Signal-Regulating Kinase 1 and IκB kinase (IKK) (Kaneko et al 2003; Hetz 2012; Hetz et al 2013; 2015; Cao et al 2016; Grootjas et al 2016; Martins et al 2016). The subsequent phosphorylation of IκB leads to its degradation, which releases Nuclear Factor-κB (NF-κB) for nuclear translocation (Christian et al 2016). Moreover, the TRAF2 possibly interacts with the pattern recognition receptors Nucleotide-Binding Oligomerization domain protein 1 (NOD1) and NOD2 with requires of the adaptor Protein Receptor-Interacting Serine/Threonine-Protein Kinase 2 (RIP2) (Byndloss et al 2016; Keestra-Gounder et al 2016). The aforementioned pathway modulates proinflammatory genes at different levels as well as autophagy and apoptosis (Byndloss et al 2016; Cao et al 2016; Grootjas et al 2016; Martins et al 2016; Hetz and Saxena 2017; Niu et al 2017). Inositol-requiring enzyme 1 alpha finely controls switches between adaptive

and pro-apoptotic mechanisms of the UPR (Hetz and Glimcher 2009; Hetz et al 2011; Hetz 2012; Urra et al 2013).

Immunoglobulin-heavy-chain-binding protein releases activates the PERK autophosphorylation (see Fig. 2) (Tood et al 2008). It subsequently phosphorylates Eukaryotic Translation-Initiation Factor 2α (EIF2α), which blocks the translation of most proteins (Walter and Ron 2011). As a result, the quantity of proteins that enter the ER is reduced (Grootjans et al 2016). The grow arrest and DNA Damage-Inducible Protein (GADD34) forms a complex with the catalytic subunit of protein Phosphatase 1 promoting the dephosphorilation of eIF2α, reinstating the mRNA translation (Connor et al 2001; Novoa et al 2001). The eIF2a-phosphorylated protein induces translation of the protein Activating Transcription Factor 4 (ATF4), even when the translation process is inhibited (Tood et al 2008; Walter and Ron 2011). That is possible because the ATF4 has on its sequence an upstream Open Reading Frame (ORF) that allows its translation even (Tood et al 2008; Walter and Ron 2011).

Protein ATF4 translocates to the nucleus where it activates a set of UPR target genes (Tood et al 2008). The ATF4 supports an antioxidant response; controls the expression of genes involved on proteostasis increasing the ER folding capacity and up-regulates macroautophagy (Harding et al 2000; Han et al 2013; Urra and Hetz 2017; Hetz and Papa 2018).

During chronic ER stress the ATF4 up-regulates the expression of CCAAT/Enhancer-Binding Protein Homologous Protein (CHOP), which can induce apoptosis towards the increase of Reactive Oxygen Species (ROS) production (Tood et al 2008; Walter and Ron 2011; Urra et al 2013; Pakos-Zebrucka et al 2016). The CHOP can also increase expression of Canopy Homolog 2, a newly described regulator factor of PERK, via direct transactivation (Hong et al 2017; Urra and Hetz 2017). Additionally, the ATF4 can induce the expression of GADD34, which also increases the production of ROS, which may initiate proteotoxicity (Kojima et al 2003; Urra et al 2013). ATF4 regulates as well the expression of B-Cell Lymphoma 2 (BCL-2) family members, hampering the expression of anti-apoptotic BCL-2 proteins, together with an increase in the expression of pro-apoptotic BCL-2 members in order to accelerate cell death (Urra et al 2013; Cao et al 2016; Urra and Hetz 2017; Hetz and Papa 2018).

Through elevated levels of persistent ER stress both proteins PERK and IRE1a control many signaling pathways that result in cell dysfunction, activation of inflammasome and apoptosis (Cao et al 2016; Urra and Hetz 2017; Hetz and Papa 2018).

Activating Transcription Factor 6 (ATF 6) (see Fig. 2) encodes a Basic Leucin Zipper Transcription Factor (bZIP) (Hetz 2012). After being released by BiP, ATF6 Golgi-Localization Sequence (GLS) is exposed (Tood et al 2008). The ATF6 interacts with Coat Protein II (COPII) and is transported to the Golgi apparatus (Schindler and Schekman 2009). Attached to Golgi body, the ATF6 suffers a proteolytic activity by the Site-1- and Site-2-Protease (S1P, S2P), at the ATF6 cytoplasmic domain and ATF6 fragment (ATF6f) is released (Ye et al 2000).

The ATF6 fragment has a bZIP domain, it translocates to the nucleus and works as transcription factor (Hetz 2012). It binds the ATF/cAMP response element as well as ERSE, thereby induces the transcription of genes involved in protein folding, ERAD components and autophagy (Haze et al 1999; Ye et al 2000; Lee et al 2002; Schröder and Kaufman 2005; Yamamoto et al 2007; Tood et al 2008; Hetz 2012; Martins et al 2016). Additionally, it induces the transcription of chaperone proteins, pro-survival molecules, such as BiP, XBP1, Homocysteine-Induced Endoplasmic Reticulum Protein, and $P58^{IPK}$ (also termed DnaJ Heat Shock Protein Family (Hsp40) Member C3) (Schröder and Kaufman 2005; Tao et al 2010; Hetz 2012; Hughes and Mallucci 2018). Besides, ATF6 triggers NF-κB through transient phosphorylation of Proteinkinase B (AKT, serine/threonine kinase) and also promotes the Interferon Regulatory Factor (IRF) 3 phosphorylation (Yamazaki et al 2009; Liu et al 2012; Boriushkin et al 2014; Martins et al 2016). The ATF6 can also regulate the expression of CHOP (Oyadomari and Mori 2004; Li et al 2014; Martins et al 2016; Hetz and Papa 2018).

Several authors have shown that UPR intersects with inflammatory pathways at various levels, possibly having major functions in inflammation (Martins et al 2016; Sarvani et al 2017; Frakes and Dilli 2017; Urra and Hetz 2017). In an UPR independent manner the ER overload can activate inflammatory pathways (Martins et al 2016; Grootjans et al 2016). The high amounts of cytosolic calcium can affect the mitochondria homeostasis causing ROS production, which

possibly activates NFκB (Martins et al 2016; Chernorudskiy and Zito et al 2017; Carreras-Sureda et al 2018). The Ca^{2+} and potassium efflux from the ER can interact with ROS triggering NLR pirin domain 3 (NLRP3) inflammasome (Martins et al 2016; Hetz and Papa 2018). Furthermore, if BiP enters the cytoplasm it connects with IKK, leading to phosphorylation of IκBα and subsequent proteasomal degradation (Martins et al 2016).

The UPR also has conserved functions in immunity; its signaling crosses many levels with innate and adaptive immune responses (Janssens et al 2014; Grootjans et al 2016). Moreover, the integrated stress response and the UPR seem to be closely intertwined with host immune responses (Janssens et al 2014). There is a partial overlap in the genes induced by them and those induced by microbial infection or stimulation of Toll-Like Receptor (TLR) (Tattoli et al 2012; Clavarino et al 2012; Janssens et al 2014). One example is the IFN3, which is expressed on ER stress response, and IFNs are part of the innate and adaptive immune system being involved with Pattern Recognition Receptors (PRRs) and activation of TLR (Liu et al 2012). Some pathogens also subvert the UPR mechanism (Tattoli et al 2012; Clavarino et al 2012; Janssens et al 2014). In some cells of the immune system, for instance in dendritic- and B-cells, the activation of some UPR sensors are part of the typical cell differentiation program (Janssens et al 2014). The UPR seems to be constitutively active, regardless of the lack of conventional trigger mechanisms, the UPR activation seems to be crucial for antigen presentation and immunoglobulin synthesis (Ma et al 2003; Janssens et al 2014).

Understanding the cross-linking among the various elements of the UPR can help the drug manipulation of pro-death or pro-survival pathways (Senf and Ronai 2015). This may lead to novel therapeutic approaches for many diseases e.g. as autoimmune diseases, metabolic disorders, neurodegenerative disorders, several eye, heart and renal diseases, whose pathogenesis is characterized by chronic activation of these pathways (Park and Ozcan 2013; Senf and Ronai 2015; Liu et al 2016a; Cybulsky 2017; Hetz and Saxena 2017; Sarvani et al 2017; Hetz and Papa 2018).

3. Mesencephalic astrocyte-derived factor

3.1. MANF/CDNF family proteins

Mesencephalic Astrocyte-Derived Factor (MANF), also known as arginine-rich, mutated in early stage tumors (ARMET) was described by Petrova et al (2003), as a factor that promotes *in vitro* survival of midbrain dopaminergic neurons in culture medium of rat type-1 astrocyte ventral mesencephalic cell line.

Analyses of the MANF protein sequence showed homology with an earlier described predicted protein that has an Arg-rich N-terminal region. Of the first 55 amino acids in MANF, 22 are arginine (Shridhar et al 1996). Because of this, the protein was named human arginine-rich protein (hARP) or, alternatively, ARMET (Shridhar et al 1996). Nevertheless, studies of different organisms concluded that the putative arginine-rich region of human ARP is not translated and consequently the protein terminology was changed to MANF (Petrova et al 2003).

Human MANF is 179 amino acids protein, which has a predicted signal peptide of 21 amino acids (Petrova et al 2003). Cleavage produces a mature protein of 158 amino acids (Petrova et al 2003). MANF and the cerebral dopamine neurotrophic factor (CDNF), previously known as conserved dopamine neurotrophic, constitute an evolutionarily conserved family of neurotrophic factors (Petrova et al 2003; Lindholm et al 2007; 2010; Parkash et al 2009).

Mesencephalic astrocyte-derived factor exists in vertebrate and invertebrate species (Petrova et al 2003), but CDNF is a paralog that is only found in vertebrates (Lindholm et al 2007). Human CDNF is a protein of 187 amino acids with a predicted signal peptide of 26 amino acids; the mature protein has 161 amino acids (Lindholm et al 2007). Human CDNF exhibits an amino acid identity of 59% with human MANF, 49% identity with *Drosophila melanogaster (D. melanogaster)* MANF and 46% identity with *Caenorhabditis elegans* (*C. elegans*) MANF proteins (Lindholm et al 2007).

The two proteins, MANF and CDNF are structurally different from the typical neurotrophic factors; their capability to activate cell surface receptors remains uncertain as well as their intracellular activity following internalization (Niu et al 2011; Henderson et al 2013; Lindahl et al 2017). Additionally, the pro-sequence for enzymatic activation that is common for classical NTFs seems absent (Airaksinen

and Saarma 2002; Henderson et al 2013; Lindahl et al 2017). Another difference of them is the number of cysteine residues in their primary structure: glial cell line-derived neurotrophic factor family ligands, have seven cysteine residues in their primary structure, whereas CDNF and MANF have eight cysteine residues, forming four disulphide bridges and (Airaksinen and Saarma 2002; Petrova et al 2003; Lindholm et al 2007; 2008; 2010; Parkash et al 2009; Hoseki et al 2010). Moreover, the space between the cysteine residues in MANF and CDNF (Fig. 3) is evolutionary conserved (Voutilainen et al 2015).

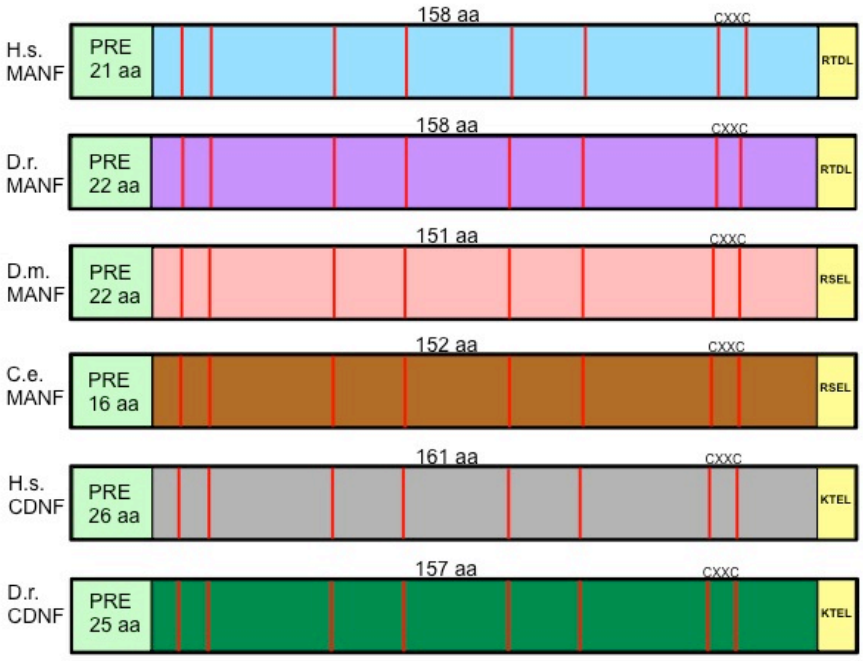

Figure 3: Conserved position of cysteine residues of MANF and CDNF on vertebrates and invertebrates. Schematic organization of the conserved spacing between the eight-cysteine residues (red bars) on Mesencephalic Astrocyte-Derived Factor (MANF) and Cerebral Dopamine Neurotrophic factor (CDNF). The CXXC motif is highly conserved in many metazoan species. The signal peptide (PRE) is16–26 amino acids (aa) long (light green). The mature proteins have a length of 152–161 aa. The KDEL receptor retention sequence is located at the C-terminus (yellow). H.s. *Homo sapiens*; D.r. *Danio rerio*; D.m. *Drosophila melanogaster;* C.e. *Caenorhabditis elegans*. Not on scale. Image modified from Voutilainen et al 2015.

Both proteins, MANF and CDNF are small proteins, highly soluble and monomeric in neutral solution (Lindholm et al 2007; Mizobuchi et al 2007; Hoseki et al 2010; Hellman et al 2011; Latge et al 2015; Lindahl et al 2017). They have

two domains; an N-terminal signal peptide and ER retention signal (Fig. 4) (Mizobuchi et al 2007; Parkash et al 2009).

The N-terminal domains of MANF and CDNF resemble Saposin-Like Proteins (SAPLIPs) (see Fig. 4) (Parkash et al 2009; Hellman et al 2011; Hoseki et al 2010). The SAPLIPs protein group possesses diverse activities for example lipid- or membrane-binding activities (Bruhn 2005). Besides the porcine NK-lysin and human granulysin were identified as the closest structural homologs for the N-terminal domain of CDNF and MANF; both proteins have cytolytic activity (Parkash et al 2009; Lindahl et al 2017). Bai et al (2018) showed that MANF has the ability to directly bind sulfatide, the binding probably occurs via the evolutionarily conserved surface lysine residue K112 in Human MANF. CDNF does not bind to sulfatide (Bai et al 2018). Sulfatide is a sulfoglycolipid produced in ER and Golgi body and diffuses to the extracellular fluid of several cell types, in mammals it can also diffuse into the extracellular space and circulation (Bai et al 2018).

The C-terminal domain of human MANF and CDNF is homolog of the C-terminal SAF-A/B Acinus and PIAS (SAP) (see Fig. 4) domain of Lupus Ku Autoantigen Protein p70 (Ku70) (Hellman et al 2011; Lindahl et al 2017). Ku70 blocks BCL-2- Associated X Protein-Dependent (BAX) apoptosis by binding BAX (Gomez et al 2007; Hada et al 2016).

Moreover, the CXXC motif at the carboxy-(C) terminal domain of MANF possibly has reductase or disulphide isomerase activity (Parkash et al 2009). The CXXC motif is a consensus sequence of proteins of the thiol-protein oxidoreductase superfamily; other members are for example metal-binding proteins, thioredoxins, as well as glutaredoxins and peroxiredoxins (Collet et al 2003; Mizobuchi et al 2007). Common for this enzyme superfamily is that all members are involved in disulphide mediated redox reactions and glutathione metabolism in which the CXXC domain is central (Horibe et al 2004; Mizobuchi et al 2007). In spite of that, no evidence of oxidoreductase activity was detected in MANF so far (Mizobuchi et al 2007; Mätlik et al 2015). Mutations in the CXXC motif totally revoke the protective effect of MANF but do not change MANF's localization, demonstrating the motif’s necessity for MANF's intracellular and extracellular activity (Mätlik et al 2015).

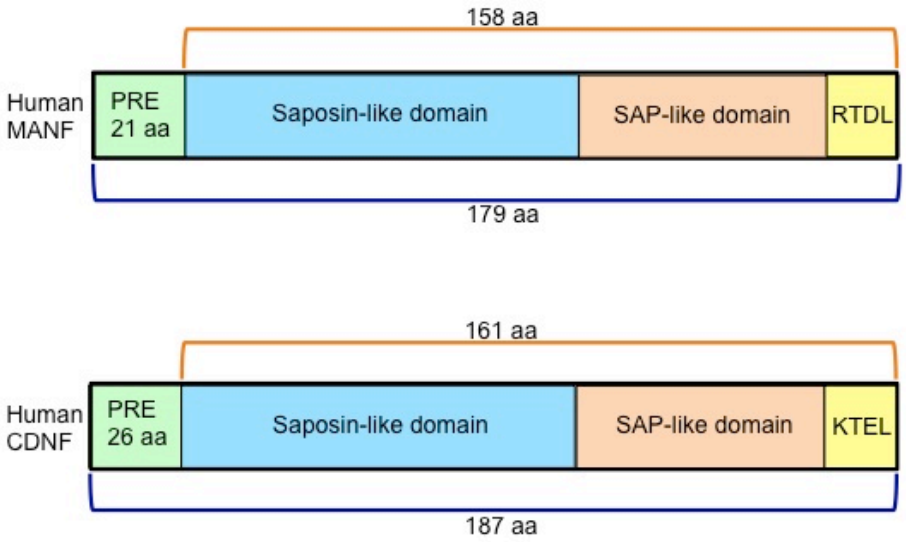

Figure 4: Schematic representation of human MANF and CDNF. The N-terminal domain of MANF and CDNF terminal domains of Mesencephalic Astrocyte-Derived Factor (MANF) and Cerebral Dopamine Neurotrophic factor (CDNF) resemble saposin-like protein, in light blue (Parkash et al 2009; Hellman et al 2011). MANF and CDNF also possess at the N-terminal domain a signal sequence (PRE in green), that is cutoff forming the mature protein, the orange line indicates the mature protein (Voutilainen et al 2015). The blue line shows the complete protein sequence. The C-terminal domain of human MANF and CDNF is homolog of the C-terminal SAF-A/B Acinus and PIAS (SAP) domain of Lupus Ku Autoantigen Protein p70, in orange (Hellman et al 2011; Lindahl et al 2017). The proteins also have a KDEL receptor retention sequence (yellow) at the C-terminal domain (Voutilainen et al 2015). aa; amino acids. Not on scale.

Petrova and colleagues 2003 reported that human MANF is a glycosylated protein, but subsequent studies by Lindholm et al 2008 did not identify post-translational modifications of mouse MANF secreted *in vitro.* Additionally, human and mouse MANF do not have glycosylation sites (Lindholm and Saarma 2010). Human CDNF is presumed to have one N-glycosylation and one O-glycosylation site (Lindholm et al 2007; Sun et al 2011). Cells overexpressing CDNF have been reported to secrete glycosylated (Apostolou et al 2008; Sun et al 2011) and unglycosylated forms of CDNF (Lindholm et al 2007). According to Sun et al 2011 the glycosylation of CDNF is not necessary for its secretion or biological activity. Putative glycosylation sites are missing on mouse CDNF (Lindholm et al 2007).

Only a fraction of MANF and CDNF is secreted from the ER and Golgi body due to their C-terminal ER retention signal, the so-called KDEL-like motif (see Fig

4), most of both proteins remain in the ER and Golgi body (Mizobuchi et al 2007; Tadimalla et al 2008; Apostolou et al 2008; Oh-Hashi et al 2012; Glembotski et al 2012; Norisada et al 2016; Lindahl et al 2017).

Research on MANF intracellular traffic shows that MANF is secreted from ER to the Golgi body (Apostolou et al 2008; Oh-hashi et al 2012). Studies on MANF overexpressing cells exposed to brefeldin A (a Golgi disrupter) present almost fully inhibition of MANF secretion, while the amount of intracellular MANF increases (Apostolou et al 2008; Oh-hashi et al 2012). Furthermore, a study that induced overexpression of MANF and dominant negative Sar1 (Sar1[H79G] compromises COPII-mediated transport from the ER to the Golgi apparatus) in cells also found inhibition of MANF secretion (Oh-hashi et al 2012).

These results showed that COPII mediated the transport and regulated the secretion of MANF (Oh-hashi et al 2012). Besides, the overexpression of BiP reduces secretion of MANF and causes intracellular accumulation of the latter (Oh-hashi et al 2012). Like MANF, the CDNF transport is mediated by COPII and its secretion is also regulated by BiP and KDEL receptor (Norisada et al 2016).

The KDEL receptors (KDEL-Rs), which exist on *cis*-Golgi network, recognize the KDEL-like motifs of MANF and CDNF and mediate their trafficking from the Golgi apparatus back to the ER (Henderson et al 2013; Liu et al 2015a; 2015b; Mätlik et al 2015; Norisada et al 2016; Kim et al 2017a). The experimental removal of the KDEL-like motif of mouse MANF and CDNF decreased their extracellular levels, however, a significant increase in the intracellular amounts was only observed for MANF (Norisada et al 2016). The secretion of Cysteine-Rich with EGF-like Domains 2 (CRELD2), an endoplasmic reticulum stress-inducible protein, is affected by MANF, but only if the KDEL-like motif is present (Oh-hashi et al 2009; 2015). However in contrast to MANF, mouse CDNF only slightly affected the secretion of CRELD2 (Norisada et al 2016).

Mätlik and colleagues (2015) observed, if the KDEL-like motif of MANF is deleted, the entire intracellular pro-survival activity of MANF is revoked and the protein localizes in the Golgi complex. The MANF C-terminal domain is also important for the protection against BAX-dependent apoptosis on sympathetic neurons (Hellman et al 2011). Furthermore, MANF mutation experiments show the KDEL-like motif is not required for the neuroprotective activity on extracellular

application in *in vivo* stroke models (Mätlik et al 2015). This result supports the hypothesis that MANF has at least two different targets: an intracellular target that works with the endoplasmic reticulum and an extracellular target it is modulated by the secreted protein (Oh-hashi et al 2012; Glembotski et al 2012; Mätlik et al 2015; Latge et al 2015).

Even if MANF and CDNF have two domains with distinct functions, the intact full-length protein is required to function (Hoseki et al 2010; Hellman et al 2011). As an example, only mature MANF (and none of its isolated domains) rescued larval lethality in *D. melanogaster* (Lindström 2013). Besides, on the same study, CDNF was not able to rescue the lethal phenotype, demonstrating that probably both paralogs behave differently (Cordero-Llana et al 2015; Latge et al 2015). Supporting that view, Renko et al (2018) observed that rats injected with MANF or CDNF show differences in dopamine neurotransmission, dopamine synthesizing and metabolizing enzymes.

3.2. MANF expression

The MANF protein and mRNA are widely expressed in neuronal and non-neuronal tissues (Kim et al 2017a). MANF expression in human splenocytes is mainly localized in the plasma cells and macrophages, but not in T- and B-cells (Liu et al 2015c). Because of these findings, it can be assumed that splenocytes expressing MANF are probably involved in plasma cell differentiation and immune regulation (Liu et al 2015c).

Mesencephalic astrocyte-derived factor mRNA is expressed in several brain areas, high levels were detected especially in the cortical neurons, hippocampus, and in the cerebellar Purkinje cells, which also expressed high levels of CDNF (Lindholm et al 2008; 2007). MANF mRNA is also expressed in non-neuronal tissues, such as heart (Tadimalla et al 2008), adult liver, testis, salivary gland (Lindholm et al 2008), and also found in human blood (Galli et al 2016). Additionally, MANF was also found in the retina, vitreous body and optic nerve of humans and rodents (Gao et al 2017a; 2017b). The urinary excretion of MANF occurs during podocyte or tubular cell ER stress (Kim et al 2016). Because MANF is secreted, it is extremely high expressed in secretory cells and tissues (Gao et al 2017b).

Dopaminergic neurons are selectively protected by MANF MANF, but not GABAergic or serotonergic neurons *in vitro* or *in vivo* experiments (Petrova et al 2003; Lindholm et al 2007). Rats pre-treated with MANF by injection on the striatum show after induced stimulus-evoke an increase in dopamine release and turnover (Renko et al 2018).

Wang et al (2014b) analyzed the spatiotemporal expression of MANF in the brain of postnatal and adult rats and observed that MANF expression is wide spread among the brain, mainly localized in neurons. The expression level of MANF was high in the early postnatal days and declined slowly as the brain matured; the lowest level of MANF expression was detected in the adult rat brain (Wang et al 2014b). However, the high expression level of MANF in the hypothalamus persisted into adulthood (Wang et al 2014b).

Mesencephalic astrocyte-derived factor protein probably plays an important role in the mature hypothalamus (Yang et al 2017). Several hypothalamic nuclei, which critically regulate energy intake, are rich in MANF and the expression of MANF rises in the hypothalamus of fasting mice (Yang et al 2017).

Mice knockout for MANF had a severe diabetes-independent growth defect, the reason was uncertain; however, it was probably related to a deficiency of MANF in the hypothalamus and adenohypophysis resulting in an impairment of the hormonal control of growth (Lindahl et al 2014; 2017). Additionally, the dopamine system of the MANF knockout mice was affected. This phenotype was already expected, due to earlier experiments with *D. melanogaster* and *Danio rerio* (*D. rerio*) knockout systems that showed the same phenotype (Palgi et al 2009; Chen et al 2012). Moreover, MANF is known to be involved in protecting and repairing dopaminergic neurons from apoptosis (Hellman et al 2011). In contrast to $MANF^{-/-}$ mice, the CDNF knockout mice are viable, fertile and do not present obvious defects in growth, lifespan or glucose metabolism (Lindahl et al 2017).

Tseng et al (2017a) showed that MANF expression is high in the developing cortex as well as in neural lineage cells, including neural stem cells of the subventricular zone. The same scientists observed that the lack of MANF disturbs the neurite growth and migration of developing neurons into the cortex, showing that MANF is involved in neurite extension. On the other hand, the removal of MANF does not change stem cell proliferation; an unexpected fact compared to

the effects of other NTFs (Tseng et al 2017a). The MANF protein is developmentally regulated and may play a role in the maturation of the central nervous system (Wang et al 2014b). In zebra fish MANF regulated the development of dopaminergic neurons, in adult zebra fish the MANF expression was high in liver, but lower in kidney and eyes and knockdown of the MANF mRNA affected the dopamine system (Chen et al 2012; Lindahl et al 2017).

In several invertebrate-sequencing projects MANF homologs were predicted. However, until today analyses of sequences and functions of MANF in invertebrates were conducted for homologs of fruit fly *D. melanogaster,* pea aphid *Acrythosiphon pisum* and *C. elegans* (Palgi et al 2009; Wang et al 2015a; Bai et al 2018).

The protein (DmMANF) found in *Drosophila melanogaster* is closer related to MANF than to CDNF (Palgi et al 2009). DmMANF takes part in the regulation and development of dopaminergic neurons of *Drosophila* (Palgi et al 2009). It is predominantly expressed in garland cells and is extensively expressed in the adults visual system, which raises the idea a possible role in this context (Palgi et al 2012, Walkowicz et al 2017). In the central nervous system of adult *Drosophila* specimen DmMANF co-localizes strongly with glial processes; it is localized specifically in dopaminergic cell somas, and during embryonic phases DmMANF is also expressed in the salivary glands and body fat (Palgi et al 2009; 2012). DmMANF protein is extensively distributed during embryonic and larval stages in contrast with the most concentrated distribution of MANF expression in mature fruit flies, demonstrating the dynamic expression pattern of DmMANF during development (Stratoulias and Heino 2015b). Moreover, *in vivo* screening shows that DmMANF genetically interacts with Irbp, the *Drosophila* homolog of Ku70; besides, partially localizes to mitochondria and genetically interacts with the ubiquinone synthesis pathway (Lindström et al 2017).

The knockout of DmMANF results in lethality at early developmental stages with neuronal defects, exhibit specific and significant reduction of dopaminergic neurite and cuticular defects (Palgi et al 2009), and knockdown of DmMANF paired with Dicer-2 overexpression in glia resulted in the appearance of an unusual macrophage-like cell type in the pupal brain (Stratoulias and Heino 2015a). The silencing of DmMANF in glia diminishes the lifespan of the flies

(Walkowicz et al 2017). Furthermore, the reduction of DmMANF levels in either glia or neurons influences the sleep and the locomotor activities of flies (Walkowicz et al 2017).

The MANF homolog (ARMET), of the pea aphid *Acrythosiphon pisum* is a secreted protein that modulates the hosting plant's defense mechanisms, as part of the parasite-plant interaction (Wang et al 2015a).

The *C. elegans* MANF homolog is extensively expressed in a variety of tissues as intestine, hypoderm, spermatheca and nervous system and plays a role on ER stress response mechanisms (Bai et al 2018).

Mesencephalic astrocyte-derived factor is a widely expressed protein that has functions during embryogenic and adult phases of the animal's life (Wang et al 2014b; Stratouilias and Heino 2015b; Lindahl et al 2017; Tseng et al 2017a; Yang et al 2017; Bai et al 2018; Lu et al 2018).

3.3. MANF expression and secretion upon ER stress

Several studies have shown that MANF can protect cells from ER stress on many different disease models, and also on experiments using reduction agents and ER inhibitors (Voutilainen et al 2015; Wang et al 2015b; Kim et al 2016; 2017a; Li-na et al 2017; Liu et al 2016b; Bai et al 2018; Guo et al 2018).

Mesencephalic astrocyte-derived factor expression is up-regulated in cell lines derived from bone tissue (U2OS), Human Embryonic Kidney cells (HEK 293), and neuroblastoma (SH-SY5Y) in response ER stress induce by tunicamycin (TM) thapsigargin (TG) and lactacystin (Apostolou et al 2008). Tunicamycin is a nucleoside antibiotic that inhibits protein glycosylation, thapsigargin (TG) is a specific inhibitor of the sarcoplasmic/endoplasmic reticulum Ca^{2+}-ATPase (SERCA) (Mizobuchi et al 2007) Lactatystin is a cell-permeable and irreversible proteasome inhibitor (Apostolou et al 2008).

The expression of MANF was also enhanced on embryo fibroblasts (NIH 3T3) exposed to TM, TG, and Dithiothreitol (DTT, that change the ER redox status) (Mizobuchi et al 2007). The treatment of neuron Neuro2a cells with TG raised the levels of MANF; ATF6α powerfully increased the MANF promoter function; however the effect of ATF6b and XBP1s were modest (Oh-hashi et al 2013; Kim et al 2017a). In spleens of human patients it was observed, that

splenocytes, which express MANF also express ER stress-related proteins, including ATF6, XBP1s, BiP, and CHOP (Liu et al 2015c).

The MANF promoter comprises an ER Stress Response Element (ERSE-II) motif (ACGTGGNCCAAT), which is directly downstream of -160 bp in the promoter region (Mizobuchi et al 2007; Tadimalla et al 2008). The ERSE-II includes two transcriptional factor recognition sequences: ACGTGG is recognized by ATF6 or XBP1, while CCAAT is recognized by nuclear transcriptional factor (NF)-Y, the two binding sites are necessary for activation of MANF in response to ER stress (Mizobuchi et al 2007). XBP1s up-regulates trough the ERSE elements MANF expression (Lindahl et al 2017; Wang et al 2018).

Trafficking and secretion of MANF are regulated by ER stress, but the increase in protein secretion is not a universal response (Kim et al 2017a). Cardiomyocytes, HeLa cells and neurons primary cell culture, it constitutively expresses MANF at moderated levels presents an up-regulation of MANF after exposition to TM (Tadimalla et al 2008; Yu et al 2010; Glembotski et al 2012; Liu et 2016a). Besides, cardiomyocytes and HeLa cells also show increase in MANF expression upon exposition to TG and DTT (Glembotski et al 2012). On the other hand Henderson and colleagues 2013 did not observe an increase in MANF expression in SH-SY5Y cells treated with TM or DTT.

The ER stress, enhances not only expression, but also secretion of MANF (Apostolou 2008; Tadimalla et al 2008; Glembotski et al 2012). The secretion of MANF was induced by TM in cardiomyocytes (Tadimalla et al 2008). On the other hand Glembotski et al (2012) observed on cardiomyocytes and HeLa cells significant increased in MANF secretion only upon tapsigargin exposition.

Furthermore, CDNF expression in osteosarcoma U2OS cells did not increase upon TM exposition In contrast to the MANF expression, it was up-regulated (Apostolou et al 2008). The knowledge of CDNF activity on ER stress is slight, but it may also play a protective role against ER stress, like MANF. So far, some studies have shown that CDNF can mitigate ER stress-induced damage (Cheng et al 2013; Zhou et al 2016; Liu et al 2017).

The lack of MANF in mice activates ER stress response as well as unfolded protein response pathways (Lindahl et al 2014). The MANF deficient mice developed severe diabetes, caused by postnatal reduction on the β-cell mass, due

to decreased proliferation and increased apoptosis on pancreatic islets, a chronic UPR response (Lindahl et al 2014). This was also observed in zebra fish, *D. melanogaster* and *C. elegans* (Palgi et al 2009; 2012; Chen et al 2012; Lindström et al 2016; Bai et al 2018).

Besides, *C. elegans* MANF null mutants can be rescued by human MANF, in the presence of sulfatide, in some cases through a dependent activity of endocytosis machinery (Bai et al 2018). The enrollment of BiP on MANF uptake was demonstrated by the co-localization of MANF and BiP, raising the idea of an endocytosis following a cell surface binding (Bai et al 2018). Another hypothesis was that MANF is involved in the degradation process of lysosomes, due to its Saposin-like domain (Bai et al 2018). Saposin family proteins normally work on the solubilization of many sphingolipids for degradation inside lysosomes (Kolter and Sandhoff 2005). Indeed MANF binds to sulfatide, but without inducing degradation processes, in contrast leading to efficient cellular endocytosis (Bai et al 2018).

Mesencephalic astrocyte-derived factor activity during UPR is not completely clear yet, one raised hypothesis is that during unstressed situations, MANF is retained in the ER by KDELR via the C-terminal RTDL sequence and by calcium dependent interaction with BiP/GRP78 (Glembotski et al 2012; Henderson et al 2013; Lindahl et al 2017). A change in calcium concentration could trigger dissociation of the MANF/-BiP complex causing a subsequent MANF secretion (Glembotski et al 2012), extracellular MANF could function in an autocrine and/or paracrine capacity to protect cells from death in response to ER calcium depletion (Apostolou et al 2008; Glembotski et al 2012).

Another function of MANF and CDNF has been hypothesized from the structural homology were C-terminal, SAP domain, protects the cell from BAX-mediated cell death (Hellman et al 2011). Furthermore, MANF is a major component regulating the secretion of the ER inducible protein CRELD2 through the C-terminal amino acids (RTDL) (Hartley et al 2013; Oh-hashi et al 2015). Chen and colleagues (2015b) demonstrates the interaction between MANF and RTN1-C, a protein from the reticulons family.

Mesencephalic astrocyte-derived factor may also be part of the regulation of inflammatory response (Zhao et al 2013; Chen et al 2015a; Gao et al 2017a; 2017b; Yang et al 2017). In a study where astrocytes were pre-treated with MANF

and then exposed to ER stress by oxygen–glucose deprivation-induced cell damage, a suppression of ER stress was observed (Zhao et al 2013). Additionally, the levels of BiP, NF-kB p65 and secretion of proinflammatory cytokines, Interleukin 1 beta (IL-1β), interleukin 6, as well as Tumor Necrosis Factor alpha (TNF-α) were reduced (Zhao et al 2013).

Corroborating that results, MANF's negative regulates NF-kB signaling, the C-terminal SAP-like domain of MANF interacts with the DNA binding domain of NF-kB p65 subunit after translocation of MANF into the nucleus under inflammation and ER stress (Chen et al 2015a). Besides, MANF decreased the expression level of IL-1β, TNF-α, and Interferon Gamma (IFN-γ) induced by Lipopolysaccharide (LPS) treatment, regulating NF-kB and phosphorylation of p38-Mitogen-Activated Protein Kinases (P38-MAPKs) pathways, but not n p-JNK or p-ERK signaling (Zhu et al 2016).

Induced cell damage of SH-SY5Y cells through neurotoxin 6-hydroxydopamine (6-OHDA) is protected by MANF, thru suppressing ER stress, activating the pathway PI3K/Akt/mTOR (phosphatidylinositol 3-kinase (PI3K)/Akt/Mammalian Target of Rapamycin (mTOR)) and inhibiting autophagy (Hao et al 2017; Zhang et al 2017a). The AMPK/mTOR signalling pathways are also involved in the inhibiting of autophagy by MANF on energy depletion conditions (Zhang et al 2017a).

Nonetheless, MANF up-regulates the expression of nuclear factor Erythroid 2-Related Factor (Nrf2), which is a transcription factor in the phase II antioxidant response pathway, and promotes its translocation into the nucleus, potentiating the Nrf2-related survival mechanism through the PI3K/Akt/GSK3β (Glycogen synthase kinase 3 beta) pathway (Alfieri et al 2011; Zhang et al 2017b).

3.4. MANF on disease models

Neurodegenerative diseases are characterized by progressive loss of neuronal function in defined area of the nervous system, ending up in malfunction (Majdi et al 2016; Hetz and Saxena 2017). Disorders such as Alzheimer's, Parkinson and Huntington disease, as well as, amyotrophic lateral sclerosis, prion-related, retinitis pigmentosa and some myelin-related disorders have different pathophysiological and clinical hallmarks (Soto 2003; Bertram and Tanzin 2005; Aguzzi and

O´Connor 2010; Hetz and Saxena 2017). However, they share a pathological trait: abnormal aggregation of misfolded proteins and this accumulation generates ER stress, which triggers UPR (Soto 2003; Oakes and Papa 2015; Rivas et al 2015; Plate and Wiseman 2017).

The long-term activation of UPR is present in numerous neurodegenerative diseases based on animal models and post-mortem studies of tissue from patients with disorders related to protein aggregation (Hetz and Saxena 2017). But the link between ER stress and UPR is also present in inflammatory disease and traumatic injury to the nervous system (Hetz and Saxena 2017). The possibility of influencing UPR controlling secretory proteostasis can provide a remarkable therapeutic possibility to treat humans (Plate and Wiseman et al 2017).

The role of MANF and CDNF on ER stress and UPR response highlight them as possible treatments to neurodegenerative diseases; both proteins have neuroprotective and neurorestorative effects (Lindholm et al 2016; Liu et al 2015b; Nasrolahi et al 2018). As well, their role on ER stress and UPR can make then target to treat not only neurodegenerative disorders but also many other diseases (Glembotski et al 2012; Lindahl et al 2014; Liu et al 2016a; Neves et al 2016; Kim et al 2017a; Guo et al 2018).

The expression, activity and protective effect of MANF has been studied on many ER stress and disease models. MANF rescues apoptotic superior cervical ganglion (SCG) neurons (Hellman et al 2011) and also non-neuronal cells (Petrova et al 2003; Apostolou et al 2008; Mätlik et al 2015). It inhibits oxygen glucose deprivation induced cell damage and inflammation in rat primary astrocytes (Zhao et al 2013) and is up-regulated on mice chronic restrain stress model (Huang et al 2015).

Mesencephalic astrocyte-derived factor plays an important role in nervous system diseases (Li-na et al 2017). Studies on MANF on Parkinson´s disease models, show a neuroprotective and neurorestorative effect on rats treated with 6-OHDA (Voutilainen et al 2009; 2011; Cordero-Llana et al 2014; Hao et al 2017) and C57BL/6 mice model (Liu et al 2018). Moreover, MANF *in vitro* inhibits apoptosis and decreases the damage on SH-SY5Y cells challenged with 6-OHDA or with overexpression of alpha-synuclein (Huang et al 2016; Sun et al 2017; Zhang et al 2017a; 2017b). The infusion potential of MANF in a large animal

model, were studied on porcine putamen and substantia nigra following Convection-Enhanced Delivery (CED), and validates the translational potential of infusing MANF as a novel treatment strategy for PD (Barua et al 2015).

The neuroprotective effects of MANF have been also researched on others disease models as: cerebral ischemia in mice (Lindholm et al 2008; Yang et al 2014a), rats (Airavaara et al 2009; 2010; Yu et al 2010; Shen et al 2012; Yue et al 2014; Mätlik et al 2015; 2018; Wang et al 2016; Tseng et al 2017b; Xu et al 2018) and piglets (Olson et al 2013), also on spinal cord (Gao et al 2018) and traumatic brain injury models (Li et al 2018). As well as, on knock-in mouse model of spinocerebellar ataxia 17, that inducibly expressed one copy of mutant TATAbox binding protein (Yang et al 2014b; Guo et al 2018). Furthermore, the treatment of an epilepsy mouse model (Lindholm et al 2008), as well as of rats and neural stem cell with valproic acid, a drug clinically used as mood stabilizer, resulted in the up-regulation of MANF (Niles et al 2012; Almutawa et al 2014).

Moreover, in a rat model for chronic glaucoma and on an *in vitro* model of hypoxia-induced cell injury, MANF was able to protect retina ganglion cells (Gao et al 2017b). Besides, Neves et al (2016) showed that intravitreal injection of recombinant MANF induces neuroprotection, improves tissue repair, and increases the success of photoreceptor replacement therapies in the retina, through an alternative activation of innate immune cells. MANF is a novel prospective therapeutic agent to treat retinal degenerative disorders (Gao et al 2017b; Lu et al 2018).

Besides, MANF possibly plays a role in cardiac diseases (Tadimalla et al 2008; Glembotski et al 2012; Liu et al 2016a; 2016b). MANF is able to protect neonatal rat cardiomyocytes (Liu et al 2016b), and also has a cytoprotective effect on induced myocardial infarction and inducible ischemia models (Tadimalla et al 2008; Glembotski et al 2012). Furthermore, it has the ability of reducing cardio hypertrophy and heart failure, therefore it is considered as a cardioprotective factor with a possible future in treating cardiac diseases (Glembotski et al 2011; 2012 Liu et al 2016a). Shimano et al (2012) described MANF as cardiokine. This protein type is secreted from cells that play crucial roles in intercellular and intertissue communication during tissue development, growth and in response to various pathological stresses.

Moreover, in rabbit fibroblast-like synoviocytes antigen induced arthritis model, MANF is up-regulated (Chen et al 2015a). It is also up-regulated in cell and mouse models of chondrodysplasias (Hartley et al 2013), as well as in metaphyseal chondrodysplasia, Schmid type disease model; were the ER stress was analyzed through the replication of the disease phenotype by expressing misfolded types of collagen X (Schmid) or thyroglobulin (Cog) in the hypertrophic zone (Cameron et al 2011). Furthermore, rabbits with antigen-induced arthritis, and patients with rheumatoid arthritis or Systemic Lupus Erythematosus (SLE) show a decreased expression of MANF in the peripheral white blood cells (Wang et al 2014a; Chen et al 2015a). Otherwise, in 2017 Almlöf et al presented MANF as predicted novel risk gene for SLE according to the SLE random forest classification.

The MANF protein can also easily be detected in urine samples taken from mouse model of human Nephrotic Syndrome (NS) caused by mutant laminin b2 at the initial stage of NS. Urinary MANF excretion increased during disease progression in the mutants, but not in the controls (Kim et al 2016). Due to this, MANF can possibly be used as urinary biomarker for detecting ER stress in podocytes or renal tubular cells (Kim et al 2016). The usage of noninvasive biomarkers for detecting ER stress in podocytes or tubular cells on the initial phases of the disease is relevant to identified the illness when a kidney biopsy is not yet clinically indicated (Kim et al 2016). In a rodent bladder outlet obstruction disease model an increased expression of MANF and others ER-stress markers, as the ER expands, were observed (Krawczyk et al 2016). The ER expansion is a phenotypic modulation of smooth muscle cells that is an indicator of the bladder outlet obstruction (Krawczyk et al 2016).

Moreover, probably MANF plays a role in Diabetes Mellitus (DM) (Lindahl et al 2014). DM is a group of metabolic disorders characterized by the loss of functional pancreatic β cell mass, leading to insufficient insulin secretion (Talchai et al 2012; Weir and Bonner-Weir 2013; Lindahl et al 2014). The MANF protein is essential for proliferation and survival of pancreatic β cells and is also able to protect them from ER stress (Lindahl et al 2014; Cunha et al 2017). Beyond that, on children recently identified with type I DM newly diagnosed pre diabetic and as well diabetic patients type II, presented increased levels of circulating MANF in

serum (Galli et al 2016; Wu et al 2017). Along with, the serum levels of MANF were well correlated with indices of insulin resistance (Wu et al 2017).

Besides, Yang and colleagues (2017) showed that *in vivo* hypothalamic MANF overexpression leads to insulin resistance and *in vitro* the overexpression of MANF in cultured cells leads to a reduced insulin sensitivity. The same research group also demonstrated that MANF does not trigger insulin resistance via enhanced of inflammation (Yang et al 2017).

Overweight and obesity evolve when the energy intake exceeds expenditure; the excess energy is deposited as body tissue (Romieu et al 2017). The idea of a possible role of MANF in obesity is raised by the functional balancing of MANF associated with food intake on hypothalamus (Yang et al 2017). Hypothalamic MANF overexpression leads to hyperphagia and MANF hypothalamic reduction leads to hypophagia (Yang et al 2017). It also influences food intake and body weight by modulating hypothalamic insulin signaling (Yang et al 2017). Analyzes with transgenic mice overexpressing MANF, which become highly obese, show the increasing on energy intake is the sole cause of the observed animal obesity (Yang et al 2017).

4. Sponge

The sponges (Phylum Porifera) are among the oldest existing multicellular animals (Metazoa) lineages dating back to Precambrian, preceding the radiation of all other animal phyla (Li et al 1998; Love et al 2009, Botting and Muir 2018). Sponges have been considered the earliest branching of metazoan taxon, and, therefore, present great significance in the reconstruction of early metazoan evolution (Müller et al 2004a; Wörheide et al 2012). However, there are conflicting phylogenetic hypotheses concerning evolutionary relationships among some of major metazoan lineages based on molecular data: Porifera, Placozoa, Ctenophora, Cnidaria (Nosenko et al 2013). In some phylogeny analysis Ctenophora are placed at the basis of metazoan clade (Dunn et al 2008; Hejnol et al 2009; Ryan et al 2013). The majority of phylogeny analysis sponges are placed at the basis of metazoan clade (Medina et al 2001; Philippe et al 2009; Schierwater et al 2009; Sperling et al 2009; Pick et al 2010; Erwin et al 2011; Wörheide et al 2012; Feuda et al 2017; Simion et al 2017, Renard et al 2018).

The conflicting results presented by the deep metazoan phylogenies can be caused by many factors, as example most of the phylogenies diverge on taxon and gene sampling, on applications of phylogenetic methods and thresholds, as well as different models of amino acid substitution (Philippe et al 2011; Nosenko et al 2013; Riesgo et al 2014). Furthermore, solving the deep animal phylogenetic relation is important because it can contribute to a better comprehension of the evolution and function of many animal characteristics such as body plans, and nervous system (Philippe et al 2009; Dunn et al 2015).

4.1 Sponge biology

Sponges are exclusively aquatic animals that inhabit a variety of marine and freshwater systems (Bergquist 1978; Hooper and van Soest 2002). Approximately 8.500 sponges species have already been described, although some authors estimate that as many as the double of this number exist (van Soest et al 2012; Appeltans et al 2012). Phylum Porifera is currently divided into four classes, Hexactinellida, Demospongiae, Calcarea and Homoscleromorpha (Gazave et al 2012; van Soest et al 2012; Riesgo et al 2014). Marine sponges are distributed worldwide, ranging from polar to tropical regions and are an important component of the benthic communities (Maldonado et al 2005; van Soest et al 2012).

Sponge body is structured around a system of water channels that may exhibit four different forms: ascon, sycon, leucon and solenoid (Bergquist 1978; Bavestrello et al 1988; Cavalcanti and Klautau 2011). These water channels are vital for feeding, respiration and reproduction (Bergquist 1978; Bavestrello et al 1988). The sponge body plans show a huge variety among the four sponge classes, though the majority of the adult sponge's body is assembled by the same components: pinacocytes, choanocytes, and a selection of mesohyl cells (Adamsk 2018). The skeleton is made of calcareous or siliceous spicules and, siliceous spicules give structural support to almost all demosponges (Rupert and Barnes 1996; Hentschel et al 2012). The external body wall is formed by the pinacoderm, which is made by epithelioid cells named pinacocytes (Rupert and Barnes 1996). The inhalant orifices in the outside of pinacoderm (called pores) are formed by specialized cells called porocytes, which forms a ring that extends from the outer surface to the espongiocele (Rupert and Barnes 1996). Below, the pinacoderme is

the mesohyle, which is a gelatinous and protein matrix that contains both skeletal material and amoeboid cells (Rupert and Barnes 1996). Internal to the mesohyle is the choanocyte chamber, which is formed by lined up flagellated cells called choanocytes (Hentschel et al 2012). The beating movement of the choanocytes generates a water flow through the sponge body, which is micro-filtered by a microvillous collar at the flagellum base and used to collect food particles from the surrounding water (Hentschel et al 2012; Mah et al 2014).

The sponges are filter-feeding organisms that are remarkably efficient in obtaining food from the surrounding water (Reiswig 1971; Vogel 1977; Pile et al 1996; Taylor et al 2007). However, some sponge species are carnivorous, which is the case of *Chondrocladia grandis* (Vacelet and Boury-Esnault 1995; Verhoeve and Dufour 2018).

Moreover, sponges are capable to filter huge amounts of water (0.002 to 0.84 ml/s per cm^3 of sponge tissue) through its aquifer channel system. Through this process, sponges obtain food while retaining a wide range (0.1 to 50 mm) of particulates organic materials, bacteria, unicellular algae and even viruses (Reiswig 1971; 1975; Vogel 1977; Larsen and Riisgård 1994; Hadas et al 2006; Pile et al 1996; De Goeij et al 2008; Hentschel et al 2012). The food particles or microorganism retained on choanocyte microvillous collar is moved to the inner mesohyl layer, where they are digested via phagocytosis by archaeocyte cells, which are totipotent cells (Custódio et al 1998; Müller et al 2006; Taylor et al 2007; Hentschel et al 2012; Mah et al 2014). Besides, sponge morphology is very diverse and can be strongly influenced by natural factors and interaction with other organisms (Bergquist 1978; Leys and Hill 2012).

Despite the phenotypic simplicity of sponges, their genome displays an amazing complexity with a comprehensive set of genes characteristic of metazoan multicellularity (Harcet et al 2010; Srivastava et al 2010; Conaco et al 2012b; Riesgo et al 2014; Pita et al 2016). Sponges express a variety of signaling genes, which includes core genes of the bilaterian signaling pathways such as Wnt, TGF-b, Hedhog, receptor tyrosine kinase, JAK/STAT and Notch signaling pathway (Müller et al 1999d; Nichols et al 2006). They also present a complex repertoire of developmental transcription factors (Larroux et al 2006; Müller 2006; Fortunato et al 2015). These findings corroborate the idea that sponge genetics can play an

important role in the understanding of metazoan development (Müller 2006; Srivastava et al 2010; Leys and Hill 2012).

Regarding reproduction, sponges can reproduce through both asexually and sexually reproduction methods. Asexually, reproduction occurs by budding off portions of the adult body or by separating cells into an overwintering cyst or gemule (Leys et al 2005). Sexually, through a widely different mechanism of sexual reproduction and larval development (Leys and Ereskovsky 2006), which may show phototaxis and geotaxis behaviors (Leys and Degnan 2001; Maldonado and Bergquist 2002; Maldonado et al 2003). These larvae go through a metamorphic transition after settlement which includes extensive reorganization of undifferentiated cells and trans-differentiation of functional larval cells toward the adult system (Amano and Hori 1996; Leys and Degnan 2002; Leys and Ereskovsky 2006; Conaco et al 2012b), with nitric oxide (NO) playing a role in regulation of sponge pelagic/benthic life cycle (Ueda et al 2016).

4.2. Components of neuronal processes identified in sponges

The sponge epithelium is the better recognizable tissue, being composed of rudimentary epithelial cells that are poorly differentiated, and sensory cells that seems to be also involved in a conducting pathway (Leys et al 2009; Leys and Riesgo 2012; Leys 2015; Littlewood et al 2017). Although, the presence of a “true” ephithelia in sponges still being debated (Belahbib et al 2018).

The sponge epithelium has functions on cell communication and coordination, along with the ability to seal and control ionic composition of the internal milieu, keeping the animal integrity and homeostasis (Leys et al 2009; Leys and Riesgo 2012). Sponges seems to have an epithelial genetic toolkit with the presence of collagen IV, epithelial polarity complexes, adherent junctions, as well as an E-cadehrin complex a Metazoa novelty (Srivastava et al 2010; Nichols et al 2012; Riesgo et al 2014; Belahbib et al 2018). The presence of occluding junctions, as parallel membrane and septate junctions has also been reported in sponges and at least some groups (e.g., Demospongiae, Haplosclerida) have functional epithelia that occludes the passage of ions (Nichols et al 2006; Leys et al 2009; Adams et al 2010; Leys and Hill 2012; Whitmer 2018). The adhesion molecules of the MAGUK family of transmembrane proteins have also been

reported for sponges. Since these proteins are also involved in the framework of post-synaptic molecules, some authors have suggested that the MAGUK proteins might have functions not only on cell–cell adhesion, but also on signaling at cell junctions in sponges (De Mendoza et al 2010; Fahey and Degnan 2010; Leys and Hill 2012).

Sponges do not have nerves in the prevailing sense; i.e. they lack a specific cell type that transmits signals using electrical impulses that travel along the cell membrane and convey to other cells via a chemical synapse (Leys and Hill 2012). Genomic and transcriptomic analyses demonstrate that sponges have a huge collection of genes that are linked to neuronal processes in other animals (Leys 2015). Different ions form the basis of action potentials, with calcium triggering a rapid signal in sponges that causes a behavioral response: as the inward current is carried with calcium, the influx of Ca^{2+} into the cells of the flagellated chamber stops their pumping (Leys et al 1999; Leys and Meech, 2006; Leys 2015; Meech 2015).

Moreover, the osculum is the main sponge sensory organ; it is able of sensing stimuli from the surroundings and triggering a reaction of the whole body, as a “sneeze” behavior (Meech 2008; Leys 2015). As a result, the sponge disrupts the water flow stopping the water cycle, which is a defensive action in response to damage to any part of the system (Meech 2008; Leys 2015). Studies that scanned sponges on electron microscopy showed that they present small cilia (4-6 μm long) lined up inside of the oscula (Nickel 2010; Ludeman et al 2014; Leys 2015). Leys 2015 suggests that sensory cilia are probably a common sensory organ of Poriferan. The sensory cilia can produce coordinated effector responses that alter, filter-feeding behavior and if either the cilia or the whole osculum is removed the animal loses its ability to “sneeze” (Nickel 2010; Ludeman et al 2014; Leys 2015).

Furthermore, both external mechanical stimuli and chemical molecules such as caffeine, acetylcholine esterase, nicotine, nitric oxide, cyclic adenosine monophosphate and serotonin are known to trigger contractions of the osculum, ostia or whole body of sponges (Ellwanger and Nickel 2006; Nickel 2010; Leys 2015). Dopamine and epinephrine bath applications are also known to cause contractions on sponges (Ellwanger and Nickel 2006). However, the signaling functions of biogenic amines, such as catecholamines, dopamine, epinephrine and

norepinephrine, are not fully understood in sponges (Riesgo et al 2014). Although, sponges probably coordinate their behavior using common chemical messenger systems also present on other animals (Leys and Meech 2006; Ellwanger and Nickel 2006; Ramoino et al 2007; Elliott and Leys 2010).

Sponges have a complex intercellular communication and signaling system that permits them to have coordinated behaviors, which is thought to be the root of both nervous and endocrine systems in other animal groups (Müller and Müller 2003b; Leys and Meech 2006). Almost a whole set of genes homologous to those related to the mammalian synapse formation is present on the genome and transcriptome of demosponge, *Amphimedon queenslandica* (*A. queenslandica*) (Conaco et al 2012a; Riesgo et al 2014). As gamma-amino butyric acid (GABA) and the glutamate decarboxylase, which carries out the synthesis of GABA from glutamate, were identified in sponges (Perovic et al 1999; Ramoino et al 2007; Sakarya et al 2007; Riesgo et al 2014). GABA is believed to be the main inhibitory neurotransmitter in the mammalian central nervous system, a function that has been also reported to a number of invertebrate systems (Ramoino et al 2007).

This corroborates previous reports that show that NO, glutamate and GABA are physiologically active in demosponges (Ellwanger et al 2007; Ramoino et al 2007; 2011; Elliott and Leys 2010). For example, two glutamate receptor inhibitors, AP3 (a competitive inhibitor) and kynurenic acid (Kyn, a non-competitive inhibitor) have been shown to block the sneeze behavior in a concentration-dependent and $GABA_B$ receptors have also been shown to modulate feeding behavior in *Leucandra aspera* (Perović et al 1999; Ramoino et al 2007; 2011; Elliott and Leys 2010). Finally, a transcriptome assay also identifies an ionotropic glutamate receptor (iGluR), with good similarity to vertebrate homologue (Riesgo et al 2014; Leys 2015).

4.3. Sponges microbiome

Sponges host an abundant community of organisms (i.e. nematodes, copepods, bacteria), which forms the poriferan endofauna (Magnino et al 1999; Ribeiro et al 2003; Skilleter et al 2005). The sponge-associated microorganisms generally live in the sponge extracellular matrix (mesohyle) concentrated around the choanocyte chambers (Webster and Thomas 2016). However, some sponge species also host

high densities of cyanobacteria or microalgae just under the pinacoderm cell layer, where they are highest exposed to sunlight (Wilkinson et al 1978b; Webster and Thomas 2016). Furthermore, some sponge species also host bacterial cells intracellularly within specialized bacteriocyte cells that have different kinds of bacteria that might be both symbiotic or food resource (Vacelet and Donadey 1977; Woollacott 1993; Ilan and Abelson 1995; Taylor et al 2007; Hentschel et al 2012; Uriz et al 2012).

Sponge-associated microbiota is complex, with 47 phyla of bacteria known to live in association with sponges, with phyla Poribacteria being specific to sponges (Fieseler et al 2004; Thomas et al 2010; Hentschel et al 2012; Moitinho-Silva et al 2014; Reveillaud et al 2014; Gardères et al 2015b). Thousands of symbionts lineages were described per sponge individuals, and up to 35% of the total sponge biomass may be composed of microorganisms. These may reach densities above 10^9 microbial cells per cubic centimeter of sponge tissue, which are 3 to 4 orders of magnitude higher than the density in the surrounding sea water (Taylor et al 2007; Hentschel et al 2012; Pita el al 2016; Thomas et al 2016). However, that while many sponge species have a dense and diverse microbial community (“high microbial abundance”) other species are virtually lacking of microorganisms (“low microbial abundance”) (Wilkinson et al 1978a; Hentschel et al 2006; Taylor et al 2007; Bayer et al 2014; Gloeckner et al 2014; Ryu et al 2016).

Symbionts of sponges perform a wide range of functional roles, including vitamin synthesis, production of bioactive compounds, and biochemical transformations of nutrients or waste products (Taylor et al 2007; Siegl et al 2011; Hentschel et al 2012; Wilson et al 2014; Moitinho-Silva et al 2017). Sponges ability to house a huge, dense and diverse community of presumed symbiotic bacteria, archaea and unicellular eukaryotes – despite the presence of the bacterium-digesting archaeocytes –, arises the idea that sponge cells are able to recognize different microbial kinds and/or protect the symbionts cells, inhibiting consumption (Wilkinson et al 1984; Hentschel et al 2003; 2012; Taylor et al 2007).

Sponge feeding studies show that putative symbionts, which are those ingested by their sponge hosts, pass through unharmed, although ingested non-symbiont bacteria are normally consumed (Wilkinson et al 1984; Wehrl et al 2007; Hentschel et al 2012). The mechanisms of interaction between marine sponges

and bacteria, being they consumed as food, or establishing opportunistic and commensal relationships are not fully clarified (Gardères et al 2015a). So far, a molecular crosstalk between sponge and bacteria have been shown for bacterial homoserine lactones, where the 3-oxo-C_{12}-HSL may play a role in the tolerance of the sponge apoptosis and immune systems towards the presence of bacteria (Gardères et al 2014). The sponge may sense the 3-oxo-C_{12}-HSL as a molecular proof of the bacterial presence and/or density to control the populations of symbiotic bacteria in the sponge (Gardères et al 2014). Ankyrin-repeat proteins from sponge symbionts may also interfere with phagocytosis pathways and that may be one of the mechanisms used by symbionts to avoid being digested by a sponge host (Nguyen et al 2014). Lectins may also have a role in the sponges defense mechanisms and possibly in the association between the sponge and its microorganisms due to their ability to identify different carbohydrates (Gardères et al 2015a; 2016). Furthermore, there are differences in the lipopolysaccharides (LPS) structure from *Endozoicomona* sp., a commensal *of S. domuncula*, and *Pseudoalteromonas* sp. opportunistic bacteria. Therefore, LPS patterns can have a function on sponge discrimination between symbionts and food (Gardères et al 2015b). The sponge innate immune system is probably involved in the mechanism used to distinguish between food and symbiotic microorganisms (Degnan 2015).

The symbiotic relationships of sponges, and the knowledge of hosting density, specificity, and often highly diverse microbial communities in sponges are raising studies of sponge hologenome, that the collective genomic content of a host (holobiont) and its microbiome (Moran and Sloan 2015; Ryu et al 2016; Theis et al 2016; Webster and Thomas 2016; Moitinho-Silva et al 2017; Slaby et al 2017). The emerging use of sponges as a model of animal-microbe symbioses can contribute to the understanding host–microbe interactions in basal metazoans (Pita et al 2016).

5. Metazoan immunity

The ability to distinguish between self and non-self is a key element of life, and since the foremost eukaryotic cells a variety of defense mechanisms have been developed to assure cellular integrity, homeostasis, and survival of the host (Custódio et al 2004; Boehm et al 2006; Dzik et al 2010; Buchmann et al 2014).

Consequently, all animals have immunity components that differentiate self from non-self (Hoffman et al 1999; Buchmann et al 2014). When a foreign factor somehow triggers the animal recognition mechanisms, it induces a variety of signaling pathways on the host immune response system, which aim to eliminate the threat by killing or isolation (Custódio et al 2004).

The immune response in vertebrates is structured in two main components, the innate and adaptive immune system and they use fundamentally different approaches to deal with the molecular diversity of pathogens (Medzhitov and Janeway 1998; Medzhitov 2007b; Palm and Medzhitov 2009; Vivier and Medzhitov 2016). The major differences are related to how the systems develop their recognition repertoire (Medzhitov and Janeway 1997; Palm and Medzhitov 2009; Medzhitov 2007a; 2007b).

The innate immunity is the first-line of host defense, the response is virtually immediate, and works without former exposure (Medzhitov and Janeway 1997; 1998; Hoffmann et al 1999; Kimbrell and Beutler 2001; Medzhitov 2007a; 2007b; Palm and Medzhitov 2009; Vivier and Medzhitov 2016). Innate immune response works via the pattern recognition repertoire detection, through the pattern recognition receptors (PRR) (Hoffmann et al 1999; Kimbrell and Beutler 2001; Medzhitov 2007a; 2007b; Delbridge and O´Riordan 2007; Palm and Medzhitov 2009).

The PRR are a limited set of germline-encode receptors that can detect a big number of molecules that have a typical structural motif or pattern shared by classes of microorganisms (Medzhitov and Janeway 1997; 1998; Kimbrell and Beutler 2001; Kabelitz and Medzhitov 2007; Medzhitov 2007a; 2007b; Palm and Medzhitov 2009; Vivier and Medzhitov 2016). These pattern molecules are also named Pathogen-Associated Molecules (PAMPs), however they are not only preset on pathogenic microorganisms (Medzhitov 2007b). Besides, the innate immunity has appeared prior to the separation of vertebrates and invertebrates and most of multicellular organisms rely entirely on it (Kimbrell and Beutler 2001).
The adaptive immune response, on the other hand, is present only in vertebrates (Medzhitov and Janeway 1997; 1998). The adaptive immunity relies on somatically generated antigen receptors that are clonally expressed (Medzhitov and Janeway 1997; 1998). The receptors are highly specific and randomly generated (Palm et al

2009). It evolved to be able to express a huge array of recombinant receptors with apparently limitless possibilities of specificity (Medzhitov and Janeway 1997; 1998; Kimbrell and Beutler 2001; Cooper and Alder 2006; Medzhitov 2007b; Vivier and Medzhitov 2016). The receptor activates the effectors mechanisms in a challenge-specific manner and offers long-term protection, although the response takes days or weeks to reach the level of maximum efficacy (Kimbrell and Beutler 2001; Kurtz and Armitage 2006; Kabelitz and Medzhitov 2007; Medzhitov 2007b; Chaplin 2010). There is a crosstalk between innate and adaptive immunity, with the innate immunity playing a role on the control of adaptive immunity (Kabelitz and Medzhitov 2007; Iwasaki and Medzhitov 2015).

5.1. Immunity in sponges

Findings on the comparative immunology research field corroborate the importance of understand the molecular and functional characteristics of the immune systems on many different organisms (Flanjnik and Pasquier 2004). Genes related to the innate immunity tend to be conserved in metazoans (van der Burg et al 2016). Therefore, the phylogenic position of Porifera as a sister clade of Eumetazoa can help to understand evolutionary mechanisms related to innate immunity (Wiens et al 2005; 2007; Gauthier et al 2010; Yuen et al 2014; Feuda et al 2017). Several proteins associated to self and non-self in deuterostomian, have also been described in sponges (Müller et al 1999a; Srivastava et al 2010; Riesgo et al 2014; Guzman and Conaco 2016).

Sponges depend on cell aggregation and allorecognition properties to maintain tissue integrity (Blumbach et al 1999; Müller et al 1999a; Gauthier and Degnan 2008; Guzman and Conaco et al 2016). Poriferan possesses cell-cell and cell-matrix adhesion systems (Pancer et al 1996; 1997a; 1998; Müller 1997; Müller et al 1999b; Fernàndez-Busquets and Burger 1999; Srivastava et al 2010; Leys and Hill 2012; Grice et al 2017; Schippers and Nichols 2018).

On the cell-cell adhesion system the intercellular Aggregation Factor (AF) is a mediator of cell recognition, binding the Aggregation Receptor (AR) that is inserted into the plasma membrane to one galectin molecule in the presence of Ca^{2+}, and a second galectin molecule to the first (Müller 1997; Fernàndez-Busquets and Burger 1999; Müller et al 1999c). The AFs are very different

between for different species; two sponge species do not have an equal AF repertoire or domain organization (Grice and Degnan 2017). The AFs carry features of allorecognition molecules as well, which induce a downstream reaction (Müller et al 1999a; 1999c; Müller et al 2002; Müller and Müller 2003a; Grice et al 2017).

Molecules involved on histocompatibility response of sponges were studied through autograph/allograph transplantation, as well at a cellular level using mixed sponge cell reaction (Müller et al 1999a; 1999e; Müller et al 2002; Grice and Degnan 2017). A series of chemokines, cytokines and molecules involved on host and graft interaction have also been reported (Müller et al 2000; 2003; 2009b) such as Allograft Inflammatory Factor-1 (Kruse et al 1999; Müller et al 1999a; 1999c; 1999e; 2002; Müller and Müller 2003a), glutathione peroxidase (Kruse et al 1999), endothelial-monocyte-activating polypeptide (Pahler et al 1998), pre-B colony enhencing factor (Müller et al 1999e), leukotrin B4 (Wiens et al 2000a) and phenylalanine hydroxylase (Wiens et al 1998).

Since sponges are surrounded by microorganism that can be symbionts, parasites, pathogens or food source to them (Hentschel et al 2012), sponges require a versatile mechanisms of defense (Hentschel et al 2012). Moreover, families of pattern recognition receptors have been described in sponges (Wiens et al 2007; Müller and Müller 2007; Srivastava et al 2010; Riesgo et al 2014; Guzman and Conaco 2016; Ryu et al 2016; Webster and Thomas 2016) such as the scavenger receptors (Pancer 1997b; Blumbach et al 1998; Müller et al 1999b; Srivastava et al 2010; Guzman and Conaco 2016; Ryu et a 2016), and the Nucleotide Oligomers Domain (NOD)-Like Receptor (NLR) encoding genes, which contains a NACHT domain in combination with leucine-rich repeatitions that have been described on *A. quenslandica* genome in a high amount (Srivastava et al 2010; Yuen et al 2014; Degnan 2015; Ryu et a 2016; Webster and Thomas 2016). Lectin family proteins (Schröder et al 2003; Gardères et al 2015a; 2016) and manose-banding associated serine protease, which activates lectin complement pathway (Riesgo et al 2014) have also been reported. Additionally, the Toll-Like Receptor (TLR) and Interleukin Receptor 1 (ILR-1) pathways proteins, as Myeloid Differentiation Primary Response 8 (MyD88) Kappa-Light-Chain-Enhancer of Activated B Cells (NF-kB), the Interleukin Receptor-Associated Kinase 1/4 (IRAK

1/4), TGF- Activated Kinase (TAK-1), the Tumor Necrosis Factor (TNF) Receptor-Associated Factors (TRAF), the Interferon Regulatory Factor (IRF), and the TNF superfamily have also been reported (Wiens et al 2005; 2007; Gauthier et al 2010; Riesgo et al 2014; Pozzolini et al 2016; Ryu et al 2016).

Other proteins related to host defense mechanisms that have also been described include (2'-5') oligoadenylate synthetase (Wiens et al 1999; Grebenjuk et al 2002), (1→3) -β-D-glucan (Perović-Ottstadt et al 2004), alpha2-macroglobulin (Riesgo et al 2014), *Ascaris suum* Antibacterial Factor (ASABF) (Wiens et al 2011), guanylate-binding proteins 1 (Ryu et al 2016) and aquaporin (Müller et al 2009a).

As filter feeders, sponges are in contact with a huge amount of bacteria existing in the surrounding aqueous milieu (Wiens et al 2005; Hentschel et al 2012). This raises the possibility that perhaps they may suffer microbial infections, such as gram-positive and gram-negative bacteria, which can cause disintegration of fibers and tissues, and even cause death (Webster et al 2002; Taylor et al 2007; Müller et al 2009b). Studies carried to evaluate the immunity pathways activated in response to infections have shown that sponges react differently to commensal and opportunistic bacteria, and also to gram-positive and gram-negative bacteria (Böhm et al 2001; Schröder et al 2003; Thakur et al 2003; 2005; Wiens et al 2005; Müller et al 2009b; Gardères et al 2015b).

Some of the proteins and pathways described above play a role on bacterial response, which is the case of TLR and interleukin 1 (Wiens et al 2005; 2007; Müller et al 2009b; Gauthier et al 2010), MAPK, JNK, macrophage expressed gene 1, perforin-like molecule, adaptor gene (AdaPTin 1) and lysozyme (Böhm et al 2000; 2001; 2002; Schröder et al 2003; Thakur et al 2003; 2005; Wiens et al 2005; Müller et al 2009b). Besides, sponges use also chemical strategies to control infections, producing a variety of bioactive compounds (Wiens et al 2003a; Müller and Müller 2003a; Müller et al 2004b; 2004c; 2004d; Schröder et al 2006; Blunt et al 2013; He et al 2017).

6. Metazoan apoptosis

Cell death is a basic cellular response, that is triggered either via Accidental Cell Death (ACD) or via Regulated Cell Death (RCD), also generally referred on as

programmed cell death (PCD) (Ashkenazi and Salvesen 2014; Fan et al 2018; Galluzzi et al 2014; 2016).

The ACD is a result of critical damage that is uncontrolled and often harmful to the organism (Galluzzi et al 2014; 2016). The PCD is mediated through a tightly regulated intracellular program that follows the activation of specific molecular mechanisms (Degterev and Yuan 2008; Fuchs and Steller 2011; Ouyang et al 2012; Ashkenazi and Salvesen 2014; Galluzzi et al 2014; 2016; Fan et al 2018). Different types of programmed cell death have been described such as apoptosis, autophagic cell death, pyroptosis and necroptosis (Venderova and Park 2012; Fearnhead et al 2017; Fan et al 2018; Heneka et al 2018).

According to Ashkenazi and Salvesen 2014 (see also Lemasters 2018) PCD is mainly carried out by apoptosis. Apoptosis plays a role in embryogenesis, development, aging, and homeostasis mechanism as well as on immune reactions (Elmore 2007; Hedrick 2010; Miura 2011). Problems on apoptosis regulation mechanisms and pathways are also associated with many diseases such as autoimmune disorders, immunodeficiency, inflammation, cancer, neurodegenerative diseases, and diabetes (Ekert and Vaux 1997; Favaloro et al 2012; Kaczanowski 2016; Hetz and Saxena 2017; Gupta et al 2018).

Apoptosis can be triggered through intrinsic or extrinsic pathways (Jeng et al 2018). Both pathways activate the cysteine proteases of the caspase family that are mediators and executors of apoptosis, which then leads to the final phase of cell apoptosis where the cells present altered morphological and biochemical features, such as chromatin condensation, internucleosomal DNA degradation, cell shrinkage, formation of numerous small surface blebs (zeiosis), and phosphatidylserine externalization on the plasma membrane (Lemaster 2005; 2018; Galluzzi et al 2016; Bell and Megeney 2017; Jeng et al 2018).

The apoptotic extrinsic pathway (Fig. 5) is initiated by the activation of the cell surface death receptors (e.g. First Apoptosis Signal Receptor (FAS), (TNF) receptor superfamily member 1A receptors), after binding of the cognate ligands (Galluzzi et al 2018; Jeng et al 2018). The death receptors ligation triggers the intracellular adaptor proteins like FAS-Associated Death Domain (FADD) that dimerizes with procaspase 8 building the Death-Inducing Signaling Complex (DISC) (Ashkenazi and Salvesen 2014; Galluzzi et al 2018; Jeng et al 2018).

When the DISC complex is formed it triggers the auto-activation of procaspase 8, the now active caspase 8 directly activates the effectors caspase 3 and 7, which consequently causes apoptosis (Ashkenazi and Salvesen 2014; Galluzzi et al 2018; Jeng et al 2018). Besides, the caspase 8 (see Fig. 5) also controls the proteolytic cleavage of BH3 Interacting Domain Death Agonist (Bid) toward truncated (tBid) (Choi 2018; Jeng et al 2018). The tBid induces the oligomerization of BAX (BCL-2-Associated X Protein) and BAK (BCL-2 Antagonist Killer), activating BAX/BAK-dependent Mitochondrial Outer Member Permeabilization (MOMP), linking the extrinsic pathway and the intrinsic mitochondrial apoptosis pathways (Westphal et al 2011; 2014; Suhaili et al 2017; Jeng et al 2018). The MOMP (see Fig. 5) allows the release of Cytochrome c (Cyt-c) and Second Mitochondria-Derived Activator of Caspases (SMAC) from the mitochondrial intermembrane space to the cytosol (Verhagen et al 2000; Galluzzi et al 2008; Gyrd-Hansen 2018; Jeng et al 2018). On cytosol, Cyt-c connects with Apoptotic Protease Activating Factor 1 (Apaf1) and caspase 9 to form the apoptosome (Zhang et al 2015; Gyrd-Hansen 2018; Galluzzi et al 2018). Consecutively, the active caspase 9 triggers caspase 3 and 7 activation, inducing apoptosis (Suhaili et al 2017; Galluzzi et al 2018; Jeng et al 2018). The SMAC protein sequesters X-Linked Inhibitor of Apoptosis (XIAP), therefore promoting the activation of effector caspase (caspase 3 and 7), which also leads to apoptosis (Deveraux and Reed 1999; Ashkenazi and Salvesen 2014; Suhaili et al 2017; Galluzzi et al 2018).

The induction or inhibition of the apoptotic mitochondrial event is finely regulated by several positive and negative regulators, among which the proteins of the B-cell Lymphoma 2 (BCL-2) family have a crucial role (Elmore 2007; Westphal et al 2011; 2014; Czabotar et al 2014; Galluzzi et al 2014; 2018; Pihán et al 2017).

The intrinsic pathway of apoptosis (see Fig. 5) can be triggered by a huge number of intracellular perturbations of the cell homeostasis such as DNA damage, viral infections, oxidative stress, cytosolic Ca^{+2} overload, accumulation of unfolded proteins in the endoplasmic reticulum, replication stress, microtubular alterations, among others (Lemaster 2005; Ashkenazi and Salvesen 2014; Pihán et al 2017; Galluzzi et al 2012; 2014; 2016; 2018).

Upon sensing suitable apoptotic stimuli, the BH3-only proteins (BH3s), that are part of the BCL-2 family of proteins, become active by transcriptional and post-

translational mechanisms (Du et al 2011; Moldoveanu et al 2014; Birkinshaw and Czabotar 2017). The BH3s proteins induce the homo-oligomerization of BAX and BAK initiating MOMP, driving to apoptosis (Du et al 2011; Birkinshaw and Czabotar 2017; Suhaili et al 2017; Jeng et al 2018).

The proteins that compose the mammalian BCL-2 family have homologies at the structural and sequence levels (Czabotar et al 2014). They share one or more regions of the BLC-2 sequence homology (BH) domains: BH1, BH2, BH3 and BH4 (Birkinshaw and Czabotar 2017; Galluzzi et al 2018; Saidak et al 2018). Functionally, the BCL-2 family proteins are divided on pro-survival or pro-apoptotic (Czabotar et al 2014; Birkinshaw and Czabotar 2017; Galluzzi et al 2018; Saidak et al 2018;). The pro-survival members can inhibit apoptosis by blocking pro-apoptotic proteins, consequently inhibiting MOMP (Birkinshaw and Czabotar 2017). They either bind to the BH3 domain from pro-apoptotic BH3-only proteins or bind to a pro-apoptotic effector protein (BAK and BAX) (Birkinshaw and Czabotar 2017).

The BCL-2 pro-apoptotic family is divided in activator or sensitizer, which is established according to their mechanism action (Birkinshaw and Czabotar 2017). The activators are able to activate BAX and BAK by physically interaction, inducing homo-oligomerization of BAX and BAK, which leads first to MOMP and consequently to apoptosis (Moldoveanu et al 2014; Birkinshaw and Czabotar 2017; Galluzzi et al 2018). The activators of BH3s includes BCL-2 interacting mediator of cell death (Bid), BCL2-Interacting Mediator of Cell Death)-Dependent of Triggering Apoptosis, II (BIM), p53 up-regulated modulators of apoptosis (Puma) and Noxa (Du et al 2011; Moldoveanu et al 2014; Birkinshaw and Czabotar 2017; Saidak et al 2018). The sensitizers works in a different way, interacting only with pro-survival proteins by blocking their activity (Moldoveanu et al 2014; Birkinshaw and Czabotar 2017). Furthermore, DNA damage leads to activation of the p53 nuclear transcription factor which induces the expression of genes involved in apoptosis and/or cell-cycle arrest especially the pro-apoptotic Puma, Noxa and Bid (Haupt et al 2003; Lemaster 2018).

Perturbations in ER homeostasis, oxidative stress as well as unfolding protein response can also lead to apoptosis (Hetz and Saxena 2017; Hetz and Papa 2018). The calcium accumulation in the cytosol, induced by ER

perturbations, can be absorbed by the mitochondria inducing Ca^{2+} dependent Mitochondrial Permeability Transition (MPT) (Lemaster et al 2005; 2018; Darling and Cook 2014; Görlach et al 2015). The MPT prompts dissipation of the mitochondrial membrane potential and osmotic swelling of the mitochondrial matrix. When the surface area of the inner membrane overreaches the outer membrane the MPT then leads to MOMP (Song et al 2011).

The UPR also promotes apoptosis via different pathways (see Fig. 5), which is the case of Inositol-Requiring Enzyme 1 (IRE1) that associates with TNF Receptor-Associated Factor 2 (TRAF2) and activates caspase 12, that consequently activates caspase 3 and 7 leading to apoptosis (Lemaster et al 2005; 2018; Hetz and Saxena 2017; Pihán et al 2017; Hetz and Papa 2018). The IRE1/TRAF2 association can activate Jun N-terminal kinase (JNK) as well, which triggers MPT (Lemaster et al 2005; 2018; Perri et al 2016; Sarvani et al 2017). Moreover, during UPR the activation of IRE1 and PERK (PKR-like Endoplasmic Reticulum Kinase) receptors, induces the expression of CCAAT/ Enhancer-Binding Protein Homologous Protein (CHOP) that triggers MPT (Lemaster et al 2005; 2018; Pihán et al 2017; Hetz and Papa 2018). The CHOP protein is involved on the expression of pro-apoptotic proteins of the BCL-2 family as well, such as Noxa, BIM, Puma (Perri et al 2016; Pihán et al 2017; Sarvani et al 2017; Hetz and Papa 2018).

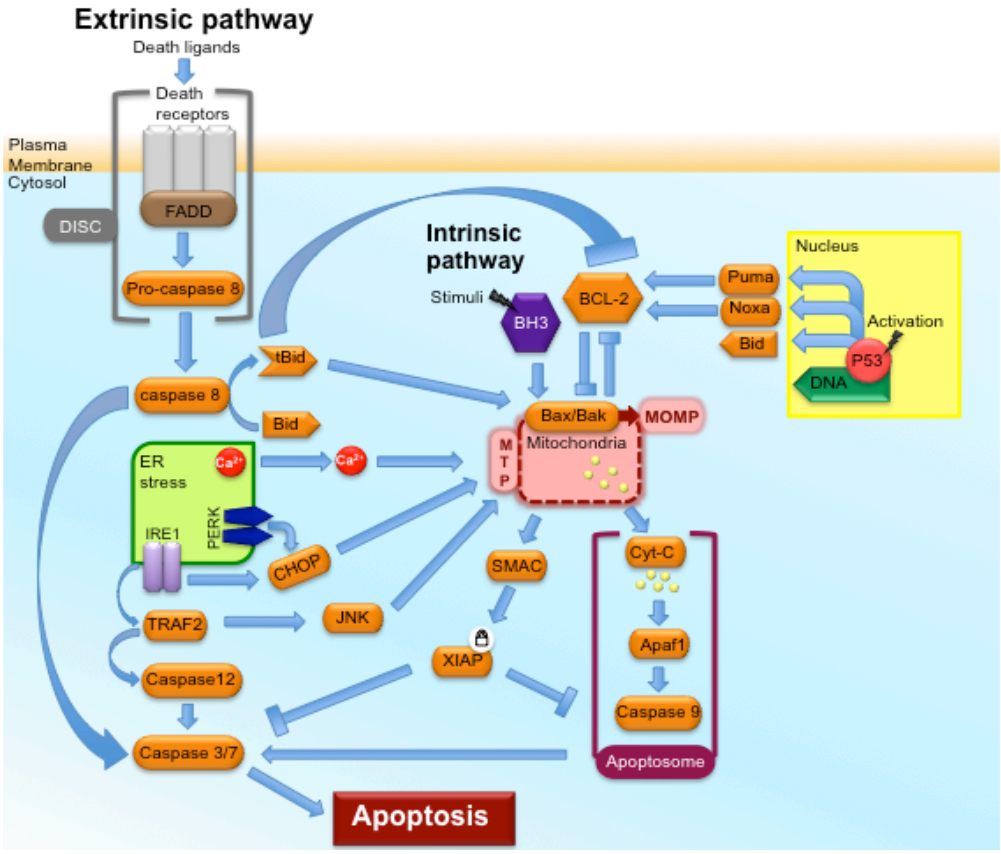

Figure 5: Schematic of the extrinsic, intrinsic and ER stress induced pathways of apoptosis. For a better overview not all the pathways were described. The death ligands activate the death receptors and trigger the dimerization FAS-Associated Death Domain (FADD) and procaspase 8, forming the Death-Inducing Signaling Complex (DISC), then caspase 8 directly activates the effectors caspase 3 and 7, inducing apoptosis (Ashkenazi and Salvesen 2014; Galluzzi et al 2018; Jeng et al 2018). Besides, caspase 8 also controls the proteolytic cleavage of BH3 Interacting Domain Death Agonist (Bid) toward Truncated Bid (tBid) (Jeng et al 2018, Choi 2018). The tBid blocks pro-survival B-Cell Lymphoma 2 (BCL-2) proteins (Westphal et al 2011; Ashkenazi and Salvesen 2014; Jeng et al 2018). Moreover, the tBid induces the oligomerization of BCL-2-Associated X Protein (BAX) and BAK (BCL-2 antagonist killer), activating BAX/BAK-dependent Mitochondrial Outer Member Permeabilization (MOMP) (Suhaili et al 2017; Westphal et al 2011; 2014; Jeng et al 2018). The MOMP allows the release of Cytochrome c (Cyt-c) and Second Mitochondria-Derived Activator of Caspases (SMAC), the Cyt-c connects with apoptotic protease activating factor 1 (Apaf1) and caspase 9 to forming the apoptosome (Verhagen et al 2000; Galluzzi et al 2008; 2018; Zhang et al 2015; Gyrd-Hansen 2018; Jeng et al 2018). Consecutively, the activated caspase 9 triggers caspase 3 and 7 activation, inducing apoptosis (Suhaili et al 2017; Jeng et al 2018; Galluzzi et al 2018). The SMAC protein sequesters X-Linked Inhibitor of Apoptosis (XIAP), therefore allowing the activation of effector caspase (caspase 3 and 7), which also leads to apoptosis (Deveraux and Reed 1999; Ashkenazi and Salvesen 2014; Suhaili et al 2017; Galluzzi et al 2018). Furthermore, the activation of p53 nuclear transcription factor induces the expression of the pro-apoptotic subset of the BCL-2 family genes, as p53 up-

regulated modulators of apoptosis (Puma), Noxa and Bid (Haupt et al 2003; Lemaster 2018). The intrinsic pathway of apoptosis is activated when BH3-only proteins (BH3s) senses apoptotic stimuli (Jeng et al 2018). The BH3s become active and induce the homo-oligomerization of BAX and BAK initiating MOMP (Du et al 2011; Moldoveanu et al 2014; Birkinshaw and Czabotar 2017; Suhaili et al 2017; Jeng et al 2018). Moreover, ER stress can induces calcium release, thereby the absorption may induce Ca^{2+} dependent Mitochondrial Permeability Transition (MPT), them drives to MOMP (Lemaster et al 2005; 2018; Song et al 2011; Darling and Cook 2014; Görlach et al 2015; Hetz and Papa 2018). Besides, during acute or chronic ER stress the UPR (unfolding protein response) promotes apoptosis via different pathways (Lemaster et al 2005; 2018; Hetz and Papa 2018). Which in the case of Inositol-Requiring Enzyme 1 (IRE1) it associates with Tumor Necrosis Factor Receptor-Associated Factor 2 (TRAF2), then activates caspase 12, it activates caspase 3 and 7 leading to apoptosis (Lemaster et al 2005; 2018; Hetz and Saxena 2017; Pihán et al 2017; Hetz and Papa 2018). The IRE1/TRAF2 association can activate Jun N-Terminal Kinase (JNK) as well, which triggers MPT (Lemaster et al 2005; 2018; Perri et al 2016; Sarvani et al 2017). Moreover, during UPR the activation of IRE1 and (PKR)-Like Endoplasmic Reticulum Kinase (PERK) receptors, induces the expression of CCAAT/ Enhancer-Binding Protein homologous protein (CHOP) that triggers MPT (Lemaster et al 2005; 2018; Pihán et al 2017; Hetz and Papa 2018).

6.1. Apoptosis in Porifera

Several components of the apoptosis machinery have been identified on sponges (Wiens and Müller 2006), such as the proteins from the BCL-2 family, both pro-survival and pro-apoptotic, among others (Wiens et al 2000a; 2000b; 2001, 2003b; 2004; 2005; 2006; Wiens and Müller 2006; Caria et al 2017; Kenny et al 2018). It has been identified in *Geodia cydonium* (*G. cydonium)* and *S. domuncula* molecules with BCL-2 homology proteins regions BH1 and BH2 (Wiens et al 2000b; 2001). Besides it was shown that *G. cydonium* BCL-2 homolog protein was able to protect mammalian cells against apoptosis (Wiens et al 2001).

Furthermore, the study of Caria et al (2017) evaluated the structural binding mechanisms of pro-survival BCL-2 and pro-apoptotic BCL-2 of sponge *Lubomirskia baicalensis* (*L. baicalensis).* They demonstrated that the BHP2 motif of LB-BCL-2 is able to bind the BH3 motif of LB-Bak-2 with high affinity (Caria et al 2017). These results indicate that the molecular mechanism used by BCL-2 to mediated apoptosis are evolutionary ancient and resemble the roles of mammalian BCL-2 proteins (Wiens et al 2000b; 2001; Wiens and Müller 2006; Caria et al

2017).

A pro-apoptotic protein named DD2 was also identified in Porifera, this protein has high sequence homology to human FAS and FADD (Wiens et al 2000a; 2000b; Wiens and Müller 2006). Although, this protein contains two death domains, which is a characteristic uncommon to any other know protein of TNF signaling pathway (Wiens et al 2000a).

Several caspase-like proteins have also been identified in sponges (Wiens et al 2003b; Wiens and Müller 2006; Luthringer et al 2011; Kenny et al 2018). The caspases have a well know apoptotic function and also play roles on inflammation, genomic stability, metabolism, autophagy and aging (Shalini et al 2015).

The mechanisms of apoptosis have been studied in sponges on many different conditions such as development, body plan, cell-turnover, feeding, regeneration mechanism and immunity (Müller and Müller 2003b; Wiens et al 2006; Wiens and Müller 2006; De Goeij et al 2009; Martinand-Mari et al 2012; Conaco et al 2012b; Kenny et al 2018).

Furthermore, the phylogenetically position of sponges as oldest Metazoan make then an interesting model to study the evolution of apoptosis mechanisms and its key elements (Wiens 2000b; 2001; Wiens and Müller 2006). In addition to that, more knowledge on the evolution mechanisms of apoptosis can contribute to a better understanding of the imbalance on apoptosis mechanisms that are present on many diseases (e.g. cancer, neurodegenerative disorders, ischemia, heart failure, auto immune disorders, diabetes mellitus (Elmore 2007; Favoloro et al 2012; Zmasek and Godzik 2013; Anuradha et al 2014; Kaczanowski 2016).

D. AIM OF THE STUDY

The mesencephalic astrocyte-derived neurotrophic factor (MANF) together with cerebral dopamine neurotrophic factor (CDNF) compose a family of evolutionary conserved neurotrophic factors. Previous studies have identified MANF in vertebrates as well as in invertebrates, such as human, mouse, *D. melanogaster* and *C. elegans.* MANF is involved in a broad range of activities in neuronal and non-neuronal tissues. It promotes the survival of dopaminergic neurons and is a protective factor against ER stress. However, the functional mechanism of MANF is still not fully understood yet.

Sponges (Phylum Porifera) are at the base of the animal tree of life, and therefore offer a unique vantage point to study the evolution of molecular pathways. Furthermore, several components of apoptosis and innate immunity pathways have already been described in sponges. Even though sponges have no neuronal cells or a nervous system, molecular components of the conventional metazoan nervous system (such as protosynaptic proteins) have been identified in sponges. These unique characteristics offer an enticing opportunity to explore the evolutionary aspects and ancient functional roles of such molecules.

The aims of the present study are to identify a MANF homolog in the marine sponge *Suberites domuncula* (SDMANF), and to evaluate its function in an Evolutionary ancient model organism that lacks a conventional neuronal system.

To achieve that, the complete DNA/protein sequence of MANF needed to be acquired followed by sequence characterization and structural analyses for the presence of MANF/CDNF family specific features. To study the functions of poriferan MANF, the SDMANF protein need to be detected and localized in sponge tissue. For that purpose, an antibody should be developed.

Moreover, to evaluate the functional roles of SDMANF, the protein should be stably transfected in mammalian cells to assess protein expression, secretion, localization and function such as the previously described protective activities against apoptosis induced by certain stressors.

The results of this study can help establishing the evolutionary conserved role of MANF in pathways of apoptosis and immunity.

E. MATERIAL AND METHODS

1. Animal model

Suberites domuncula (Olivi, 1792)

Systematic

Kingdom: Animalia

Phylum: Porifera

Class: Demospongiae

Order: Hadromerida (Topsent, 1894)

Family: Suberitidae (Schimidt, 1870)

Genera: *Suberites* (Nardo, 1833)

Specie: *Suberites domuncula*

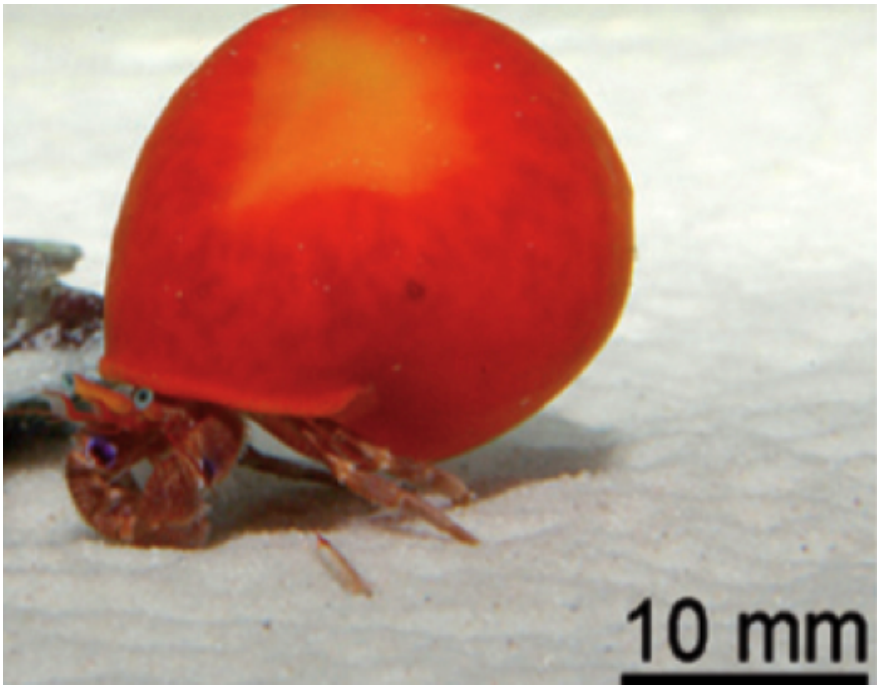

Figure 6: Photo of *Suberites domuncula* (Olivi, 1792). Reproduced from Schröder et al 2008 with permission from The Royal Society of Chemistry.

The genus *Suberites* is cosmopolitan, although most common in cold water. (Hooper and van Soest 2002). They are able to survive in sediment environments or rooting stalks, as well as living on gastropod´s shell (Hooper and van Soest 2002). They are often massive lobate or spherical sponges, usually presenting a

velvety mooth surface and compressible skeleton (Hooper and van Soest 2002). Most *Suberites* species are bright orange colored, sometimes mottled with brown, red or bluish spots (Hooper and van Soest 2002). *Suberites domuncula* (Fig. 6) reproduces asexually by gemules, which are in general deposited on gastropod shells. This is similar to some freshwater sponges, although *S. domuncula* gemules are structurally simpler (Hooper and van Soest 2002).

1.2 *Suberites domuncula* in captivity

Living *S. domuncula* specimens were collected by scuba diving from depths ranging from 10 to 30 meters near Rovinj (North Adriatic Sea, Croatia). The collection expeditions were done in partnership with the Center for Marine Research (CMR) of the Ruđer Boškovic.

The sponges were brought to Mainz and kept in a 200 l salt-water aquarium at 16°C to 18°C under controlled aeration. Aquarium salinity balance was kept with artificial salt (Tropic Marin™). Aquarium water was supplemented with commercial NutriMarine™ (GroTech) and Artemia™ (Amtra) was used to feed the hermit crabs, on whose shells the sponges live.

2. Materials

2.1. Chemicals and ready solutions

4-Nitro blue tetrazolium chloride / 5-bromo-4-chloro-3-indolyl-phosphate, 4-toluidine salt (NBT/BCIP) solution	Roche, Mannheim
Acetone	Roth, Karlsruhe
Agarose	Roth, Karlsruhe
Albumin bovine fraction V	Roth, Karlsruhe
Ammonium persulfate	Sigma-Aldrich, Darmstad
Blocking reagent	Roche, Mannheim
Brefeldin A (BFA)	Sigma-Aldrich, Darmstad
Bromophenol blue sodium salt	Serva, Heidelberg
Cadmium ($CdCl_2$) 50 µM	Sigma-Aldrich, Darmstad
Dimethyl sulfoxide (DMSO)	Sigma-Aldrich, Darmstad

Dithiothreitol solution (DTT)	Sigma-Aldrich, Darmstad
DNA (desoxyribonucleic acid) loading dye 6X	Fermentas, St. Leon-Rot
DRAQ5™	Thermo Scientific, Schwerte
Ethanol	Roth, Karlsruhe
Ethidium bromide (EtBr)	Boehringer, Mannheim
Fetal bovine serum (FBS)	Life Technologies, Darmstad
Floromount™ antifade mounting medium	Sigma-Aldrich, Darmstad
Formamide	Sigma-Aldrich, Darmstad
Gel code™ blue safe	Thermo Scientific, Schwerte
Glycerol	AppliChem, Darmstad
Goat serum	Sigma-Aldrich, Darmstad
Imidazole ($C_3H_4N_2$)	Roth, Karlsruhe
Isopropanol	AppliChem, Darmstad
Isopropyl-β-D-thiogalactoside (IPTG)	Roth, Karlsruhe
L-Arabinose	Roth, Karlsruhe
Lipopolysaccharides (LPS) from Escherichia coli 026:B6	Sigma-Aldrich, Taufkirchen
Milk powder	Roth, Karlsruhe
Paraformaldehyde (PFA)	Sigma-Aldrich, Darmstad
Potassium chloride (KCl)	Roth, Karlsruhe
Potassium dihydrogen phosphate (KH_2PO_4)	Roth, Karlsruhe
Roti-Load™ 1	Roth, Karlsruhe
Roti-Phorese™ 10X tris-borate-EDTA (TBE) buffer	Roth, Karlsruhe
Saccharose	Roth, Karlsruhe
Sheep serum	Sigma-Aldrich, Darmstad
Sodium chloride (NaCl)	Roth, Karlsruhe
Sodium hydrogen phosphate (Na_2HPO_4)	Roth, Karlsruhe
Trichloroacetic acid (TCA)	MERCK, Darmastad
Tris (2-carboxyethyl) phosphine (TCEP)	Roth, Karlsruhe
Tris ($C_4H_{11}NO_3$)	Roth, Karlsruhe
Triton X-100	Sigma-Aldrich, Darmstad

Tween 20	Sigma-Aldrich, Darmstad
Urea (CH_4N_2O)	Roth, Karlsruhe
Xylene cyanol FF	Sigma-Aldrich, Darmstad

2.2. Consumables

Used consumables such as Parafilm™, disposable pipettes, disposable pipette tips, sterile scalpels, and syringe filters were purchased from Roth (Karlsruhe). Centrifuge tubes of 15 ml and 50 ml volumes, petri dishes, pipette filtered tips, plastic disposable pipettes, and cell culture materials were bought from Greiner Bio-One (Frickenhausen). Syringes and needles from BD (USA) were used. Reaction tubes sizes 1.5 ml and 2 ml were acquired from Brand (Wertheim), and 0.2 ml and 0.5 ml tubes were obtained from Thermo Scientific (Schwerte).

2.3. Kits

7-Deaza-2′-deoxy-guanosine-5′-triphosphate (7-deaza-dGTP)	Sigma-Aldrich, Darmstad
E. coli Expression system with Gateway™ technology	Life Technologies, Darmstad
GF-AFC peptide substrate	Promega, Mannheim
High pure PCR product purification kit	Roche, Mannheim
High pure plasmid isolation kit	Roche, Mannheim
Lipofectamine™ 2000	Invitrogen, Karlsruhe
NucView™ 488 caspase 3 assay kit for live cells	VWR, Darmstad
Pierce™ 660nm protein assay kit	Thermo Scientific, Schwerte
Plasmid midi kit	Qiagen, Hilden
ProteoExtract™ Subcellular proteome extraction kit	Merck Millipore, Darmstad
pTrcHis TOPO™TA expression kit	Invitrogen, Karlsruhe
ReadyProbes Cell viability imaging kit	Thermo Scientific, Schwerte
SequaGel™ XR	National Diagnostics, Atlanta, USA
TC-FlAsH™ II In-cell tetracysteine tag	Life Technologies,

detection kit	Darmstad
Technovit 3040™	HeraeusKulzer, Wehrheim
Technovit 8100™	HeraeusKulzer, Wehrheim
TOPO TA cloning kit	Invitrogen, Karlsruhe

2.4. Commercial Buffers

DNA gel loading dye (6x)	Thermo Scientific, Schwerte
Dulbecco's phosphate buffered saline (PBS) 1X	Merck Millipore, Darmstad
M-PER™ Mammalian Protein Extraction Reagent	Thermo scientific, Schwerte
NuPAGE™ MOPS SDS running buffer (20X)	Invitrogen, Karlsruhe
3-(N-Morpholino) propane sulfonic acid MOPS, SDS	
Roti-Load™ 1-protein loading buffer	Roth, Karlsruhe
Roti-Phorese™ 10X TBE buffer	Roth, Karlsruhe
Tris-buffered saline (TBS) 20x	AppliChem, Darmstad
Tris-EDTA buffer (TE)	Life technologies, Darmstad
Trypsin-EDTA (0.05%)	Thermo scientific, Schwerte

2.5. Enzymes

DreamTaq™ Green PCR master mix (2x)	Thermo scientific, Schwerte
Gateway™ BP Clonase™ II enzyme mix.	Life technologies, Darmstad
Gateway™ LR Clonase™ II enzyme mix	Life technologies, Darmstad
PCR master mix (2x)	Fermentas, St. Leon-Rot
Proteinase K	Life technologies, Darmstad

2.6. Vectors

Gateway™ pcDNA™ 6.2/cTC-Tag-DEST vector	Life technologies, Darmstad
Gateway™ pDEST17™ vector	Life technologies, Darmstad
Gateway™ pDONR™ 221 vector	Life technologies, Darmstad

pCR™II-TOPO™ TA vector	Thermo scientific, Schwert
pTrcHis2™ TOPO™ TA vector	Thermo scientific, Schwert

2.7. Bacterial strains

BL21-AI™One Shot™ Chemically competent *E. coli*	Life technologies, Darmstad
BL21(DE3) pLysS, Singles™ chemically competent *E. coli*	Calbiochem, San Diego, USA
One Shot™ TOP10 Chemically competent *E. coli*	Life technologies, Darmstad
One Shot™ *ccd*B Survival T1^{R} chemically competent *E. coli*	Life technologies, Darmstad

2.8. Cell line

Homo sapiens HEK 293 hTLR4/MD2/CD14	InvivoGen, Toulouse, FR

2.9. Medium

DMEM (Dubelcco's modified Eagles medium) high glucose with stable glutamine	Merck Millipore, Darmstad
FluroBrite™ DMEM	Thermo Fisher Scientific, Schwerte
LB-Broth (Luria/Miller)	Roth, Karlsruhe
LB-Broth (Luria/Miller) Agar	Roth, Karlsruhe
Opti-MEM™	Invitrogen, Karlsruhe
S.O.C Medium	Life technologies, Darmstad

2.10. Antibiotics

Ampicillin	Roth, Karlsruhe
Blasticidin	InvivoGen, Toulouse, FR
Carbenicillin	Roth, Karlsruhe
Normocin	InvivoGen, Toulouse, FR

2.11. Antibodies

Anti-BAX	Santa Cruz Biotecnology, Heidelberg
Anti-His (C-term) AP conjugated antibody	Life technologies, Darmstad
Anti-rabbit-IgG- AP conjugated	Sigma-Aldrich, Taufkirchen
Anti-SDMANF raised in rabbit	Developed at the research group
Anti-V5 tag antibody	Life technologies, Darmstad
Anti-V5-Alkaline Phosphatase (AP) conjugated	Life technologies, Darmstad
Anti-α-tubulin	Abcam, Cambridge, UK
Cy™ 2-conjugated affiniPure F(ab´)$_2$ fragment goat anti-rabbit IgG	Jackson ImmunoResearch Cambridge, UK,

2.12. Markers

GeneRuler™ DNA ladder mix	Fermentas, St. Leon-Rot
Precision Plus Protein™ dual color standard	Bio-Rad, München
See Blue™ Plus 2 pre-stained protein standard	Life technologies, Darmstad

2.13. Instruments

Agarose gel electrophoresis device	Wide Mini-Sub™ Cell GT, Bio-Rad, München
Automated cell counter	Scepter 2.0, Merck Millipore, Darmstad
Automated protein purification system	Profinia, Bio-Rad, München
Automatic DNA sequenator	Li-Cor 4300, Bad Homburg
Centrifuge	Mini centrifuge: Spectrafuge, neoLab, Heidelberg Refrigerated centrifuge 5415R R, Eppendorf, Wesseling-Berzdorf

	Refrigerated centrifuge 5804 R, Eppendorf, Wesseling-Berzdorf
	Stand refrigerated centrifuge: Sorvall RC-5B, Firma Du Pont Instruments, USA
CO_2 incubator	Queue, NUNC, Wiesbaden
Dot-Blot device	Bio-Dot, Bio-Rad, München
Electronic scale	PB 300, Mettler-Toledo, Giessen
	Sartorius, Göttingen
Homogenization	Precellys ™24 Peqlab, Erlangen
Incubator with agitation system	WiseCube, Witeg, Wertheim
Laminar flow hood	Slee, BioNova, Roma (IT)
Live cell imaging system	JuLI™ Stage; VWR, Darmstad
Magnetic stir bars	Roth, Karlsruhe
Magnetic stirrer	Roth, Karlsruhe
Microscope	Digital, inverte fluorescente microscope: EVOS™fl, AMG, USA
Microtome	RM2145 Firma Leica, Wetzlar
Multichannel precision pipette200 µl	Gilson, Limburg
PCR thermocycler	PeqSTAR 2 x Gradient, Peqlab, Erlangen
PCR work station	Ultraviolet PCR Work station, Peqlab, Erlangen
pHmeter	Seven Compact, Mettler -Toledo, Giessen
Power-supply	Power Pac 2000, Bio-Rad, München
Precision pipette2/ 10/ 20/ 100/ 200/ 1000/ 5000 µl	Gilson, Limburg
Printer for agarose gels	P93, Mitsubishi Electrics, Ratingen
Scanner for documentation of gels	Odyssey, Li-Cor Biosciences, Bad Homburg

SDS-PAGE device polyacrylamide gel electrophoresis (PAGE)	XCell sure lock system, Life Technologies, Darmstad
Slide warmer	Guwina-Hofmann, Berlin
Spectrophotometer	Nanodrop2000, Peqlab, Erlangen Smartspec™ Plus, Bio-Rad, München Varioskan™ Flash Multi mode reader, Thermo scientific, Schwerte
Steam autoclave	DX-23, Systec, Wettenberg
Thermal block	Wealtec HB-1, Peqlab, Erlangen
Ultrasonicator	Sonifier Cell Disruptor B-12, Branson Ultrasonicator, Dietzenbach
UV-transilluminator	E-Box 1000, Peqlab, Erlangen
Vortex	Reax 2000, Heidolph, Lodz
Water bath	KottermanLabortechnick, Uetze
Western blot device	iBlot, Life Technologies, Darmstad

3. General Precautions

Molecular biological, microbiological and cell culture materials, as well as, laboratory equipment, solutions and supplies were sterilized by autoclaving. Autoclaving temperature was set to at least 121°C with 1 bar of pressure for 30 minutes. Demineralized water or double-distilled water (dd H_2O) was used in the preparation of buffers and solutions. Filtration techniques were applied to remove impurities, aggregates, or to complete solutions sterility when necessary. Filtration of larger volumes was performed on vacuum filtration bottle-top devices with sterile devices and membranes with a minimum porosity of 0.22 µm. In case of small volumes, the solutions were filtered through syringe filter units with variable membrane types and cutoffs. To avoid sample contamination – as well for self-protection purposes – latex disposable gloves were used. When dealing with more hazardous chemicals – such as ethidium bromide nitrile – disposable gloves were used. A DNase-free condition was applied while working with DNA. Proteins,

enzymes, and nucleic acids were always cooled worked and stored on ice.

4. Polymerase chain reaction methods

4.1. Primers generation

Primers (Oligolenucleotides) were designed with the online program Primer 3 and double-checked for hairpins and dimers with the program OligoAnalizer.
To design a primer a few rules are followed:

- Length should be between 18 to 25 nucleotides;
- Primer pairs (forward and reverse) should have about the same melting temperature (Tm). Tm= 4 x (G+C) + 2 x (A+T);
- Guanine-Cytosin (G+C) content should be about 50%;
- No self-compatibility, i.e. there must be no possibility to build primer-dimer or secondary structure;
- No palindrome sequence;
- When possible, five nucleotides G or C should be the end of the primer (3´-end) to ensure a tight binding.

The primers were ordered at Eurofins MWG, lyophilized. The Oligonucleotides were resuspended in diethyl pyrocarbonate treated water (DEPC H_2O) with the recommended volume of 100 pmol (stock solution) and then diluted 1:10 to prepare the working aliquots with 10 pmol/µl.

4.2 Polymerase chain reaction

The Polymerase Chain Reaction (PCR) is a technology developed by Kary Mullis (Mullis et al 1986, Mullis and Fallona 1987) that allows the amplification of a few copies of DNA into thousands of millions of copies (Kratz 2009). The specific region to be copied is defined by the pair of primers. Both primers need to be complementary to the region 3´, because that is the direction that the DNA polymerase needs to add the first nucleotide in order to make the elongation of the new sequence 5´-3´. One primer is designed to the sense strand of the DNA target (forward primer) and the other is designed to the antisense strand of the DNA target (reverse primer). A PCR requires several reagents to amplify the *DNA template*: a pair of primers, one DNA polymerase – such as Taq (*Thermus*

aquaticus) polymerase –, the Deoxynucleoside Triphosphates (dNTPs), a buffer solution that offers proper conditions, and bivalent cations. The PCR is made with the following basic steps, using different temperatures cycles:

1. An initial denaturation phase at 94°C to 95°C is done for two to five minutes to assure primer annealing and extension efficiency.
2. PCR Cycles (25x-35x) proceed as following:

   a. Denaturation: denaturation is done at temperatures between 94°C to 95°C for 20-30 sec, to induce the separation of the newly formed DNA dimmer.

   b. Primer annealing: primer annealing phase lasts for 20-30 sec at ideal temperature. This temperature is set by the melting temperature of the pair of primers used in the reaction.

   c. Primer extension: at 72°C DNA polymerase takes 45 sec to synthesize one kilobase (Kb) o the new DNA fragment. This is the last step of the cycle. The PCR have in general 25-35 cycles.
3. The last step is extension at 72°C for 5 to 15 min. This procedure is carried to complete extension of partial products and annealing of single-stranded complementary products.

4.2.1. Touchdown PCR

In a touchdown PCR program, the melting temperature for the primer annealing phase is slowly reduced during the course of PCR reaction. The PCR program begins using the primer calculated Melting Temperature (Tm) or even a bit higher Tm value. However, the melting temperature is not kept constant in all cycles, being slowly reduced instead. The temperature reduction procedure can be done by reducing a defined temperature once per second during the cycles or once per each cycle.

A touchdown PCR program takes advantage of the exponential characteristic of the PCR, since any difference in melting temperature between the correct and incorrect annealing will give an advantage of 2-fold per cycle, which helps amplifying the more specific DNA in less time-consuming adjustments (Don et al 1991).

4.2.2. Standard PCR program

The PCR program used in the present study was composed by an initial denaturation phase at 95°C for three minutes, followed by 35 primer extension cycles (Fig. 7). As previously stated, each cycle is composed of three phases: a) a denaturation phase at 95 °C for 30 sec; b) a primer annealing phase, 30 sec at the primer specific Melting Temperature (Tm), with a temperature reduction of 0.1°C per cycle; c) the last cycle phase is the extension at 72°C for two min. The ending step was a final extension at 72°C for 10 min.

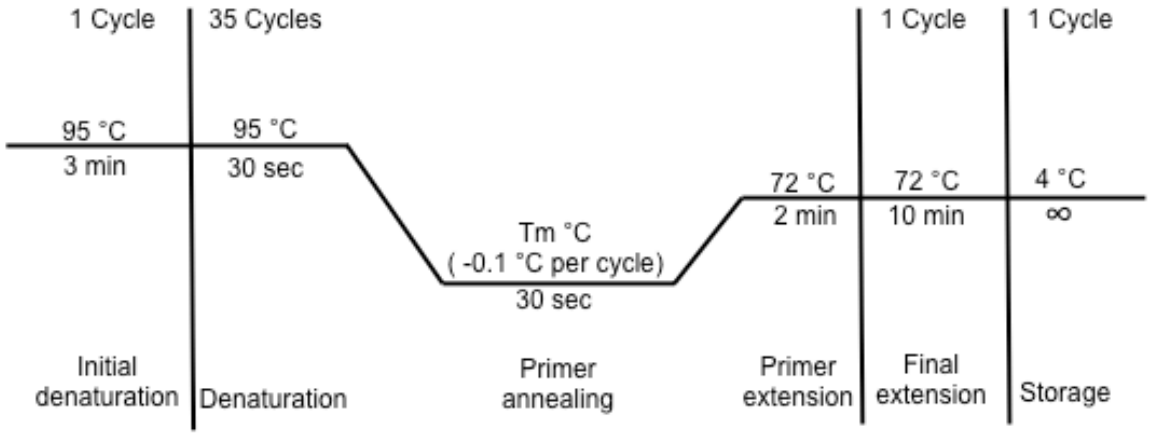

Figure 7: Schematic diagram of the PCR program used in the present study. Polymerase Chain Reaction (PCR) cycles, respective temperatures and duration of each phase are show. Tm, Melting Temperatures; sec, seconds; min, minutes, °C, Celsius grad, ∞ infinite.

4.2.3. PCR *S. domuncula* complementary DNA library

Polymerase chain reaction program used to obtain the DNA sequence of MANF from *Suberites domuncula* (SDMANF) through the *S. domuncula* complementary DNA library (cDNA). The PCR was executed with a denaturation step at 95°C for 5 min, sequenced by 35 amplification cycles: step 1) at 95°C for 25 s, step 2) Tm of 54°C for 45 s, step 3) 74°C for 1 min. The elongation step was done at 74°C for 10 min.

4.2.4. SDMANF gene specific PCR

The gene specific PCR was done with the PCR standard reaction and with the standard PCR program using the melting temperature of 58°C. A combination of cDNA, forward primer: 5−ATG GAG CTA AAG GTG TTA−3´ and reverse primer: 5´−AAG TTC TAC ATG TTG ATG CT−3´ was used to obtain the complete SDMANF ORF (nt 1-516, excluding the stop codon) (Sereno et al 2017).

4.2.5. PCR SDMANF recombinant protein expression in *E. coli*

The PCR of the complete SDMANF (ORF, nt_{1-516}, excluding the stop codon), for the expression in *E. coli* (vector pTrcHis2™), was done using the same specifications of the SDMANF gene specific PCR. To amplify by PCR the SDMANF fragment ($nt_{279-516,}$ aa_{72-172}) used for expression in *E. coli* (Gateway™pDONR™ 221 vector entry constructs and destination vector Gateway™pDEST17™), for later preparation of antiserum, a combination of *S. domuncula* cDNA forward primer: 5´−GGG GAC AAG TTT GTA CAA AAA AGC AGG CTT AAT GTC CTT CAG TAA GCC T−3´ and reverse primer: GGG GAC CAC TTT GTA CAA GAA AGC TGG GTA TTA AAG TTC TAC ATG TTG—3′ (attB1 and attB2 extension for integration into the entry vector pDONR21 are underlined respectively) were used. The PCR was carried out with standard condition and Tm 56°C (Sereno et al 2017).

4.2.6. PCR SDMANF recombinant protein expression in HEK cells

The complete ORF of SDMANF, including the Kozak translation initiation sequence with an ATG initiation codon and excluding the first stop codon, was amplified using the forward primer 5´−G GGG ACA AGT TTG TAC AAA AAA GCA GGC TTA ACC ATG GAG CTA AAG GTG TTA−3´ and the reverse primer 5´−G GGG ACC ACT TTG TAC AAG AAA GCT GGG TAA AGT TCT ACA TGT TGA TG−3´(attB1 and attB2 extension for integration into the entry vector pDONR21 are respectively underlined) (Sereno et al 2017).

4.3. Standard PCR reaction

The PCR standard reactions were done to a volume of 50 µl, using Fermentas™ PCR master mix (2x).

- 25 µl PCR master mix 1X
- 10 pmol forward primer (1µl of 10 pmol/µl)
- 10 pmol reverse primer (1µl of 10 pmol/µl)
- DNA 30 ng
- dd H_2O up to 50 µl

4.3.1. Checking PCR of bacterial colonies

The bacterial colonies were analyzed to verify if the cloned had the inserted DNA on the right direction. The primers pairs (forward and reverse primer) used in the reaction were a combination of one primer specific of the vector (the vector used in the cloning) and one gene specific primer.

The PCR reaction was done with Dream Taq™ master mix (2x). The reaction was scaled to a small volume (12.5 µl) per colony to be tested.

- 6.5 µl DreamTaq™ PCR master mix 1X
- 0.5 pmol forward primer (0.5 µl of 10 pmol/µl)
- 0.5 pmol reverse primer (0.5 µl of 10 pmol/µl)
- 0.5 µl DNA of bacterial colony culture
- dd H_2O up to 12.5 µl

4.4. PCR product purification

PCR products suitable for downstream applications were purified with high pure PCR product purification kit.

4.5. Agarose gel electrophoresis

The agarose gel matrix allows the separation of the DNA elements by size. Chosen gels were usually a 1% (weight/volume (w/v)) agarose in Tris-Borate-EDTA (TBE) buffer. Before loaded on the gel the PCR products were mixed with a DNA loading dye (GeneRuler™ DNA Ladder Mix) to make them visible during run, the exception being PCR products made with DreamTaq™, which were already conjugated with a loading buffer. A DNA molecular weight marker was used to allow the calculation of DNA fragments length. After the run, gels were stained on a bath of EtBr 1% (Volume/Volume (v/v)). The EtBr fluoresces under UV light,

intercalating the DNA base pairs allowing visualization. The gels were photographed for documentation.

4.5.1. DNA isolation from agarose gel

DNA target bands were excised from the gels when suitable for a downstream application. The excised bands were purified with high pure PCR product purification kit.

Gel DNA 6x loading Dye	**Rotiphorese™ 10x TBE-Buffer**
10 mM tris-HCl, pH 7.6	1 M tris-HCl, pH 8.3
0.03% (w/v) bromophenol blue	20 mM EDTA
0.03% (w/v) xylene cyanol FF	in ddH_2O
60% (v/v) glycerol 60 mM EDTA	

4.6. Measurements of concentration and purity of nucleic acids

Purines and pyrimidines absorb UV light at 260 nm wavelengths, which allows the estimation of the nucleic acid concentration. The purity of the nucleic acid preparation was calculated through a ratio between the absorbance at 260 nm and at 280 nm wavelengths. Pure preparations of DNA had OD260:OD280 values of 1.8. phenol or protein contaminations could disturb the quantification of nucleic acids. Nucleic acid concentration and purity were measured with the spectrophotometer NanoDrop™ 2000c.

5. DNA sequencing

5.1. DNA sequencing reaction

The DNA was sequenced in accordance with Sanger method (Sanger et al. 1977). The PCR for sequencing were performed with the kit 7-Deaza-2′-deoxy-guanosine-5′-triphosphate (7-deaza-dGTP) according with manufacture recommendations. Four batches were obtained and the separated reactions for A, C, T and G of labeled DNA fragments were performed. The PCR program was defined according with by the material of interest to be sequenced (see 4.2). After the last cycle 3 µl of the stop buffer was add to each batch. The final denaturation

step was executed at 95°C for 3 min.

Stop solution:

95% (v/v) formamide

10 mM EDTA

0.1% (w/v) xylene cyanol FF

0.1% (w/v) bromophenol blue

5.2. Automated DNA sequencing

DNA was sequenced using a LI-COR 4300 sequencer. The polyacrylamide gel (41 cm × 66 cm × 0.25 mm) was prepared with the SequaGel™ XR system. The solution was poured between two glass plates, kept apart by a spacer and a comb was added, which creates the sample slots. After polymerization the comb was removed, the gel placed in the sequencer and 1.5 µl of stop solution was added to each well. Then a pre-run at 50 °C for 30 min was performed with 1x TBE-Buffer (diluted from Rotiphorese™10x TBE-Buffer). After that, the samples were loaded, and the electrophoresis executed at 1500V for 6-7 hours under the control of the software program BaseImagIR/Data Collection V02.31. After the gel run was completed the image information was stored automatically and processed with the software BaseImagIR / Image Analysis V4.

SequaGel™ XR

6 ml SequaGel™ XR buffer

24 ml of SequaGel™ monomerconcentrate

175 µl of 10% (w/v) ammonium persulfate

Rotiphorese™ 10x TBE-Buffer

1 M Tris-Borat, pH 8.3

20 mM EDTA

6. Acquire of MANF from *S. domuncula* DNA sequence

The cDNA of SDMANF was isolated from a *S. domuncula* (Wiens et al 2007) with the degenerated primer (5´−A/TG/CI G/ATI GAT/C C/TTG/A AAG IT−3´) that was designed against a stretch of conserved (NH2−T/S-V/I-D-L-K-K-L/M−COOH) within the ARMET domain of MANF homologs (protein family (Pfam) accession

number PF10208), in combination with a library specific primer. The fragment thus obtained, with a size of ≈ 200 bp. Ultimately, the SDMANF sequence was completed through primer walking (Sereno et al 2017).

7. Bioinformatics methods

7.1. Bioinformatics analysis

The homology searches of MANF-like protein were conducted via the server at National center for Biotechnology Information. Phylogenetic and molecular evolutionary analyses and graphic output were carried out using SeaView-Multiplatform GUI for molecular phylogeny.

Multiple sequence alignment was done with Clustal Omega at SeaView. It also drives the Gblocks program to select blocks of evolutionarily conserved sites. SeaView computes the phylogenetic tree using PHYLIP's algorithm for parsimony and the Maximum Likelihood (ML) with PhyML 3.1 software. Model of choice on ML analyses was the LG model from Le and Gascuel 2008. The distance analyses were performed on SeaView with Neighbor-Joining (NJ) method in order to evaluate the degree of bootstrapping (1.000 bootstrap replicates) were assessed in all methods (NJ, ML and Parsimony) in order to evaluate the support for tree internal branches. To root the resulting phylogenetic tree, a distantly related hypothetical protein bearing an ARMET-like domain of the diatom *Thalassiosira pseudonana* was used as outgroup.

Potential domains and functional sites were predicted after searching SMART and EXPASY/PROSITE databases respectively. The protein subcellular localization and signal peptide were checked with WoLF PSORT and SignalP 4.1 respectively. Sequence similarities together with secondary structure information from aligned sequences were predicted with ESPript 3.0.

Sequence similarities and identity from aligned sequences were calculated using the software Sequence Manipulation Suite. Amino acid and DNA sequences graphic presentations were prepared with GeneDoc. Densitometric analyses of individual bands detected on non-saturated western blots were performed with the NIH ImageJ 1.46r software.

The 3D structural homology modeling was performed with UCSF Chimera and Modeller using the archive-information about the 3D shapes of proteins from the Research Collaboratory for Structural Bioinformatics (RCSB) Protein Data Bank (PDB). Two models of SDMANF were developed: first model uses as template the structure of human MANF solved by crystallography, PKB accession number 2W51, 2.05116e-59 E-value, mature MANF (25-181aa) (Parkash et al 2009). Second model uses as template the structure of human MANF solved by Nuclear Magnetic Resonance (NMR), PKB accession number 2KVD, 2.11586e-59 E-value, mature MANF (25-182aa) (Hellman et al 2011).

7.2. Computer programs and online software

BLAST	http://www.ncbi.nlm.gov/BLAST/ (Altschul et al 1990)
EXPASY/PROSITE	http://www.expasy.org/ (Gasteiger et al 2003)
Gblocks 0.91b	http://molevol.cmima.csic.es/castresana/Gblocks.html (Castresana 2000; Talavera and Castresana 2007).
GeneDoc	http://genedoc.software.informer.com/ (Nicholas et al 1997)
Modeller	https://salilab.org/modeller/ (Webb and Sali 2016)
OligoAnalizer	http://eu.idtdna.com/calc/analyzer Copyright© 2016 Integrated DNA Technologies, Inc.
PHYLIP's algorithm	http://evolution.genetics.washington.edu/phylip.html
Primer 3	http://primer3.ut.ee/ (Koressaar and Remm 2007; Untergasser et al 2012)
Research Collaboratory for	https://www.rcsb.org/

Structural Bioinformatics (RCSB) Protein Data Bank (PDB)	(Berman et al 2000)
Sequence Manipulation Suite	http://www.bioinformatics.org/sms2/ident_sim.html (Stothard 2000)
SMART	http://smart.embl-heidelberg.de/index2.cgi (Schultz et al 1998; Letunic et al 2015)
UCSF Chimera	https://www.cgl.ucsf.edu/chimera/ (Pettersen et al 2004)
WoLF PSORT	https://wolfpsort.hgc.jp/ (Horton et al 2007)
NIH ImageJ 1.46r software	http://imagej.nih.gov/ij/
Image processing and analysis in java	Wayne Rasband, National Institute of Health, USA
ESPript 3.0	http://espript.ibcp.fr/ESPript/ESPript/ (Robert and Gouet 2014)
Sea View 4.6.4	http://doua.prabi.fr/software/seaview (Gouy et al 2010)
PhyML 3.1 program	http://www.atgc-montpellier.fr/phyml/binaries.php (Guindon et al 2010)
SignalP 4.1	http://www.cbs.dtu.dk/services/SignalP/ (Petersen et al 2011)
Clustal Omega 1.2	http://www.clustal.org/omega/ (Sievers et al 2011)

8. Recombinant protein expression

8.1. Cloning for recombinant protein expression

The vector used defines the cloning method. The cloning methods used in the present work were TOPO™ TA (vector pCR™II-TOPO™ and vector pTrcHis2™) and Gateway™ (Gateway™ pDONR™ 221, Gateway™ pDEST17™, Gateway™ pcDNA™ 6.2/cTC-Tag-DEST) vector cloning technologies.

8.1.1. TOPO™ TA cloning

The vector developed to a TOPO™ TA cloning has a single overhanging 3´deoxythymidine (T) residue that allows the ligation with the single overhang deoxyadenosine (A) to the 3´ ends of the PCR product. The deoxyadenosine (A) is added by the terminal transferase activity of Taq polymerase to the PCR products.

8.1.2. TOPO™ TA cloning reaction

The PCR product is mixed with the vectors (pCR™II-TOPO™ and pTrcHis2™-TOPO™) for five minutes at room temperature and then placed on ice where it proceeds to the chemical transformation protocol.

8.2 Gateway™ cloning

The entry clone efficiently transfer the DNA fragment to the gateway destination vector, that is the vector used on the protein expression. The entry clone (ex: Gateway™ pDONR 221 vectors) contains the DNA fragment flanked by attL sequences. The attL sequences present on the entry clone are used to shuttle the DNA to a secondary plasmid, the destination vector (expression vector), has an attR. This reaction is mediated by LR Clonase II enzyme mix, which contains the protein machinery necessary to excise the gene of interest from the entry clone and integrate it into the destination vector (ex: Gateway™ pDEST17™, Gateway™ pcDNA™ 6.2/cTC-Tag-DEST) which then becomes your expression clone.

8.2.1. Gateway™ cloning reaction

The Gateway cloning steps are the generation of the entry clone and the generation of the destination vector:

1.Generation of entry clone (pDONR 221)

The attB PCR product at the concentration of 50 femtomoles (fmol) was mixed with 50 fmol of the pDONR 221™ and Tris-EDTA (TE) buffer to a volume of 8 µl and then 2 µl of Gateway™ BP Clonase™ II enzyme mix was added and incubated for one hour at 25°C. Then 1 µl of the proteinase K solution was mixed and incubated for 10 minutes at 37°C, before transforming the competent cells.

2.Generation of destination vector (Gateway™ pDEST17™ or Gateway™ pcDNA™ 6.2/cTC-Tag-DEST™)

The purified pDONR 221™ plasmid vector at the concentration of 150 ng was mixed with 150 ng of the destination vector (Gateway™pDEST17™ for the expression in *E. coli* or pcDNA™ 6.2/cTC-Tag-DEST™ for the transfection of the mammalian cells). The reactive described above was mixed with TE buffer to a volume of 8 µl. Then 2 µl of Gateway™ LR Clonase™ II enzyme mix was added and incubated for one hour at 25°C. Finally, 1 µl of the proteinase K solution was added and incubate for 10 min at 37°C, before transforming the competent cells.

TE Buffer

10 mM tris-HCl

1 mM EDTA

in ddH_2O

pH 8.0

8.3. Transformation of competent cells

Transformation is the transference of the recombinant vector with the target DNA from the mixed reaction produced on the cloning reaction or vector solution into the bacterial strains. Transformation is done with competent cells that are able to uptake extracellular DNA from their environment. The bacterial strains can be chemically or electroporation competent cells. The bacterial strains used during this work were chemically competent cells, which are bacterial cells treated with calcium chloride to facilitate attachment of the plasmid DNA.

The vector DNA produced during the cloning procedure (1 µl) was mixed with the bacterial strain that was defined in accordance with the downstream use. The mix was incubated on ice for 30 min and then heat-shocked at 42°C for 30 sec to open the cell membrane pores in order to allow entry of the plasmid. Afterwards, it was transferred back to ice and 250 µl of S.O.C medium (Super Optimal Broth With Catabolite Repression Medium) was added to the bacteria, and then incubated at 37°C under 200 rpm agitation for one hour.

The bacteria were grown on LB-agar plates (containing the appropriate antibiotic for the selection) and incubated overnight at 37°C. The plates were

prepared using two different volumes (50 µl and 200 µl) of S.O.C medium culture to prevent bacterial overgrowing.

- The bacterial strain One Shot™ TOP10 chemically competent *E. coli* were transformed with the vector pCR™II-TOPO™ The vector has an ampicillin and kanamycin antibiotic resistance genes.
- The bacterial strain BL21 (DE3) pLysS, Singles™ Chemically competent *E. coli* were transformed with vector pTrcHis2-TOPO™. The vector has an ampicillin antibiotic resistance gene.
- The bacterial strain One Shot™ ccdB Survival 2 T1^R chemically competent *E. coli* were transformed with the vector Gateway™ pDONR 221™. The vector has chloraphenicol and Kanamycin antibiotic resistance genes.
- The bacterial strain BL21-AI™One Shot™ chemically competent *E. coli* were transformed with the vector Gateway™ pDEST17™ for SDMANF recombinant expression. For library storage the bacterial strain Library Efficiency™DH5α™ chemically competent *E. coli* was used. The vector has chloramphenicol and ampicillin antibiotic resistance genes.
- The bacterial strain One Shot™ ccdB Survival 2 T1^R chemically competent *E. coli* were transformed with the vector Gateway™ pcDNA™ 6.2/cTC-Tag-DEST™. The vector has chloramphenicol, ampicillin and blasticidin antibiotic resistance genes.

S.O.C Medium

2% (w/v) tryptone
0.5% (w/v) yeast extract
10 mM NaCl
2.5 mM KCl
10 mM $MgCl_2$
10 mM $MgSO_4$
20 mM glucose

LB-Broth (Luria/Miller) Agar

10 g/l tryptone
5 g/l yeast extract
10 g/l NaCl
15 g/l agar
pH 7.0
With the suitable antibiotic

8.4. Antibiotic selection

The vectors used in this work have an antibiotic resistant gene that allows a selection of the bacterium; i.e. only bacteria that have the plasmid inserted are

able to grow on antibiotic enriched LB-Agar.

8.5. Checking PCR of positive cloned bacterial colonies

The 10 most appropriate colonies for the experiment were selected to be used on the PCR. These colonies were then allowed to grow on 50 µl of LB medium for one hour under agitation at 37°C. One microliter of the bacteria cultured was taken to run the colony checking PCR in order to evaluate if the inserted DNA was on the right position and size in the bacterial cells. Only those that passed this checking were selected to grow overnight.

LB-Broth (Luria/Miller)

10 g/l Tryptone
5 g/l Yeast extract
10 g/l NaCl
pH 7.0
With the suitable antibiotic

8.6. Overnight culture

The bacterial overnight cultures were prepared at 37°C under 250 rpm agitation for at least 18 hours in LB medium with suitable antibiotics. The amount of volume of bacterial overnight culture was prepared according to the downstream application.

8.7. Plasmid DNA isolation

Small preparations (3 ml) were isolated using high pure plasmid isolation kit, following the manufacturer's protocol. Plasmid DNA isolated from a larger amount of culture (50 ml) was purified with the plasmid Midi kit. Preparations with 150 ml were used to purify DNA for the HEK cell transfection.

8.8. Bacterial cryopreservation

Bacteria containing the plasmid of interest were long term preserved using Roti™-Store cryo-vials. Approximately 0.5 ml of the fresh overnight culture was added to the tube and shaken several times. Supernatants were removed and frozen at -

20°C for several weeks or below -70°C for years. When defrosting the plasmid culture, a glass bit was added to specific culture media.

8.9. Vector of choice for recombinant SDMANF protein expression

The vector used for expression was chosen according to the cell model (e.g. bacterial and mammalian cells). The expression of SDMANF on the prokaryotic system was done with pTRCHis2™ vector, the SDMANF open reading frame, nt_{1-516} and the vector Gateway™ pDEST17™ for the SDMANF ($nt_{279-516}$; aa_{72-172}). The eukaryotic expression in HEK cells was done with Gateway™ pcDNA™ 6.2/cTC-Tag-DEST™**.** The primers for expression were designed following the manufacturers' specifications.

8.9.1. Vector construct pTrcHis2™ for expression of whole SDMANF protein in *E. coli*

The SDMANF complete amino acid sequence (nt_{1-516}; aa_{1-172}) was done using the vector pTrcHis2™, with *E. coli* bacterial strain BL21 (DE3) pLysS, Singles™ chemically competent *E. coli.* The vector adds a c-terminal HIS-tag (a sequence of 6 histidines) that was used for the protein purification and for western blot analysis through anti-His antibody. The expected size of the recombinant protein was 23,48 kDa.

8.9.2. Vector construct Gateway™ pDEST17™ for expression of SDMANF fragment in *E. coli*

The expression of a SDMANF recombinant fragment ($nt_{279-516,}$ aa_{72-172}) was done using the vector Gateway™ pDEST17™, with the *E. coli* bacterial strain BL21-AI™One Shot™ Chemically competent. The vector adds n-terminal HIS-tag (a sequence of 6 amino acid histidine) that can be used for protein purification and for western blot analysis via anti-His antibody. The recombinant MANF has 11.6 kDa.

8.10. Recombinant expression of SDMANF in *E. coli*

8.10.1. Time-course analysis of SDMANF expression with pTrcHis 2™

To establish the best expression conditions a time-course test of the construct expression was run. A 50 ml LB media with 50 µg/ml ampicillin was inoculated with 2 ml of an overnight culture. The culture was kept at 37°C under 250 rpm agitation.

When the cell culture reaches mid-log phase it presents an optical density at 660 nm (OD_{660}) of 0.6. The recombinant protein expression was induced by isopropyl-β-D-thiogalactoside (IPTG) to a final concentration of 2 mM. The time-course samples of the culture were collected at 0, 1, 2, 3, 4, 5, 6, 12, 18 and 24 hours.

After each sampling time, 2 ml of the culture were collected and centrifuged at 13.000 rpm for 10 min at 4°C. The obtained pellets were frozen after removing supernatant. The frozen pellets were defrosted and mixed with Roti™Load buffer and denaturated for 15 min at 95°C. For each time-course sample, 15 µl were loaded on the SDS gel, which was posteriorly used on western blot.

8.10.2. Recombinant expression of SDMANF complete sequence with pTrcHis2™

The expression was started with 10 ml of an overnight culture in LB medium. The 10 ml primary culture was used to inoculate a 600 ml of LB medium enriched with 50 µg/ml ampicillin. This culture was kept at 37°C under agitation. When the culture reached 0.6 of OD_{660} the recombinant protein expression was stimulated with IPTG to a final concentration of 2 mM. The culture was kept under these conditions for 5 hours, after which it was centrifuged at 6.000 rpm for 15 min. The pellet obtained was then washed with Phosphate Buffer Saline (PBS) and centrifuged again at 6.000 rpm for 15 min. Finally, the pellet was frozen for further purifications.

Phosphate buffer saline (PBS)

137 mM NaCl

2.7 mM KCl

10 mM Na_2HPO_4

8.10.3 Recombinant expression of SDMANF sequence fragment with Gateway™ pDEST17™

The bacterial culture was done in LB medium containing 50 µg/ml carbenicillin, at 37°C under agitation at 250 rpm. The cryopreserved *E.coli* modified with SDMANF fragment was defrosted in 10 ml of LB medium and let to grow for at least 8 hours. This initial culture was used to inoculate 600 ml of LB medium. The OD_{660} was checked frequently to verify the bacterial grow. When the bacterial culture reached OD_{660} 0.6, the expression of the recombinant protein ($SDMANF_{fragment}$) was stimulated with L-arabinose to a final concentration of 0.2% (w/v), for approximately 18 hours. Afterwards, the bacterial culture was centrifuged at 6.000 rpm for 15 min. The pellet was washed with PBS and centrifuged again at 6.000 rpm for 15 min and then frozen to future purification protocol of the targeted recombinant protein.

8.11. Purification of recombinant SDMANF expressed in *E. coli*

The purification method of choice was the Immobilization on Metal Affinity Chromatography (IMAC) with the Profinia™- Protein Purification System. The Profinia protein purification system is an automated chromatography system, which uses the IMAC binding affinity to the Histidine Tag (HIS-tag) to purify the recombinant protein.

The recombinant SDMANF proteins were purified under denaturing condition. The pellet was thawed and resuspended with the lysis buffer with a mixing ratio of 1 g pellet to 10 ml buffer. The lysate was mixed using a magnetic stir bar for one hour at room temperature, then centrifuged at 10.000 rpm for 10 min. The supernatant was collected, and then sonicated for 3 times. The pause between each run was 2 min long. The lysate was filtered with 0.8 µm filter followed by another filtration with 0.45 µm filters before being loaded at the Profinia™. The clear lysate was loaded at flow rate of 1 ml/min to a 1 ml bed volume (IMAC/ Ni-NTA) column. The column was washed with the washing buffer I using 6 times the column volumes, and then washed with the same volume of the washing buffer II. The washing buffer has a progressive amount of imidazole to

release unspecific bound protein to the column. The recombinant protein was eluted with four bed volumes of elution buffer. The recombinant protein was analyzed by SDS-PAGE, western blot and quantified using the kit Pierce™ protein 660 nm.

Lysis buffer
6 M urea
5 mM imidazol
50 mM KH_2PO_4
300 mM KCl
pH 8.0

Washing buffer I
6 M urea
10 mM imidazol
50 mM KH_2PO_4
300 mM KCl
pH 8.0

Washing buffer II
6 M urea
20 mM imidazol
50 mM KH_2PO_4
300 mM KCl
pH 8.0

Elution buffer
6 M urea
250 mM imidazol
50 mM KH_2PO_4
300 mM KCl
pH 8.0

9. Antibody development against *Suberites domuncula* MANF

In order to identify MANF on *S. domuncula* tissue and cell compartments a polyclonal antibody was developed by [redacted] Besides, she were performed the rabbit immunization, serum production, quality and concentration analysis.

The purified *S. domuncula* recombinant protein fragment ($nt_{279-516,}$ $aa_{101-172}$) expressed in *E. coli* was used as antigen; the polyclonal antibody was raised in New Zealand white rabbits. Prior to rabbit immunization a blood sample was collected. This pre-immune serum is used to demonstrate the absence of immunity response before the immunization with the recombinant protein. The rabbit was immunized with recombinant SDMANF twice (12 mg/injection, containing Freud´s adjuvant) with a lapse of 5 weeks between each immunization. After that time another blood sample was collected and the serum separated (1h, 37°C, centrifugation at 13.000 rpm, 10 min). The serum was aliquoted and stored at -

20°C.The antibody specificity was tested by western blot.

10. Protein extraction of sponge tissue

The sponge was cut into small pieces (1~2 mm^2), which were gently squeezed to remove water. Pieces were divided into Precellys™ tubes (ceramic, 1.4 mm 50x 2.0ml) and buffer was added. Samples were incubated at room temperature on a horizontal shaker for 2 hours and homogenized afterwards on Precellys™ with the program 5000, 2 times for 15 sec on 90 sec. Following homogenization, sponge samples were centrifuged at 15.000 rpm for 20 min. Finally, the supernatant (total protein extract) was transferred into a new vessel and succeeded by protein precipitation protocol.

Protein extraction buffer

10 mM tris-HCl
7M urea
4% (w/v) chaps
60 mM DTT (add just on the moment of extraction)
pH 7.5

10.1 Protein precipitation with trichloroacetic acid / acetone

The total protein extract was mixed with ice-cold acetone and trichloroacetic acid (TCA) in the ration 1:8:1 and then let to precipitate at -20°C for 1 hour. The solution was then centrifuged at 11.500 rpm for 15 min at 4°C. The supernatant was discarded and the pellet remains were washed with 1 ml ice-cold acetone and then centrifuged at 11.500 rpm for 15 min at 4°C. These steps were repeated 2 times. After the last centrifugation, acetone was discharged and the pellet was allowed to dry at room temperature. After dried, the pellets were rehydrated with rehydration buffer at room temperature for one hour, with a vortexing step every 10 min. At the end, samples were centrifuged at 14.000 rpm for 10 min at room temperature and the supernatant was transferred to a new tube and stored at -80°C.

Protein precipitation buffer	Protein rehydration buffer
Mix the solution in a ratio 1:8:1	10 mM tris-HCl
1 ml supernatant	2 M thiourea
8 ml 100% ice-cold acetone	7 M urea
1 ml 100% TCA (100% TCA, w/v)	4% (w/v) chaps
	pH 7.5

11. Protein quantification

The chosen method for protein quantification was Pierce™ 660 nm protein assay reagent kit. The procedure was executed according to the manufacturer's specifications. To measure protein concentration of each sample, a linear regression was calculated using a standard curve with known concentrations of BSA.

12. Sodium dodecyl sulfate-polyacrylamide gel electrophoresis

The separation of charged molecules induced by an electric field is called electrophoresis. Migration speed is determined by the physical characteristics of both the electrophoresis system and the proteins, in units of $cm^2/Vsec$. Factors affecting protein electrophoresis include the strength of the electric field, the temperature of the system, the pH, ion type, and concentration of the buffer as well as the size, shape, and the electrical charge of the proteins (Garfin 1990).

When electrophoresis is performed with Polyacrylamide Gel Electrophoresis (PAGE) or agarose gels, the gel serves as a size-selective sieve during separation. As proteins move through a gel in response to an electric field, applying an electrical field across the buffer chambers forces proteins to move into and through the gel (Hames 1998). The percentage of acrylamide/bis-acrylamide defines the pore structure of the gel matrix and can be adapted to the wanted resolution.

In 1970 Laemmli included the anionic detergent Sodium Dodecyl Sulfate (SDS), creating the electrophoresis in a denaturation condition (SDS-PAGE). The SDS applies a negative charge to the protein in proportion to its mass (1.4 g of SDS per 1 g protein, a stoichiometry of about one SDS molecule per two amino acids), and, as a consequence, protein migration on the gel is directly related to its

size (Weber and Osborn 1969). Laemmli protein loading buffer has reagents as SDS, glycerol, reducing agents as DTT or ß-mercaptoethanol that also help protein denaturation and a tracking dye as bromophenol blue to visualize the course of the migration into the gel.

The protein electrophoresis were performed with the XCell sure lock system using NuPAGE™ 12% Bis-Tris mini, 10 wells, pre cast gel using NuPAGE™ MOPS SDS Running Buffer (1X). Prior to loading, the samples were mixed with the Roti-Load™ 1- protein loading buffer and boiled, 10 min at 95°C.

The sponge total protein extracts were precipitated with a buffer containing thiourea in order to concentrate the protein content. Proteins extracts that contain thiourea should not be heated above 37°C. Above this temperature hydrolyzed thiocyanate may be formed. This can modify amino acids via carbamylation, which may cause artifacts charge heterogeneity (Rabilloud 1999). Therefore, to avoid the heating phase at 95 °C, the sponge samples were mixed a SDS loading buffer containing TCEP (Tris(2-Carboxyethyl)Phosphine) as reduction agent. The TCEP was chosen as the reducing agent because it functions at room temperature eliminating the need of heating at 95°C.

In all approaches 30 µg of extracted proteins were subjected to electrophoresis. After the run, the gel was prepared to protein visualization by staining with the Gel code™ blue safe following the procedures determined in the manual. The documentation of the gel was either done with Odyssey, Li-Cor Biosciences, documentation system or used to the western blot procedure.

NuPAGE™ MOPS SDS Running Buffer (1X)

50 mM MOPS
50 mM tris base
0.1% (w/v) SDS
1 mM EDTA
pH 7.3

Roti-Load™ 1 (4X) SDS sample loading buffer

in phosphate buffered saline.
8% (w/v) SDS
20% (v/v) β-mercaptoethanol
40% (v/v) glycerol
0.015% (w/v) bromophenol blue

SDS-sample loading buffer (2X)
with (TCEP)
100 mM tris-Cl
4% (w/v) SDS
0.2% (w/v) bromophenol blue
20% (v/v) glycerol
pH 6.8
50 mM TCEP was add to each
sample prior to use

13. Western Blot

Western Blot is a method of electrophoretic transfer of proteins from polyacrylamide gels to nitrocellulose sheets (Towbin 1979). Membranes made from other materials, such as Polyvinylidene Difluoride (PVDF), can also be used in the electrophoretic transfer. An electric current makes the protein move from the gel to the membrane while keeping spatial separation. Once transferred to the membrane, the proteins are accessible for detection, which can be done by many different techniques. The method of transferring used was the iBlot™ DryBlotting System 6 min with 20 volts to nitrocellulose membrane, following the instructions of the manufacturer.

13.1. Detection of SDMANF recombinant expressed with the vector pTrcHis2-TOPO™ with anti-His (C-term) AP antibody

After the transference, the membrane was incubated with 1.5% (v/v) blocking solution for one hour at room temperature, under gentle shaking. On the sequence, the membrane was incubated with anti-His antibody at the dilution 1:1000 on TBS overnight at 4°C. On the following day, the anti-His antibody incubation continued at room temperature for two hours under gentle shaking. Since the anti-His antibody is already conjugated with alkaline phosphatase a second antibody was not required for detection. The membrane was washed three times for five min each with TBS-T then stabilized with NBT/BCIP buffer for five minutes. The membrane was then incubated with colorimetric substrate, prepared

as manufacture´s specification, until the color development. Finally, the process was stopped with water.

13.2. Detection of SDMANF in sponge tissue

After the transfer, the membrane was incubated with 1% (w/v) milk in TBS-T for one hour at room temperature under gentle shaking and then incubated with the first antibody (SDMANF antibody, rabbit) at the dilution 1:500 in TBS-T overnight. On the next day, SDMANF antibody incubation continued at room temperature for three hours under gentle shaking. After that, SDMANF antibody was discharged and a subsequent incubation was done with the secondary antibody (rabbit) for two hours at room temperature under gentle shaking. After the antibody incubation time the membrane was washed three times for 10 min each with TBS-T and then stabilized with NBT/BCIP buffer for five minutes. The next step was the incubation with the colorimetric substrate NBT/BCIP until color development, prepared as manufacture´s specification, and then stopped with water.

13.3. Detection of SDMANF recombinant protein tagged with V5 expressed in transfected HEK cells for stable cell line cloning selection with Dot Blot

A similar approach as that used to detect the SDMANF recombinant protein expressed in HEK cells tagged with V5 was used with the dot-blot. The detection of a specific protein, in this case, relies only on the specificity of the antibody; i.e. there is no protein separation by size as on electrophoresis. The membrane was incubated with 1.5% (v/v) blocking solution for two hours at room temperature under gentle shaking followed by overnight incubation with V5 antibody at the dilution 1:1.000 in TBS-T. The V5 is already conjugated with alkaline phosphatase therefore a second antibody was not required for detection. The membrane was washed three times for five min each with TBS-T and then stabilized with NBT/BCIP buffer for five minutes. The next step was incubation with the colorimetric substrate NBT/BCIP, prepared as manufacture´s specification, until the color development.

13.4 Detection of the SDMANF recombinant protein tagged with V5, BAX, and α-tubulin in HEK cells

After the transfer, the membrane was incubated with 1.5% (v/v) blocking solution for one hour at room temperature under gentle shaking and then incubated with V5 antibody at the dilution 1:1.000 or anti-BAX at the dilution 1:200 or anti-α-tubulin at the dilution 1:1.000 in TBS overnight. On the second day, the membrane was incubated for three hours at room temperature under gentle shaking. A subsequent incubation, when needed, was done with the secondary antibody (anti-rabbit for anti-BAX and anti-α-tubulin) for two hours at room temperature under gentle shaking. After the antibody incubation time, the membrane was washed three times for 10 min each with TBS-T and then stabilized with NBT/BCIP buffer for five minutes. The next step was the incubation with the colorimetric substrate NBT/BCIP, prepared as manufacture´s specification until the color developed, which is then stopped with water (Sereno et al 2017).

14. Immunohistochemistry

The technique of Immunohistochemistry (IHC) allows visualizing the distribution and localization of specific cellular components within cells or tissue context. IHC combines anatomical and immunological techniques to identify discrete tissue components by the interaction of target antigens with specific antibodies conjugated with a visible label.

14.1. Poriferan tissue IHC

A few pieces (ca. 5x5 mm and 1 mm thickness) were cut from three different sponges kept alive in the aquarium. The tissue pieces were fixated in Paraformaldehyde (PFA) 4% (w/v) in PBS at 4°C, overnight. To wash the PFA, the samples were incubated with 6.8% (w/v) saccharose solution in PBS at 4°C, overnight. The tissue was dried in 100% (v/v) acetone (the acetone was changed until becoming clear) for 60 min at 4°C. After acetone drying procedure, the tissue was infiltrated with infiltration solution (100 ml Technovit 8100™ plus the hardener I package of 0.6 g) overnight at 4°C. The infiltration solution was mixed with the hardener II (Embedding solution), which make the infiltration solution polymerases, for around 10 min. Before the solution gets polymerized a bit was loaded on the

Teflon cast and the tissue piece was carefully settled up. The tissue piece was covered with the embedding solution, then covered with plastic foil and incubated overnight at 4°C.

A block was used to pull out the sample that gets harder inside the Teflon plate and also the blocks are the holding apparatus to the microtome. A second polymer mix made with Technovic 3040™ (2 parts of powder to 1 part of liquid) was used to make the blocks. Before polymerization the liquid was loaded on the top of the block above the tissue fragment and let to dry overnight at 4°C. The blocks were sectioned with ca. 10 µm with a microtome. The sections were placed to stretching bath with ddH_2O and then mounted on a glass slide. The section adheres to the slide drying at 37°C on a slide warmer for two hours.

14.2 Immunostaining

The slides were washed three times for 10 min with PBS, and then placed in a dark humidity chamber. To reduce unspecific antibody binding, the sections were blocked with 2% (v/v) goat serum. The sections were incubated with pre-immune serum or primary antibodies against SDMANF (rabbit anti-SDMANF; 1:100 dilution with 0.02% (v/v) sheep serum), followed by incubation with secondary antibodies labeled with Cy™ 2 (goat anti-rabbit,1:50 dilution). Nuclei were counterstained with DRAQ5™**.** The slides were mounted with Fluoromount™ mounting medium. The slides were observed with an EVOS™fl fluorescence microscope, using the GFP ($Ex_{470\ nm}/Em_{510\ nm}$) and Cy5 ($Ex_{628\ nm}/Em_{692\ nm}$) light cube.

15. Cell culture

15.1. Culture of human embryonic kidney cells

Human Embryonic Kidney Cells (HEK) are adherent with epithelial morphology. The HEK cells were cultured in 75 cm^2 flasks with Dulbecco's modified Eagle's medium (DMEM, high glucose and with L-glutamine) supplemented with 10% (v/v) fetal bovine serum (FBS) and Normocin™ 50 mg/ml. The SDMANF transfected cells (HEK_{SDMANF}) and the HEK transfected with the empty vector (mock transfected cells, HEK_{Mock}) were grown in the presence of Normocin™ 50 mg/ml and 15 µg/ml Blasticidin. To avoid overgrow, the cells were split when they

reached 80-90% of confluence. The cultivation ratio was 1:6 to 1:10 weekly, with medium renewal every 2 or 3 days. To split the cells, first the medium was removed and the cells washed once with sterile DPBS 1X. These cells were detached with 1 ml of trypsin-EDTA (0.05%) solution for 1-3 min. The trypsin activity was stopped by adding the complete medium with the same amount of trypsin. After centrifugation at 800 rpm for 10 min, the cells were resuspended in fresh complete media. The desired number of cells was transferred to 10 ml of complete medium in a 50 ml cell culture flask.

Dubelcco´s Phosphate Buffer Saline (DPBS) 1X (free of Ca^{2+} and Mg^{2+}	**Complete medium**
25 mM tris	DMEM medium
2.68 mM KCl	10% (v/v) FBS
137 mM NaCl	50 mg/ml Normocin™
pH 7.4	* 15 µg/ml blasticidin, were add with working with HEK_{SDMANF} and HEK_{Mock}

15.2. Cell counting

Cell counting was performed using the handheld automated cell counter Scepter™ 2.0. A dilution of the cell culture to be counted is prepared and aspirated into the Scepter sensor. The Scepter cell counter counts any particle that passes through the orifice within the cell diameter range and display a histogram of size distribution, excluding deviant large and small cells, and debris from the count.

15.3 Cryopreservation of mammalian cells

For long-term cell storage, HEK cells were trypsinized, pelleted for 10 min at 800 rpm and resuspended in medium to freezing process; this solution was transferred to cryogenic vials. The vials were allocated on a cell-freezing container that ensure a temperature rate of -1°C/min at - 80°C. After 24h, the cryogenic vials were transferred to liquid nitrogen.

Freezing medium

DMEM medium

20% (v/v) FBS

10% (v/v) DMSO

16. Transfection of HEK cells with SDMANF

Transfection is the process of intentionally introducing nucleic acids into eukaryotic cells. The chosen method for transfection was the Lipofectamin™ 2000 reagent. The HEK cells were transfected with the vector Gateway™ pcDNA™ 6.2/cTC-Tag-DEST carrying a MANF of *Suberites domuncula* construct. The vector adds a V5 tag to the recombinant protein that allows its identification by antibody detection. The vector also adds a tetracysteine Lumio™ tag (FlAsh) that allows the visualization of the fluorescent recombinant protein by bi-arsenical labeling reagent (TC-FlAsH™ In-cell tetracysteine tag detection kit) and a Blasticidin antibiotic resistant gene. SDMANF expected size is 23.8 kDa (Sereno et al 2017).

On the eve prior to transfection, the cells were seeded to approximately 80-90% confluence on DMEM medium with 10% (v/v) FBS without antibiotic. On the next day the plasmid isolated DNA, with either vector Gateway™ pcDNA™ 6.2/cTC-Tag-DEST with SDMANF vector construct or empty vector, was diluted in Opti-MEM™ medium at the concentration of 2.5 µg DNA per well of a 6-wells plates and mixed with the appropriated amount of Lipofectamin™ 2000 transfection reagent (Sereno et al 2017). The transfection was monitored after 48 hours. SDMANF expression was microscopically assessed via fluorescence in live cells and immunological on western blots. For the former analyses, the TC-FlAsH-EDT_2 labeling reagent of the cell TC-FlAsH™ In-cell tetracysteine tag detection kit was employed according to manufacturer's specifications. FlAsH-EDT_2 is membrane-permeable and becomes fluorescent upon binding to tetracysteine (TC)-tagged proteins ($Ex_{508\ nm}/Em_{528\ nm}$). Upon addition of FlAsH-EDT_2 to the medium, cells were inspected with an EVOS™fl fluorescence microscope, using the GFP ($Ex_{470\ nm}/Em_{510\ nm}$) light cube (Sereno et al 2017).

16.1 Establishment of HEK SDMANF transfected stable cell line and clonal selection

The pool of HEK SDMANF transfected cells (HEK_{SDMANF}) was cultured in the presence of the antibiotic blasticidin at 15 µg/ml, which allows the selection of stable transfected cells. The media containing blasticidin were changed every 2-3 days. To prepare clones of the stable transfected cell line, the pools of antibiotic selected cells were seeded at the concentration of 0.3 cells/wells in a 96 wells plate and let to grow until reach 90% of confluence. When confluence was reached, each well was trypsinized and the volume divided in two plates of 96 wells, making two equal plates. One plate was used to keep the clones and the second for total protein extraction to be used in Dot-Blot test.

16.2 Dot-Blot for clonal selection

The expression of the recombinant protein was evaluated using the dot-blot technique. The aim was to select and cryopreserve a clone of stable transfected HEK_{SDMANF} that highly express SDMANF. The medium was removed, and the cells on the 96 wells plate were lysate with the Mammalian Protein Extraction Reagent Buffer (M-PER), and then transferred using the Bio-Dot device directly to a PVDF membrane. The membrane was immunostained with the V5-tag antibody. The cell clone that presented higher recombinant protein HEK_{SDMANF} expression was cultivated for future experiments.

17. SDMANF expression in transfected cells

17.1. Secretion of SDMANF on culture medium

To verify the presence of secreted SDMANF in the culture medium of HEK_{SDMANF}, an aliquot of the medium was dried by lyophilization and resuspended in SDS sample buffer.

17.2. Mammalian cell total protein extraction

The protein extraction was done using M-PER buffer. The culture medium was carefully decanted, after which 500 µl of M-PER was added. The cell scraper was used to help lysis process. The lysate was collected and transferred to a 1.5 ml

tube; and then centrifuged at 13.200 rpm for 10 minutes to pellet the cell debris. The supernatant (total protein extract) was transferred to a new tube for the downstream analysis, protein quantification and western blot.

17.3. ProteoExtract™ Subcellular proteome extraction kit (S-PEK)

The S-PEK kit enables the differential extraction of proteins according to their subcellular localization. It takes advantage of the differential solubility of subcellular compartments. It uses a special reagent mixtures it preserves the subcellular structures during the extraction, allowing the separation in four different fractions. ProteoExtract™ Subcellular Proteome Extraction kit yields the total proteome fractionated into four sub proteomes of decreased complexity. With extraction buffer I cytosolic proteins are released (fraction 1). Subsequently, membranes and membrane organelles are solubilized with extraction buffer II, without impairing the integrity of nucleus and cytoskeleton (fraction 2). Next, nucleic proteins are enriched with extraction buffer III (fraction 3). Finally, components of the cytoskeleton are solubilized with extraction buffer IV (fraction 4). The HEK_{SDMANF} cells stably transfected grow in 50 ml cell culture flasks at the concentration of 3 $x10^6$ cells. The S-PEK protein extraction was done according the manufacture protocol for adherent tissue culture.

18 Cell treatments

18.1 Treatment of HEK_{SDMANF} with Brefeldin A or cadmium

The HEK_{SDMANF} were seeded at 50 ml cell culture flasks at the concentration of 3 $x10^6$ cells. After 24 hours, the medium was changed either to new medium Control (Co) or the medium containing the stressor 1, Brefeldin A (BFA) or 2, cadmium ($CdCl_2$).

1. The HEK_{SDMANF} cells were incubated with BFA 5 µg/ml for 6 h or kept untreated for the same time (control).
2. The HEK_{SDMANF} cells were incubated with cadmium 25 µM or 50 µM for 0 h, 6 h and 24 h or kept untreated for the same time (control).

Following the treatment the total proteins were extracted, size-separated, and blotted onto membranes. On the western blots SDMANF was probed for with V5 antibody.

18.2 Cell assays upon LPS exposure

The HEK_{SDMANF} and HEK_{wt}, were seeded at 50 ml cell culture flasks at the concentration of 3 $x10^6$ cells, 24 hours prior to treatment. For the treatment the medium was changed to a medium containing the toxic reagent LPS at 0.1 or 1.0 µg/ml concentration and incubated for 1 h, 6 h or 12 hours. Control cells were kept untreated for the same time. Following the treatment, proteins were extracted, size-separated, and blotted onto membranes (Sereno et al 2017). On these western blots, SDMANF, BAX, and α-tubulin were probed for with respective antibodies. The densitometric analyses of individual bands detected on non-saturated western blots and the relative band densities were normalized according to the α- tubulin loading controls to calculate the adjusted density (Sereno et al 2017).

19. Viability and caspase activity of HEK cells upon LPS exposure

To analyze cell viability and caspase activity, the fluorogenic GF-AFC peptide substrate and the NucView™ 488 caspase 3 substrate were used. GF-AFC is a cell-permeant and non-fluorescent peptide substrate that is cleaved by live-cell protease activity to generate fluorescent signal in viable cells (Ex_{400nm}/Em_{505nm}). Similarly, cell-permeant NucView™ 488 becomes fluorescent ($Ex_{488\ nm}/Em_{520\ nm}$) upon hydrolysis at the DEVD recognition sequence by cytoplasmic caspase 3 (Sereno et al 2017).

For this purpose, cells were seeded (HEK_{SDMANF}, HEK_{wt}, HEK_{Mock}) in 96-well plates 12 hours prior treatment. The medium was changed to FluoroBrite™ DMEM, which reduces background fluorescence, with 10% (v/v) fetal bovine serum and incubated after 12 hours with 1.0 µg/ml LPS. Finally, the substrates were added to each well according to the manufacturer's specifications. Fluorescence was monitored with a Varioskan Flash multimode reader (Sereno et al 2017).

19.1. Live cell imaging viability and caspase activity in HEK wild-type and SDMANF upon LPS exposure

For live cell imaging, cells (HEK_{SDMANF} and HEK_{wt}) were cultivated in 24-well plates to 40% confluence before treatment. The medium was changed to FluoroBrite™ DMEM, with 10% (v/v) fetal bovine serum and LPS 0.1 µg/mL and 1µg/ml. At the same time, each well in the medium was supplement with (1) 5 µM NucView™ 488 caspase 3 substrate, (2) 50 µl propidium iodide (PI), and (3) 50 µl Hoechst 33342. The latter two reagents were part of the ReadyProbes™ Cell Viability Imaging kit and used for staining nuclei of dead cells with compromised cell membranes (PI) or nuclei of all cells (Hoechst). Fluorescence was monitored in real-time with an automated cell imaging system (JuLI™ Stage; VWR) using the following wavelength settings: Ex_{466nm}/Em_{525nm} (NucView™ 488), Ex_{525nm}/Em_{580nm} (PI), and Ex_{390nm}/Em_{452nm} (Hoechst) (Sereno et al 2017).

20. Statistic analyses

To analyze the statistical significance of differences between groups a one-way analysis of variance (ANOVA) followed by a Tukey post hoc test was performed, with α level set at 0.001.

F. RESULTS

1. The isolation of poriferan MANF homolog

The MANF DNA sequence from *Suberites domuncula* (SDMANF) was isolated from the *S. domuncula* cDNA library (see E. 6) through polymerase chain reaction using a degenerate primer which was designed against a conserved region of the ARMET domain (the DNA fragment with a size of ≈ 200 bp was already available in the research group). The DNA fragment was extended through primer walking technic obtains SDMANF DNA sequence.

The ARMET domain can be found present in all described MANF homologs. The whole DNA sequence of SDMANF (516 nt, excluding the first stop codon) was isolated from the sponge cDNA by using primers directed against regions comprising Met_{start} and the first stop codon. The DNA sequence was translated on EXPASY. The deduced sequence has 172 amino acids and has an expected size of 19745 Da (Fig. 8). The *Suberites domuncula* Mesencephalic Astrocyte-Derived Neurotrophic Factor (SDMANF) cDNA sequence was deposited on European Molecular Biology Laboratory (EMBL) accession number LT605074.

```
atggagctaaaggtgttagttgtcctgggactgtgtttcctctgttgtgaagtgaaggcg
 M  E  L  K  V  L  V  V  L  G  L  C  F  L  C  C  E  V  K  A
aagctaaaaggagatgattgtgaagtgtgtatatctttcttgaacaagtttggtaaacga
 K  L  K  G  D  D  C  E  V  C  I  S  F  L  N  K  F  G  K  R
ctaaaagaaagagctgtggacatgcccaatcaagatcagatggagattgaactgctcaag
 L  K  E  R  A  V  D  M  P  N  Q  D  Q  M  E  I  E  L  L  K
acatgcagagaagcaaaaggaaaagatgagagattttgttactacattggagcctctgat
 T  C  R  E  A  K  G  K  D  E  R  F  C  Y  Y  I  G  A  S  D
atagctgctaccaagttggtcaggttagtgacaaagccaatgtccttcagtaagcctgct
 I  A  A  T  K  L  V  R  L  V  T  K  P  M  S  F  S  K  P  A
gagaagatttgtgaagacttgaaaaagaaagatggagagatttgtgaattaaaatatgaa
 E  K  I  C  E  D  L  K  K  K  D  G  E  I  C  E  L  K  Y  E
aaagagattgactttagtactgttgacctgaagaagctccgagtcaaggaactcaagaag
 K  E  I  D  F  S  T  V  D  L  K  K  L  R  V  K  E  L  K  K
attttgagcaactggggcgaggactgtcggggatgtgcagagaaaacagactttattagc
 I  L  S  N  W  G  E  D  C  R  G  C  A  E  K  T  D  F  I  S
aagatcaatgccattaagcatcaacatgtagaactt
 K  I  N  A  I  K  H  Q  H  V  E  L
```

Figure 8: Deduced desoxyribonucleic acid and amino acid sequence of *Suberites domuncula* MANF.

2. Characterization of SDMANF protein sequence

The MANF of *S. domuncula* shows the predicted (see E. 7) ARMET domain (Fig. 9), (aa_{26-172}, E: value 2.6e-59; Pfam accession number PF10208). Analysis via the SMART server also predicted a Saposin B domain ($aa_{25-115,}$ E value: 3.23 SMART accession number SM000741), and the motif SAF-A/B, Acinus and PIAS Scaffold Attachment Factors A and B (SAP motif), ($aa_{130-166,}$ E value: 17.500, SMART accession number SM000513). The SDMANF shows the eight-conserved cysteine residues (See Fig. 9) with the characteristic conserved spacing between then.

A cleavable N-terminal signal sequence (aa_{1-20}, see Fig. 9) has been predicted in SDMANF with signalIP 4.1 Server as well (Fig. 10). Moreover, SDMANF has at the C-terminus sequence (see Fig. 10) a "KDEL like" sequence. The WoLF PSORT protein subcellular localization prediction tool estimated the SDMANF localization with 48.0% vesicles of secretory system, 36.0% plasma membrane and 16.0% at cytoskeletal.

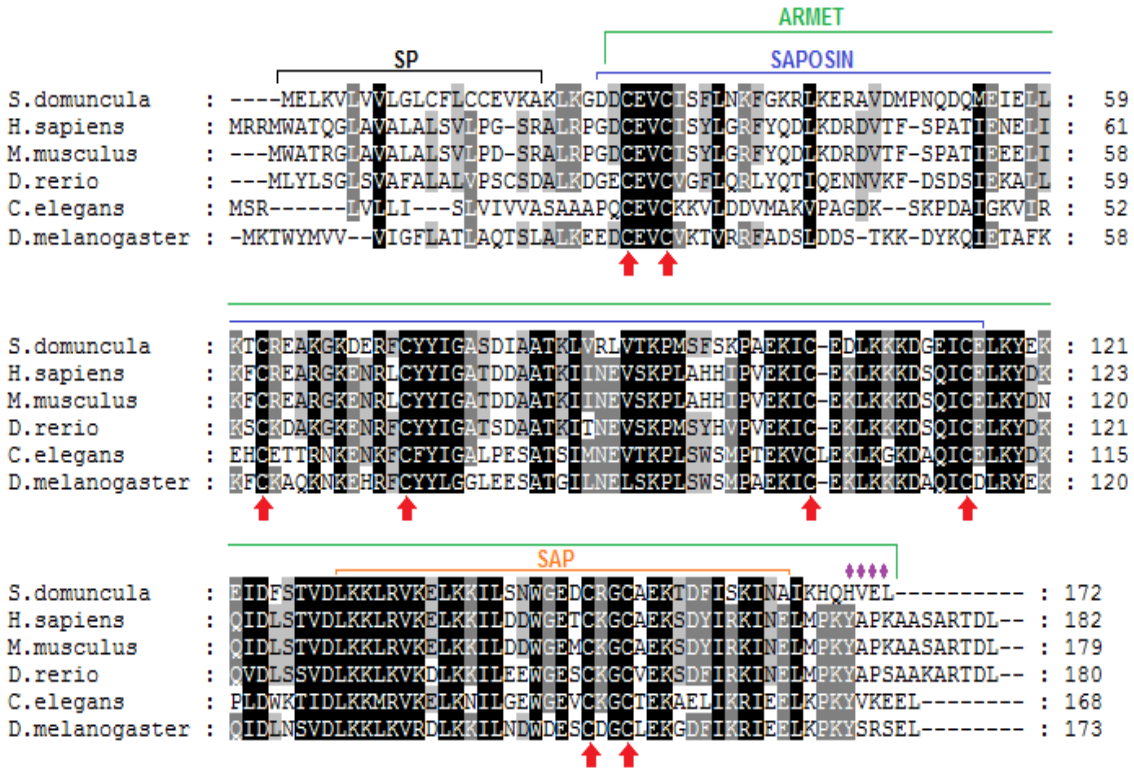

Figure 9: SDMANF protein sequence characterization and alignment. The deduced domains presents on of *Suberites domuncul*a Mesencephalic Astrocyte-Derived Neurotrophic Factor (SDMANF) aa sequence were depicted. The ARMET domain is depicted with a green line (aa_{26-172}), the Saposin B domain (aa_{25-115}) is

depicted in blue and the SAP domain ($aa_{130-166}$, SAF-A/B, Acinus and PIAS Scaffold Attachment Factors A and B) is depicted in orange. Besides, SDMANF presents eight conserved cysteine residues with the characteristic conserved spacing, (Cys residues, indicated by red arrows). The N-terminal signal sequence (SP, aa_{1-20}) is depicted in black. The ER retention signal is featured in purple (◆). The deduced aa sequence of SDMANF was aligned and analyzed in comparison with the mesencephalic astrocyte-derived neurotrophic factor (MANF) homologs of *Homo sapiens* (Uniprot identification entry codes, P55145), *Mus musculus* (Q9CX15), *Danio rerio* (Q08CA7), *Caenorhabditis* elegans (Q9N3B0) and *Drosophila melanogaster* (Q9XZ63). The residues conservation (identical or similar with respect to physicochemical properties) in all sequences are shown: those with 100% conservation in white letters on black background, those with 80% are in white letters on gray background; those with 60% are written in black on light gray. Sequence alignment was performed with Clustal Omega 1.2 at Sea View 4.6.4 and graphical manipulation was performed with GeneDoc.

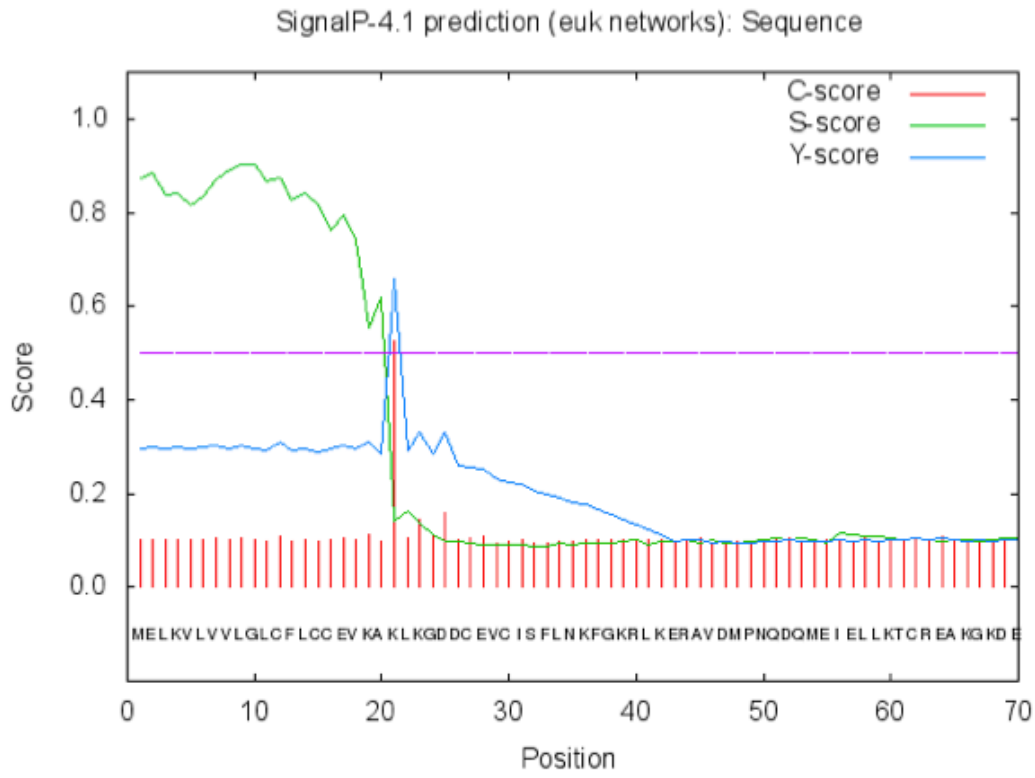

Figure 10: Screening of SDMANF protein for the presence of a signal peptide
The graphic shows a cleavage site position between the amino acids 20 and 21:VKA-KL. The C-score (raw cleavage site score) is output from the CS network, which distinguish signal peptide cleavage site from everything else. The S-score (signal peptide score) is output from the SP network, which distinguishes signal peptide from positions in the mature part of proteins and from proteins without peptide. Y-score (combined cleavage score) a geometric average of the C-score and the slope of the S-score (Petersen et al 2011). Analysis was performed with the neural networks in SignalP 4.1 Server.

3. SDMANF homologies and phylogenetic relationships

S. domuncula MANF presents higher sequence identities to MANF (see E. 7) from vertebrates such as *Homo sapiens* MANF (with 182 aa, an expect value [E value] of 5e-58, identities 60%, BLAST accession number P55145.3), *Mus musculus* (179 aa, 2e-57 and 60%; NP_083379.2), *D. rerio* (180 aa, 9e-47, 53%; NP_001070097.1), then, to MANF-like proteins from invertebrates such as *D. melanogaster* (173 aa, 1e-45 and 45% NP_477445.1), *C. elegans* (168 aa, 4e-37, 44%; NP_500273.2) and *A. queenslandica* predicted MANF-like protein (165 aa, 2e-51 and 54%, XP_003389510.1) by BLAST. Moreover, MANF-like protein of *Amphimedon queenslandica* (which, like *S. domuncula, is* a sponge from the demosponge class) was predicted from NCBI's automated computational analysis based on whole genome shotgun sequences of *A. queenslandica.* Furthermore, the percentage of identities and similarities performed with *Sequence Manipulation Suite server* are present at the table 1.

Table 1: SDMANF homologs identities and similarities. The MANF protein sequences from The *S. domuncula* (S.d.), *Amphimedon queenslandica,* predicted MANF-like protein (A.q. UniProt identification code A0A1X7TYG8), *Caenorhabditis elegans* (C.e, Q9N3B0) and *Drossphila melanogaster* (D.m. Q9XZ63), *Danio rerio* (D.r. Q08CA7), *Mus musculus* (M.s. Q9CX15), *Homo sapiens* (H.s., P55145) were aligned and percentage of identity and similarity calculated. MANF identity and similarity are higher when compared with vertebrates than to invertebrates. The percent of identity highlighted on yellow and the percent of similarity highlighted on blue. The alignment was performed with Clustal Omega 1.2, together with Gblocks software it selects blocks of evolutionarily conserved sites were performed at SeaView 4.6.4 and the percentage of identity and similarity were calculated with Sequence Manipulation Suite server.

	S.d.	A.q.	C.e	D.m.	D.r.	M.m	H.s.
S.d.		63.95	56.00	61.02	66.30	66.85	65.22
A.q.	48.26		54.44	56.25	58.56	59.12	57.61
C.e	39.43	40.24		62.92	57.69	54.40	54.59
D.m.	41.81	40.91	44.38		67.58	64.29	65.03
D.r.	48.62	44.75	41.76	51.65		81.11	80.87
M.m	50.28	43.65	42.31	47.25	68.33		96.15
H.s.	50.00	57.61	42.16	47.54	67.76	96.50	

To study the phylogenetic relationship of MANF proteins molecular phylogenetic analyses a consensus tree (see E. 7), (Fig. 11) was developed using the resulting trees of NJ, ML and Parsimony analyses. The first and second clade comprised the Ecdysozoa group (representing the well-supported lineages of Nematoda, Crustacea, and Hexapoda), that was positioned as the sister group to the third clade, in which are the poriferan SDMANF (*S. domuncula*) and predicted MANF-like protein of *A. queenslandica.* The third clade comprised deuterostomian MANF sequences with strong support at almost all key nodes of consensus tree (only missing support on ML between the branches of *Homo sapiens* and *Pan troglodytes*), and resolving Osteichthyes, amphibian, reptilian and mammals. These phylogenetic analyses show that poriferan MANF shares a common ancestor with the MANF homologs of invertebrate and vertebrate origin.

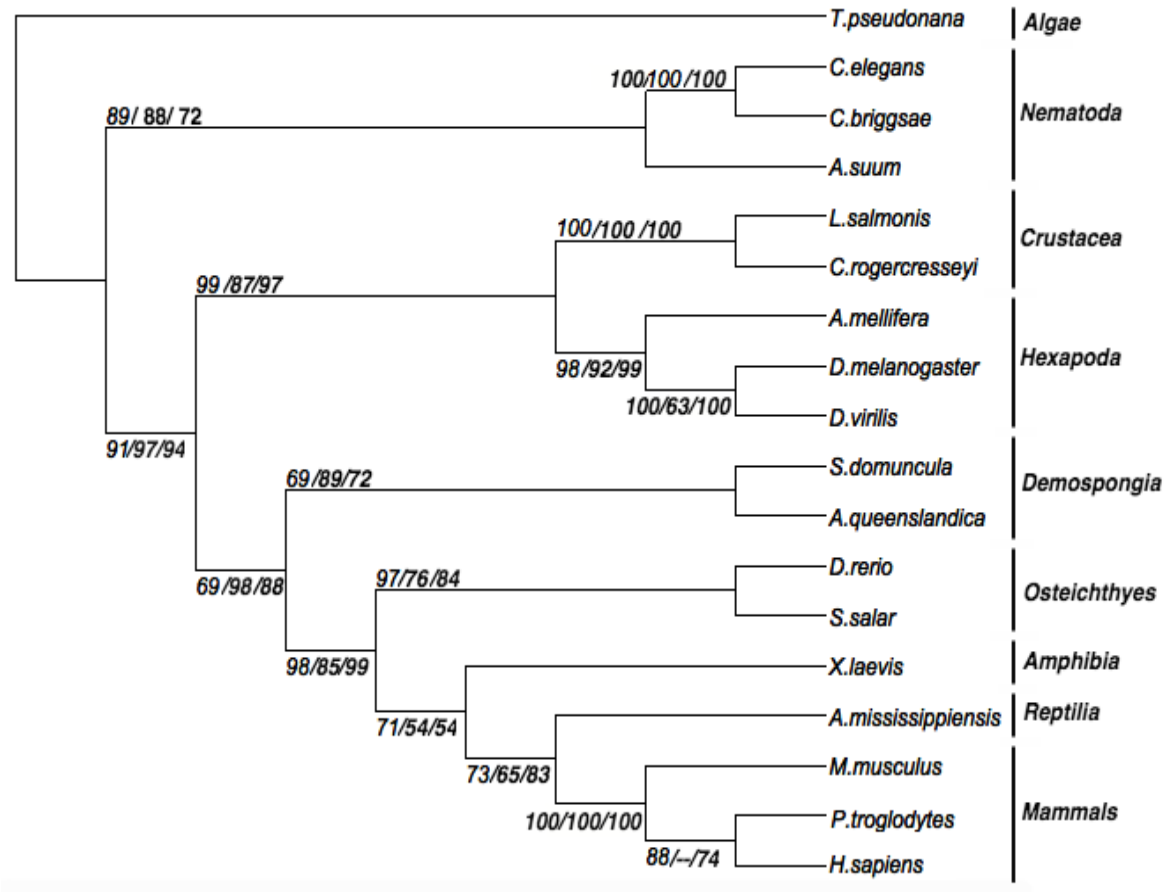

Figure 11: Phylogenetic consensus tree with MANF protein sequences. The rooted consensus phylogenetic tree was constructed with the outcome trees from Neighbor-Joining (NJ), Maximum Likelihood (ML) and parsimony. To root the resulting phylogenetic tree, a distantly related hypothetical protein bearing an ARMET-like domain of the diatom *Thalassiosira pseudonana* (B8BWT8) was used

as outgroup. The trees were constructed with SDMANF, MANF protein or predicted MANF of *Amphimedon quenslandica* (UniProt identification code A0A1X7TYG8)*, Caenorhabditis elegans* (Q9N3B0), *Caenorhabditis briggsae* (A8XI39), *Ascaris suum* (F1LCB4), *Lepeophtheirus salmonis* (C1BS72)*, Caligus rogercresseyi* (C1BMK0), *Apis mellifera* (A0A088AAX0)*, Drosophila melanogaster* (Q9XZ63), *Drosophila virilis* (B4LX78), *Danio rerio* (Q08CA7), *Salmo salar* (B5XGI6)*, Alligator mississippiensis* (A0A151MEM0), *Mus musculus* (Q9CX15), *Pan troglodytes (*K7BGP3) and *Homo sapiens* (P55145). The degree of bootstrapping (1.000 bootstrap replicates) was assessed in all three methods (NJ, ML and Parsimony) in order to evaluate the support for tree internal branches. Bootstrap values are displayed at the nodes of the consensus tree at the order NJ, ML, and Parsimony. The phylogenetic analyses and tree were constructed on SeaView 4.6.4.

4. Expression of recombinant SDMANF on *E. coli* for the developmental of polyclonal antibody

The development of an SDMANF polyclonal antibody (pAbs) was necessary to study the expression and cellular localization of SDMANF in sponge tissue via an immunodetection approach (see E. 9). A SDMANF recombinant protein was required to raise the polyclonal antibodies (anti-SDMANF pAbs). The SDMANF was expressed on a bacterial system conjugated with a 6xHis-tagged (HIS-tagged) to allow the purification and detection of the recombinant protein. The recombinant SDMANF expression was carried out using two different constructs.

The first construct (see E. 8) presented the complete protein sequence (pTrcHis2™, $SDMANF_{1-516}$, aa_{1-172}) conjugated with a 6xHis-tagged. The protein expected size was 23.4 kDa. However, the amount of recombinant protein obtained was lower then amount necessary to develop the antibody. Because of this, to evaluate the expression of recombinant SDMANF a time course expression evaluation was carried out at 0, 1, 2, 3, 4, 5, 6, 12, 18 and 24 hours. The recombinant SDMANF was visualized through immunodetection on western blot using anti-HIS antibody (Fig. 12 A). The expressed recombinant SDMANF was visualized through the presence of bands until around 5 hours after the stimulation of expression, after which was not possible anymore to visualize the bands. On Fig. 13 B is the western blot of purified recombinant SDMANF. Due to the problems on the expression of the recombinant protein the yield of purified recombinant SDMANF was not enough to the antibody development.

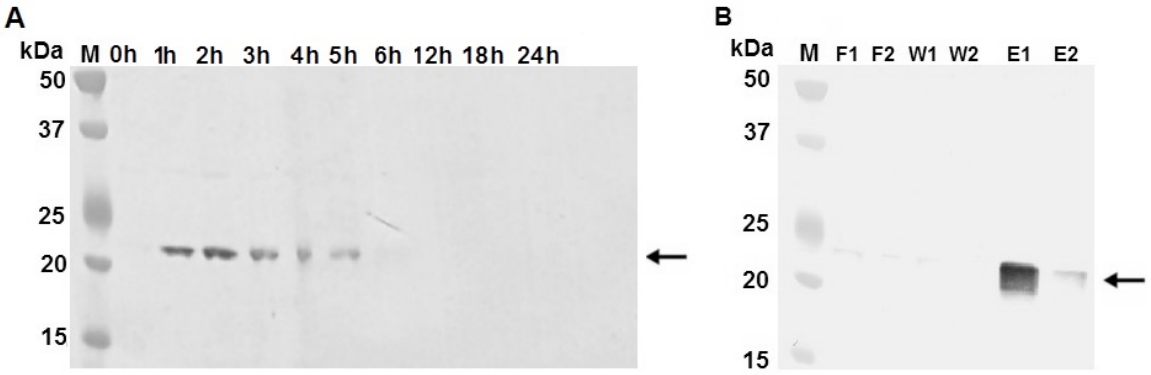

Figure 12: SDMANF recombinant protein expressed in *E. coli* with vector pTrcHis2™. A- Immunodetection of recombinant *Suberites domuncula* mesencephalic astrocyte-derived neurotrophic factor (SDMANF) expressed on time course (0h, 1h, 2h, 3h, 4h, 5h, 6h, 12h, 18h and 24 hours). The expressed recombinant SDMANF was visualized by the presence of bands until around 5 hours after the stimulation of expression, after which was not possible anymore to visualize the bands. B- Recombinant SDMANF purified by Immobilization on Metal Affinity Chromatography (IMAC) with the Profinia™- Protein Purification System. Immunodetection of size-separated protein blotted and probed with anti-HIS tag antibody. The protein was detected at the expected size as indicated by arrow, kDa, Kilodalton; M, Marker. F1, flow through 1; F2, Flow Through 2; W1, Washing Fraction 1; W2, Washing Fraction 2; E1, Elution Fraction 1; E2, Elution Fraction 2.

The production of a second construct (pDEST17™, $nt_{279-516,}$ aa_{28-172}) was required to improve the efficiency of expression of recombinant SDMANF. Therefore, obtain the amount of recombinant SDMANF necessary to develop the antibody. The second construct was developed using a different expression vector (pDEST17™) and contains only a fragment of SDMANF ($nt_{279-516,}$ aa_{28-172}) protein sequence for expression. The recombinant SDMANF was also conjugated with a 6xHis-tagged (HIS-tagged) and expressed on *E. coli.* The protein expected size was 11.6 kDa. The recombinant SDMANF was purified by IMAC purification method on Profinia™-protein purification system. The elution fractions of purified recombinant SDMANF were size-separated (SDS-PAGE) and the gel stained (Fig. 13). The elution fraction 1 was used to raise the polyclonal antibody on rabbit (see E. 4.9) (see Fig 13).

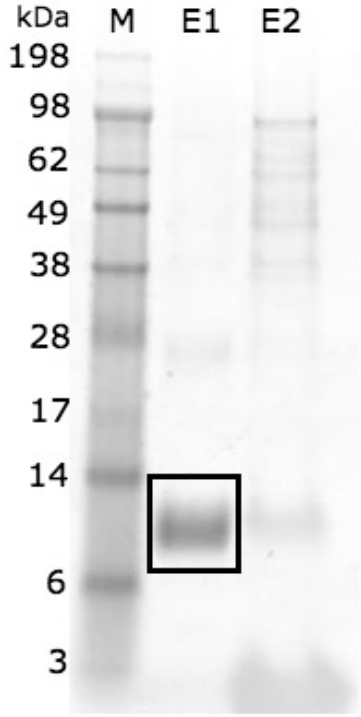

Figure 13: SDMANF recombinant protein expressed in *E. coli* with vector pDEST17™. *Suberites domuncula* Mesencephalic Astrocyte-Derived Neurotrophic Factor (SDMANF) purified recombinant fragment protein ($nt_{279-516}$) expressed in *E. coli*, ca.11.6 kDa, size-separated in SDS-PAGE gel 12%, stained with Gel code™. The E1 fraction used to develop the antibody is marked by a black square. M, Marker; E1, Elution Fraction 1; E2, Elution Fraction 2.

5. Expression of SDMANF within *S. domuncula* tissue

The SDMANF protein was detected on *S. domuncula* tissue preparations by western blots using anti-SDMANF pAbs to assess the expression of SDMANF on sponge tissue (see E. 10). A band with a slightly lower molecular weight (≈ 17 kDa) than expected (≈ 20 kDa), was detected in all total proteins extracts, size-separated (SDS-PAGE) and blotted of eight different *S. domuncula* specimens (Fig. 14).

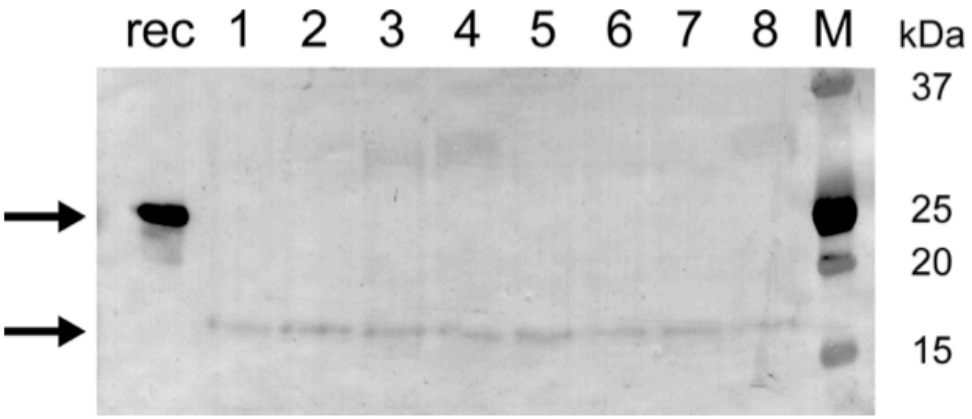

Figure 14: Immunodetection of SDMANF in *S. domuncula* tissue. Immunodetection of *Suberites domuncula* Mesencephalic Astrocyte-derived Neurotrophic Factor (SDMANF), ca. 17 kDa in size-separated and blotted total protein extracts of eight different *S. domuncula* specimens. The recombinant SDMANF (rec) was used as positive control. It was detected at a higher molecular weight than native SDMANF as presumed, due to the presence of to His-tag and other vector-specific aa (ca. 24 kDa). M, Marker; kDa, Kilodalton (Sereno et al 2017).

6. Localization of SDMANF within *S. domuncula* tissue

In order to investigate the cellular localization of SDMANF an immunohistological analysis were performed with tissue sections of *S. domuncula* (see E. 14). The overall staining intensity of sponge tissue can be seen in Fig. 15 A - F. Figures 15 A and D show the prokaryotic/eukaryotic DNA labeled with DRAQ5™ (in Blue). Figure 15 A revealed a bacteriocyte that is composed by the DRAQ5™-stained nucleoids (indicated by a white solid arrow), within bacterial cells that were individually smaller in size than the stained nuclei of the surrounding sponge cells. On Figure 15 D the DRAQ5™-stained nucleus is displayed in a round form, what looks like a multicellular endobiont organism, the Blue stained nucleus are bigger in size than the stained nuclei of the surrounding sponge cells. Figures 15 B and E show the fluorescence labeled SDMANF. The Fig. 15 B revealed a considerable intense and spotted staining pattern of SDMANF indicated by a white solid arrow, a weak and spotted staining of could be observed also a part of it. Figure 15 E shows an intense spotted staining of SDMANF in a round format and a weak and spotted staining of could be observed also a part of it. The fluorescence patterns of the merge SDMANF (in green) and DNA (in Blue) fluorescence patterns of (Fig.

15 C and F) revealed a considerable intense and spotted staining pattern of SDMANF mainly restricted to sponge cells close to the bacteriocyte (indicated by a white solid arrow) (Fig. 15 C) or at the vicinity of what looks like a multicellular endobiont organism (Fig. 15 F).

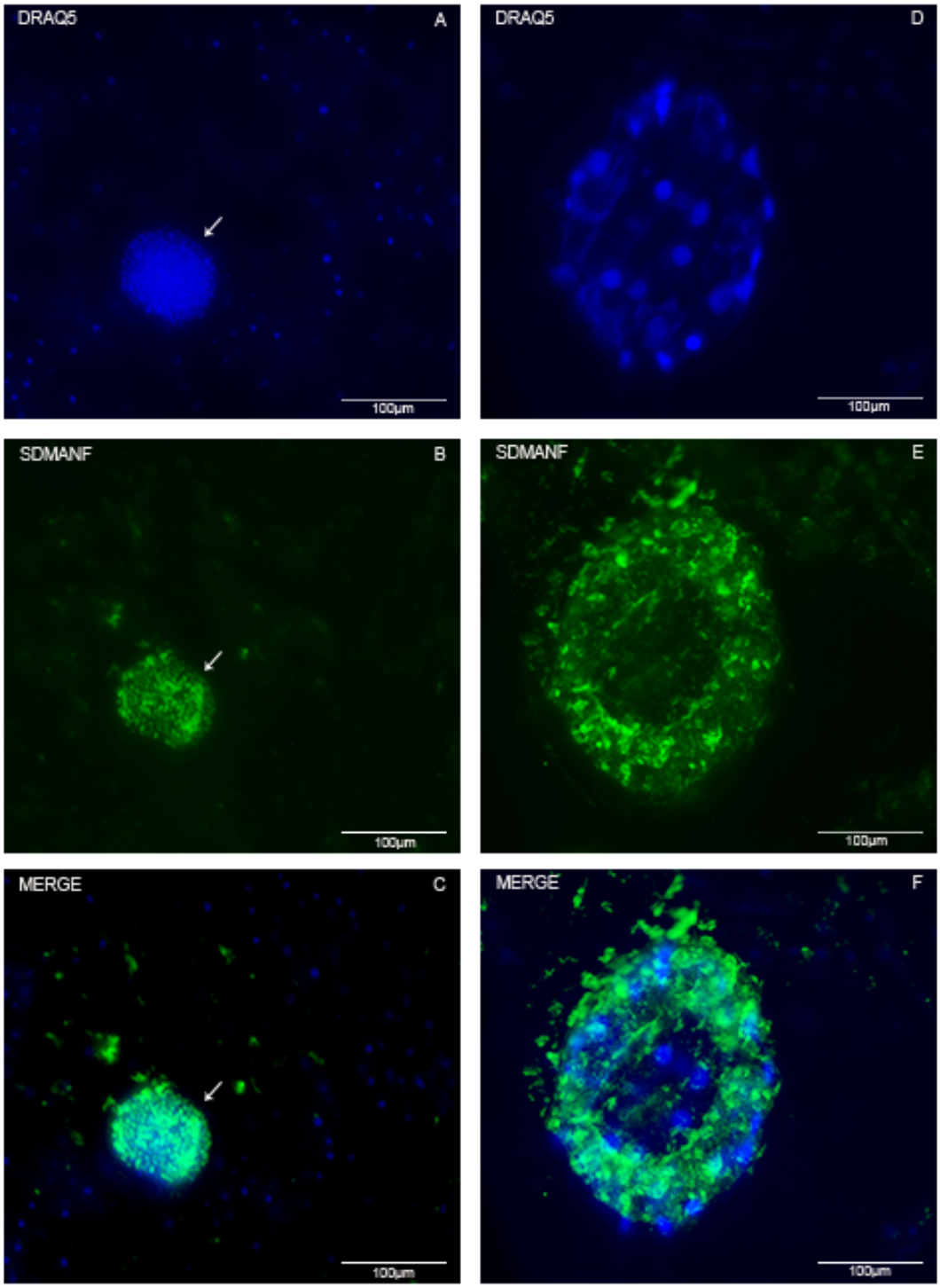

Figure 15: Immunohistological analysis of SDMANF in *Suberites domuncula* tissue. The tissue sections were incubated with *Suberites domuncula*

Mesencephalic Astrocyte-Derived Neurotrophic Factor (SDMANF) antiserum. SDMANF immune complexes were visualized through treatment with Cy™ 2 (green) conjugated secondary antibody and subsequent microscope analysis. The deoxyribonucleic acid (DNA) was counterstained with DRAQ5™ (blue). Merge pictures were used to assess protein co-localization. The prokaryotic/eukaryotic DNA labeled for (A and D; blue), SDMANF (B and E; green). The fluorescence patterns of the merge (C and F) revealed a considerable intense and spotted staining pattern of MANF mainly restricted to sponge cells close to the bacteriocyte (C, indicate by a white solid arrow). This was also observed in the vicinity of what might be an endobiont multicellular organism (F). A weak and spotted staining of SDMANF positive cells could be observed also apart of bacteriocytes (B). Scale bars, 100µm.

7. Development of SDMANF stably transfected HEK cell line

To assess the functional mechanisms of SDMANF the technique of stably transfection of mammalian cells (HEK cells) was applied. The vector construct then expresses the recombinant SDMANF tagged with a tetracysteine Lumio™ tag (TC-tag), which becomes fluorescent upon binding with labeling reagent FlAsH-EDT_2. To confirm the expression of SDMANF on transfected HEK cells, the membrane-permeable FlAsH-EDT2 was applied (Fig. 16 A-C). The two controls (non-transfected (HEK_{wt}) and mock-transfected cells (HEK_{Mock}) presented only weak cellular background fluorescence (see Fig. 16 A and B). The SDMANF-transfected cells (HEK_{SDMANF}), however, show an intense fluorescent staining (Fig. 17 C).

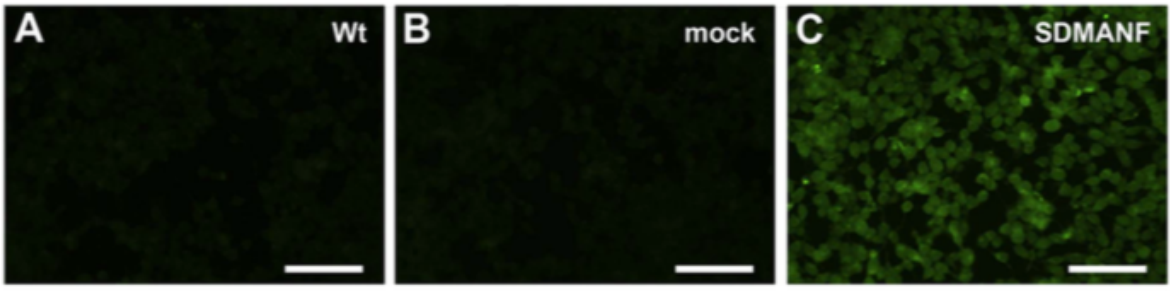

Figure 16: Expression and secretion of SDMANF in stably transfected HEK cells. (A-C) Fluorescence micrographs of (A) non-transfected wild-type, (B) mock transfected, and (C) SDMANF tetracysteine Lumio™ tag (TC-tag)-transfected cells. The recombinant SDMANF that posses a TC-tag, became green fluorescent upon the binding with labeling reagent FlAsH-EDT_2. Scale bars, 100 µm (Sereno et al 2017).

7.1 Clonal selection of stably transfected HEK_{SDMANF}

A pool of transfected HEK_{SDMANF} was selected with Blasticidin antibiotic and a clonal expansion was performed (see E. 17). Thereafter, the selection of a clone that better expressed SDMANF was done through immunodetection by dot blot. The selected clone is indicated by a black square in (Fig. 17). The SDMANF recombinant protein expressed by the transfected cells besides the TC-tag possesses a V5 epitope that allows immunodetection by V5 antibody.

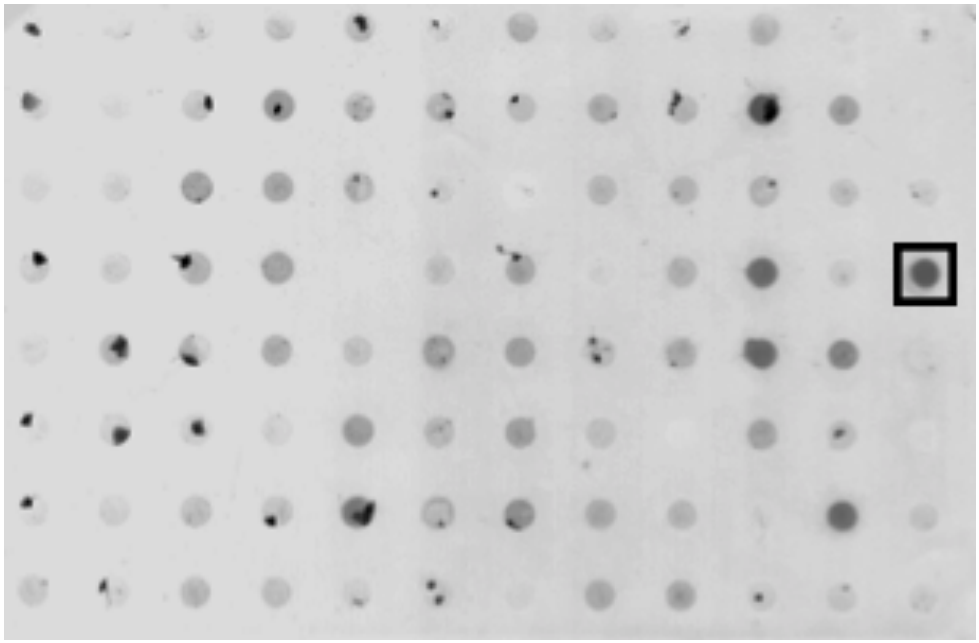

Figure 17: Immunodetection of SDMANF on stably transfected HEK cells. Immunodetection through dot blot of V5 epitope from recombinant *Suberites domuncula* Mesencephalic Astrocyte-Derived Neurotrophic Factor expressed by transfected cells clones. The black square highlights the clone selected for downstream experiments. HEK, Human Embryonic Kidney Cells.

8. SDMANF expression and subcellular localization in transfected cells

In a complementary approach to confirm SDMANF expression and secretion (see E. 18), the total proteins of the different cell lines, i.e. non-transfected wild-type (a), mock transfected (b), and (c) SDMANF-transfected, were extracted, size-separated via SDS-PAGE, blotted, and probed for SDMANF using V5 antibody (Fig. 18 A). The same approach was used to investigate the presence of SDMANF in the cell supernatants (i. e., culture medium) (see Fig. 18 B).

A band was only immunodetected on the blots within the total protein extract of SDMANF transfected cells (Fig. 18 A, lane c) and in the culture medium of SDMANF transfected cells (Fig. 18 B, lane c) but not in the protein extracts of the controls, i.e. wild-type and mock transfected cells. SDMANF was detected at the expected size of ca. 24 kDa (SDMANF including V5 epitope and TC tag). Simultaneously, the subcellular localization of expressed SDMANF was also assayed using the subcellular fractionated protein samples of SDMANF transfected cells. The chromogenic immunodetection shows a band on the blot at the expected size ca. 24 kDa, in the organelle/membrane protein fraction (see Fig. 18 F, lane c) but not in the cytoskeletal (lane a), nuclear (lane b), or cytosolic fractions (lane d).

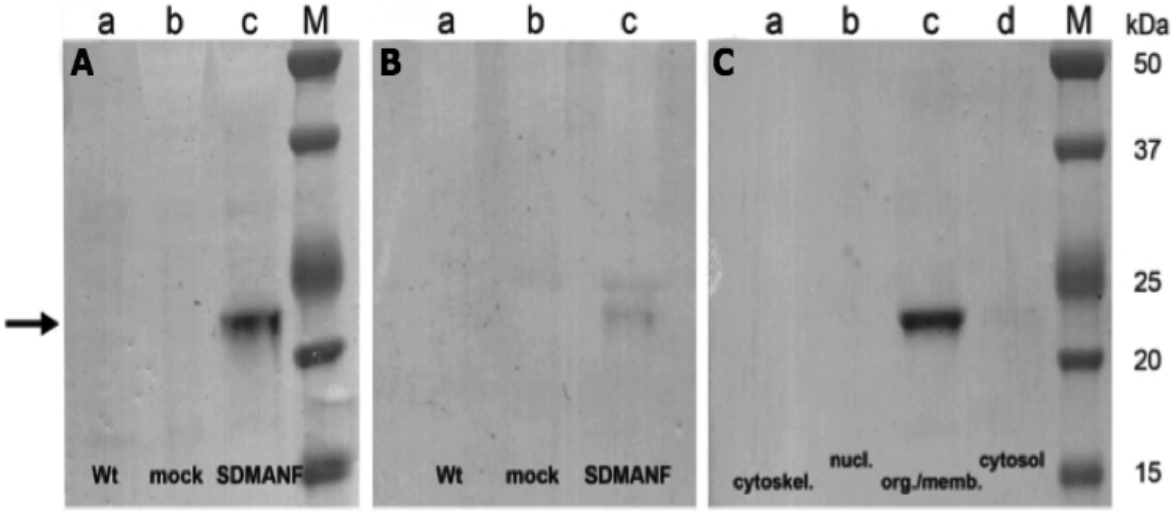

Figure 18: Immunodetection of SDMANF in HEK cell lines. (A-C) Immunodetection of *Suberites domuncula* Mesencephalic Astrocyte-Derived Neurotrophic Factor (SDMANF) in size-separated and blotted protein lysates or culture medium. A- Total protein extracts of (a) non-transfected cells (wild-type), (b) mock transfected, and (c) SDMANF transfected cells. B- Lyophilized medium of the cell culture lines (a) wild-type, (b) mock transfected, and (c) SDMANF transfected cells. C- Protein extracts of different subcellular compartments of SDMANF-transfected cells, extracted with ProteoExtract™ kit: (a) cytoskeleton (cytoskel.), (b) nucleus (nucl.), (c) organelles/membranes (org./memb.), (d) cytosol. SDMANF (including V5 epitope and TC tag) was identified in the total protein extracts of lysates, culture medium, and the organelle/membrane fraction of SDMANF- transfected cells at the expected size ca. 24 kDa (arrow). M; Marker; kDa, Kilodalton; HEK, Human Embryonic Kidney Cells (Sereno et al 2017).

9. Expression of SDMANF in transfected cells upon Brefeldin A and cadmium exposure

To characterize the intracellular transport as a component of secretory pathways, the level of SDMANF was analyzed in transfected cells that had been treated for 6 h with the Golgi/ER transport inhibitor Brefeldin A (BFA). The incubation with BFA (see E. 19) caused a notably rise (i. e., 2.5-fold) on the intracellular level of SDMANF as compared to the untreated control (Fig. 19).

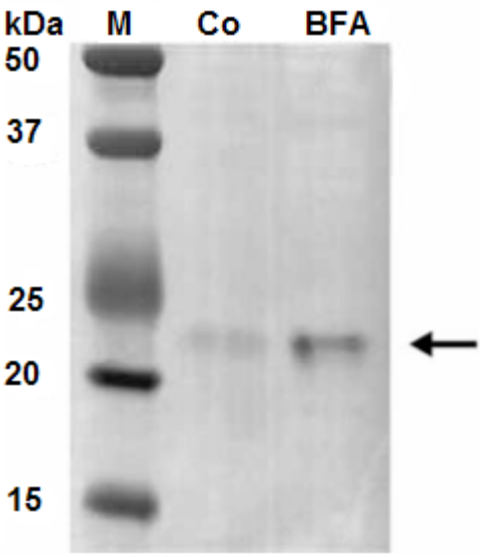

Figure 19: Immunodetection of SDMANF in transfected cells treated with brefeldin A. The *Suberites domuncula* Mesencephalic Astrocyte-derived Neurotrophic Factor (SDMANF) stably transfected cells that had been exposed to Brefeldin A (BFA) for 6 hours or stayed untreated as a control (Co). The SDMANF levels were immunodetected with V5 antibody on size-separated and blotted total protein extracts at the expected size, ca. 24 kDa (arrow). M, Marker; kDa, Kilodalton (Sereno et al 2017).

Furthermore, to assess the SDMANF activity upon a different stressor, the transfected cells were exposed to cadmium concentrations of 25 µm and 50 µm for 0, 6 and 20 hours (see E. 19). The incubation with the stressor caused an increased intracellular level of SDMANF, when compared to the untreated cells (control, Co). An increase of SDMANF levels was observed after cadmium exposition (i.e., 3.1 fold (25 µm) and 3.0 fold (50 µm), 4.8 fold (25 µm) and 8.3 fold (50 µm); 15.9 fold (25 µm) and 39.7 fold (50 µm), in comparison to unchallenged

cells, respectively at 0, 6 and 20 hours (Fig. 20). The levels of SDMANF untreated cells were barely above the detection limit.

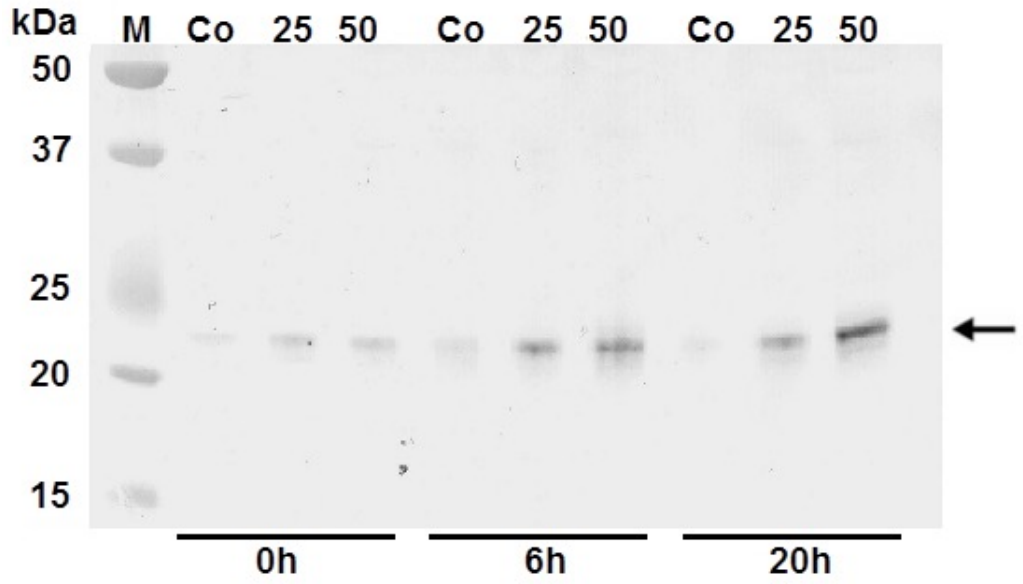

Figure 20: Immunodetection of SDMANF in transfected HEK cells exposed to cadmium. The *Suberites domuncula* Mesencephalic Astrocyte-Derived Neurotrophic Factor (SDMANF) of stably transfected cells that had been exposed to cadmium 25 µm and 50 µm remained untreated, control (Co) for 0, 6 and 20 hours. The SDMANF levels were immunodetected with the V5 antibody on size-separated and blotted total protein extracts at the expected size, ca. 24 kDa (arrow). M, Marker; kDa, Kilodalton; HEK, Human Embryonic Kidney Cells

10. Detection of SDMANF levels and BAX expression on cells upon LPS exposure

To assess the levels of SDMANF and BCL-2-Associated X Protein (BAX) expression after exposure to the endotoxin lipopolysaccharide (LPS) (see E. 19), HEK cells (wild-type, HEK_{wt} and SDMANF transfected, HEK_{SDMANF}) were treated with 0.1 or 1.0 µg/ml LPS for 1, 6 and 12 hours. The control cells remained untreated for the same time period. Afterwards, the total protein extracts were size-separated, blotted, and probed with respective antibodies (V5 antibody to detect SDMANF, BAX antibody, and α-tubulin (Fig 21 A-F). As already demonstrated in Fig. 18 A, the non-transfected cells (HEK_{wt}) showed no expression of SDMANF (see Fig. 21 A). Moreover, in SDMANF transfected cells (HEK_{SDMANF}) controls (not treated with LPS). However, the transfected samples

(HEK_{SDMANF}), treated with LPS presented an increased level of SDMANF (Fig. 21 B).

A positive correlation between SDMANF levels and increase on LPS concentration and incubation time (Fig. 21 B and G) was observed. An increase in SDMANF levels was observed after LPS exposure. The detected levels of SDMANF upon LPS exposure were calculated comparing the levels of SDMANF on controls cells (HEK_{SDMANF} not exposed to LPS) with the levels of SDMANF on HEK_{SDMANF} cells exposed to LPS with there respective incubation time. Thus, the levels of SDMANF increase upon exposure to LPS for 6 h a ca. 3-fold (0.1 µg/ml LPS), 6-fold (1 µg/ml), for 12 h an 11-fold (0.1 µg/ml LPS) and 18-fold (1 µg/ml) was calculated (Fig. 21 G).

The same approach was used to investigate BAX expression. The expression of BAX increased 3-fold on the average upon LPS exposure in a time- and concentration-independent manner in all HEK_{wt} samples, when compared with unchallenged HEK_{wt} control with very low expression levels (see Fig. 21 C and G). However, independent whether the HEK_{SDMANF} samples had been exposed to LPS or not, their BAX expression was barely above the detection limit (see Fig. 21 D and G). The housekeeping gene α-tubulin was applied as a loading control (see Fig. 21 E and F).

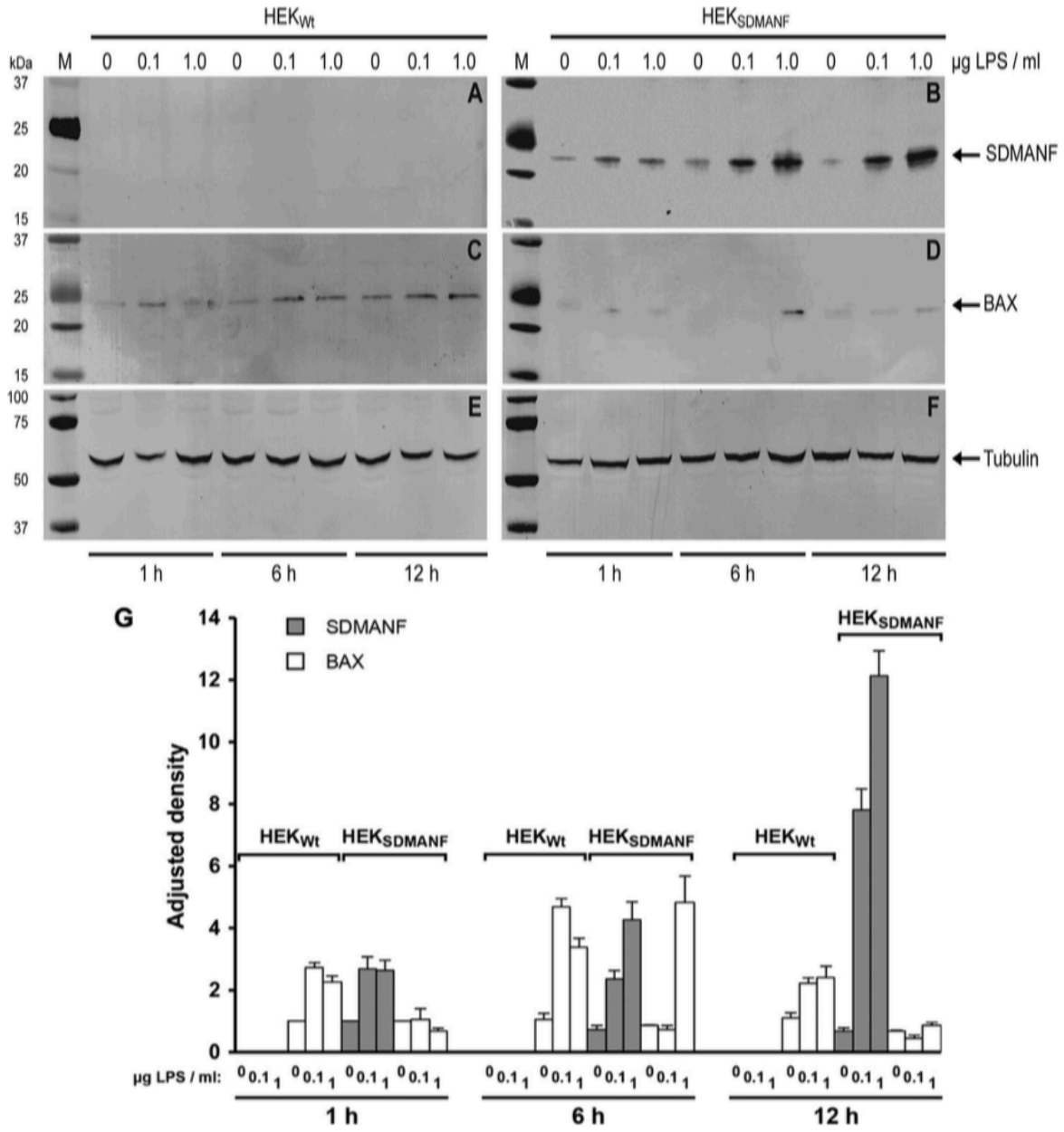

Figure 21: Immunodetection and quantitative analysis of SDMANF and BAX protein expression in HEK cells lines upon exposure to LPS. The *Suberites domuncula* Mesencephalic Astrocyte-Derived Neurotrophic Factor (SDMANF), BCL-2-Associated X Protein (BAX) and α-tubulin (loading control) were probed for in size-separated and blotted protein extracts of wild-type (HEK_{wt}; A, C, E) and SDMANF stably transfected (HEK_{SDMANF}; B, D, F) cells using respective antibodies. Cells had been incubated with 0, 0.1, or 1 µg of lipopolysaccharide (LPS) per ml for 1, 6 or 12 h. Proteins were detected at the respective expected size (arrows). Blots are representative of three independent experiments. (G) Densitometric analysis of immunodetected SDMANF (grey columns) and BAX (white) in HEK cells for quantification of protein levels. The relative density of each sample protein band was divided by the relative density of respective α-tubulin loading control band to calculate the adjusted density. Values are means ± standard deviation (n = 3). M, Marker; h, Hours; HEK, Human Embryonic Kidney Cells (Sereno et al 2017).

11. Viability and caspase activity of transfected cells upon LPS exposure

To evaluate both viability and caspase activity of HEK_{SDMANF} transfected cells upon LPS exposure (see E. 19), cells were exposed to 1 µg/ml LPS for 12 h and then assayed. To analyze cell viability, cells were incubated with the peptide substrate GF-AFC. It is cell-permeant and becomes fluorescent when cleaved by live-cell proteases. The ensuing quantitative fluorescence analyses showed no significant differences between the untreated control samples (wild-type, mock transfected, and SDMANF-transfected cells) (Fig. 22 A). Nevertheless, the incubation with LPS reduced the viability of wild-type cells by 40% and mock transfected cells by 34% respectively (Fig. 22 A). However, in SDMANF-transfected cells, the viability was reduced by only 11% (see Fig. 22 A). Concomitantly, to assess caspase 3 activity, cells were incubated with cell-permeant NucView™ 488 that only becomes fluorescent in apoptotic cells, because the activated caspase 3 facilitates cleavage and consequently the releases of a green fluorescent stain. A comparative analysis of the fluorescence signals showed no significant differences between the untreated samples, i. e. controls (Fig. 22 B). However, in all treated samples LPS significantly induced caspase activity above the control levels, in wild-type the caspase activity increased by 42%; in mock-transfected cells the increase was 46%, while in SDMANF-transfected cells the increase on caspase activity was considerably lower with 18%, when compared to the control (see Fig. 22 B).

Caspase 3 activity was also assessed by visualization in real-time with an automated cell imaging system (see E. 19). The cells were exposed to 1 µg/ml LPS for up to 15 h. The NucView™ 488, mentioned above, was used to detect caspase 3 activity; Propidium Iodide (PI) was used to stain nuclei of dead cells/cells with compromised cell membranes; and Hoechst 33342 was used for staining all cells. As a result, the untreated control samples (wild-type and SDMANF-transfected cells) presented almost no caspase 3 activity with scarce green fluorescence signals that barely increased with time. Additionally, no significant red staining of dead cells/cells with compromised cell membranes was detected by PI (Fig. 23). Wild-type cells (HEK_{wt}) exposed to LPS presented a considerably higher green staining as soon as after 6 h exposure to the endotoxin, followed by a significant enhancement of fluorescence up to 15 h exposure time. In SDMANF-transfected (HEK_{SDMANF}) cells, however, the LPS treatment weakly

induced caspase 3 activity, barely above the background fluorescence. Besides, the caspase activity stayed constant throughout the 15 h of exposure. In both cell lines, HEK_{wt} and HEK_{SDMANF}, PI elicited only few red fluorescence signals (Fig. 23).

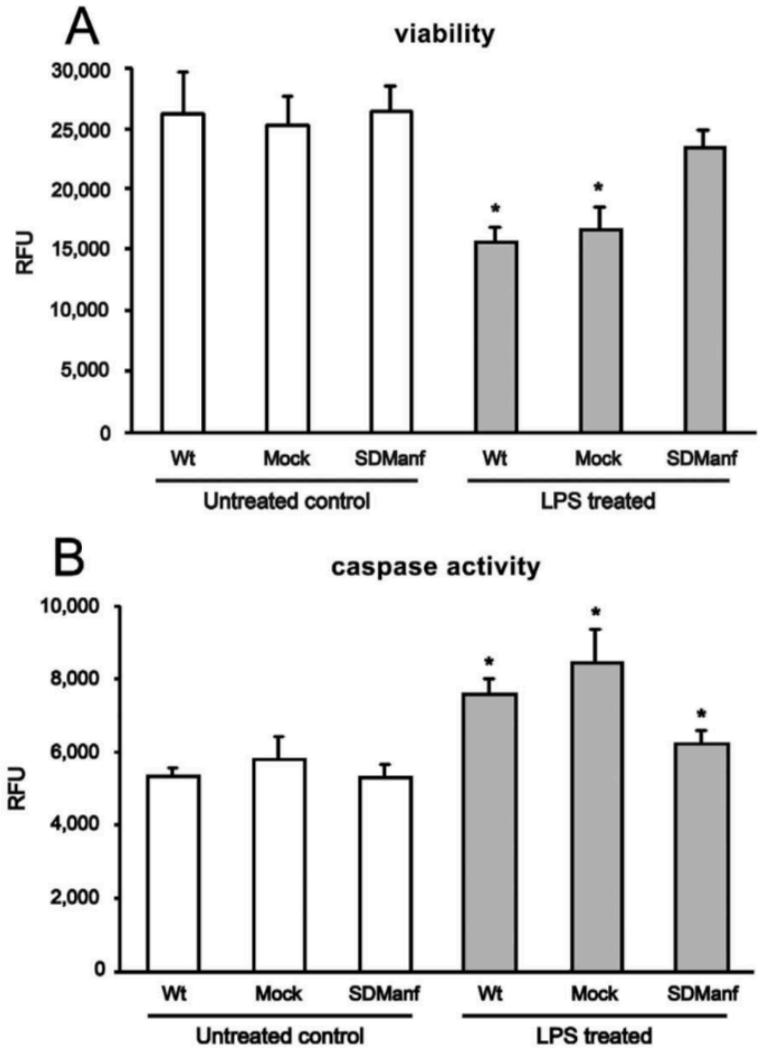

Figure 22: Viability and caspase activity of HEK cells upon LPS exposure. Activities of intracellular live-cell proteases (viability, A) and caspase 3 (B) were assessed with the cell-permeant fluorogenic substrates peptide GF-AFC and NucView™ 488 respectively. Fluorescence was quantified in wild-type (wt), mock transfected, and SDMANF-transfected cells that had remained untreated (controls, white bars) or that had been incubated with Lipopolysaccharide (LPS) for 12 h (grey). Values are expressed as the mean ± standard deviation of four independent experiments, compared by ANOVA, followed by the post-hoc Tukey HSD test. *$p < 0.01$ versus untreated control. RFU, Relative Fluorescence Units (Sereno et al 2017).

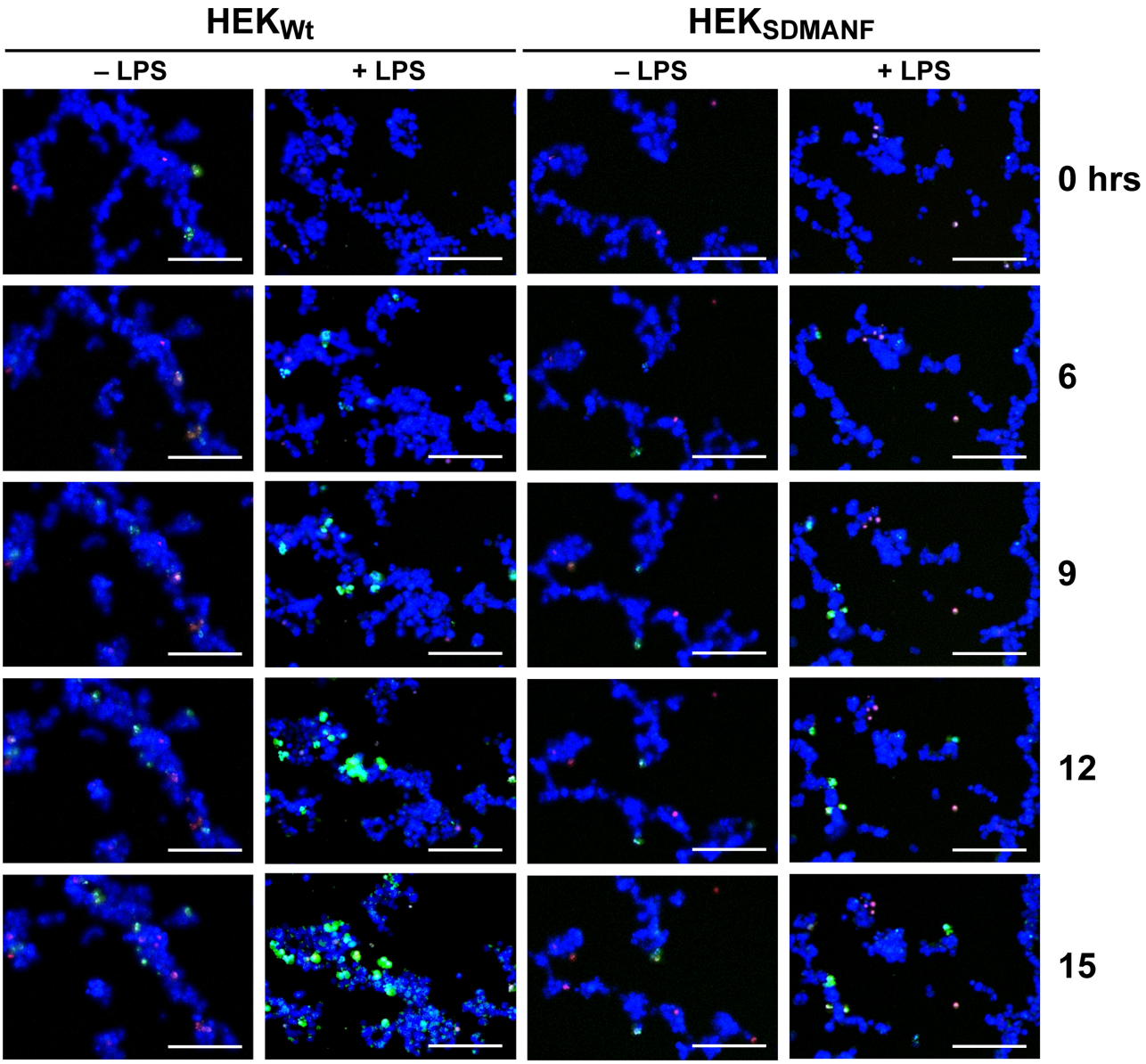

Figure 23: Fluorescence micrographs of HEK cells recorded in real-time with an automated cell imaging system. The wild-type cells (HEK_{wt}) and SDMANF-transfected cells (HEK_{SDMANF}) were exposed to 1 µg/ml LPS for up to 15 hours. The NucView™ 488 dye (green) (see text) was used to detected caspase 3 activity, Propidium Iodide (magenta) was used to stain nuclei of dead cells/cells with compromised cell membranes and Hoechst 33342 (blue) for staining of all cells. HEK, Human Embryonic Kidney Cells. Scale bars, 200 µm. (Sereno et al 2017).

G. DISCUSSION

The Cerebral Dopamine Neurotrophic Factor (CDNF) and Mesencephalic Astrocyte-Derived Factor (MANF) form the most recently discovered family of neurotrophic factors, that are evolutionary conserved, posses a distinctive structure and a mode of action mode that differ from the classic NTFs (Voutilainen et al 2015; Lindström et al 2017; Li-na et al 2017; Zhang et al 2018).

Mesencephalic astrocyte-derived factor presents neurotrophic and neuroprotective activities as well as neurorestorative effects in different neurodegenerative disease models, including Parkinson's disease, ischemia and traumatic brain injury (see C.3.4; Lindahl et al 2017). Furthermore, MANF also protects neuronal and non-neuronal tissue against ER stress (Wang et al 2018). This particular set of characteristics leads to its introduction as a potential therapeutic agent for the treatment of pathological conditions such as stroke, diabetes, glaucoma and retinal disorders (see C.3.4; (Mätlik et al 2018, Gao et al 2017b; Li-na et al 2017; Lu et al 2018; Hakonen et al 2018). Not by chance, in 2018 MANF was approved by the United States Food and Drug Administration (US-FDA) to be tested for treatment of retinitis pigmentosa and retinal artery occlusion (Amarantus bioScience Inc).

Despite the promising therapeutic applications of MANF and its multiple functions on neuronal and non-neuronal tissue, ER stress and development (Wang et al 2014b; Stratouilias and Heino 2015b; Kim et al 2017a; Lindahl et al 2017; Tseng et al 2017a; Xu et al 2018), the MANF homologs underlying mechanisms of activities have not yet been fully understood (Voutilainen et al 2015; Lindahl et al 2017; Wang et al 2018). Hence, the use of a new organism model, as sponges, can rise new insights on MANF mechanisms of function.

The aim of the present work was to identify and functionally characterize MANF in sponges. The Phylum Porifera is among the oldest Metazoa lineages and has been considered the earliest branching of Metazoa (Li et al 1998; Love et al 2009; Müller et al 2004a; Wörheide et al 2012; Renard et al 2018). Thus, sponges are important in the reconstruction of early metazoan evolution (Müller et al 2004a; Wörheide et al 2012). Sponges lack a conventional metazoan nervous system, however, structural and molecular evidence has been gathered for some kind of neuronal-like signaling and a (pre-)nervous system is present in sponges

(Leys and Meech 2006; Conaco et al 2012a; Leys 2015; Whitmer 2018). In view of these particular characteristics, sponges can be used as an animal model system to study the evolution of the nervous system, and furthermore, sponges offer an enticing opportunity to explore the evolutionary aspects and ancient roles of MANF before the advent of nervous system.

1. SDMANF homologies and phylogenetic relationships

The deduced *Suberites domuncula* MANF protein (SDMANF) established in this study shows similarities with the MANF homolog as expected, because MANF protein exists in both vertebrate and invertebrate species (Petrova et al 2003), while CDNF is a paralog that can only be found in vertebrates (Lindholm et al 2007).

The SDMANF protein shows a significant degree of sequence homology to both invertebrates and vertebrates MANF, although with higher homology to vertebrates (see Table 1 and Fig. 11). The phylogenetic analysis through the consensus tree shows that both *S. domuncula* and *Amphimedon quenslandica* poriferan MANF (predicted, using SDMANF for comparison, from NCBI's automated computational analysis based on the whole *A. quenslandica* genome shotgun sequences) have particularly high homology to Deuterostomia (see Fig. 11). Therefore, sponges were placed at the basis of a clade comprising well-supported deuterostomian lineages with robust bootstrap values. These overall characteristics are in accordance with former studies (Halanych 2004; Mallat and Winchell 2007; Pisani et al 2015). Moreover, the MANF sequences from Ecdysoza (Nematoda, Crustacea and Hexapoda) composed a sister group to the Porifera clade.

On the majority of phylogeny analysis, sponges are placed at the basis of Metazoa clade (Feuda et al 2017; Simion et al 2017, Renard et al 2018). However, on the phylogenetic analysis of MANF gene, Porifera was placed at the basis of the Deuterostomian clade. This apparently closer similarity between sponge and deuterostomian protein sequences than compared to Ecdysozoan sequences has already been previously observed (Harcet et al 2010). This is possibly an effect of the relatively rapid rate of gene evolution, which is a trait facilitated by shorter generation times and larger population sizes, all features that are common for

Ecdysozoa (Harcet et al 2010, Babenko and Krylov 2004). Together with, uses of only one gene, as we only uses MANF gene, to build the phylogeny analysis provide insufficient information for resolving the relationships between major metazoan lineages because the variable rates of evolution among lineages affect the resolution (Rokas et al 2003; Nosenko et al 2013).

1.1. The likely presence of unfolded protein response mechanism in Poriferan

Mechanism of unfolded protein response (See C. 2) are evolutionary conserved and have many important functions on development and homeostasis of Metazoa (Hetz 2015; Godin et al 2016; Kratochvílová et al 2016; Hetz and Papa 2018).

Considering that proteins components of the UPR pathway I) Activating Transcription Factor 6 (ATF6), ER stress sensor protein, II) X-Box Binding Protein 1 (XBP1) component of the IRE1 ER stress sensor pathway, III) Activating Transcription Factor 4 (ATF4) component of the PERK ER stress sensor pathway, have been identified in sponges (Tood et al 2008; Hollien 2013; Jindrich and Degnan 2016); the identification of *S. domuncula* MANF is not unexpected. Sponge MANF probably play roles on ER stress response, a characteristic that have been described for all MANF homologs so far (Lindström et al 2016; Lindahl et 2017; Bai et al 2018). Here I suggest the possibility that UPR response mechanism or a similar mechanism is present in Porifera.

2. Characteristics of the SDMANF sequence

The results show that SDMANF has the same characteristic features described for other MANF protein from vertebrates and invertebrates (Hellman et al 2011; Richman et al 2018). As the ARMET, Saposin and SAP domains, CXXC motif, a N-terminal signal peptide sequence and the ER retention signal motif, a KDEL-like sequence (see Fig. 9).

The ARMET domain of poriferan MANF begins a few amino acids after the N-terminal predicted signal peptide and covers approximately the whole MANF protein sequence (SDMANF $aa_{25\text{-}172}$). A pair of consensus sequences of the ARMET domain has been deduced from SDMANF and other metazoan MANF sequences: ARMET domain N-terminal pattern NH_2—C-[KRHNQMLAS]-

[EDSTAGK]-[ATLVS]-[KRN]-[GS]-K-[DE]-[ENSH]-[RL]-[FLM]-C-Y-Y-[VLI]—COOH (aa_{62-76} of the SDMANF sequence) and a C-terminal patternNH_2—[VAIMT]-[DEN]-L-[KRWQSNGL]-[KST]-[LM]-[RK]-V-[KRTAV]-[EDKQ]-L-[KR]-[KRQ]-[IV]-L—COOH ($aa_{128-142}$ of the SDMANF sequence) (Sereno et al 2017).

Moreover, SDMANF and also MANF protein from other representative Metazoa present, within the ARMET domain, a highly conserved amino acid residue region termed MANF/BCL-2 Homology Domain [MBHD]; ($aa_{130-156}$) (Sereno et al 2017). MANF homologs, including the poriferan MANF, present a region in which C-terminal overlaps with the conserved BH2 domain of BCL-2 proteins ($aa_{145-156}$ of SDMANF) following the motif signature of the BH2 domain (PROSITE PS01258), NH_2—W-[LIMG]-x(3)-[GR]-G-[WQC]-[DENSAV]-x-[FLGAK]-[LIVFTC]—COOH; with three exceptions (marked in bold), where the poriferan sequence is concerned (Sereno et al 2017).

The BH2 sequence motif is present in most pro- and anti-apoptotic BCL-2 proteins and the BH2 domain has important activities on apoptosis modulation, because of its function in protein–protein interactions and homo- and heterodimerization with BAX protein and other members of the BCL-2 family (Gurudutta et al 2005; Westphal et al 2011; 2014; Aouacheria et al 2013; Moldoveanu et al 2014; Jeng et al 2018). In this context, it is also important to mention that BAX interacts not only with members of the BCL-2 family (Vogel et al 2012; Garner et al 2016). It has been also suggested that an inactive dimer conformation of BAX has an auto-inhibitory function, playing a part in apoptosis mechanism (Vogel et al 2012; Garner et al 2016).

The identification of MANF/BCL-2 homology domain supports the idea that SDMANF and others MANF homologs partake in the competitive interactions entailing BCL-2 proteins, having a role in regulating apoptosis mechanisms. Although to confirm this proposed protein interaction experimental evidence is necessary (Sereno et al 2017).

Some possible interplays of MANF homologs and BCL-2 family proteins have been observed: I) Cunha et al (2017) show that Thrombospondin 1 cytoprotective effect involves the maintenance of expression of human MANF on β-cells, and then MANF prevents BH3-only protein BIM (BCL2-Interacting Mediator of Cell Death)-Dependent of Triggering Apoptosis. II) Treatment with

recombinant human MANF induce a increase of BCL-2/BAX ration and show reduced neuronal death on rat model of intracerebral hemorrhage or spinal cord injury (Gao et al 2018; Xu et al 2018).

A few others BH2-bearing BCL-2 homologs have been described in *S. domuncula* and other sponges (Wiens et al 2004; 2006). Caria et al (2017), in a study on BCL-2 homologs of sponges showed that the BCL-2 BHP2 homolog of *L. baicalensis* and of *G. cydonium* are able to bind the *L. baicalensis*- BCL-2 antagonist killer (BAK)-2. This demonstrates that sponge BHP2 binds to multi-motif BAX-like proteins and the binding groove is conserved across pro-survival BCL-2 proteins, functioning in a similar way to the mammalian apoptotic mechanisms (Caria et al 2017).

The SDMANF protein presents the eight-conserved cysteine residues (See Fig. 9 and Fig. 3), which are a trademark of MANF homologs (Parkash et al 2009; Hellman et al 2011). The position of the eight-conserved cysteine residues in SDMANF, according to the amino acid sequence matches the other MANF homologs. Also resembling other MANF homologs, SDMANF possess the CXXC motif (See Fig. 9 and Fig. 3), within the cysteine residue (Mätlik et al 2015).

Poriferan SDMANF as the majority of metazoan homologs comprises the characteristic eight conserved cysteine residues and their conserved spacing, within the context of NH_2—C-x(2)-C-x(29,30,**31**)-C-x(10)-C-x(30)-C-x(10)-C-x(33)-C-x(2)-CCOOH (aa_{27-152}), with one exception marked in bold (Sereno et al 2017). Very few sequences lack the first cysteine residue, which is the case of *Myotis brandtii* MANF (EPQ17481.1) (Sereno et al 2017).

Subeites domuncula MANF protein has an N-terminal signal peptide (See Fig. 10) for protein targeting to ER, as other MANF homologs (Parkash et al 2009; Hoseki et al 2010; Hellman et al 2011). As shown by Oh-hashi et al (2013), and also Norisada et al (2016), the protein targeting through the signal peptide has also roles in secretion, when the signal peptide is lacking, MANF loses the ability to be secreted.

Furthermore, SDMANF possesses a C-terminal ER retention KDEL-like motif sequence (see Fig. 9), a feature that has been reported from all MANF sequences (Mizobuchi et al 2007; Oh-hashi et al 2012; Henderson et al 2013). KDEL is a canonical ER retention signal sequence that prevents secretion of

soluble ER resident proteins (Raykhel et al 2007). The KDEL motif binds to the KDEL receptors, localized in the intermediate compartments and Golgi apparatus, which triggers the retrieval of the protein to the ER via coat protein I (Raykhel et al 2007), while the coat protein II mediates the transport and secretion of MANF (Ohhashi et al 2012).

Mesencephalic astrocyte-derived factor homologs, including SDMANF, also possess a variation pattern on the canonical KDEL motif NH2—[R,P,K,Q,**H**]-[T,A,S,R,P,**V**]-[D,E]-L—COOH pattern (with two exceptions concerning SDMANF, marked in bold) (Sereno et al 2017). Although most deuterostomian MANF homologs have an RTDL sequence as variant of the KDEL-like motif (Henderson et al 2013). For invertebrates it displays a wider range of sequences with a consensus of [R,K,H]-[S,T]-E-L for Hexapoda, R-E- [D,G]-L for Crustacea, and [R,K]-[D,E]-E-L for Nematoda (Sereno et al 2017).

The SDMANF KDEL-like motif is formed by the HVEL amino acids. Supporting the functionality of SDMANF KDEL-like motif, this sequence has already been reported as a functional ER retention signal in vertebrate cells (Robbi and Beaufay 1991; Raykhel et al 2007).

The establishment of the consensus sequences for ARMET, BH2 domain and CXXC motif and KDEL motif demonstrate the conservation of general features from MANF homologs from invertebrates and vertebrates and the evolutionary conservation of MANF characteristics features also extend to *S. domuncula* MANF. It is accordance with the observation that MANF and CDNF compose the first family of NTF with a well-conserved protein sequences on multicellular organisms (Zhang et al 2018).

3. Structural homology model of SDMANF

As mentioned before, MANF is a bi-functional protein with roles in survival of dopaminergic neurons and in ER stress (Petrova et al 2003; Voutilainen et al 2015; Richman et al 2018). The main hypothesis to explain MANF's bi-functional activity suggests that it is associated with two well-defined domains, N- and C-terminal, each one possibly have two different targets: an intracellular target that is associated with the endoplasmic reticulum and an extracellular target that is modulated by the secreted MANF (Mätlik et al 2015; Kim et al 2017a; Lindahl et al

2017). However, the two domains may have distinct functions since the intact full-length protein is required for MANF function (Hoseki et al 2010; Hellman et al 2011) and only the mature MANF - and none of its isolated domains - was able to reduce larval lethality in *D. melanogaster* (Lindström 2013).

Structural analyses of MANF show that the N-terminal domain of MANF resembles Saposin-Like Proteins (SAPLIPs), being structurally close to the membrane-lytic proteins such as granulysin and NK-Lysin (Parkash et al 2009). The saposin-like proteins are phylogenetically conserved proteins with a diverse range of functions such as lipid-membrane interactions, immunity response and apoptosis (Anderson et al 2003; Bruhn 2005; Kolter and Sandhoff 2005; Linde et al 2005; Wei et al 2016). Lipids also interplay with the immune response, having roles at different phases of host–pathogens interactions such as primary recognition and host cell signaling during invasion (Helms et al 2006; Walpole et al 2018). The granulysin and NK-Lysin are cytolytic effectors involved in antimicrobial defense; acting against microorganisms such as bacteria, fungi, mycobacteria and parasites, and intracellular parasites (Bruhn 2005; Linde et al 2005; Nagasawa et al 2014; Wei et al 2016; Dotiwala et al 2016). As predicted by the N-terminal domain similarities with SAPLIPs, both human and *C. elegans* MANF are able to directly bind sulfatide, this lipide-sulfatide construct is possibly involved in MANF endocytic processes (see C3.1 and 3.3; Bai et al 2018).

The C-terminal domain of human MANF and CDNF is a structural homolog of the C-terminal SAF-A/B Acinus and PIAS (SAP) domain of Lupus Ku Autoantigen Protein p70 (Ku70) (Hellman et al 2011; Lindahl et al 2017). Ku70 blocks BCL-2- Associated X Protein-dependent (BAX) inhibiting apoptosis (Gomez et al 2007; Hada et al 2016).

Besides, to assess the possible three-dimensional structure of SDMANF, two 3D homolog models of the mature SDMANF ($aa_{20\text{-}172}$) were developed with UCSF chimera and Modeller (see D 7.1). The first model uses the human MANF crystal structure PKB 2W51, described by Parkash et al (2009), as backbone. The second model uses the human MANF structure PKB 2KVD, obtained through NMR and described by Hellman et al 2011, as backbone. Initially, PKB 2W51 was used for structural comparison of the N-terminal domain of human MANF with SAPLIP domain, whereas PKB 2KVD was used for structural comparison of the C-

terminal domain of human MANF with the SAP domain. These two different approaches elicited, two homologous structural models of SDMANF, of which the one of Hellman et al (2011) remains the most accepted one (Voutilaine et al 2015; Lindahl et al 2017). The modeled 3D structure of SDMANF (Fig. 24) has two well-defined N-and C-terminal domains that resemble the aforementioned SAPLIP and SAP domains (Parkash et al 2009; Hoseki et al 2010; Hellman et al 2011). Thus, the N-terminal and C-terminal domain of SDMANF comprise five (α1 to α5) and three helices (α 6 to α8) respectively. SDMANF model based on the 2W51 structure of Parkash et al (2009) shows an almost complete overlap of the helices of both proteins (Fig. 25 A). On the other hand, the SDMANF model that is based on the 2KVD structure by Hellman et al (2011) have as the template eight alpha helices, although the alpha helices positions do not overlap, concerning the SDMANF amino acid sequence (Fig. 25 B).

The N-terminal domain of SDMANF predicted by both 3D models (see Fig. 24) is formed by five alpha helices (α1 to α5) that are connected by a flexible linker to the C-terminal domain. The structural conformation of SDMANF N-terminal domain resembles the structure of human MANF described by Parkash et al (2009) and Hellman et al (2011).

Then, the C-terminal domain of SDMANF (see Fig. 24 B) was predicted to have three alpha helices (α6, α7 and α8) according to the 2KVD structure. Contrarily, the SDMANF model predicted by the 2W51 structure has only two helices (α6, α7). This divergence of the number of C-terminal alpha helices was already described for human MANF (Hellman et al 2011): the structure of human MANF described by Parkash et al (2009) has only two C- terminal alpha helices (see Fig. 25 A) whereas according to Hellman et al (2011) it has three C- terminal alpha helices (see Fig. 25 B). It is important to note that, as Parkash et al (2009) reported, a poor quality of the electron density maps at the C-terminus may induce a lower resolution of the C-terminal model. This issue is the most probable cause of the differences observed between the structures of human MANF.

The structurally homolog model suggest SDMANF has a protein structural similar to other MANF homologs. The MANF and CDNF proteins compose a novel family of evolutionary conserved neurotrophic factors, each are structurally different from the typical neurotrophic factors, such as the glia cell-line derived

neurotrophic factor family of ligands (Nasrolahi et al 2018; Axelsen and Wolabye 2018; Zhang et al 2018).

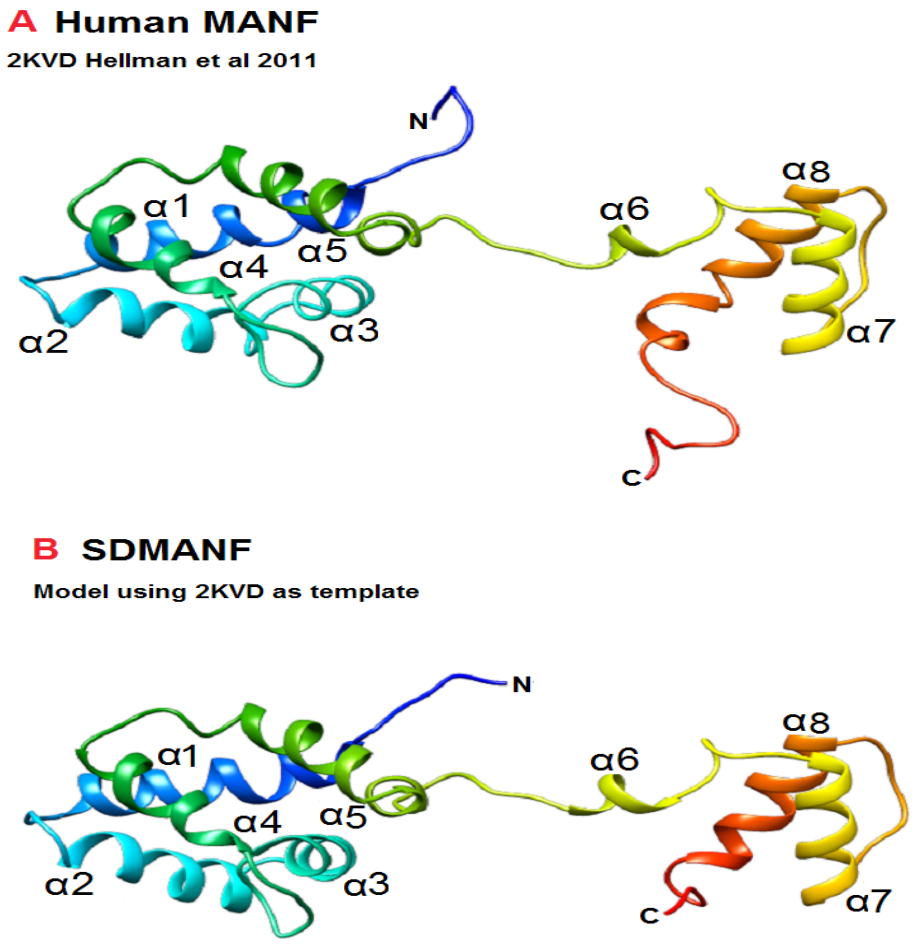

Figure 24: Schematic ribbon presentation of folding of human and *S. domuncula* MANF. A- Schematic representation of mature human Mesencephalic Astrocyte-Derived Neurotrophic Factor (MANF, $aa_{25\text{-}182}$, PKB accession number 2KVD, Hellman et al 2011) ribbon color-coded from blue to red. All helices are labeled. B-Schematic representation of mature *Suberites domuncula* Mesencephalic Astrocyte-Derived Neurotrophic Factor (SDMANF, 20-172aa) protein homolog model using protein data bank accession number 2KVD, Hellman et al 2011 as template. It is represented in the same scheme, orientation and color as (A). For both proteins, the N- terminal (N) and C-terminal (C) domains are well defined. The N-terminal domain has five alpha helices (α1 to α5), while the C-terminal is formed by three helices (α6 to α8). Both domains (N- and C-) are connected with a flexible linker followed by the alpha helices (α6 to α8) that form the C-terminus. The schematic representation and analysis was performed with UCSF Chimera and Modeller.

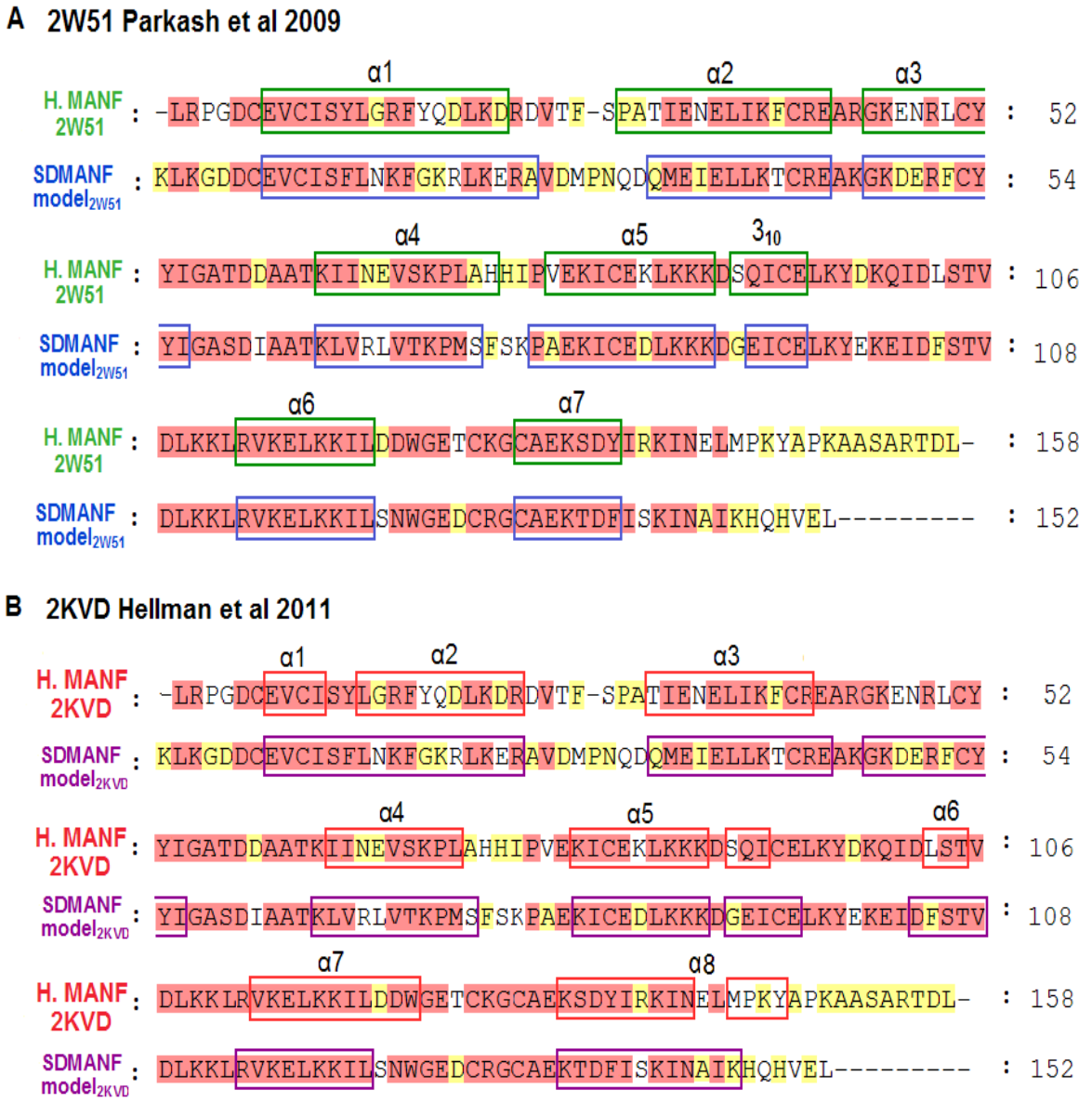

Figure 25: SDMANF homology model. A- Amino acid sequence alignment of *Suberites domuncula* Mesencephalic Astrocyte-Derived Neurotrophic Factor (SDMANF) and human Mesencephalic Astrocyte-Derived Neurotrophic Factor MANF (H.MANF), depicting secondary protein structures: marked in green, the human MANF model 2W51 and in blue the SDMANF model 2W51, based on the protein data bank (PDB) structural model 2W51 as template. B- Amino acid sequence alignment of SDMANF and human, depicting secondary protein structures: marked in red, the human MANF model 2KVD and in purple the SDMANF model 2KVD, with the PDB structural model 2W51 as template. The structural models were built with UCSF Chimera and Modeller. The residue conservation in the sequences (identical or similar with respect to physicochemical properties) at 80% are highlighted in a pink background and at 60% are highlighted in yellow background.

4. Expression and localization of SDMANF in *S. domuncula tissue*

4.1. Expression of SDMANF in *S. domuncula tissue*

The expression of SDMANF was detected on *S. domuncula* tissue as expected. Although, it presents a slightly lower molecular weight than expected and this difference in weight could be an indication of either the proteolytic cleavage of the presumed signal peptide sequence or abnormal protein migration during SDS-PAGE.

4.2. Localization and putative function of SDMANF in *S. domuncula tissue*

A few roles of MANF on immunity modulation have been suggested. For instance, as MANF transitorily enhances the amount of phagocytic macrophages and also improves behavioral recovery upon treatment with recombinant human MANF of ischemic stroke in a mouse model (Mätlik et al 2018). In *Drosophila,* an increase of MANF expression was identified during the activation of the immune response (Stratoulias and Heino 2015a). In addition, the expression of MANF was also induced in *Drosophila* hemocytes (macrophage-like innate immune cells) and in murine microglia cells after light-induced retinal damage, MANF immune modulation induces the switch from proinflammatory to pro-repair profile, promoting tissue repair and regeneration of the retina (Neves et al 2016).

Moreover, human MANF reduces the levels of pro-inflammatory cytokines such as IL-1β, IFN-γ and, TNF-α upon LPS exposition in neural stem cells (Zhu et al 2016) and also under different stress stimuli (Zhao et al 2017; Chen et al 2015a; Cunha et al 2017; Li et al 2018). Cytokines contribute to immune response and have a critical role mediating host defense against parasites and also on autoimmune processes (Kabelitz and Medzhitov 2007; Smith et al 2018).

The possibility of MANF protein also has a role in autoimmune diseases have been considered because patients with autoimmune disorder as rheumatoid arthritis and systemic lupus erythematosus show enhanced levels of MANF in isolated peripheral white blood cells, along with patients recently diagnosed with Type 1 diabetes presented higher serum concentration of MANF (Wang et al 2014a; Chen et al 2015a; Galli et al 2016).

A few activities of MANF on immune modulation have been reported,

although the roles of MANF on immune system remain unknown. In the same fashion, it also remains unknown whether MANF has antimicrobial functions like other proteins from the SAPLIPs granulysin and NK-lysin.

In the present study, both SDMANF expression in sponge tissue and SDMANF functions in sponges were evaluated. SDMANF expression was identified mainly restricted to sponge cells close to bacteriocytes and in the vicinity of what might be a multicellular endobiont (see Fig. 15). Sponges host a community of organisms, like nematodes, brittle-stars, copepods, bacteria, etc. (Magnino et al 1999; Ribeiro et al 2003; Skilleter et al 2005), which forms the poriferan intracellular and/or extracellular endofauna. Bacteriocytes are specialized cells present in some sponges that host different kinds of bacterial cells that might be either symbiotic or a food resource. *S. domuncula* bacteriocytes are mostly filled with gram-negative bacteria (Vacelet and Donadey 1977; Woollacott 1993; Ilan and Abelson 1995; Böhm et al 2001; Uriz et al 2012). Even with the highly diverse community of multicellular organisms and bacteria in the mesohyle hosted by sponges (See C.4; Taylor et al 2007; Hentschel et al 2012), SDMANF was detected mainly in the vicinity of bacteriocytes, suggesting some activity on recognition/response mechanisms. The mechanisms sponges uses to differentiate between bacteria (food, pathogens or symbionts) have not been completely elucidated (See C.4). These mechanisms are probably connected to immune system pathways (Hentschel et al 2012; Gardères et al 2015a; Degnan 2015).

Furthermore, as was previously demonstrated (Sereno et al 2017), SDMANF expression was co-localized with the expression of *S. domuncula* toll-like receptor, which corroborates the role of MANF on immunity.

Toll-Like Receptors (TLRs) are crucial components of the immune system (i.e. pattern recognition receptors) that are involved in recognition and defense mechanism against pathogens (Medzhitov 2007a; 2007b). It has been identified in Poriferan the toll-like receptors and interplay components as Interleukin Receptor 1 (ILR-1) pathway proteins, as Myeloid Differentiation Primary Response 8 (MyD88), kappa-light-chain-enhancer of activated B cells (NF-κB), the Interleukin Receptor-Associated Kinase 1/4 (IRAK 1/4), the Tumor Necrosis Factor (TNF), Receptor-Associated Factors (TRAF), Macrophage Expressed Protein (MPEG),

and caspase family among others (Wiens et al 2005; 2007; Gauthier et al 2010; Riesgo et al 2014).

As described for other organisms, the *S. domuncula* toll-like receptor (SDTLR) and molecules of its activation pathways are involved in the innate immune response against potential microbial invaders in Porifera and are expressed on *S. domuncula* cells upon bacteria exposition (Wiens et al 2005; 2007; Gardères et al 2014). Studies carried to evaluate the immunity pathways activated in response to infections have shown that sponges react differently to commensal and opportunistic bacteria, and also to gram-positive and gram-negative bacteria (Böhm et al 2001; Schröder et al 2003; Thakur et al 2003; 2005; Wiens et al 2005; 2007; Müller et al 2009b; Gardères et al 2014; 2015b).

The findings regarding the co-localized expression of SDTLR and SDMANF mainly restricted to sponge cells close to bacteriocytes suggest a common function of both molecules as part of the innate immune system on bacterial recognition/response mechanisms (Sereno et al 2017).

Immunity mechanisms - such as TLR activation upon bacterial activation - trigger defense mechanisms required to fight foreign invaders and frequently entail downstream modulation of UPR, cytokines, NF-κB and apoptosis mechanism (Salaun et al 2007; Martinon 2010; Janssens et al 2014; Celli and Tsolis 2015; Hetz et al 2015; Schmitz et al 2018). The UPR has multiple roles during bacterial infection and activation of immunity; pathways of UPR also interplay with innate and adaptive immune responses at different levels as via the partial overlap in the genes induced by UPR and those induced by microbial infection or stimulation TLR (Janssens et al 2014; Celli and Tsolis 2015; Hetz et al 2015; Grootjans et al 2016; Smith et al 2018).

Regarding MANF, the homologs from vertebrates and invertebrates are reported to be a protective factor against ER stress and apoptosis (Mätlik et al 2015; Lindström et al 2016; Liu et al 2016a; Lindahl et al 2017; Bai et al 2018). In addition to that, on human beta cell line EndoC-βH1, the exogenous administration of MANF inhibit NF-κB signaling pathway and specifically downregulated of B-cell lymphoma/leukemia (BCL10) (Hakonen et al 2018). NF-κB and BCL10 (do not belong to the BCL-2 family) have roles on immunity and apoptosis (Medzhitov and Janeway 2000; Fan et al 2008; Rech de Laval et al 2014; Gehring et al 2018).

BCL10 induces apoptosis acting up-stream of NF-κB and has a role on adaptive and innate immune activation, although how BCL-10 influences MyD88-dependent innate immune response is not clear yet (Gehring et al 2018).

Further studies on MANF homologs (including SDMANF) potential activities during bacterial recognition/response mechanism might give new insights on the interplay mechanism of immunity, unfolding protein response and cell death.

5. Studies of SDMANF functions in transfected mammalian cells

Since no cell line from Poriferan is available to date, in the present work, a heterologous system was employed to assess the functional mechanisms SDMANF is putatively involved in. A heterologous system, a stable cell line of SDMANF allowed for reproducibility of the analyzes under standardized conditions and a quantitative analysis of the results, which are difficult to achieve when using sponge individuals or primary cell lines. This type of heterologous vertebrate cell model has been previously employed to study the pro-proliferative and anti-apoptotic role in *S. domuncula* (Luthringer et al 2011). The SDMANF cell line was generated by transfection with a vector construct, in which SDMANF expression is constitutive and controlled by the CMV promoter/enhancer to avoid differential SDMANF transcription.

5.1. SDMANF in stably transfected HEK cells upon BFA and cadmium exposure

The SDMANF protein was expressed in HEK stable transfected cells (see Fig. 19 A). SDMANF was localized in the organelle/membrane (including Golgi) as expected due to the presence of the KDEL-like motif (see Fig. 19 C). This result corroborates previous studies that also reported the detection of MANF homologs in the ER and Golgi apparatus (Oh-hashi et al 2012; Henderson et al 2013). Despite the fact that the pattern showed by proteins that possess a KDEL-like motif are confined to the ER and Golgi apparatus, the MANF homologs, within SDMANF, can be secreted (Oh-hashi et al 2012; Henderson et al 2013). Most of the SDMANF protein was detected in the organelle/membrane subcellular fraction. However, SDMANF could also be detected in the cell culture medium (see Fig. 18 B).

Besides, to evaluate the intracellular SDMANF protein transport HEK_{SDMANF} cells were treated with the Golgi/ER transport inhibitor BFA. The HEK_{SDMANF} cells treated with BFA present enhanced SDMANF intracellular levels (see Fig. 19) when compared with non-treated cells. This indicates that BFA blocks SDMANF translocation and subsequent secretion, inducing increased intracellular SDMANF levels. This pattern has already been observed in cell lines as neuroblastoma cells SH-SY5Y) and in human embryonic kidney cells (HEK 293 cells) overexpressing human MANF challenged with BFA (Apostolou et al 2008; Henderson et al 2013). As well as, on HEK cells expressing mouse MANF upon BFA exposition (Oh-hashi et al 2012). The BFA blocks the translocation of MANF (human and mouse) from ER to Golgi and subsequent secretion, inducing an increase of intracellular MANF (Apostolou et al 2008; Oh-hashi et al 2012; Henderson et al 2013).

The SDMANF secretion showed the protein had access to secretory pathways of HEK cells, together with SDMANF enhance on intracellular levels upon BFA exposition indicate the transport and secretory pathways of MANF homologs could be evolutionary conserved.

In order to assess a possible role of SDMANF on stress mechanisms, HEK_{SDMANF} cells were also challenged with cadmium. Cadmium has been chosen as a stressor agent because it is able to induce ER stress and apoptosis (Mao et al 2007; Pathak et al 2013; Chen et al 2015c; Kim et al 2017b). In addition, it has also been previously used to study anti-apoptotic function of the survivin protein from *S. domuncula* in a similar heterologous model of stable-transfected HEK cells (Luthringer et al 2011). Here, HEK_{SDMANF} cells showed up-regulation of SDMANF corresponding to both increased cadmium concentration and incubation time, when compared to non-challenged HEK_{SDMANF}, which suggests that SDMANF is probably involved in ER stress mechanisms.

The increase of SDMANF levels in HEK_{SDMANF} transfected cells upon cadmium exposition was in accordance with previous studies that demonstrated that MANF is up-regulated during ER stress and also upon drug induced ER stress (See C 3.3; 3.4; Voutilainen et al 2015; Wang et al 2015b; Kim et al 2016; 2017a; Li-na et al 2017; Liu et al 2016b; Bai et al 2018; Guo et al 2018). For example in cell lines overexpressing human MANF, as HEK 293, bone osteosarcoma (U2OS), and SH-SY5Y showed an increase of MANF in response to ER stress induce by

Tunicamycin (TM) Thapsigargin (TG) and lactacystin (Apostolou et al 2008). Along with an increase of mouse MANF levels was also observed in embryo fibroblasts (NIH 3T3) exposed to TM, TG, and Dithiothreitol (DTT) (Mizobuchi et al 2007). In addition to that an up-regulation of rodent MANF was also detected in neuron Neuro2a cells treated with TG and on cardiomyocytes after exposition to TM, TG and DTT (Tadimalla et al 2008; Yu et al 2010; Glembotski et al 2012; Liu et 2016a). Moreover, have been also observed that MANF levels also increase in different animal diseases models that are associated with ER stress, as in rodent models of bladder obstruction, in rabbit fibroblast-like synoviocytes antigen induced arthritis model, and in a *C. elegans* human α-synuclein induced Parkinson's disease model (Chen et al 2015a; Liu et al 2015c; Lindström et al 2016; Gao et al 2017b; Zhang et al 2018).

5.2. Levels of SDMANF, BAX expression, caspase activity and cell viability upon LPS exposure

The endotoxin Lipopolysaccharide (LPS) is a component of the outer membrane of most gram-negative bacteria that triggers the innate immune response in host organisms through TLR pathways and Invading microbial pathogens triggers a cellular stress that activates UPR pathways (Salaun et al 2007; Wang and Quinn 2010; Brown et al 2011; Celli and Tsolis 2015; Rosadini and Kagan 2017; Cheng et al 2018). UPR has pivotal roles in the modulation of immunity, autophagy and also apoptosis pathways on multiple levels (Hetz et al 2015; Grootjans et al 2016; Cybulsky 2017; Niu et al 2017; Hetz and Papa 2018; Schmitz et al 2018; Smith 2018).

Mesencephalic astrocyte-derived factor proteins (i.e. human, mouse, *Drosophila*, *C. elegans*) have been described to be involve at multiple levels with UPR, attenuates inflammation, autophagy and apoptosis (Chen et al 2015a; Stratoulias and Heino 2015a; Lindström et al 2016; Zhu et al 2016; Gao et al 2017a; 2017b; Lindahl et al 2017; Zhang et al 2017a; 2017b; 2018; Hakonen et al 2018; Li et al 2018; Richman et al 2018; Zhang et al 2018).

The previously describe roles of MANF proteins together with the aforementioned results were SDMANF up-regulation upon stress and co-localization with SDTLR led to further analyses of SDMANF functions on apoptosis

mechanism triggered by LPS. The levels of SDMANF, expression of BAX, activity of caspase 3 and cell viability were analyzed.

SDMANF protein (in HEK_{SDMANF}) levels increased in a time- and concentration-dependent manner upon LPS challenged (see Fig. 21 B and G). LPS triggers a cellular stress that activates UPR pathways (Hetz et al 2015) the increased on intracellular level of SDMANF was probably affected by downstream regulatory pathways of the ER stress responses. For instance: LPS induces expression of the ER-resident chaperon ORP150 (150-kD oxygen-regulated protein) in murine macrophages, the ORP150 binding of free calcium and maintains Ca^{2+} homeostasis having a similar protective function as BiP (Kitao et al 2001; Nakagomi et al 2004). As well as, have been described that human MANF interacts with BiP in a calcium dependent manner on cultured cardiomyocytes and HeLa cells, It was proposed that under normal ER calcium concentrations MANF is retained in the ER by BiP (Glembotski et al 2012; Lindahl et al 2017). Therefore, SDMANF might be protected from degradation through targeting downstream proteases that are activated by free calcium. MANF (Human; *Droshophila*; *C. elegans*) levels increase during ER stress, although, the complete mechanisms of MANF homologs transcriptional regulation remain undefined (Lindstrom et al 2016; Lindahl et al 2017; Richman et al 2018; Wang et al 2018).

Furthermore, During LPS-induced ER-stress several responsive genes such as BAX is regulate, and the pro-apoptotic programs is activated (Hetz et al 2006; 2015; Dong et al 2013; Hetz and Papa 2018). LPS induce as well activation of caspase 3 (Karahashi et al 1998; Munshi et al 2002; Guo et al 2014). Likewise, in the present study were observed an increased on expression of BAX expression a higher caspase 3 activity and a reduced cell viability upon LPS exposition in HEK wild-type (HEK_{wt}, not transfected cells) when compared with HEK_{SDMANF} cells upon LPS exposition (See Fig. 21, 22 and 23). However, the expression of BAX in HEK_{SDMANF} remained barely undetectable (with one enigmatic exception: BAX was markedly detected after incubation with 1 µg/ml LPS for 6h HEK_{SDMANF} cells present as well a lower caspase 3 activity and a higher cell viability (See Fig. 21, 22 and 23).

These findings suggest that SDMANF might block the LPS-induced activation of pro-apoptotic transcription factors directly or indirectly and, therefore,

regulates BAX expression. Accordingly, during LPS-induced ER stress SDMANF might not only regulate BAX activity by protein interaction via MANF/BCL-2 Homology Domain MBHD (see above), but it might also regulate BAX expression (Sereno et al 2017). If this holds true, then SDMANF would mediate access to apoptotic pathways. This hypothesis is also supported by the decreased caspase 3 activity and increased cell viability of HEK_{SDMANF} cells after exposition to LPS when compared to HEK_{wt}, treated with LPS.

The results are in agreement with former findings on MANF, where: (I) MANF homologs (human, mouse, *Drosophila*, *C. elegans*) are protective factors against apoptosis induce by a variety of stimulus in cells on *in vivo* (see C3.3 and 3.4; Palgi et al 2009; Mätlik et al 2015; Voutilainen et al 2015; Kim et al 2017; Lindahl et al 2017; Liu et al 2018; Richman et al 2018), (II) The treatment with recombinant human MANF on a rat model of intracerebral hemorrhage and, on rat model of traumatic spinal cord injury reduce neuronal death, decrease caspase 3 activity an the levels of BAX, increase the levels of MANF and BCL-2 (Gao et a 2018; Xu et al 2018), (III) Pre-treated of cells SH-SY5Y cells (neuroblastoma) with human MANF upon exposition to metabolite 1-methyl- 4-phenylpyridinium ion, a Parkinson´s Diseases (PD) model, restore the cell viability, inhibited Bax expression and increased the levels of BCL-2 (Liu et al 2018), (IV) Treatment with human MANF also protects from cell damage upon exposition to neurotoxin 6-hydroxydopamine (6-OHDA) PD model on SHSY-5Y MANF reduce caspase 3/7 activity and cell apoptosis (Sun et al 2017) and (VI) Treatment of *ex vivo* culture of retinal explants of mice with recombinant human MANF, upon tunicamycin, reduced caspase 3 activation and also improve cell viability (McLaughlin et al 2018)

Finally, the several results indicate SDMANF-mediated access to apoptotic pathways conferring a cytoprotective activity. Therefore SDMANF might have a role on the crossroads of innate immune and apoptotic pathways.

H. Conclusion

In the present work the protein Mesencephalic Astrocyte-Derived Neurotrophic Factor (MANF) was identified in the sponge *Suberites* domuncula (SDMANF). Sponges belong to the earliest branching Metazoa phyla and they lack a conventional nervous system. The discovery of SDMANF in sponges is evidence that MANF homologs belong to an especial category of neurotrophic factors that emerged during the early evolution of Metazoa, prior even to the advent of complex neuronal signal networks.

The SDMANF complete DNA/protein sequence was acquired. The SDMANF protein presents all the characteristics features of MANF/CDNF family protein, as the ARMET, Saposin-like and SAP-like domains. As well as the CXXC motif and the KDEL-like ER-retention sequence. A three-dimensional structural homologue model of SDMANF, using human MANF as backbone structure, show similarities between the human MANF and the possible structural of SDMANF.

The sponge tissue expression of SDMANF was mainly restricted to sponge cells close to bacteriocytes, that are specialized cells that host intracellularly different kinds of bacterial cells, which might be either symbiotic or a food resource. Along with the SDMANF expression was reported the co-localized expression of *S. domuncula* Toll-like Receptor (SDTLR). The SDTLR have roles on innate immune response of Poriferan against potential microbial invaders as bacterial as the other metazoan TLRs. These findings suggest a common function of SDMANF and SDTLR as part of innate bacterial recognition/response mechanisms.

The functional mechanisms were SDMANF is putatively involved were also studied through a heterologous system (HEK cells stable transfected with SDMANF, HEK_{SDMANF}). The SDMANF was localized in the organelle organelle/membrane subcellular fraction and in the cell culture medium indicating the SDMANF protein was also secreted. The secretion of SDMANF showed the protein had access to secretory pathways of HEK cells, together with the enhancement of SDMANF intracellular levels upon BFA exposition (Golgi transport inhibitor) indicated the transport and secretory pathways of MANF homologs could be evolutionary conserved. Moreover, as the other MANF homologs, SDMANF is probably involved in ER stress mechanisms and apoptosis taking in consideration

the up-regulation of SDMANF levels on HEK_{SDMANF} after exposition to cadmium wich induces both ER stress and apoptosis.

The roles of SDMANF as a cytoprotective factor, a characteristic that has been described to MANF homologs, was also studied in HEK cells upon exposition to endotoxin lipopolysaccharide and the HEK_{SDMANF} cells showed an up-regulation of SDMANF levels and BAX levels remained barely undetectable. Also, the HEK_{SDMANF} presented a decreased activity of caspase 3 and higher cell viability when compared with non-transfected HEK cells. These results suggest SDMANF mediated access to apoptotic pathways.

Taken together the results on SDMANF sequence, localization, expression, and functions suggest an ER-resident protein with roles on ER stress, it interplays on innate immune and apoptotic pathways. The SDMANF have an evolutionary ancient functional role beyond of conventional neurotrophic factors.

The study of SDMANF can increase the interest of research on the evolutionary conserved roles of others neurotrophic factors and discover their function before the advent of the nervous system.

I. REFERENCES

Adams ED, Goss GG, Leys SP (2010) Freshwater sponges have functional, sealing epithelia with high transepithelial resistance and negative transepithelial potential. PLoS One 5(11):e15040. doi:10.1371/journal.pone.0015040

Adamsk M (2018) Differentiation and transdifferentiation of sponge sells In: Marine organisms as model systems in biology and medicine. Results and Problems in Cell Differentiation 65. Eds: Kloc M, Jacek JZ. Springer. doi:10.1007/978-3-319-92486-1

Aguzzi A, O'Connor T (2010) Protein aggregation diseases: pathogenicity and therapeutic perspectives. Nat. Rev. Drug Discov. 9(3):237-248. doi:10.1038/nrd3050

Airaksinen MS, Saarma M (2002) The GDNF family: signaling, biological functions and therapeutic value. Nat. Rev. Neurosci. 3:383-394. doi:10.1038/nrn812

Airavaara M, Chiocco MJ, Howard DB, Zuchowski KL, Peränen J, Liu C, Fang S, Hoffer BJ, Wang Y, Harvey BK (2010) Widespread cortical expression of MANF by AAV serotype 7: localization and protection against ischemic brain injury. Exp. Neurol. 225(1):104-13. doi:10.1016/j.expneurol.2010.05.020

Airavaara M, Shen H, Kuo CC, Peränen J, Saarma M, Hoffer B, Wang Y (2009) Mesencephalic astrocyte-derived neurotrophic factor reduces ischemic brain injury and promotes behavioural recovery in rats. J. Comp. Neurol. 1;515(1):116-24. doi:10.1002/cne.22039

Alfieri A, Srivastava S, Siow RC, Modo M, Fraser PA, Mann GE (2011) Targeting the Nrf2-Keap1 antioxidant defence pathway for neurovascular protection in stroke. J. Physiol. 589(17):4125-4136. doi:10.1113/jphysiol.2011.210 294

Almlöf JC, Alexsson A, Imgenberg-Kreuz J, Sylwan L, Bäcklin C, Leonard D, Nordmark G, Tandre K, Eloranta ML, Padyukov L, Bengtsson C, Jönsen A, Dahlqvist SR, Sjöwall C, Bengtsson AA, Gunnarsson I, Svenungsson E, Rönnblom L, Sandling JK, Syvänen AC (2017) Novel risk genes for systemic lupus erythematosus predicted by random forest classification. Sci. Rep. 7(1):6236. doi:10.1038/s41598-017-06516-1

Almutawaa W, Kang NH, Pan Y, Niles LP (2014) Induction of neurotrophic and differentiation factors in neural stem cells by valproic acid. Basic Clin. Pharmacol. Toxicol. 115(2):216-221. doi:101111/bcpt.12201

Alsina FC, Ledda F, Paratcha G (2012) New insights into the control of neurotrophic growth factor receptor signaling: implications for nervous system development and repair. J. Neurochem. 123(5):652-661. doi:10.1111/jnc.12021

Altschul SF, Gish W, Miller W, Myers EW, Lipman DJ (1990) “Basic local alignment search tool.” J. Mol. 215:403-410. doi:10.1016/S0022-2836(05)80360-2

Amano S, Hori I (1996) Transdifferentiation of larval flagellated cells to choanocytes in the metamorphosis of the demosponge *Haliclona permollis*. Biol. Bull. 190:161-172. doi:https://doi.org/10.2307/1542536

Anderson DH, Sawaya MR, Cascio D, Ernst W, Modlin R, Krensky A, Eisenberg D (2003) Granulysin crystal structure and a structure-derived lytic mechanism. J. Mol. Biol. 325(2):355-365. doi:https://doi.org/10.1016/S0022-2836(02)01234-2

Anuradha R, Saraswati M, Kumar KG, Rani SH (2014) Apoptosis of beta cells in diabetes mellitus. DNA Cell Biol. 33(11):743-748. doi:10.1089/dna.2014.2352

Aouacheria A, de Laval VR, Combet C, Hardwick JM (2013) Evolution of Bcl-2 homology (BH) motifs – homology versus homoplasy. Trends cell biol. 23(3):103-111. doi:10.1016/j.tcb.2012.10.010

Apostolou A, Shen Y, Liang Y, Luo J, Fang S (2008) Armet, a UPR-upregulated protein, inhibits cell proliferation and ER stress-induced cell death. Exp. Cell Res. 1;314(13):2454-2467. doi:10.1016/j.yexcr.2008.05.001

Appeltans W, Ahyong ST, Anderson G, Angel MV, Artois T, Bailly N, Bamber R, Barber A, Bartsch I, Berta A, Błażewicz-Paszkowycz M, Bock P, Boxshall G, Boyko CB, Brandão SN, Bray RA, Bruce NL, Cairns SD, Chan TY, Cheng L, Collins AG, Cribb T, Curini-Galletti M, Dahdouh-Guebas F, Davie PJ, Dawson MN, De Clerck O, Decock W, De Grave S, de Voogd NJ, Domning DP, Emig CC, Erséus C, Eschmeyer W, Fauchald K, Fautin DG, Feist SW, Fransen CH, Furuya H, Garcia-Alvarez O, Gerken S, Gibson D, Gittenberger A, Gofas S, Gómez-Daglio L, Gordon DP, Guiry MD, Hernandez F, Hoeksema BW, Hopcroft RR, Jaume D, Kirk P, Koedam N, Koenemann S, Kolb JB, Kristensen RM, Kroh A, Lambert G, Lazarus DB, Lemaitre R, Longshaw M, Lowry J, Macpherson E, Madin LP, Mah C, Mapstone G, McLaughlin PA, Mees J, Meland K, Messing CG, Mills CE, Molodtsova TN, Mooi R, Neuhaus B, Ng PK, Nielsen C, Norenburg J, Opresko DM, Osawa M, Paulay G, Perrin W, Pilger JF, Poore GC, Pugh P, Read GB, Reimer JD, Rius M, Rocha RM, Saiz-Salinas JI, Scarabino V, Schierwater B, Schmidt-Rhaesa A, Schnabel KE, Schotte M, Schuchert P, Schwabe E, Segers H, Self-Sullivan C, Shenkar N, Siegel V, Sterrer W, Stöhr S, Swalla B, Tasker ML, Thuesen EV, Timm T, Todaro MA, Turon X, Tyler S, Uetz P, van der Land J, Vanhoorne B, van Ofwegen LP, van Soest RW, Vanaverbeke J, Walker-Smith G, Walter TC, Warren A, Williams GC, Wilson SP, Costello MJ (2012) The magnitude of global marine species diversity. Curr. Biol. 22(23):2189-2202. doi:10.1016/j.cub.2012.09.036

Appenzeller-Herzog C, Simmen T (2016) ER-luminal thiol/selenol-mediated regulation of Ca^{2+} signaling. Biochem. Soc. Trans. 44(2):452-459. doi:10.1042/BST20150233

Araki K, Nagata K (2011) Protein folding and quality control in the ER. Cold Spring Harb. Perspect. Biol. 3(11):a007526. doi:10.1101/cshperspect.a007526

Ashkenazi A, Salvesen G (2014) Regulated cell death: signaling and mechanisms. Annu. Rev. Cell Dev. Biol. 30(1):337-356. doi:10.1146/annurev-cellbio-100913-013226

Axelsen TM, Woldbye DPD (2018) Gene therapy for Parkinson's disease, an update. J. Parkinson's Dis. 8(2):195-215. doi:10.3233/JPD-181331

Babenko VN, Krylov DM (2004) Comparative analysis of complete genomes reveals gene loss, acquisition and acceleration of evolutionary rates in Metazoa, suggests a prevalence of evolution via gene acquisition and indicates that the evolutionary rates in animals tend to be conserved. Nucleic Acids Res. 32(17):5029-5035. doi:10.1093/nar/gkh833

Bai M, Vozdek R, Hnízda A, Jiang C, Wang B, Kuchar L, Li T, Zhang Y, Wood C, Feng L, Dang Y, Ma DK (2018) Conserved roles of *C. elegans* and human MANFs in sulfatide binding and cytoprotection. Nat. Commun. 9(1):897. doi:10.1038/s41467-018-03355-0

Ballard SL, Miller DL, Ganetzky B (2014) Retrograde neurotrophin signaling through Tollo regulates synaptic growth in Drosophila. J. Cell. Biol. 204(7):1157-1572. doi:10.1083/jcb.201308115

Bartus RT, Johnson EM Jr. (2017) Clinical tests of neurotrophic factors for human neurodegenerative diseases, part 2: Where do we stand and where must we go next? Neurobiol. Dis. 97:169-178. doi:10.1016/j.nbd.2016.03.026

Barua NU, Bienemann AS, Woolley M, Wyatt MJ, Johnson D, Lewis O, Irving C, Pritchard G, Gill S (2015) Convection-enhanced delivery of MANF-volume of distribution analysis in porcine putamen and substantia nigra. J. Neurol. Sci. 357(1-2):264-269. doi:10.1016/j.jns.2015.08.003

Bavestrello G, Burlando B, Sara M (1988) The architecture of the canal systems of *Petrosia ficiformis* and *Chondrosia reniformis* studied by corrosion casts (Porifera, Demospongiae). Zoomorphology 108(3):161-166. doi:https://doi.org/10.1007/BF00363932

Bayer K, Kamke J, Hentschel U (2014) Quantification of bacterial and archaeal symbionts in high and low microbial abundance sponges using real-time PCR. FEMS Microbiol. Ecol. 89(3):679-90. doi:10.1111/1574-6941.12369

Belahbib H, Renard E, Santini S, Jourda C, Claverie JM, Borchiellini C, Le Bivic A (2018) New genomic data and analyses challenge the traditional vision of animal epithelium evolution. BMC Genomics. 19(1):393. doi:10.1186/s12864-018-4715-9

Bell RAV, Megeney LA (2017) Evolution of caspase-mediated cell death and

differentiation: twins separated at birth. Cell Death Differ. 24(8):1359-1368. doi:10.1038/cdd.2017.37

Bergquist PR (1978) Sponges. UC Press, Berkeley. 268 pp.

Berman HM, Westbrook J, Feng Z, Gilliland G, Bhat TN, Weissig H, Shindyalov IN, Bourne PE (2000) The protein data bank. Nucleic Acids Res. 28(1):235-42. doi:https://doi.org/10.1093/nar/28.1.235

Bertolotti A, Zhang Y, Hendershot LM, Harding HP, Ron D (2000) Dynamic interaction of BiP and ER stress transducers in the unfolded protein response. Nat. Cell Biol. 2(6):326-32. doi:10.1038/35014014

Bertram L, Tanzi RE (2005) The genetic epidemiology of neurodegenerative disease. J. Clin. Invest. 115:1449-1457 doi:10.1172/JCI24761

Birkinshaw RW, Czabotar PE (2017) The BCL-2 family of proteins and mitochondrial outer membrane permeabilization. Semin. Cell Dev. Biol. 72:152-162. doi:10.1016/j.semcdb.2017.04.001

Blumbach B, Diehl-Seifert B, Seack J, Steffen R, Müller IM, Müller WEG (1999) Cloning and expression of new receptors belonging to the immunoglobulin superfamily from the marine sponge *Geodia cydonium*. Immunogenetics 49:751-763. doi:https://doi.org/10.1007/s002510050549

Blumbach B, Pancer Z, Diehl-Seifert B, Steffen R, Münkner J, Müller I, Müller WEG (1998) The putative sponge aggregation receptor. Isolation and characterization of a molecule composed of scavenger receptor cysteine-rich domains and short consensus repeats. J. Cell Sci. 111(7):2635-2644.

Blunt JW, Copp BR, Keyzers RA, Munro MHG, Prinsep MR (2013) Marine natural products. Nat. Prod. Rep. 30:237-323. doi:10.1039/c2np20112g

Boehm T (2006) Quality control in self/nonself discrimination. Cell 125(5):845-858. doi:10.1016/j.cell.2006.05.017

Böhm M, Gamulin V, Schröder HC, Müller WE (2002) Evolution of osmosensing signal transduction in Metazoa: stress-activated protein kinases p38 and JNK. Cell Tissue Res. 308(3):431-438. doi:10.1007/s00441-002-0535-x

Böhm M, Hentschel U, Friedrich A, Fieseler L, Steffen R, Gamulin V, Müller IM, Müller WEG (2001) Molecular response of the sponge *Suberites domuncula* to bacterial infection. Mar. Biol. 139: 1037-1045. doi:10.1007/s002270100656

Böhm M, Schröder HC, Müller IM, Müller WE, Gamulin V (2000) The mitogen-activated protein kinase p38 pathway is conserved in metazoans: cloning and activation of p38 of the SAPK2 subfamily from the sponge *Suberites domuncula*. Biol. Cell. 92(2):95-104.
doi:https://doi.org/10.1016/S0248-4900(00)89017-6.

Boriushkin E, Wang JJ, Zhang SX (2014) Role of $p58^{IPK}$ in endoplasmic reticulum stress-associated apoptosis and inflammation. J. Ophthalmic Vis. Res. 9(1):134-143

Bothwell M (2006) Evolution of the neurotrophin signaling system in invertebrates. Brain Behav. Evol. 68:124-132. doi:10.1159/000094082

Bothwell M (2014) NGF, BDNF, NT3, and NT4. 220:3-15. In: Lewin G, Carter B. (eds) Neurotrophic factors. Handb. of Exp. Pharmacol. vol. 220. Springer, Berlin, Heidelberg. doi:10.1007/978-3-642-45106-5_1

Bothwell M (2016) Recent advances in understanding neurotrophin signaling. F1000 Faculty Rev-1885:5. doi:10.12688/f1000research.8434.1

Botting JP, Muir LA (2018) Early sponge evolution: A review and phylogenetic framework. Palaeoworld 27(1): 1-29. doi: 10.1016/j.palwor.2017.07.001

Braakman I, Hebert D (2013) Protein folding in the endoplasmic reticulum. Cold Spring Harb. Perspect. Biol. 5:a013201. doi:10.1101/cshperspect.a013201

Bravo R, Parra V, Gatica D, Rodriguez AE, Torrealba N, Paredes F, Wang ZV, Zorzano A, Hill JA, Jaimovich E, Quest AF, Lavandero S (2013) Endoplasmic reticulum and the unfolded protein response: dynamics and metabolic integration. Int. Rev. Cell. Mol. Biol.301:215-290. doi:10.1016/B978-0-12-407704-1.00005-1

Brett AC, Rosenstock TR, Rego AC (2014) Current therapeutic advances in patients and experimental models of Huntington's disease. Curr. Drug Targets. 15(3):313-334. doi:10.2174/1389450114666131124140704

Brown J, Wang H, Hajishengallis GN, Martin M (2011) TLR-signaling networks: an integration of adaptor molecules, kinases, and cross-talk. J. Dent. Res. 90(4):417-427. doi:10.1177/0022034510381264

Bruhn, H (2005) A short guided tour through functional and structural features of saposin-like proteins. Biochem. J. 389:249-257. doi:10.1042/BJ20050051

Buchmann K (2014) Evolution of innate immunity: clues from invertebrates via fish to mammals. Front. Immunol. 23(5):459. doi:10.3389/fimmu.2014.00459

Byndloss MX, Keestra-Gounder AM, Bäumler AJ, Tsolis RM (2016) NOD1 and NOD2: new functions linking endoplasmic reticulum stress and inflammation. DNA Cell Biol. 35(7):311-313. doi:10.1089/dna.2016.3396

Calfon M, Zeng H, Urano F, Till JH, Hubbard SR, Harding HP, Clark SG, Ron D (2002) IRE1 couples endoplasmic reticulum load to secretory capacity by processing the XBP-1. Nature 415:92-96. doi:10.1038/415092a

Cameron TL, Bell KM, Tatarczuch L, Mackie EJ, Rajpar MH, McDermott BT,

Boot-Handford RP, Bateman JF (2011) Transcriptional profiling of chondrodysplasia growth plate cartilage reveals adaptive ER-stress networks that allow survival but disrupt hypertrophy. PLoS One. 6(9):e24600. doi:10.1371/journal.pone.0024600

Cao SS, Kaufman RJ (2012) Unfolded protein response. Curr. Biol. 22(16):R622-626. doi:10.1016/j.cub.2012.07.004

Cao SS, Luo KL, Shi L (2016) Endoplasmic reticulum stress interacts with inflammation in human diseases. J. Cell. Physiol. 231(2):288-294. doi:10.1002/jcp.25098

Caria S, Hinds MG, Kvansakul M (2017) Structural insight into an evolutionarily ancient programmed cell death regulator - the crystal structure of marine sponge BHP2 bound to LB-Bak-2. Cell Death Dis. 8(1):e2543. doi:10.1038/cddis.2016.469

Carreras-Sureda A, Pihán P, Hetz C (2018) Calcium signaling at the endoplasmic reticulum: fine-tuning stress responses. Cell Calcium. 70:24-31. doi:10.1016/j.ceca.2017.08.004

Castresana J (2000) Selection of conserved blocks from multiple alignments for their use in phylogenetic analysis. Mol. Biol. Evol. 17(4):540-552. doi:10.1093/oxfordjournals.molbev.a026334

Cavalcanti FF, Klautau M (2011) Solenoid: a new aquiferous system to Porifera. Zoomorphology 130(4): 255-260. doi:10.1007/s00435-011-0139-7

Celli J, Tsolis RM (2015) Bacteria, the endoplasmic reticulum and the unfolded protein response: friends or foes? Nat. Rev. Microbiol. 13(2):71-82. doi:10.1038/nrmicro3393

Chakrabarti A, Chen AW, Varner JD (2011) A review of the mammalian unfolded protein response. Biotechnol. Bioeng. 108(12):2777-2793. doi:10.1002/bit.23282

Chaplin DD (2010) Overview of the immune response. J. Allergy Clin. Immunol. 125 (2)2:S3-23. doi:10.1016/j.jaci.2009.12.980

Chen CY, Zhang SL, Liu ZY, Tian Y, Sun Q (2015c) Cadmium toxicity induces ER stress and apoptosis via impairing energy homoeostasis in cardiomyocytes. Biosci. Rep. 35(3). pii: e00214. doi:10.1042/BSR20140170

Chen J, Zhang M, Zhu M, Gu J, Song J, Cui L, Liu D, Ning Q, Jia X, Feng L (2018) Paeoniflorin prevents endoplasmic reticulum stress-associated inflammation in lipopolysaccharide-stimulated human umbilical vein endothelial cells via the IRE1α/NF-κB signaling pathway. Food Funct. 9(4):2386-2397 doi:10.1039/c7fo01406f

Chen L, Wan L, Du J, Shen Y (2015b) Identification of MANF as a protein interacting with RTN1-C. Acta Biochim. Biophys. Sin. 47(2):91-97. doi:10.1093/abbs/gmu125

Chen LJ, Feng LJ, Wang X, Du J, Chen Y, Yang W, Zhou C, Cheng Li, Shen Y, Fang S, Li J, Shen Y (2015a) Mesencephalic astrocyte-derived neurotrophic factor is involved in inflammation by negatively regulating the NF-kappa B pathway. Sci. Rep. 5:8133. doi:10.1038/srep08133

Chen YC, Sundvik M, Rozov S, Priyadarshini M, Panula P (2012) MANF regulates dopaminergic neuron development in larval zebra fish. Dev. Biol. 370(2):237-249. doi:10.1016/j.ydbio.2012.07.030

Cheng L, Zhao H, Zhang W, Liu B, Liu Y, Guo Y, Nie L (2013) Overexpression of conserved dopamine neurotrophic factor (CDNF) in astrocytes alleviates endoplasmic reticulum stress-induced cell damage and inflammatory cytokine secretion. Biochem. Biophys. Res. Commun. 435:34-39. doi:10.1016/j.bbrc.2013.04.029

Chernorudskiy AL, Zito E (2017) Regulation of calcium homeostasis by ER Redox: a close-up of the ER/mitochondria connection. J. Mol. Biol. 429(5):620-632. doi:10.1016/j.jmb.2017.01.017

Choi S (2018) BID (BH3 interacting domain death agonist). Encyclopedia of signaling molecules. Springer, Cham. doi:https://doi.org/10.1007/978-3-319-67199-4

Chow CY, Wang X, Riccardi D, Wolfner MF, Clark AG (2015) The genetic architecture of the genome-wide transcriptional response to ER stress in the mouse. PLoS Genet. 11(2):e1004924. doi:10.1371/journal.pgen.1004924

Christian F, Smith EL, Carmody RJ (2016) The regulation of NF-κB subunits by phosphorylation. Cells. 5(1):E12. doi:10.3390/cells5010012

Clavarino G, Cláudio N, Couderc T, Dalet A, Judith D, Camosseto V, Schmidt EK, Wenger T, Lecuit M, Gatti E, Pierre P (2012) Induction of GADD34 is necessary for dsRNA-dependent interferon-β production and participates in the control of Chikungunya virus infection. PLoS Pathog. 8(5):e1002708. doi:10.1371/journal.ppat.1002708

Collet JF, D'Souza JC, Jakob U, Bardwell JC (2003) Thioredoxin 2, an oxidative stress-induced protein, contains a high affinity zinc binding. site. J. Biol. Chem. 278(46):45325-45332. doi:10.1074/jbc.M307818200

Conaco C, Bassett DS, Zhou H, Arcila ML, Degnan SM, Degnan BM, Kosik KS (2012a) Functionalization of a protosynaptic gene expression network. Proc. Natl. Acad. Sci. USA 109(1):10612-8. doi:10.1073/pnas.1201890109

Conaco C, Neveu P, Zhou H, Arcila ML, Degnan SM, Degnan BM, Kosik KS (2012b) Transcriptome profiling of the demosponge *Amphimedon*

queenslandica reveals genome-wide events that accompany major life cycle transitions. BMC Genomics. 13:209. doi:10.1186/1471-2164-13-209

Connor JH, Weiser DC, Li S, Hallenbeck JM, Shenolikar S (2001) Growth arrest and DNA damage-inducible protein GADD34 assembles a novel signaling complex containing protein phosphatase 1 and inhibitor 1. Mol. Cell. Biol. doi:10.1128/MCB.21.20.6841-6850.2001

Cooper MD, Alder MN (2006) The evolution of adaptive immune systems. Cell 124(4):815-822. doi:10.1016/j.cell.2006.02.001

Cordero-Llana Ó, Houghton BC, Rinaldi F, Taylor H, Yáñez-Muñoz RJ, Uney JB, Wong LF, Caldwell MA (2015) Enhanced efficacy of the CDNF/MANF family by combined intranigral overexpression in the 6-OHDA rat model of Parkinson's disease. Mol. Ther. 23:244-254. doi:10.1038/mt.2014.206

Cunha DA, Cito M, Grieco FA, Cosentino C, Danilova T, Ladrière L, Lindahl M, Domanskyi A, Bugliani M, Marchetti P, Eizirik DL, Cnop M (2017) Pancreatic β-cell protection from inflammatory stress by the endoplasmic reticulum proteins thrombospondin 1 and mesencephalic astrocyte-derived neurotrophic factor (MANF). J. Biol. Chem. 292(36):14977-14988. doi:10.1074/jbc.M116.769877

Custódio MR, Hajdu E, Muricy G (2004) Cellular dynamics of in vitro allogeneic reactions *of Hymeniacidon heliophila* (Demospongiae: Halichondrida). Mar. Biol. 144:999-1010. doi:https://doi.org/10.1007/s00227-003-1265-7

Custódio MR, Prokic I, Steffen R, Koziol C, Borojevicb R, Brümmer F, Nickel M, Müller WEG (1998) Primmorphs generated from dissociated cells of the sponge *Suberites domuncula*: a model system for studies of cell proliferation and cell death. Mech. Ageing and Dev. 105(1-2):45-59. doi:https://doi.org/10.1016/S0047-634(98)00078-5

Cybulsky AV (2017) Endoplasmic reticulum stress, the unfolded protein response and autophagy in kidney diseases. Nat. Rev. Nephrol. 13(11):681-696. doi:10.1038/nrneph.2017.129

Czabotar PE, Lessene G, Strasser A, Adams JM (2014) Control of apoptosis by the BCL-2 protein family: implications for physiology and therapy. Nat. Rev. Mol. Cell Biol. 15(1):49-63. doi:10.1038/nrm3722

Darling NJ, Cook SJ (2014) The role of MAPK signaling pathways in the response to endoplasmic reticulum stress. Biochim. Biophys. Acta. 1843(10):2150-63. doi:10.1016/j.bbamcr.2014.01.009

De Goeij JM, De Kluijver A, Van Duyl FC, Vacelet J, Wijffels RH, De Goeij AF, Cleutjens JP, Schutte B (2009) Cell kinetics of the marine sponge *Halisarca caerulea* reveal rapid cell turnover and shedding. J Exp Biol. 212(Pt 23):3892-900. doi:10.1242/jeb.034561

De Goeij JM, Van den Berg H, Van Oostveen MM, Epping EHG, Van Duyl FC (2008) Major bulk dissolved organic carbon (DOC) removal by encrusting coral reef cavity sponges. Mar. Ecol. Prog. Ser. 357: 139-151. doi:https://doi.org/10.3

De Mendoza A, Suga H, Ruiz-Trillo I (2010) Evolution of the MAGUK protein gene family in premetazoan lineages. BMC Evol. Biol. 10:93. doi:10.1186/1471-2148-10-93

Degnan SM (2015) The surprisingly complex immune gene repertoire of a simple sponge, exemplified by the NLR genes: a capacity for specificity? Dev. Comp. Immunol. 48(2):269-274. doi:10.1016/j.dci.2014.07.012

Degterev A, Yuan J (2008) Expansion and evolution of cell death programmes. Nat. Rev. Mol. Cell. Biol. 9(5):378-90. doi:10.1038/nrm2393

Delbridge LM, O'Riordan MX (2007) Innate recognition of intracellular bacteria. Curr. Opin. Immunol. 19(1):10-16. doi:10.1016/j.coi.2006.11.005

DeLotto Y, DeLotto R (1998) Proteolytic processing of the Drosophila Spätzle protein by easter generates a dimeric NGF-like molecule with ventralising activity. Mech. Dev. 72(1-2):141-148. doi:https://doi.org/10.1016/S0925-4773(98)00024-0

Deveraux QL, Reed JC (1999) IAP family proteins-suppressors of apoptosis. Genes Dev. 13(3):239-252.

Don RH, Cox PT, Wainwright BJ, Baker K, Mattic JS (1991) “Touchdown” PCR to circumvent spurious priming during gene amplification. Nucleic. Acids Res. 19:14. doi:https://doi.org/10.1093/nar/19.14.4008

Dong M, Hu N, Hua Y, Xu X, Kandadi MR, Guo R, Jiang S, Nair S, Hu D, Ren J (2013) Chronic Akt activation attenuated lipopolysaccharide-induced cardiac dysfunction via Akt/GSK3β-dependent inhibition of apoptosis and ER stress. Biochim. Biophys. Acta, Mol. Basis Dis.1832(6):848-863

Dotiwala F, Mulik S, Polidoro RB, Ansara JA, Burleigh BA, Walch M, Gazzinelli RT, Lieberman J (2016) Killer lymphocytes use granulysin, perforin and granzymes to kill intracellular parasites. Nat. Med. 22(2):210-216. doi:10.1038/nm.4023

Du H, Wolf J, Schafer B, Moldoveanu T, Chipuk JE, Kuwana T (2011) BH3 domains other than Bim and Bid can directly activate Bax/Bak. J. Biol. Chem. 286(1):491-501. doi:10.1074/jbc.M110.167148

Dunn CW, Hejnol A, Matus DQ, Pang K, Browne WE, Smith SA, Seaver E, Rouse GW, Obst M, Edgecombe GD, Sørensen MV, Haddock SH, Schmidt-Rhaesa A, Okusu A, Kristensen RM, Wheeler WC, Martindale MQ, Giribet G (2008) Broad phylogenomic sampling improves resolution of the animal tree of

life. Nature 452:745-749. doi:10.1038/nature06614
Dunn CW, Leys SP, Haddock SH (2015) The hidden biology of sponges and ctenophores. Trends Ecol. Evol. 30(5):282-291.doi:10.1016/j.tree.2015.03.003.

Dzik JM (2010) The ancestry and cumulative evolution of immune reactions. Acta Biochim. Pol. 57(4):443-466.

Ekert PG, Vaux DL (1997) Apoptosis and the immune system. Br. Med. Bull. 53(3):591-603. doi:https://doi.org/10.1093/oxfordjournals.bmb.a011632

Ellgaard L, McCaul N, Chatsisvili A, Braakman I (2016) Co- and post-translational protein folding in the ER. Traffic. 17(6):615-638. doi:10.1111/tra.12392

Elliott GRD, Leys SP (2010) Evidence for glutamate, GABA and NO in coordinating behaviour in the sponge, *Ephydatia muelleri* (Demospongiae, Spongillidae). J. Exp. Biol. 213:2310–2321. doi:10.1242/jeb.039859

Ellwanger K, Eich A, Nickel M (2007) GABA and glutamate specifically induce contractions in the sponge *Tethya wilhelma*. J. Comp. Physio. l A Neuroethol. Sens. Neural. Behav. Physiol. 193(1):1-11. doi:10.1007/s00359-006-0165-y

Ellwanger K, Nickel M (2006) Neuroactive substances specifically modulate rhythmic body contractions in the nerveless metazoon *Tethya wilhelma* (Demospongiae, Porifera). Front. Zool. 3:7. doi:10.1186/1742-9994-3-7

Elmore S (2007) Apoptosis: a review of programmed cell death. Toxicol. Pathol. 35(4):495-516.doi:10.1080/01926230701320337

Erwin DH, Laflamme M, Tweedt, SM, Sperling EA, Pisani D, Peterson KJ (2011) The Cambrian conundrum: early divergence and later ecological success in the early history of animals. Science 334:1091-1097. doi:10.1126/science.1206375

Fahey B, Degnan BM (2012) Origin and evolution of laminin gene family diversity. Mol. Biol. Evol. 29(7):1823-1836. doi:10.1093/molbev/mss060

Fan Y, Dutta J, Gupta N, Fan G, Gélinas C (2008) Regulation of programmed cell death by NF-kappaB and its role in tumorigenesis and therapy. Adv. Exp. Med. Biol. 615:223-250. doi:10.1007/978-1-4020-6554-5_11

Fan L, Yin S, Zhang E, Hu H (2018) Role of p62 in the regulation of cell death induction. Apoptosis 23(3-4):187-193. doi:10.1007/s10495-018-1445-z

Favaloro B, Allocati N, Graziano V, Di Ilio C, De Laurenzi V (2012) Role of apoptosis in disease. Aging 4(5):330-349. doi:10.18632/aging.100459

Fearnhead HO, Vandenabeele P, Vanden Berghe T (2017) How do we fit ferroptosis in the family of regulated cell death? Cell Death Differ. 24(12):1991-

1998. doi:10.1038/cdd.2017.149

Fernàndez-Busquets X, Burger MM (1999) Cell adhesion and histocompatibility in sponges. Microsc. Res. Tech. 44(4):204-218. doi:10.1002/(SICI)1097-0029(19990215)44:4<204::AID-JEMT2>3.0.CO;2-I

Feuda R, Dohrmann M, Pett W, Philippe H, Rota-Sabelli O, Lartillot, Wörheide G, Pisani D (2017) Improved modeling of compositional heterogeneity supports sponges as sister to all other. Curr. Biol. 27:1-7. doi: 10.1016/j.cub.2017.11.008

Fewell SW, Travers KJ, Weissman JS, Brodsky JL (2001) The action of molecular chaperones in the early secretory pathway. Ann. Rev. Genet. 35:149-191. doi:10.1146/annurev.genet.35.102401.090313

Fieseler L, Horn M, Wagner M, Hentschel U (2004) Discovery of the novel candidate phylum "Poribacteria" in marine sponges. Appl. Environ. Microbiol. 70(6):3724-3732. doi:10.1128/AEM.70.6.3724-3732.2004

Flajnik MF, Du Pasquier L (2004) Evolution of innate and adaptive immunity: can we draw a line? Trends Immunol. 25(12):640-644 doi:10.1016/j.it.2004.10.001.

Fortunato SA, Adamski M, Adamska M (2015) Comparative analyses of developmental transcription factor repertoires in sponges reveal unexpected complexity of the earliest animals. Mar. Genomics. 24(2):121-129 doi:10.1016/j.margen.2015.07.008.

Frakes AE, Dillin A (2017) The UPR (ER): Sensor and Coordinator of Organismal Homeostasis. Mol. Cell. 66(6):761-771. doi:10.1016/j.molcel.2017.0
Fuchs Y, Steller H (2011) Programmed cell death in animal development and disease. Cell. 147(4):742-758. doi:10.1016/j.cell.2011.10.033

Fulda S, Gorman AM, Hori O, Samali A (2010) Cellular stress responses: cell survival and cell death. Int. J. Cell. Biol. 2010:214074. doi:10.1155/2010/214074

Galli E, Härkönen T, Sainio MT, Ustav M, Toots U, Urtti A, Yliperttula M, Lindahl M, Knip M, Saarma M, Lindholm P (2016) Increased circulating concentrations of mesencephalic astrocyte-derived neurotrophic factor in children with type 1 diabetes. Sci. Rep. 30(6):29058. doi:10.1038/srep29058

Galliot B, Quiquand M, Ghila L, de Rosa R, Miljkovic-Licina M, Chera S (2009) Origins of neurogenesis, a cnidarian view. Dev. Biol. 332:2-24. doi:10.1016/j.ydbio.2009.05.563

Galluzzi L, Bravo-San Pedro JM, Kroemer G (2014) Organelle-specific initiation of cell death. Nat. Cell Biol. 16(8):728-736. doi:10.1038/ncb3005.

Galluzzi L, Joza N, Tasdemir E, Maiuri MC, Hengartner M, Abrams JM, Tavernarakis N, Penninger J, Madeo F, Kroemer G (2008) No death without life: vital functions of apoptotic effectors. Cell Death Differ. 15(7):1113-1123. doi:10.1038/cdd.2008.28

Galluzzi L, López-Soto A, Kumar S, Kroemer G (2016) Caspases connect cell-death signaling to organismal homeostasis. Immunity 44(2):221-231. doi:10.1016/j.i mmuni.2016.01.020

Galluzzi L, Vitale I, Aaronson SA, Abrams JM, Adam D, Agostinis P, Alnemri ES, Altucci L, Amelio I, Andrews DW, Annicchiarico-Petruzzelli M, Antonov AV, Arama E, Baehrecke EH, Barlev NA, Bazan NG, Bernassola F, Bertrand MJM, Bianchi K, Blagosklonny MV, Blomgren K, Borner C, Boya P, Brenner C, Campanella M, Candi E, Carmona-Gutierrez D, Cecconi F, Chan FK, Chandel NS, Cheng EH, Chipuk JE, Cidlowski JA, Ciechanover A, Cohen GM, Conrad M, Cubillos-Ruiz JR, Czabotar PE, D'Angiolella V, Dawson TM, Dawson VL, De Laurenzi V, De Maria R, Debatin KM, DeBerardinis RJ, Deshmukh M, Di Daniele N, Di Virgilio F, Dixit VM, Dixon SJ, Duckett CS, Dynlacht BD, El-Deiry WS, Elrod JW, Fimia GM, Fulda S, García-Sáez AJ, Garg AD, Garrido C, Gavathiotis E, Golstein P, Gottlieb E, Green DR, Greene LA, Gronemeyer H, Gross A, Hajnoczky G, Hardwick JM, Harris IS, Hengartner MO, Hetz C, Ichijo H, Jäättelä M, Joseph B, Jost PJ, Juin PP, Kaiser WJ, Karin M, Kaufmann T, Kepp O, Kimchi A, Kitsis RN, Klionsky DJ, Knight RA, Kumar S, Lee SW, Lemasters JJ, Levine B, Linkermann A, Lipton SA, Lockshin RA, López-Otín C, Lowe SW, Luedde T, Lugli E, MacFarlane M, Madeo F, Malewicz M, Malorni W, Manic G, Marine JC, Martin SJ, Martinou JC, Medema JP, Mehlen P, Meier P, Melino S, Miao EA, Molkentin JD, Moll UM, Muñoz-Pinedo C, Nagata S, Nuñez G, Oberst A, Oren M, Overholtzer M, Pagano M, Panaretakis T, Pasparakis M, Penninger JM, Pereira DM, Pervaiz S, Peter ME, Piacentini M, Pinton P, Prehn JHM, Puthalakath H, Rabinovich GA, Rehm M, Rizzuto R, Rodrigues CMP, Rubinsztein DC, Rudel T, Ryan KM, Sayan E, Scorrano L, Shao F, Shi Y, Silke J, Simon HU, Sistigu A, Stockwell BR, Strasser A, Szabadkai G, Tait SWG, Tang D, Tavernarakis N, Thorburn A, Tsujimoto Y, Turk B, Vanden Berghe T, Vandenabeele P, Vander Heiden MG, Villunger A, Virgin HW, Vousden KH, Vucic D, Wagner EF, Walczak H, Wallach D, Wang Y, Wells JA, Wood W, Yuan J, Zakeri Z, Zhivotovsky B, Zitvogel L, Melino G, Kroemer G (2018) Molecular mechanisms of cell death: recommendations of the nomenclature committee on cell death 2018. Cell Death Differ. 25(3):486-541. doi: 10.1038/ s41 418-017-0012-4

Galluzzi L, Vitale I, Abrams JM, Alnemri ES, Baehrecke EH, Blagosklonny MV, Dawson TM, Dawson VL, El-Deiry WS, Fulda S, Gottlieb E, Green DR, Hengartner MO, Kepp O, Knight RA, Kumar S, Lipton SA, Lu X, Madeo F, Malorni W, Mehlen P, Nuñez G, Peter ME, Piacentini M, Rubinsztein DC, Shi Y, Simon HU, Vandenabeele P, White E, Yuan J, Zhivotovsky B, Melino G, Kroemer G (2012) Molecular definitions of cell death subroutines: recommendations of the nomenclature committee on cell death 2012. Cell Death Differ. 19(1):107-120. doi:10.1038/cdd.2011.96

Gao FJ, Wu JH, Li TT, Du SS, Wu Q (2017b) Identification of mesencephalic astrocyte-derived neurotrophic factor as a novel neuroprotective factor for retinal ganglion cells. Front. Mol. Neurosci. 10:76. doi:10.3389/fnmol.2017.00076

Gao FJ, Zhang SH, Li TT, Wu JH, Wu Q (2017a) Expression and distribution of mesencephalic astrocyte-derived neurotrophic factor in the retina and optic nerve. Front. Hum. Neurosci. 10:686. doi:10.3389/fnhum.2016.00686

Gao L, Xu W, Fan S, Li T, Zhao T, Ying G, Zheng J, Li J, Zhang Z, Yan F, Zhu Y, Chen G (2018) MANF attenuates neuronal apoptosis and promotes behavioral recovery via Akt/MDM-2/p53 pathway after traumatic spinal cord injury in rats. Biofactors. doi:10.1002/biof.1433

Gardères J, Bedoux G, Koutsouveli V, Crequer S, Desriac F, Pennec GL (2015b) Lipopolysaccharides from commensal and opportunistic bacteria: characterization and response of the immune system of the host sponge *Suberites domuncula*. Mar. Drugs. 13(8):4985-5006. doi:10.3390/md13084985

Gardères J, Bourguet-Kondracki ML, Hamer B, Batel R, Schröder HC, Müller WE (2015a) Porifera lectins: diversity, physiological roles and biotechnological potential. Mar. Drugs. 13(8):5059-5101. doi:10.3390/md13085059

Gardères J, Domart-Coulon I, Marie A, Hamer B, Batel R, Müller WE, Bourguet-Kondracki ML (2016) Purification and partial characterization of a lectin protein complex, the clathrilectin, from the calcareous sponge *Clathrina clathrus*. Comp. Biochem. Physiol. B: Biochem. Mol. Biol. 200:17-27. doi:10.1016/j.cbpb. 2016.04.007

Gardères J, Henry J, Bernay B, Ritter A, Zatylny-Gaudin C, Wiens M, Müller WE, Le Pennec G. (2014) Cellular effects of bacterial N-3-Oxo-dodecanoyl-L-Homoserine lactone on the sponge *Suberites domuncula* (Olivi, 1792): insights into an intimate inter-kingdom dialogue. PLos One 23;9(5):e97662. doi:10.137/jornal.pone.0097662

Garea-Rodríguez E, Eesmaa A, Lindholm P, Schlumbohm C, König J, Meller B, Krieglstein K, Helms G, Saarma M, Fuchs E (2016) Comparative analysis of the effects of neurotrophic factors CDNF and GDNF in a nonhuman primate model of Parkinson's disease. PLoS One 11(2):e0149776. doi:10.1371/journal.pone.0149776

Garfin DE (1990) One-dimensional gel electrophoresis. Methods Enzymol. 182: 425-441. Re-published in Methods Enzymol. (2009) 463:497-513. doi:10.1016/ S0076-6879(09)63029-9

Garner TP, Reyna DE, Priyadarshi A, Chen HC, Li S, Wu Y, Ganesan YT, Malashkevich VN, Cheng EH, Gavathiotis E (2016) An Autoinhibited Dimeric Form of BAX Regulates the BAX Activation Pathway. Mol. Cell. 63(3):485-97. doi:10.1016/j.molcel.2016.06.010

Gasteiger E, Gattiker A, Hoogland C, Ivanyi I, Appel R D, Bairoch A (2003) ExPASy: the proteomics server for in-depth protein knowledge and analysis. Nucleic Acids Res. 31:3784-3788. doi:https://doi.org/10.1093/nar/gkg563

Gauthier M, Degnan BM (2008) Partitioning of genetically distinct cell populations in chimeric juveniles of the sponge *Amphimedon queenslandica*. Dev. Comp. Immunol. 32:1270-1280. doi:10.1016/j.dci.2008.04.002.

Gauthier MEA, Du Pasquier L, Degnan BM (2010) The genome of the sponge *Amphimedon queenslandica* provides new perspectives into the origin of Toll-like and interleukin 1 receptor pathways. Evol. Dev. 12:519-533. doi:10.1111/j.1525- 142X.2010.00436.x

Gazave E, Lapébie P, Ereskovsky AV, Vacelet J, Renard E, Cárdenas P, Borchiellini C (2012) No longer Demospongiae: Homoscleromorpha formal nomination as a fourth class of Porifera. Hydrobiologia 687:3-10. doi:https://doi.org/10.1007/s10750-011-0842-x

Gehring T, Seeholzer T, Krappmann D (2018) BCL10-bridging CARDs to immune activation. Front. Immunol. 9:1539. doi:10.3389/fimmu.2018.01539

Glembotski CC (2011) Functions for the cardiomyokine, MANF, in cardioprotection, hypertrophy and heart failure. J. Mol. Cell. Cardiol. 51(4):512-517. doi:10.1016/j.yjmcc.2010.10.008

Glembotski CC, Thuerauf DJ, Huang C, Vekich JA, Gottlieb RA, Doroudgar S (2012) Mesencephalic astrocyte-derived neurotrophic factor protects the heart from ischemic damage and is selectively secreted upon sarco/endoplasmic reticulum calcium depletion. J. Biol. Chem. 27;287(31):25893-25904. doi:10.1074/jbc.M112.356345

Gloeckner V, Wehrl M, Moitinho-Silva L, Gernert C, Schupp P, Pawlik JR, Lindquist NL, Erpenbeck D, Wörheide G, Hentschel U (2014) The HMA-LMA dichotomy revisited: an electron microscopical survey of 56 sponge species. Biol. Bull. 227(1):78-88. doi:10.1086/BBLv227n1p78

Godin JD, Creppe C, Laguesse S, Nguyen L (2016) Emerging roles for the unfolded protein response in the developing nervous system. Trends Neurosci. 39(6):394-404. doi:10.1016/j.tins.2016.04.002

Gomez JA, Gama V, Yoshida T, Sun W, Hayes P, Leskov K, Boothman D, Matsuyama S (2007) Bax-inhibiting peptides derived from Ku70 and cell-penetrating pentapeptides. Biochem. Soc. Trans. 35(4):797-801. doi:10.1042/BST0350797

Görlach A, Bertram K, Hudecova S, Krizanova O. Calcium and ROS: A mutual interplay (2015) Redox Biol. 6:260-271. doi:10.1016/j.redox.2015.08.010

Gouy M, Guindon S, Gascuel O (2010) SeaView version 4: a multiplatform graphical user interface for sequence alignment and phylogenetic tree building. Mol. Biol. Evol. 27(2):221-224. doi:10.1093/molbev/msp259

Grebenjuk VA, Kuusksalu A, Kelve M, Schütze J, Schröder HC, Müller WEG (2002) Induction of (2'-5') oligoadenylate synthetase in the marine sponges *Suberites domuncula* and *Geodia cydonium* by the bacterial endotoxin lipopolysaccharide. Eur. J. Biochem. 269:1382-1392. doi:10.1046/j.1432-1033.2002.02781.x

Grice LF, Degnan BM (2017) Transcriptomic profiling of the allorecognition response to grafting in the demosponge *Amphimedon queenslandica*. Mar. Drugs. 15(5):E136. doi:10.3390/md15050136

Grice LF, Gauthier MEA, Roper KE, Fernàndez-Busquets X, Degnan SM, Degnan BM (2017) Origin and evolution of the sponge aggregation factor gene family. Mol. Biol. Evol. 34(5):1083-1099. doi:10.1093/molbev/msx058

Grootjans J, Kaser A, Kaufman RJ, Blumberg RS (2016) The unfolded protein response in immunity and inflammation. Nat. Rev. Immunol. 16(8):469-484. doi:10.1038/nri.2016.62

Gu H (2017) Stem cell strategies for the modeling and therapy of Alzheimer´s disease. In: Frontiers in clinical drug research – Alzheimer disorders, Vol. 6. Ed. Atta-ur-Rahman. doi:10.2174/97816080587091140201

Guindon S, Dufayard JF, Lefort V, Anisimova M, Hordijk W, Gascuel O (2010) New algorithms and methods to estimate maximum-likelihood phylogenies: assessing the performance of PhyML 3.0. Syst. Biol. 59(3):307-321. doi:10.1093/sysbio/syq010

Guo C, Yuan L, Wang JG, Wang F, Yang XK, Zhang FH, Song JL, Ma XY, Cheng Q, Song GH (2014) Lipopolysaccharide (LPS) induces the apoptosis and inhibits osteoblast differentiation through JNK pathway in MC3T3-E1 cells. Inflammation. 237(2):621-631. doi:10.1007/s10753-013-9778-9

Guo J, Cui Y, Liu Q, Yang Y, Li Y, Weng L, Tang B, Jin P, Li XJ, Yang S, Li S (2018) Piperine ameliorates SCA17 neuropathology by reducing ER stress. Mol. Neurodegener. 213(1):4. doi:10.1186/s13024-018-0236-x

Gupta I, Singh K, Varshney NK, Khan S (2018) Delineating crosstalk mechanisms of the ubiquitin proteasome system that regulate apoptosis. Front. Cell Dev. Biol. 6:11. doi:10.3389/fcell.2018.00011

Gurudutta GU, Verma YK, Singh VK, Gupta P, Raj HG, Sharma RK, Chandra R (2005) Structural conservation of residues in BH1 and BH2 domains of Bcl-2 family proteins. FEBS Lett. 579(17):3503-3507. doi:10.1016/j.febslet.2005.05.015

Guzman C, Conaco C (2016) Gene expression dynamics accompanying the sponge thermal stress response. PLoS One. 11(10):e0165368. doi:10.1371/journal.pone.0165368

Gyrd-Hansen M (2018) Inhibitor of apoptosis (IAP) proteins. In: Encyclopedia of signaling molecules. Ed. Choi S. Springer. doi:https://doi.org/10.1007/978-3-319-67199-4

Hada M, Subramanian C, Andrews PC, Kwok RP (2016) Cytosolic Ku70 regulates Bax-mediated cell death. Tumour Biol. 37(10):13903-13914. doi:10.1007/s13277-016-5202-z

Hadas E, Marie D, Shpigel M, Ilan M (2006) Virus predation by sponges is a new nutrient-flow pathway in coral reef food webs. Limnol. Oceanogr. 51:1548-1550. doi:10.3354/meps141095

Hakonen E, Chandra V, Fogarty CL, Yu NY, Ustinovo J, Katayama S, Galli E, Danilova T, Lindholm P, Vartiainen A, Einarsdottir E, KrjutŠkov, Kere J, Saarma M, Lindahl M, Otonkoski (2018) MANF protects human pancreatic beta cells against stress-induced cell death. Diabetologia. doi:https://doi.org/10.1007/s00125-018-4687-y

Halanych KM (2004) The new view of animal phylogeny. Annu. Rev. Ecol. Syst. 35:229-256. doi:https://doi.org/10.1146/annurev.ecolsys.35.112202.130124

Halvorsen SW, Kaurn N (2006) CNTF and related neurokines. In: Handbook of neurochemistry and molecular neurobiology. Neuroactive proteins and peptides Eds: Lajtha A and Lim R. Springer-Verlager. 684p.

Hames BD (1998) Gel electrophoresis of proteins: a practical approach. Ed. Oxford University Press, 3rd.

Han J, Back SH, Hur J, Lin YH, Gildersleeve R, Shan J, Yuan CL, Krokowski D, Wang S, Hatzoglou M, Kilberg MS, Sartor MA, Kaufman RJ (2013) ER-stress-induced transcriptional regulation increases protein synthesis leading to cell death. Nat. Cell Biol. 15(5):481-490. doi:10.1038/ncb2738

Hao F, Yang C, Chen SS, Wang YY, Zhou W, Hao Q, Lu T, Hoffer B, Zhao LR, Duan WM, Xu QY (2017) Long-term protective effects of AAV9-mesencephalic astrocyte-derived neurotrophic factor gene transfer in parkinsonian rats. Exp. Neurol. 291:120-133. doi:10.1016/j.expneurol.2017.01.008

Harcet M, Roller M, Cetkovic H, Perina D, Wiens M, Müller WE, Vlahovicek K (2010) Demosponge EST sequencing reveals a complex genetic toolkit of the simplest metazoans. Mol. Biol. Evol. 27:2747-2756. doi:10.1093/molbev/msq174

Harding HP, Novoa I, Zhang Y, Zeng H, Wek R, Schapira M, Ron D (2000) Regulated translation initiation controls stress-induced gene expression in

mammalian cells. Mol. Cell. 6:1099-1108.
doi:http://dx.doi.org/10.1016/S1097-2765(00)00108-8

Harding HP, Zhang Y, Ron D (1999) Protein translation and folding are coupled by an endoplasmic-reticulum-resident kinase. Nature 397:271-274. doi:10.1038/16729

Hartley CL, Edwards S, Mullan L, Bell PA, Fresquet M, Boot-Handford RP, Briggs MD (2013) Armet/Manf and Creld2 are components of a specialized ER stress response provoked by inappropriate formation of disulphide bonds: implications for genetic skeletal diseases. Hum. Mol. Genet. 22(25):562-575. doi:10.1093/hmg/ddt383

Haupt S, Berger M, Goldberg Z, Haupt Y (2003) Apoptosis - the p53 network. J. Cell Sci. 116(Pt 20):4077-4085. doi:10.1242/jcs.00739

Haze K, Yoshida H, Yanagi H, Yura T, Mori K (1999) Mammalian transcription factor ATF6 is synthesized as a transmembrane protein and activated by proteolysis in response to endoplasmic reticulum stress. Mol. Biol. Cell. 10(11):3787-3799. doi:10.1091/mbc.10.11.3787

He F, Mai LH, Gardères J, Hussain A, Erakovic Haber V, Bourguet-Kondracki ML (2017) Major antimicrobial representatives from marine sponges and/or their associated bacteria. In: Prog. Mol. Subcell. Biol.55:35-89. Eds: Müller WEG, Schröder HC, Wang X. doi:10.1007/978-3-319-51284-6_2

Hedrick SM, Ch'en IL, Alves BN (2010) Intertwined pathways of programmed cell death in immunity. Immunol. Rev. 236:41-53. doi:10.1111/j.1600-065X.2010.00918.x

Hefti F, Denton TL, Knusel B, Lapchak PA (1993) Neurotrophic factors: What are they and what are they doing? In: ‘‘Neurotrophic Factors’’ Eds: Loughlin SE; Fallon HJ pp. 25-49. Academic Press.

Hejnol A, Obst M, Stamatakis A, Ott M, Rouse GW, Edgecombe GD, Martinez P, Baguñà J, Bailly X, Jondelius U, Wiens M, Müller WE, Seaver E, Wheeler WC, Martindale MQ, Giribet G, Dunn CW (2009) Assessing the root of bilaterian animals with scalable phylogenomic methods. Proc. Biol. Sci. 276(1677):4261-4270. doi:10.1098/rspb.2009.0896

Hellman M, Arumäe U, Yu LY, Lindholm P, Peränen J, Saarma M, Permi P (2011) Mesencephalic astrocyte-derived neurotrophic factor (MANF) has a unique mechanism to rescue apoptotic neurons. J. Biol. Chem. 286:2675-2680. doi:10.1074/jbc.M110.146738

Henderson MJ, Richie CT, Airavaara M, Wang Y, Harvey BK (2013) Mesencephalic astrocyte-derived neurotrophic factor (MANF) secretion and cell surface binding are modulated by KDEL receptors. J. Biol. Chem. 288:4209-4255. doi:10.1074/jbc.M112.400648

Heneka MT, McManus RM, Latz E (2018) Inflammasome signalling in brain function and neurodegenerative disease. Nat. Rev. Neurosci. [Epub ahead of print] doi:10.1038/s41583-018-0055-7

Hentschel U, Fieseler L, Wehrl M, Gernert C, Steinert M, Hacker J, Horn M (2003) Microbial diversity of marine sponges. In: Sponges (Porifera). Prog. Mol. Subcell. Biol. Ed: Müller WEG 34:59-88. Springer.

Hentschel U, Piel J, Degnan SM, Taylor MW (2012) Genomic insights into the marine sponge microbiome. Nature Rev. Microbiol. 10:641-654. doi:10.1038/nrmicro2839

Hentschel U, Usher KM, Taylor MW (2006) Marine sponges as microbial fermenters. FEMS Microbiol. Ecol. 55(2):167-177. doi:10.1111/j.1574-6941.2005.00046.x

Hetz C (2012) The unfolded protein response: controlling cell fate decisions under ER stress and beyond. Nat. Rev. Mol. Cell. Biol. 18;13(2):89-102. doi:10.1038/nrm3270

Hetz C, Bernasconi P, Fisher J, Lee AH, Bassik MC, Antonsson B, Brandt GS, Iwakoshi NN, Schinzel A, Glimcher LH, Korsmeyer SJ (2006) Proapoptotic BAX and BAK modulate the unfolded protein response by a direct interaction with IRE1α. Science. 312(5773):572-576. doi:10.1126/science.1123480

Hetz C, Chevet E, Harding HP (2013) Targeting the unfolded protein response in disease. Nat. Rev. Drug. Discov. 12(9):703-719. doi:10.1038/nrd3976

Hetz C, Chevet E, Oakes SA (2015) Proteostasis control by the unfolded protein response. Nat. Cell Biol. 17(7):829-838. doi:10.1038/ncb3184

Hetz C, Glimcher LH (2009) Fine-tuning of the unfolded protein response: Assembling the IRE1α. interactome. Mol. Cell 35(5):551-561. doi:10.1016/j.molcel.2009.08.021

Hetz C, Martinon F, Rodriguez D, Glimcher LH (2011) The unfolded protein response: integrating stress signals through the stress sensor IRE1α. Physiol. Rev. 91(4):1219-1243. doi:10.1152/physrev.00001.2011

Hetz C, Papa FR (2018) The unfolded protein response and cell fate control. Mol. Cell. 69(2):169-181. doi:10.1016/j.molcel.2017.06.017

Hetz C, Saxena S (2017) ER stress and the unfolded protein response in neurodegeneration. Nat. Rev. Neurol. 13(8):477-491. doi:10.1038/nrneurol.2017.99

Hoffmann JA, Kafatos FC, Janeway CA, Ezekowitz RA (1999) Phylogenetic perspectives in innate immunity. Science 21;284(5418):1313-1318. doi:10.1126/science.284.5418.1313

Hollien J (2013) Evolution of the unfolded protein response. Biochim. Biophys. Acta 1833:2458-2463. doi:10.1016/j.bbamcr.2013.01.016

Hollien J, Lin JH, Li H, Stevens N, Walter P, Weissman JS (2009) Regulated Ire1-dependent decay of messenger RNAs in mammalian cells. J. Cell Biol. 186(3):323-331. doi:10.1083/jcb.200903014

Hollien J, Weissman JS (2006) Decay of endoplasmic reticulum-localized mRNAs during the unfolded protein response. Science. 313(5783):104-107. doi:10.1126/science.1129631

Hong F, Liu B, Wu BX, Morreall J, Roth B, Davies C, Sun S, Diehl JA, Li Z (2017) CNPY2 is a key initiator of the PERK-CHOP pathway of the unfolded protein response. Nat. Struct. Mol. Biol. 24(10):834-839. doi:10.1038/nsmb.3458

Hooper JNA and Van Soest RWM (2002) Systema Porifera: a guide to the classification of sponges. Edited by: Hooper JNA and Van Soest RWM. Kluwer Academic/Plenum publishers.

Horibe T, Gomi M, Iguchi D, Ito H, Kitamura Y, Masuoka T, Tsujimoto I, Kimura T, Kikuchi M (2004) Gentamicin binds to the lectin site of calreticulin and inhibits its chaperone activity. J. Biol. Chem. 279:4604-4611. doi:10.1016/j.bbrc.2004.08.099

Horton P, Park KJ, Obayashi T, Fujita N, Harada H, Adams-Collier CJ, Nakai K (2007) WoLF PSORT: protein localization predictor. Nucleic Acids Res. 35:W585-587. doi:10.1093/nar/gkm259

Hoseki J, Sasakawa H, Yamaguchi Y, Maeda M, Kubota H, Kato K, Nagata K (2010) Solution structure and dynamics of mouse ARMET. FEBS Lett. 584(8):1536-1542. doi:10.1016/j.febslet.2010.03.008

Huang J, Chen C, Gu H, Li C, Fu X, Jiang M, Sun H, Xu J, Fang J, Jin L (2016) Mesencephalic astrocyte-derived neurotrophic factor reduces cell apoptosis via upregulating GRP78 in SH-SY5Y cells. Cell. Biol. Int. 40(7):803-811. doi:10.1002/cbin.10621

Huang RR, Hu W, Yin YY, Wang YC, Li WP, Li WZ (2015) Chronic restraint stress promotes learning and memory impairment due to enhanced neuronal endoplasmic reticulum stress in the frontal cortex and hippocampus in male mice. Int. J. Mol. Med. 35(2):553-559. doi:10.3892/ijmm.2014.2026

Hughes D, Mallucci GR (2018) The unfolded protein response in neurodegenerative disorders - therapeutic modulation of the PERK pathway. FEBS J. doi:10.1111/febs.14422

Ibáñez CF, Andressoo JO (2017) Biology of GDNF and its receptors - Relevance for disorders of the central nervous system. Neurobiol. Dis. 97(Pt

B):80-89. 10.1016/j.nbd.2016.01.021

Ilan M, Abelson A (1995) The life of a sponge in a sandy lagoon, Biol. Bull. 189(3):363-369. doi:https://doi.org/10.2307/1542154

Iwasaki A, Medzhitov R (2015) Control of adaptive immunity by the innate immune system. Nat. Immunol. 16(4):343-353. doi:10.1038/ni.3123

Janssens S, Pulendran B, Lambrecht BN (2014) Emerging functions of the unfolded protein response in immunity. Nat. Immunol. 15(10):910-919. doi:10.1038/ni.2991

Jeng PS, Inoue-Yamauchi A, Hsieh JJ, Cheng EH (2018) BH3-dependent and independent activation of BAX and BAK in mitochondrial apoptosis. Curr. Opin. in Physi. 3:71-81. doi:https://doi.org/10.1016/j.cophys.2018.03.005

Jindrich K, Degnan BM (2016) The diversification of the basic leucine zipper family in eukaryotes correlates with the evolution of multicellularity. BMC Evol. Biol. 16:28. doi:10.1186/s12862-016-0598-z

Joshi AS, Zhang H, Prinz WA (2017) Organelle biogenesis in the endoplasmic reticulum. Nat. Cell. Biol. 19:876-882. doi:10.1038/ncb3579

Kabelitz D, Medzhitov R (2007) Innate immunity-cross-talk with adaptive immunity through pattern recognition receptors and cytokines. Curr. Opin. Immunol. 19(1):1-3. doi:10.1016/j.coi.2006.11.018

Kaczanowski S (2016) Apoptosis: its origin, history, maintenance and the medical implications for cancer and aging. Phys. Biol. 13(3):031001. doi:10.1088/1478-3975/13/3/031001

Kaneko M, Niinuma Y, Nomura Y (2003) Activation signal of nuclear factor-kappa B in response to endoplasmic reticulum stress is transduced via IRE1 and tumor necrosis factor receptor-associated factor 2. Biol. Pharm. Bull. 26(7):931-935. doi:https://doi.org/10.1248/bpb.26.931

Karahashi H, Amano F (1998) Apoptotic changes preceding necrosis in lipopolysaccharide-treated macrophages in the presence of cycloheximide. Exp. Cell Res. 241(2):373-383. doi:https://doi.org/10.1006/excr.1998.4062

Kassabov SR, Choi YB, Karl KA, Vishwasrao HD, Bailey CH, Kandel ER (2013) A single Aplysia neurotrophin mediates synaptic facilitation via differentially processed isoforms. Cell. Rep. 3:1213-1227. doi:10.1016/j.celrep.2013.03.008

Kaufman RJ, Scheuner D, Schröder M, Shen X, Lee K, Liu CY, Arnold SM (2002) The unfolded protein response in nutrient sensing and differentiation. Nat. Rev. Mol. Cell Biol. 3(6):411-421. doi:10.1038/nrm829

Keestra-Gounder AM, Byndloss MX, Seyffert N, Young BM, Chávez-Arroyo A, Tsai AY, Cevallos SA, Winter MG, Pham OH, Tiffany CR, de Jong MF, Kerrinnes T, Ravindran R, Luciw PA, McSorley SJ, Bäumler AJ, Tsolis RM (2016) NOD1 and NOD2 signaling links ER stress with inflammation. Nature 532(7599):394-397. doi:10.1038/nature17631

Kenny NJ, de Goeij JM, de Bakker DM, Whalen CG, Berezikov E, Riesgo A (2018) Towards the identification of ancestrally shared regenerative mechanisms across the Metazoa: A transcriptomic case study in the Demosponge *Halisarca caerulea*. Mar. Genomics. 37:135-147. doi:10.1016/j.margen.2017.11.001

Kim J, Song H, Heo HR, Kim JW, Kim HR, Hong Y, Yang SR, Han SS, Lee SJ, Kim WJ, Hong SH (2017b) Cadmium-induced ER stress and inflammation are mediated through C/EBP-DDIT3 signaling in human bronchial epithelial cells. Exp. Mol. Med. 49(9):e372. doi:10.1038/emm.2017.125

Kim Y, Lee H, Manson SR, Lindahl M, Evans B, Miner JH, Urano F, Chen YM (2016) Mesencephalic astrocyte-derived neurotrophic factor as a urine biomarker for endoplasmic reticulum stress-related kidney diseases. J. Am. Soc. Nephrol. 27(10):2974-2982. doi:10.1681/ASN.2014100986

Kim Y, Park SJ, Chen YM (2017a) Mesencephalic astrocyte-derived neurotrophic fator (MANF) a new player in endoplasmic reticulum diseases: structure, biology, and therapeutic roles. Transl. Res. 29;S19315244(17):30219-0. doi:10.1016/j.trsl.2017.06.010

Kimbrell DA, Beutler B (2001) The evolution and genetics of innate immunity. Nat. Rev. Genet. 2(4):256-267. doi:10.1038/35066006

Kitao Y, Ozawa K, Miyazaki M, Tamatani M, Kobayashi T, Yanagi H, Okabe M, Ikawa M, Yamashima T, Stern DM, Hori O, Ogawa S (2001) Expression of the endoplasmic reticulum molecular chaperone (ORP150) rescues hippocampal neurons from glutamate toxicity. J. Clin. Invest. 108(10):1439-1450.

Kojima E, Takeuchi A, Haneda M, Yagi A, Hasegawa T, Yamaki K, Takeda K, Akira S, Shimokata K, Isobe K (2003) The function of GADD34 is a recovery from a shutoff of protein synthesis induced by ER stress: elucidation by GADD34-deficient mice. FASEB J. 17(11):1573-1575. doi:10.1096/fj.02-1184fje

Kolter T, Sandhoff K (2005) Principles of lysosomal membrane digestion: stimulation of sphingolipid degradation by sphingolipid activator proteins and anionic lysosomal lipids. Annu. Rev. Cell. Dev. Biol.21:81-103. doi:10.1146/annurev.cellbio.21.122303.120013

Koressaar T, Remm M (2007) Enhancements and modifications of primer design program Primer3. Bioinformatics 23(10):1289-1291. doi:10.1093/bioinformatics/btm091

Kratochvílová K, Moráň L, Paďourová S, Stejskal S, Tesařová L, Šimara P, Hampl A, Koutná I, Vaňhara P (2016) The role of the endoplasmic reticulum stress in stemness, pluripotency and development. Eur. J. Cell Biol. 95(3-5):115-123. doi:10.1016/j.ejcb.2016.02.002

Kratz RF (2009) Molecular & cell biology for dummies®. Wiley Publishing, Inc. 389p.

Krawczyk KK, Ekman M, Rippe C, Grossi M, Nilsson BO, Albinsson S, Uvelius B, Swärd K (2016) Assessing the contribution of thrombospondin-4 induction and ATF6α activation to endoplasmic reticulum expansion and phenotypic modulation in bladder outlet obstruction. Sci. Rep. 6:32449. doi:10.1038/srep32449

Kruse M, Steffen R, Batel R, Müller IM, Müller WE (1999) Differential expression of allograft inflammatory factor 1 and of glutathione peroxidase during auto- and allograft response in marine sponges. J. Cell Sci. 112(23):4305-4313.

Kültz D (2003) Evolution of the cellular stress proteome: from monophyletic origin to ubiquitous function. J. Exp. Biol. 206(18):3119-3124. doi:10.1242/jeb.005

Kurtz J, Armitage SA (2006) Alternative adaptive immunity in invertebrates. Trends Immunol. 27(11):493-496. doi:10.1016/j.it.2006.09.001

Laemmli UK (1970) Cleavage of structural proteins during the assembly of the head of bacteriophage T4. Nature 227:680-685. doi:10.1038/227680a0

Larroux C, Fahey B, Liubicich D, Hinman VF, Gauthier M, Gongora M, Green K, Wörheide G, Leys SP, Degnan BM (2006) Developmental expression of transcription factor genes in a demosponge: insights into the origin of metazoan multicellularity. Evol. Dev. 8(2):150-173. doi:https://doi.org/10.1111/j.1525-142X.2006.00086.x

Larsen OS, Riisgård HU (1994) The Sponge Pump. J. Theor. Biol. 168:53-63.

Latge C, Cabral KM, de Oliveira GA, Raymundo DP, Freitas JA, Johanson L, Romão LF, Palhano FL, Herrmann T, Almeida MS, Foguel D (2015) The solution structure and dynamics of full-length human cerebral dopamine neurotrophic factor and its neuroprotective role against α-synuclein oligomers. J. Biol. Chem. 290:20527-20540. doi:10.1074/jbc.M115.662254

Lauri A, Bertucci P, Arendt D (2016) Neurotrophin, p75, and Trk signaling module in the developing nervous system of the marine annelid *Platynereis dumerilii*. Biomed. Res. Int. 1-12. doi:10.1155/2016/2456062

Le SQ, Gascuel O (2008) An improved general amino acid replacement matrix. Mol. Biol. Evol. 25(7):1307-1320. doi:10.1093/molbev/msn067

Lee AH, Iwakoshi NN, Glimcher LH (2003) XBP-1 regulates a subset of endoplasmic reticulum resident chaperone genes in the unfolded protein response. Mol. Cell. Biol. 23:7448-7459.
doi:10.1128/MCB.23.21.7448-7459.2003

Lee K, Tirasophon W, Shen X, Michalak M, Prywes R, Okada T, Yoshida H, Mori K, Kaufman RJ (2002) IRE1-mediated unconventional mRNA splicing and S2P-mediated ATF6 cleavage merge to regulate XBP1 in signaling the unfolded protein response. Genes Dev. 16(4):452-466.
doi:10.1101/gad.964702

Lemasters JJ (2005) Dying a thousand deaths: redundant pathways from different organelles to apoptosis and necrosis. Gastroenterology. 129(1):351-360. doi:https://doi.org/10.1053/j.gastro.2005.06.006

Lemasters JJ (2018) Molecular Mechanisms of Cell Death. Chapter 1, 1-25. In: Molecular pathology, the molecular basis of human disease, 2° edition. Eds: Coleman W; Tsongalis G. Elsevier.

Lencer WI, DeLuca H, Grey MJ, Cho JA (2015) Innate immunity at mucosal surfaces: the IRE1-RIDD-RIG-I pathway. Trends Immunol. 36(7):401-409. doi:10.1016/j.it.2015.05.006

Lerner AG, Upton JP, Praveen PV, Ghosh R, Nakagawa Y, Igbaria A, Shen S, Nguyen V, Backes BJ, Heiman M, Heintz N, Greengard P, Hui S, Tang Q, Trusina A, Oakes SA, Papa FR (2012) IRE1α induces thioredoxin-interacting protein to activate the NLRP3 inflammasome and promote programmed cell death under irremediable ER stress. Cell Metab. 16(2):250-264.
doi: 10.1016/j.cmet.2012.07.007

Letunic I, Doerks T, Bork P (2015) SMART: recent updates, new developments and status in 2015. Nucleic Acids Res. 43:D257-260. doi:10.1093/nar/gku949

Levy YS, Gilgun-Sherki Y, Melamed E, Offen D (2005) Therapeutic potential of neurotrophic factors in neurodegenerative diseases. BioDrugs. 19(2):97-127. doi:https://doi.org/10.2165/00063030-200519020-00003

Lewin GR, Carter BD (2014) Neurotrophic factors. Preface. In: Handb. Exp. Pharmacol. volume 220:v-vi. Ed: Rosenthal W, Springer.

Leys SP (2015) Elements of a “nervous system” in sponges. J. Exp. Biol. 218:581-591. doi:10.1242/jeb.110817

Leys SP, Degnan BM (2001) Cytological basis of photoresponsive behavior in a sponge larva. Biol. Bull. 201:323-338. doi:10.2307/1543611

Leys SP, Degnan BM (2002) Embryogenesis and metamorphosis in a haplosclerid demosponge: gastrulation and transdifferentiation of larval ciliated cells to choanocytes. Invertebr. Biol. 121(3):171-189.

doi:10.1111/j.1744-7410.2002.tb00058.x

Leys SP, Ereskovsky A (2006) Embryogenesis and larval differentiation in sponges. Can. J. Zool. 84:262–287. doi:https://doi.org/10.1139/z05-170

Leys SP, Hill A (2012) The physiology and molecular biology of sponge tissues. Adv. Mar. Biol. 62:1-56. doi:10.1016/B978-0-12-394283-8.00001-1

Leys SP, Mackie GO, Meech RW (1999) Impulse conduction in a sponge. J. Exp. Biol. 202:1139-1150.

Leys SP, Meech RW (2006) Physiology of coordination in sponges. Can. J. Zool. 84(2):288-306. doi:https://doi.org/10.1139/z05-171

Leys SP, Nichols SA, Adams ED (2009) Epithelia and integration in sponges. Integr. Comp. Biol. 49(2):167-177. doi:10.1093/icb/icp038

Leys SP, Riesgo A (2012) Epithelia, an evolutionary novelty of metazoans. J. Exp. Zool. B. Mol. Dev. Evol. 318(6):438-447. doi:10.1002/jez.b.21442

Leys SP, Rohksar DS, Degnan BM (2005) Sponges. Curr. Biol. 15(4):R114-115. doi:10.1016/j.cub.2005.02.005

Li CW, Chen JY, Hua TE (1998) Precambrian sponges with cellular structures. Science. 279(5352):879-882. doi:10.1126/science.279.5352.879

Li QX, Shen YX, Ahmad A, Shen YJ, Zhang YQ, Xu PK, Chen WW, Yu YQ (2018) MANF prevents traumatic brain injury in rats by inhibiting inflammatory activation and protecting blood brain barrier. World Neurosurg. pii: S1878-8750(18)31156-2. doi:10.1016/j.wneu.2018.05.202

Li Y, Guo Y, Tang J, Jiang J, Chen Z (2014) New insights into the roles of CHOP-induced apoptosis in ER stress. Acta Biochim. Biophys. Sin. 46(8):629-640. doi:10.1093/abbs/gmu128

Li-na Z, Deng C, Da X, Si-Han C, Hai-Jiao W, Ling L (2017) Mesencephalic astrocyte-derived neurotrophic factor and its role in nervous system disease. Neurol. Sci. 38(10):1731-1734 doi:10.1007/s10072-017-3042-2.

Lindahl M, Danilova T, Palm E, Lindholm P, Võikar V, Hakonen E, Ustinov J, Andressoo JO, Harvey BK, Otonkoski T, Rossi J, Saarma M (2014). MANF is indispensable for the proliferation and survival of pancreatic β cells. Cell Rep. 24;7(2):366-375. doi:10.1016/j.celrep.2014.03.023

Lindahl M, Saarma M, Lindholm P (2017) Unconventional neurotrophic factors CDNF and MANF: structure, physiological functions and therapeutic potential. Neurobiol. Dis. 97:90-102. doi:10.1016/j.nbd.2016.07.009

Linde CM, Grundström S, Nordling E, Refai E, Brennan PJ, Andersson M

(2005) Conserved structure and function in the granulysin and NK-lysin peptide family. Infect. Immun. 73(10):6332-6339. doi:10.1128/IAI.73.10.6332-6339.2005

Lindholm D, Mäkelä J, Di Liberto V, Mudò G, Belluardo N, Eriksson O, Saarma M. (2016) Current disease modifying approaches to treat Parkinson's disease. Cell. Mol. Life Sci. 73(7):1365-1379. doi:10.1007/s00018-015-2101-1

Lindholm p, Peränen J, Andressoo JO, Kalkkinen N, Kokaia Z, Lindvall O, Timmusk T, Saarma M (2008) MANF is widely expressed in mammalian tissues and differently regulated after ischemic and epileptic insults in rodent brain. Mol. Cell. Neurosci. 39(3):356-371. doi:10.1016/j.mcn.2008.07.016

Lindholm P, Saarma (2010) Novel CDNF/MANF family of neurotrophic factors. Dev. Neurobiol. 70(5):360-371. doi:10.1002/dneu.20760

Lindholm P, Voutilainen MH, Laurén J, Peränen J, Leppänen VM, Andressoo JO, Lindahl M, Janhunen S, Kalkkinen N, Timmusk T, Tuominen RK, Saarma M (2007) Novel neurotrophic factor CDNF protects and rescues midbrain dopamine neurons in vivo. Nature 448:73-77. doi:10.1038/nature05957

Lindström R, Lindholm P, Kallijärvi J, Palgi M, Saarma M, Heino TI (2016) Exploring the Conserved Role of MANF in the Unfolded Protein Response in *Drosophila melanogaster.* PLoS One. 11(3):e0151550. doi:10.137/jornal.pone.0151550

Lindström R, Lindholm P, Kallijärvi J, Yu LY, Piepponen TP, Arumäe U, Saarma M, Heino TI (2013) Characterization of the structural and functional determinants of MANF/CDNF in drosophila in vivo model. PLoS One 8(9):e73928. doi:10.1371/journal.pone.0073928

Lindström R, Lindholm P, Palgi M, Saarma M, Heino TI (2017) In vivo screening reveals interactions between Drosophila Manf and genes involved in the mitochondria and the ubiquinone synthesis pathway. BMC Genet. 18(1):52. doi:10.1186/s12863-017-0509-3

Littlewood DTJ (2017) Animal evolution: last word on sponges-first? Curr. Biol. 27(7):R259-R261. doi:10.1016/j.cub.2017.02.042

Liu CL, Zhong W, He YY, Li X, Li S, He KL (2016b) Genome-wide analysis of tunicamycin-induced endoplasmic reticulum stress response and the protective effect of endoplasmic reticulum inhibitors in neonatal rat cardiomyocytes. Mol. Cell. Biochem. 413(1-2):57-67. doi:10.1007/s11010-015-2639-0

Liu H, Tang X, Gong L (2015b) Mesencephalic astrocyte-derived neurotrophic factor and cerebral dopamine neurotrophic factor: New endoplasmic reticulum stress response proteins. Eur. J. Pharmacol. 750:118-122. doi:10.1016/j.ejphar.2015.01.016. 25637781

Liu H, Yu C, Yu H, Zhong L, Wang Y, Liu J, Zhang S, Sun J, Duan L, Gong L, Yang J (2017) Cerebral dopamine neurotrophic factor protects H9c2 cardiomyocytes from apoptosis. Herz 1-6. doi:10.1007/s00059-017-4564-3

Liu H, Zhao C, Zhong L, Liu J, Zhang S, Cheng B, Gong L (2015a) Key subdomains in the C-terminal of cerebral dopamine neurotrophic factor regulate the protein secretion. Biochem. Biophys. Res. Commun. 465(3):427-432. doi:10.1016/j.bbrc.2015.08.029

Liu J, Zhou C, Tao X, Feng L, Wang X, Chen L, Li C, Huang D, Fang S, Shen Y (2015c) ER stress-inducible protein MANF selectively expresses in human spleen. Hum. Immunol. 76(11):823-830. doi:10.1016/j.humimm.2015.09.043

Liu M, Chen Z, Chen L (2016a) Endoplasmic reticulum stress: a novel mechanism and therapeutic target for cardiovascular diseases. Acta Pharmacol. Sin. 37:1-19. doi:10.1038/aps.2015.145

Liu Y, Zhang J, Jiang M, Cai Q, Fang J, Jin L (2018) MANF improves the MPP(+)/MPTP-induced Parkinson's disease via improvement of mitochondrial function and inhibition of oxidative stress. Am. J. Transl. Res. 10(5):1284-1294. eCollection 2018

Liu YP, Zeng L, Tian A, Bomkamp A, Rivera D, Gutman D, Barber GN, Olson JK, Smith JA (2012) Endoplasmic reticulum stress regulates the innate immunity critical transcription factor IRF3. J. Immunol. 189(9):4630-4639. doi:10.4049/jimmunol.1102737

Love GD, Grosjean E, Stalvies C, Fike DA, Grotzinger JP, Bradley AS, Kelly AE, Bhatia M, Meredith W, Snape CE, Bowring SA, Condon DJ, Summons R (2009) Fossil steroids record the appearance of Demospongiae during the cryogenian period. Nature 457(7230):718-721. doi:10.1038/nature07673

Lu J, Luo L, Huang D, Liu X, Xia X, Wang Z, Lam BL, Yi J, Wen R, Li Y (2018) Photoreceptor protection by mesencephalic astrocyte-derived neurotrophic factor (MANF). eNeuro 5(2):pii:0109-18.2018. doi:10.1523/ENEURO.010918.2018

Ludeman DA, Farrar N, Riesgo A, Paps J, Leys SP (2014) Evolutionary origins of sensation in metazoans: functional evidence for a new sensory organ in sponges. BMC Evol. Biol.14:3. doi:10.1186/1471-2148-14-3

Luthringer B, Isbert S, Müller WEG, Zilberberg C, Thakur NL, Wörheide G, Stauber RH, Kelve M, Wiens M (2011) Poriferan survivin exhibits a conserved regulatory role in the interconnected pathways of cell cycle and apoptosis. Cell Death Differ. 18:201-213. doi:10.1038/cdd.2010.87

Lynch JM, Maillet M, Vanhoutte D, Schloemer A, Sargent MA, Blair NS, Lynch KA, Okada T, Aronow BJ, Osinska H, Prywes R, Lorenz JN, Mori K, Lawler J, Robbins J, Molkentin JD (2012) A thrombospondin-dependent pathway for a

protective ER stress response. Cell 149:1257-1268. doi:10.1016/j.cell.2012.03

Ma Y, Hendershot LM (2003) The stressful road to antibody secretion. Nat. Immunol. 4(4):310-311. doi:10.1038/ni0403-310

Magnino G, Sarà A, Lancioni T, Gaino E (1999) Endobionts of the coral reef sponge *Theonella Swinhoei* (Porifera, Demospongiae). Invertebrate Biology 118(3): 213-220. doi:10.2307/3226993

Mah JL, Christensen-Dalsgaard KK, Leys SP (2014) Choanoflagellate and choanocyte collar-flagellar systems and the assumption of homology. Evol. Dev. 16(1):25-37. doi:10.1111/ede.12060

Mah JL, Leys SP (2017) Think like a sponge: the genetic signal of sensory cells in sponges. Dev. Biol. 431(1):93-100. doi:10.1016/j.ydbio.2017.06.012

Majdi A, Mahmoudi J, Sadigh-Eteghad S, Golzari SE, Sabermarouf B, Reyhani-Rad S (2016) Permissive role of cytosolic pH acidification in neurodegeneration: a closer look at its causes and consequences. J. Neurosci. Res. 94(10):879-887. doi:10.1002/jnr.23757

Maldonado M, Bergquist PR (2002) Phylum Porifera. In: Atlas of marine invertebrate larvae. Eds: Young CM, Sewell MA and Rice ME. CA: Academic Press. pp. 21-50.

Maldonado M, Carmona MC, Velasquez Z, Puig A, Cruzado A, Lopez A, Young CM (2005) Siliceous sponges as a silicon sink: an overlooked aspect of benthopelagic coupling in the marine silicon cycle. Limnol. Oceanogr. 50:799-809. doi:10.4319/lo.2005.50.3.0799

Maldonado M, Durfort M, McCarthy DA, Young CM (2003) The cellular basis of photobehavior in the tufted parenchymella larva of demosponges. Mar. Biol. 143:427-441. doi:https://doi.org/10.1007/s00227-003-1100-1

Mallatt J, Winchell CJ (2007) Ribosomal RNA genes and deuterostome phylogeny revisited: more cyclostomes, elasmobranchs, reptiles, and a brittle star. Mol. Phylogenet. Evol. 43:1005-1022. doi:10.1016/j.ympev.2006.11.023

Mao WP, Ye JL, Guan ZB, Zhao JM, Zhang C, Zhang NN, Jiang P, Tian T (2007) Cadmium induces apoptosis in human embryonic kidney (HEK) 293 cells by caspase-dependent and -independent pathways acting on mitochondria. Toxicol In Vitro. 21(3):343-354. doi:10.1016/j.tiv.2006.09.004

Martinand-Mari C, Vacelet J, Nickel M, Wörheide G, Mangeat P, Baghdiguian S (2012) Cell death and renewal during prey capture and digestion in the carnivorous sponge Asbestopluma hypogea (Porifera: Poecilosclerida). J. Exp. Biol. 215(22):3937-3943. doi:10.1242/jeb.072371

Martinon F, Chen X, Lee AH, Glimcher LH (2010) TLR activation of the

transcription factor XBP1 regulates innate immune responses in macrophages. Nat. Immunol. 11(5):411-418. doi:10.1038/ni.1857

Martins AS, Alves I, Helguero L, Domingues MR, Neves BM (2016) The unfolded protein response in homeostasis and modulation of mammalian immune cells. Int. Rev. Immunol. 35(6):457-476. doi:10.3109/08830185.2015.1

Mätlik K, Antila JE, Kuan-Yin T, Smolander OP, Pakarien E, Lehtonen L, Abo-Ramadam U, Lindholm P, Zhen C, Harvey B, Arumäe U, Lindahl M, Airavaara M (2018) Poststroke delivery of MANF promotes functional recovery in rats. Sci. Adv. 23;4(5):eaap8957. doi:10.1126/sciadv.aap8957

Mätlik K, Yu LY, Eesmaa A, Hellman M, Lindholm P, Peränen J, Galli E, Antilla EJ, Saarma M, Permi P, Airavaara, M, Arumäe U (2015) Role of two sequence motifs of mesencephalic astrocyte-derived neurotrophic factor in its survival-promoting activity. Cell Death Dis. 6(12):e2032. doi:10.1038/cddis.2015.371

McLaughlin T, Dhimal N, Li J, Wang JJ, Zhang SX (2018) $p58^{IPK}$ is an endogenous neuroprotectant for retinal ganglion cells. Front. Aging Neurosci. 10:267. doi:10.3389/fnagi.2018.00267

Medina M, Collins AG, Silberman JD, Sogin ML (2001) Evaluating hypotheses of basal animal phylogeny using complete sequences of large and small subunit rRNA. Proc. Natl. Acad. Sci. USA 98(17):9707-9712.

Medzhitov R (2007a) TLR-mediated innate immune recognition. Semin. Immunol. 19(1):1-2. doi:10.1016/j.smim.2007.02.001

Medzhitov R (2007b) Recognition of microorganisms and activation of the immune response. Nature 18;449(7164):819-826. doi:10.1038/nature06246

Medzhitov R, Janeway CAJ (1997) Innate immunity: the virtues of a nonclonal system of recognition. Cell. 91(3):295-298. doi:https://doi.org/10.1016/S0092-8674(00)80412-2

Medzhitov R, Janeway CAJ (1998) Innate immune recognition and control of adaptive immune responses. Semin. Immunol. 10(5):351-353. doi:https://doi.org/10.1006/smim.1998.0136

Medzhitov R, Janeway CAJ (2000) Innate immunity. N. Engl. J Med. 343(5):338-344. doi:10.1056/NEJM200008033430506

Meech RW (2008) Non-neural reflexes: sponges and the origins of behaviour. Curr. Biol. 18(2):R70-72. doi:10.1016/j.cub.2007.11.022

Meech RW (2015) Electrogenesis in the lower Metazoa and implications for neuronal integration. J. Exp. Biol. 218(Pt 4):537-550. doi:10.1242/jeb.111955

Meusser B, Hirsch C, Jarosch E, Sommer T (2005) ERAD: the long road to destruction. Nat. Cell Biol. 7:766-772. doi:10.1038/ncb0805-766

Miura M (2011) Active participation of cell death in development and organismal homeostasis. Dev. Growth Differ. 53(2):125-136. doi:10.1111/j.1440-169X.2010.01228.x

Mizobuchi N, Hoseki J, Kubota H, Toyokuni S, Nozaki J, Naitoh M, Koizumi A, Nagata K (2007) ARMET is a soluble ER protein induced by the unfolded protein response via ERSE-II element. Cell. Struct. Funct. 32:41-50. doi:https://doi.org/10.1247/csf.07001

Moitinho-Silva L, Bayer K, Cannistraci CV, Giles EC, Ryu T, Seridi L, Ravasi T, Hentschel U (2014) Specificity and transcriptional activity of microbiota associated with low and high microbial abundance sponges from the Red Sea. Mol. Ecol. 23(6):1348-1363. doi:10.1111/mec.12365

Moitinho-Silva L, Nielsen S, Amir A, Gonzalez A, Ackermann GL, Cerrano C, Astudillo-Garcia C, Easson C, Sipkema D, Liu F, Steinert G, Kotoulas G, McCormack GP, Feng G, Bell JJ, Vicente J, Björk JR, Montoya JM, Olson JB, Reveillaud J, Steindler L, Pineda MC, Marra MV, Ilan M, Taylor MW, Polymenakou P, Erwin PM, Schupp PJ, Simister RL, Knight R, Thacker RW, Costa R, Hill RT, Lopez-Legentil S, Dailianis T, Ravasi T, Hentschel U, Li Z, Webster NS, Thomas T (2017) The sponge microbiome project. Gigascience. 6(10):1-7. doi:10.1093/gigascience/gix077

Moldoveanu T, Follis AV, Kriwacki RW, Green DR (2014) Many players in BCL-2 family affairs. Trends Biochem. Sci. 39(3):101-11. doi:10.1016/j.tibs.2013.12.006

Moore KA, Hollien J (2012) The unfolded protein response in secretory cell function. Annu. Rev. Genet. 46:165-183. doi:10.1146/annurev-genet-110711-155644

Moran NA, Sloan DB (2015) The hologenome concept: helpful or hollow? PLoS Biol. 13(12):e1002311. doi:10.1371/journal.pbio.1002311

Mori K (2000) Tripartite management of unfolded proteins in the endoplasmic reticulum. Cell 101:451-454. doi:http://dx.doi.org/10.1016/S0092-8674(00)80855-7

Moroz LL, Kohn AB (2016) Independent origins of neurons and synapses: insights from ctenophores. Phil. Trans. R. Soc. B. 371:20150041. doi:10.1098/rstb.2015.0041

Müller WE (1997) Origin of metazoan adhesion molecules and adhesion receptors as deduced from cDNA analyses in the marine sponge *Geodia cydonium*: a review. Cell Tissue Res. 289(3):383-395

Müller WE (2006) The stem cell concept in sponges (Porifera): Metazoan traits. Semin. Cell Dev. Biol. 17(4):481-491. doi:10.1016/j.semcdb.2006.05.006

Müller WE, Belikov SI, Kaluzhnaya OV, Chernogor L, Krasko A, Schröder HC (2009a) Symbiotic interaction between dinoflagellates and the demosponge *Lubomirskia baicalensis*: aquaporin-mediated glycerol transport. In: Prog. Mol. Subcell. Biol. Ed: Müller WEG 47:145-170. Springer doi:10.1007/978-3-540-88552-8_6

Müller WE, Grebenjuk VA, Le Pennec G, Schröder H, Brümmer F, Hentschel U, Müller IM, Breter H (2004b) Sustainable production of bioactive compounds by sponges-cell culture and gene cluster approach: a review. Mar. Biotechnol. 6(2):105-117. doi:10.1007/s10126-002-0098-6

Müller WEG, Klemt M, Thakur NL, Schröder HC; Aiello A, D'Esposito M, Menna M, Fattorouso E (2004d) Molecular/chemical ecology in sponges: evidence for an adaptive antibacterial response in *Suberites domuncula.* Mar. Biol. 144:19-29. doi:https://doi.org/10.1007/s00227-003-1184-7

Müller WE, Koziol C, Müller IM, Wiens M (1999c) Towards an understanding of the molecular basis of immune responses in sponges: the marine demosponge *Geodia cydonium* as a model. Microsc. Res. Tech. 44(4):219-236. doi: 10.1002/(SICI)1097-0029(19990215)44:4<219::AID-JEMT3>3.0.CO;2-7

Müller WE, Kruse M, Blumbach B, Skorokhod A, Müller IM (1999b) Gene structure and function of tyrosine kinases in the marine sponge *Geodia cydonium*: autapomorphic characters in Metazoa. Gene. 238(1):179-193. doi:https://doi.org/10.1016/S0378-1119(99)00226-7

Müller WE, Perović S, Wilkesman J, Kruse M, Müller IM, Batel R (2000) Increased gene expression of a cytokine-related molecule and profilin after activation of *Suberites domuncula* cells with xenogeneic sponge molecule(s). DNA Cell Biol. 18(12):885-893. doi:10.1089/104454999314746

Müller WE, Schwertner H, Müller IM (2004c) Porifera a reference phylum for evolution and bioprospecting: the power of marine genomics. Keio J. Med. 53(3):159-165. doi:https://doi.org/10.2302/kjm.53.159

Müller WE, Skorokhod A, Müller IM (1999d) Receptor tyrosine kinase, an autapomorphic character of metazoa: identification in marine sponges. Acta Biol. Hung. 50(4):395-411.

Müller WE, Wiens M, Adell T, Gamulin V, Schröder HC, Müller IM (2004a) Bauplan of urmetazoa: basis for genetic complexity of metazoa. Int. Rev. Cytol. 235:53-92. doi:10.1016/S0074-7696(04)35002-3

Müller WEG (2003) Sponges (Porifera). Marine Molecular Biotechnology. Springer-Verlag 258 pgs. doi:10.1007/978-3-642-55519-0

Müller WEG, Blumbach B, Müller IM (1999a) Evolution of the innate and adaptive immune systems: relationships between potential immune molecules in the lowest Metazoan Phylum (Porifera) and those in vertebrates.

Transplantation 68:1215-1227

Müller WEG, Custódio MR, Wiens M, Zilberberg C, Châtel A, Müller IM, Schröder HC (2009b) Effect of bacterial infection on stem cell pattern in poriferan. In: Stem cell of marine organismo Eds: Rinkevich B, Matranga. Springer. doi:10.1007/978-90-481-2767-2_13

Müller WEG, Krasko A, Skorokhod A, Bünz C, Grebenjuk VA, Steffen R, Batel R, Müller IM, Schröder HC (2002) Histocompatibility reaction in the sponge *Suberites domuncula* on tissue and cellular level: central role of the allograft inflammatory factor 1. Immunogenetics 54:48-58. doi:https://doi.org/10.1007/s00251-002-0441-0

Müller WEG, Müller IM (2003a) Origin of the metazoan immune system: identification of the molecules and their functions in sponges. Integr. Comp. Biol. 43:281-292. doi:10.1093/icb/43.2.281

Müller WEG, Müller IM (2003b) Analysis of the sponge [Porifera] gene repertoire: implications for the evolution of the metazoan body plan. In: Sponges (Porifera). Marine Molecular Biotechnology. Springer, 258 pgs. doi:10.1007/978-3-642-55519-0

Müller WEG, Müller IM (2007) Porifera: an enigmatic taxon disclosed by molecular biology/cell biology In: Porifera Research. Biodiversity, Innovation and Sustainability. Eds: Custódio MR, Lôbo-Hajdu G, Hajdu E, Muricy G. Livros do Museu Nacional 28, Rio de Janeiro, 89-106.

Müller WEG, Perović S, Wilkesman J, Kruse M, Müller IM, Batel R (1999e) Increased gene expression of a cytokine-related molecule and profilin after activation of *Suberites domuncula* cells with xenogeneic sponge molecule(s). DNA Cell Biol. 18:885–893. doi:10.1089/104454999314746

Müller WEG, Wiens M, Müller IM, Schröder HC (2003) The chemokine networks in sponges: potential roles in morphogenesis, immunity and stem cell formation. In: Invertebrate cytokines and the phylogeny of immunity. Prog. Mol. Subcell. Biol. Eds: Beschin A, Müller WEG 34:103-143. Springer doi:http://doi.org/10.1007/978-3-642-18670-7_5

Mullis K, Faloona F (1987) Specific synthesis of DNA in vitro via a polymerase-catalyzed chain reaction. Methods Enzymol. 155**:**335-350.

Mullis K, Faloona F, Scharf S, Saiki R, Horn G, Erlich H (1986) Specific enzymatic amplification of DNA in vitro: The polymerase chain reaction. Cold Spring Harbor Symp. Quant. Biol. 51(2):63-273.

Munshi N, Fernandis AZ, Cherla RP, Park IW, Ganju RK (2002) Lipopolysaccharide-induced apoptosis of endothelial cells and its inhibition by vascular endothelial growth factor. J. Immunol. 168(11):5860-5866. doi:https://doi.org/10.4049/jimmunol.168.11.5860

Nagasawa M, Ogawa K, Nagata K, Shimizu N (2014) Granulysin and its clinical significance as a biomarker of immune response and NK cell related neoplasms. World J. Hematol. 3(4):128-137. doi:10.5315/wjh.v3.i4.128

Nakagomi T, Kitada O, Kuribayashi K, Yoshikawa H, Ozawa K, Ogawa S, Matsuyama T (2004) The 150-kilodalton oxygen-regulated protein ameliorates lipopolysaccharide-induced acute lung injury in mice. Am. J. Pathol. 165(4):1279-1288.

Nakayama Y, Endo M, Tsukano H, Mori M, Oike Y, Gotoh T (2010) Molecular mechanisms of the LPS-induced non-apoptotic ER stress-CHOP pathways. J. Biochem. 147(4):471-483. doi:10.1093/jb/mvp189

Nasrolahi A, Mahmoudi J, Akbarzadeh A, Karimipour M, Sadigh-Eteghad S, Salehi R, Farhoudi M (2018) Neurotrophic factors hold promise for the future of Parkinson's disease treatment: is there a light at the end of the tunnel? Rev. Neurosci. 29(5):475-489. doi:10.1515/revneuro-2017-0040

Neves J, Zhu J, Sousa-Victor P, Konjikusic M, Riley R, Chew S, Qi Y, Jasper H, Lamba DA (2016) Immune modulation by MANF promotes tissue repair and regenerative success in the retina. Science 353(6294):aaf3646 doi:10.1126/Science.aaf3646

Nguyen MT, Liu M, Thomas T (2014) Ankyrin-repeat proteins from sponge symbionts modulate amoebal phagocytosis. Mol. Ecol. 23(6):1635-1645. doi:10.1111/mec.12384

Nicholas KB, Nicholas HB Jr, Deerfield II DW (1997) GeneDoc: analysis and visualization of genetic variation. Embnew NEWS 4:14

Nichols SA, Dirks W, Pearse JS, King N (2006) Early evolution of animal cell signaling and adhesion genes. Proc. Natl. Acad. Sci USA 103(33):12451-12456. doi:10.1073/pnas.0604065103

Nichols SA, Roberts BW, Richter DJ, Fairclough SR, King N (2012) Origin of metazoan cadherin diversity and the antiquity of the classical cadherin/β-catenin complex. Proc. Natl. Acad. Sci. USA 109(32):13046-13051. doi:10.1073/pnas.1120685109

Nickel M (2010) Evolutionary emergence of synaptic nervous systems: what can we learn from the non-synaptic, nerveless Porifera? Invertebr. Biol. 129:1-16. doi:10.1111/j.1744-7410.2010.00193.x

Niles LP, Sathiyapalan A, Bahna S, Kang NH, Pan Y (2012) Valproic acid up-regulates melatonin MT1 and MT2 receptors and neurotrophic factors CDNF and MANF in the rat brain. Int. J. Neuropsychopharmacol. 15(9):1343-1350. doi:10.1017/S1461145711001969

Niu C, Zhang J, Mei J, Fu X (2011) Does neurotrophic factor benefit to PD

therapy via co-function with ubiquitin–proteasome system? Med. hypotheses. 76:589-592. doi:10.1016/j.mehy.2011.01.007

Niu M, Dai X, Zou W, Yu X, Teng W, Chen Q, Sun X, Yu W, Ma H, Liu P (2017) Autophagy, endoplasmic reticulum stress and the unfolded protein response in intracerebral hemorrhage. Transl. Neurosci. 8:37-48. doi:10.1515/tnsci-2017-0008

Norisada J, Hirata Y, Amaya F, Kiuchi K, Oh-hashi K (2016) A comparative analysis of the molecular features of MANF and CDNF. PLoS One. 11(1):e0146923. doi:10.1371/journal.pone.0146923

Nosenko T, Schreiber F, Adamska M, Adamski M, Eitel M, Hammel J, Maldonado M, Müller WE, Nickel M, Schierwater B, Vacelet J, Wiens M, Wörheide G (2013) Deep metazoan phylogeny: when different genes tell different stories. Mol. Phylogenet. Evol. 67(1):223-233. doi:10.1016/j.ympev.2013.01.010

Novoa I, Zeng H, Harding HP, Ron D (2001) Feedback inhibition of the unfolded protein response by GADD34-mediated dephosphorylation of eIF2α. J. Cell. Biol. 153(5):1011-1022. doi:10.1083/jcb.153.5.1011

Oakes SA, Papa FR (2015) The role of endoplasmic reticulum stress in human pathology. Annu. Rev. Pathol. 10:173-194. doi:10.1146/annurev-pathol-012513-104649

Oh-Hashi K, Hirata Y, Kiuchi K (2013) Transcriptional regulation of mouse mesencephalic astrocyte-derived neurotrophic factor in neuro2a cells. Cell. Mol. Biol. Lett. 18(3):398-415. doi:10.2478/s11658-013-0096-x

Oh-Hashi K, Koga H, Ikeda S, Shimada K, Hirata Y, Kiuchi K (2009) CRELD2 is a novel endoplasmic reticulum stress-inducible gene. Biochem. Biophys. Res. Commun. 387:504-510. doi:10.1016/j.bbrc.2009.07.047

Oh-hashi K, Norisada J, Hirata Y, Kiuchi K (2015) Characterization of a role of MANF in regulating the secretion of CRELD2. Biol. Pharm. Bull. 38:722-731. doi:10.1248/bpb.b14-00825

Oh-Hashi K, Tanaka K, Koga H, Hirata Y, Kiuchi K (2012) Intracellular trafficking and secretion of mouse mesencephalic astrocyte-derived neurotrophic factor. Mol. Cell. Biochem. 363(1-2):35-41. doi:10.1007/s11010-011-1155-0

Olson L, Faulkner S, Lundströmer K, Kerenyi A, Kelen D, Chandrasekaran M, Ådén U, Olson L, Golay X, Lagercrantz H, Robertson NJ, Galter D (2013) Comparison of three hypothermic target temperatures for the treatment of hypoxic ischemia: mRNA level responses of eight genes in the piglet brain. Transl. Stroke Res. 4(2):248-257. doi:10.1007/s12975-012-0215-4

Ouyang L, Shi Z, Zhao S, Wang FT, Zhou TT, Liu B, Bao JK (2012) Programmed cell death pathways in cancer: a review of apoptosis, autophagy and programmed necrosis. Cell Prolif. 45(6):487-498. doi:10.1111/j.1365-2184.2012.00845.x

Oyadomari S, Mori M (2004) Roles of CHOP/GADD153 in endoplasmic reticulum stress. Cell Death Differ. 11(4):381-389. doi:10.1038/sj.cdd.4401373

Pahler S, Krasko A, Schütze J, Müller IM, Müller WEG (1998) Isolation and characterization of a cDNA encoding a potential morphogen from the marine sponge *Geodia cydonium*, that is conserved in higher metazoans. Proc. R. Soc. Lond. B 265(19394):421-425. doi:10.1098/rspb.1998.0311

Pakos-Zebrucka K, Koryga I, Mnich K, Ljujic M, Samali A, Gorman AM (2016) The integrated stress response. EMBO Rep. 17(10):1374-1395 doi:10.15252/embr.201642195

Palgi M, Greco D, Lindström R, Auvinen P, Heino TI. (2012) Gene expression analysis of drosophila Manf mutants reveals perturbations in membrane traffic and major metabolic changes. BMC Genomics.13:134. doi:10.1186/1471-2164-13-134

Palgi M, Lindström R, Peränen J, Piepponen TP, Saarma M, Heino TI (2009) Evidence that DmMANF is an invertebrate neurotrophic factor supporting dopaminergic neurons. Proc. Natl. Acad. Sci. USA. 106(7):2429-2434 doi:10.1073/pnas.0810996106

Palm NW, Medzhitov R (2009) Pattern recognition receptors and control of adaptive immunity. Immunol Rev. 227(1):221-233. doi:10.1111/j.1600-065X.2008.00731.x.R

Pancer Z, Kruse M, Müller I, Müller WEG (1997a) On the origin of adhesion receptors of metazoa: cloning of the integrin subunit cDNA fromthe sponge *Geodia cydonium*. Mol. Biol. Evol. 14:391-398. doi:https://doi.org/10.1093/oxfordjournals.molbev.a025775

Pancer Z, Kruse M, Schäcke H, Scheffer U, Steffen R, Kovács P, Müller WE (1996) Polymorphism in the immunoglobulin-like domains of the receptor tyrosine kinase from the sponge *Geodia cydonium*. Cell Adhes. Commun. 4(4-5):327-339.

Pancer Z, Münkner J, Müller I, Müller WEG (1997b) A novel member of an ancient superfamily: sponge (*Geodia cydonium*, Porifera) putative protein that features scavenger receptor cysteine-rich repeats. Gene 193:211-218. doi:https://doi.org/10.1016/S0378-1119(97)00135-2

Pancer Z, Skorokhod A, Blumbach B, Müller WE (1998) Multiple Ig-like featuring genes divergent within and among individuals of the marine sponge *Geodia cydonium.* Gene. 207(2):227-233.

doi:https://doi.org/10.1016/S0378-1119(97)00631-8

Paratcha G; Ledda F (2008) GDNF and GFRα: a versatile molecular complex for developing neurons. Trends Neurosci. 31:384-391. doi:10.1016/j.tins.2008.05.003

Pardon MC (2010) Role of neurotrophic factors in behavioural processes: implications for the treatment of psychiatric and neurodegenerative disorders. Vitam. Horm. 82:185-200. doi:10.1016/S0083-6729(10)82010-2

Park SW, Ozcan U (2013) Potential for therapeutic manipulation of the UPR in disease. Semin. Immunopathol. 35(3):351-373. doi:10.1007/s00281-013-0370-z

Parkash V, Lindholm P, Peränen J, Kalkkinen N, Oksanen E, Saarma M, Leppänen VM, Goldman A (2009) The structure of the conserved neurotrophic factors MANF and CDNF explains why they are bifunctional. Protein Eng. Des. Sel. 22(4):233-241. doi:10.1093/protein/gzn080

Pathak N, Mitra S, Khandelwal S (2013) Cadmium induces thymocyte apoptosis via caspase-dependent and caspase-independent pathways. J. Biochem. Mol. Toxicol. 27(3):193-203. doi:10.1002/jbt.21468

Perović S, Krasko A, Prokic I, Müller IM, Müller WE (1999) Origin of neuronal-like receptors in Metazoa: cloning of a metabotropic glutamate/GABA-like receptor from the marine sponge *Geodia cydonium.* Cell Tissue Res. 296(2):395-404. doi:https://doi.org/10.1007/s004410051299

Perović-Ottstadt S, Adell T, Proksch P, Wiens M, Korzhev M, Gamulin V, Müller IM, Müller WE (2004) A (1→3)-beta-D-glucan recognition protein from the sponge *Suberites domuncula*. Mediated activation of fibrinogen-like protein and epidermal growth factor gene expression. Eur. J. Biochem. 271(10):1924-1937. doi:10.1111/j.1432-1033.2004.04102.x

Perri ER, Thomas CJ, Parakh S, Spencer DM and Atkin JD (2016) The unfolded protein response and the role of protein disulfide isomerase in neurodegeneration. Front. Cell Dev. Biol. 3:80. doi:10.3389/fcell.2015.00080

Petersen TN, Brunak S, von Heijne G, Nielsen H (2011) SignalP 4.0: discriminating signal peptides from transmembrane regions. Nat. Methods 8:785-786. doi:10.1038/nmeth.1701

Petrova P, Raibekas A, Pevsner J, Vigo N, Anafi M, Moore MK, Peaire AE, Shridhar V, Smith DI, Kelly J, Durocher Y, Commissiong JW (2003) MANF: a new mesencephalic, astrocyte-derived neurotrophic factor with selectivity for dopaminergic neurons. J. Mol. Neurosci. 20(2):173-188. doi:https://doi.org/10.1385/JMN:20;2:173

Pettersen EF, Goddard TD, Huang CC, Couch GS, Greenblatt DM, Meng EC,

Ferrin TE (2004) UCSF Chimera-a visualization system for exploratory research and analysis. J. Comput. Chem. 25(13):1605-1612. doi:10.1002/jcc.20084

Philippe H, Brinkmann H, Lavrov DV, Littlewood DT, Manuel M, Wörheide G, Baurain D (2011) Resolving difficult phylogenetic questions: why more sequences are not enough. PLoS Biol. 9(3):e1000602. doi:https://doi.org/10.1371/journal.pbio.1000602

Philippe H, Derelle R, Lopez P, Pick K, Borchiellini C, Boury-Esnault N, Vacelet J, Renard E, Houliston E, Quéinnec E, Da Silva C, Wincker P, Le Guyader H, Leys S, Jackson DJ, Schreiber F, Erpenbeck D, Morgenstern B, Wörheide G, Manuel M (2009) Phylogenomics revives traditional views on deep animal relationships. Curr. Biol. 19(8):706-712. doi:10.1016/j.cub.2009.02.052

Pick KS, Philippe H, Schreiber F, Erpenbeck D, Jackson DJ, Wrede P, Wiens M, Alié A, Morgenstern B, Manuel M, Wörheide G (2010) Improved phylogenomic taxon sampling noticeably affects nonbilaterian relationships. Mol. Biol. Evol. 27(9):1983-1987. doi:10.1093/molbev/msq089

Pihán P, Carreras-Sureda A, Hetz C (2017) BCL-2 family: integrating stress responses at the ER to control cell demise. Cell Death Differ. 24(9):1478-1487. doi:10.1038/cdd.2017.82

Pile AJ, Patterson MR, Witman JD (1996) *In situ* grazing on plankton <10µm by the boreal sponge *Mycale lingua*. Mar. Ecol. Prog. Ser. 141:95-102.

Pincus D, Chevalier MW, Aragón T, van Anken E, Vidal SE, El-Samad H, Walter P (2010) BiP binding to the ER-stress sensor Ire1 tunes the homeostatic behaviour of the unfolded protein response. PLoS Biol. 6;8(7):e1000415. doi:10.1371/journal.pbio.1000415

Pirvola U, Ylikoski J (2003) Neurotrophic factors during inner ear development. Curr. Top. Dev. Biol. 57:207-223. doi:https://doi.org/10.1016/S0070-2153(03)57007-7

Pisani D, Pett W, Dohrmann M, Feuda R, Rota-Stabelli O, Philippe H, Lartillot N, Wörheide G (2015) Genomic data do not support comb jellies as the sister group to all other animals. Proc. Natl. Acad. Sci. USA. 112(50):15402-1547. doi:10.1073/pnas.1518127112

Pita L, Fraune S, Hentschel U (2016) Emerging sponge models of animal-microbe symbioses. Front. Microbiol. 7:2102. doi:10.3389/fmicb.2016.02102.

Plate L, Wiseman RL (2017) Regulating secretory proteostasis through the unfolded protein response: from function to therapy. Trends Cell Biol. 27(10):722-737. doi:10.1016/j.tcb.2017.05.006

Pluquet O, Pourtier A, Abbadie C (2015) The unfolded protein response and cellular senescence. A review in the theme: cellular mechanisms of

endoplasmic reticulum stress signaling in health and disease. Cell Physiol. 308(6):C415-425. doi:10.1152/ajpcell.00334.2014

Poljšak B, Milisav I (2012) Clinical implications of cellular stress responses. Bosn. J. Basic Med. Sci. 12(2):122-126. doi:http://dx.doi.org/10.17305/bjbms.2012.2510

Pozzolini M, Scarfì S, Ghignone S, Mussino F, Vezzulli L, Cerrano C, Giovine M (2016) Molecular characterization and expression analysis of the first Porifera tumor necrosis factor superfamily member and of its putative receptor in the marine sponge *Chondrosia reniformis*. Dev. Comp. Immunol. 57:88-98. doi:10.1016/j.dci.2015.12.011

Promlek T, Ishiwata-Kimata Y, Shido M, Sakuramoto M, Kohno K, Kimata Y (2011) Membrane aberrancy and unfolded proteins activate the endoplasmic reticulum stress sensor Ire1 in different ways. Mol. Biol. Cell 22:3520-3532. doi:10.1091/mbc.E11-04-0295

Rabilloud T (1999) Proteome research: two-dimensional gel electrophoresis and identification methods. Springer science & business media, 248 pgs.

Ramoino P, Gallus L, Paluzzi S, Raiteri L, Diaspro A, Fato M, Bonanno G, Tagliafierro G, Ferretti C, Manconi R (2007) The GABAergic-like system in the marine demosponge *Chondrilla nucula*. Microsc. Res. Tech. 70(11):944-951. doi:10.1002/jemt.20499

Ramoino P, Ledda FD, Ferrando S, Gallus L, Bianchini P, Diaspro A, Fato M. Tagliafierro G, Manconi R (2011) Metabotropic γ-aminobutyric acid (GABAB) receptors modulate feeding behavior in the calcisponge *Leucandra aspera*. J. Exp. Zool. 315A(3):132-140. doi:10.1002/jez.657

Raykhel I, Alanen H, Salo K, Jurvansuu J, Nguyen VD, Latva-Ranta M, Ruddock L (2007) A molecular specificity code for the three mammalian KDEL receptors. J. Cell Biol. 179(6):1193-1204. doi:10.1083/jcb.200705180

Rech de Laval V, Deléage G, Aouacheria A, Combet C (2014) BCL2DB: database of BCL-2 family members and BH3-only proteins Database (Oxford), bau013. doi:10.1093/database/bau013

Reichardt LF (2006) Neurotrophin-regulated signaling pathways. Philos. Trans. R. Soc. Lond. B. Biol. Sci. 361:1545-1564. doi:10.1098/rstb.2006.1894

Reiswig HM (1971) Particle feeding in natural populations of three marine demosponges. Biol. Bull. 141:568-591. doi:https://doi.org/10.2307/1540270

Reiswig HM (1975) Bacteria as food for temperate-water marine sponges. Can. J. Zool. 53:582-589. doi:https://doi.org/10.1139/z75-072

Renard E, Leys SP, Wörheide G, Borchiellini C (2018) Understanding animal

evolution: the added value of sponge transcriptomics and genomics: the disconnect between gene content and body plan evolution. Bioessays. 40(9):1700237 doi:10.1002/bies.201700237

Renko JM, Bäck S, Voutilainen MH, Piepponen TP, Reenilä I, Saarma M, Tuominen RK (2018) Mesencephalic astrocyte-derived neurotrophic factor (MANF) elevates stimulus-evoked release of dopamine in freely-moving rats. Mol. Neurobiol. 55(8):6755-6768. doi:10.1007/s12035-018-0872-8

Reveillaud J, Maignien L, Murat Eren A, Huber JA, Apprill A, Sogin ML, Vanreusel A (2014) Host-specificity among abundant and rare taxa in the sponge microbiome. ISME J 8(6):1198-1209. doi:10.1038/ismej.2013.227

Ribeiro SM, Omena EP, Muricy G (2003) Macrofauna associated to Mycale *microsigmatosa* (Porifera, Demospongiae) in Rio de Janeiro State, SE Brazil, Estuar. Coast. Shelf Sci. 57(5-6):951-959. doi:https://doi.org/10.1016/S0272-7714(02)00425-0

Richman C, Rashid S, Prashar S, Mishra R, Selvaganapathy PR, Gupta BP (2018) *C. elegans* MANF homolog is necessary for the protection of dopaminergic neurons and ER unfolded protein response. Front. Neurosc. 12:544. doi:10.3389/fnins.2018.00544

Riesgo A, Farrar N, Windsor PJ, Giribet G, Leys SP (2014) The analysis of eight transcriptomes from all poriferan classes reveals surprising genetic complexity in sponges. Mol. Biol. Evol. 31(5):1102-1120. doi:10.1093/molbev/msu057

Rivas A, Vidal RL, Hetz C (2015) Targeting the unfold protein response for disease intervention. Expert. Opin. Ther. Targets 19(9):1203-1218. doi:10.1517/14728222.2015.1053869

Robbi M, Beaufay H (1991) The COOH terminus of several liver carboxylesterases targets these enzymes to the lumen of the endoplasmic reticulum. J. Biol. Chem. 266(30):20498-20503.

Robert X, Gouet P (2014) Deciphering key features in protein structures with the new ENDscript server. Nucleic Acids Res. 42:W320-324. doi:10.1093/nar/gku316

Rokas A, King N, Finnerty J, Carroll SB (2003) Conflicting phylogenetic signals at the base of the metazoan tree. Evol. Dev. 5(4):346-359. https://doi.org/10.1046/j.1525-142X.2003.03042.x

Romieu I, Dossus L, Barquera S, Blottière HM, Franks PW, Gunter M, Hwalla N, Hursting SD, Leitzmann M, Margetts B, Nishida C, Potischman N, Seidell J, Stepien M, Wang Y, Westerterp K, Winichagoon P, Wiseman M, Willett WC; IARC working group on energy balance and obesity (2017) energy balance and obesity: what are the main drivers? Cancer Causes Control. 28(3):247-258.

doi:10.1007/s10552-017-0869-z

Ron D (2002) Translational control in the endoplasmic reticulum stress response. J. Clin. Invest. 110:1383-1388. doi:10.1172/JCI16784
Ron D, Harding HP (2012) Protein-folding homeostasis in the endoplasmic reticulum and nutritional regulation. Cold Spring Harb. Perspect. Biol. 4(12). pii:a013177. doi:10.1101/cshperspect.a013177

Rosadini CV, Kagan JC (2017) Early innate immune responses to bacterial LPS. Curr. Opin. Immunol. 44:14-19. doi:10.1016/j.coi.2016.10.005

Rupert EE, Barnes RD (1996) Zoologia dos invertebrados. 6º Ed. Rocca, 1029 pgs.

Ryan JF, Pang K, Schnitzler CE, Nguyen AD, Moreland RT, Simmons DK, Koch BJ, Francis WR, Havlak P; NISC Comparative Sequencing Program, Smith SA, Putnam NH, Haddock SH, Dunn CW, Wolfsberg TG, Mullikin JC, Martindale MQ, Baxevanis AD (2013) The genome of the ctenophore *Mnemiopsis* leidyi and its implications for cell type evolution. Science. 342(6164):1242592. doi:10.1126/science.1242592

Ryu T, Seridi L, Moitinho-Silva L, Oates M, Liew YJ, Mavromatis C, Wang X, Haywood A, Lafi FF, Kupresanin M, Sougrat R, Alzahrani MA, Giles E, Ghosheh Y, Schunter C, Baumgarten S, Berumen ML, Gao X, Aranda M, Foret S, Gough J, Voolstra CR, Hentschel U, Ravasi T (2016) Hologenome analysis of two marine sponges with different microbiomes. BMC Genomics. 17:158. doi:10.1186/ s12864-016-2501-0

Saidak Z, Ezzoukhry Z, Maziere JC, Galmiche A (2018) BCL-2 Family. In: Encyclopedia of signaling molecules. Ed: Choi S. Springer, Cham. doi**:**https://doi.org/10.1007/978-3-319-67199-4

Sakai J, Cammarota E, Wright JA, Cicuta P, Gottschalk RA, Li N, Fraser IDC, Bryant CE (2017) Lipopolysaccharide-induced NF-κB nuclear translocation is primarily dependent on MyD88, but TNFα expression requires TRIF and MyD88. Scientific reports 7:1428. doi:https://doi.org/10.1038/s41598-017-01600-y

Sakarya O, Armstrong KA, Adamska M, Adamski M, Wang IF, Tidor B, Degnan BM, Oakley TH, Kosik KS (2007) A post-synaptic scaffold at the origin of the animal kingdom. PLoS One. 2(6):e506. doi:10.1371/journal.pone.0000506

Salaun B, Romero P, Lebecque S (2007) Toll-like receptors' two-edged sword: when immunity meets apoptosis. Eur. J. Immunol. 37(12):3311-3318. doi:10.1002/eji.200737744

Sampaio TB, Savall AS, Gutierrez MEZ, Pinton S (2017) Neurotrophic factors in Alzheimer's and Parkinson's diseases: implications for pathogenesis and therapy. Neural Regen. Res. 12(4):549-557.doi:10.4103/1673-5374.205084

Sano R, Reed JC (2013) ER stress-induced cell death mechanisms. Biochim. Biophys. Acta 1833:3460-3470. doi:10.1016/j.bbamcr.2013.06.028

Sarvani C, Sireesh D, Ramkumar KM (2017) Unraveling the role of ER stress inhibitors in the context of metabolic diseases. Pharmacol. Res. 119:412-421. doi:10.1016/j.phrs.2017.02.018

Scheuner D, Song B, McEwen E, Liu C, Laybutt R, Gillespie P, Saunders T, Bonner-Weir S, Kaufman RJ (2001) Translational control is required for the unfolded protein response and in vivo glucose homeostasis. Mol. Cell. 7:1165 - 1176. doi:http://dx.doi.org/10.1016/S1097-2765(01)00265-9

Schierwater B, Eitel M, Jakob W, Osigus HJ, Hadrys H, Dellaporta SL, Kolokotronis, SO, Desalle R (2009) Concatenated analysis sheds light on early metazoan evolution and fuels a modern ‘‘urmetazoon’’ hypothesis. PLoS Biol. 7:e20. doi:10.1371/journal.pbio.1000020

Schindler AJ, Schekman R (2009) In vitro reconstitution of ER-stress induced ATF6 transport in COPII vesicles. Proc. Natl. Acad. Sci. USA. 20;106(42):17775-17780. doi:10.1073/pnas.0910342106

Schippers KJ, Nichols SA (2018) Evidence of signaling and adhesion roles for β-catenin in the sponge *Ephydatia muelleri*. Mol. Biol. Evol. msy033. doi:https://doi.org/10.1093/molbev/msy033

Schmitz ML, Shaban MS, Albert BV, Gökçen A, Kracht M (2018) The crosstalk of Endoplasmic reticulum (ER) stress pathways with NF-κB: complex mechanisms relevant for cancer, inflammation and infection. Biomedicines. 6(2)pii:E58. doi:10.3390/biomedicines6020058

Schröder HC, Breter HJ, Fattorusso E, Ushijima H, Wiens M, Steffen R, Batel R, Müller WE (2006) Okadaic acid, an apoptogenic toxin for symbiotic/parasitic annelids in the demosponge *Suberites domuncula*. Appl. Environ. Microbiol. 72(7):4907-4916. doi:10.1128/AEM.00228-06

Schröder HC, Ushijima H, Krasko A, Gamulin V, Thakur NL, Diehl-Seifert B, Müller IM, Müller WE (2003) Emergence and disappearance of an immune molecule, an antimicrobial lectin, in basal metazoa. A tachylectin-related protein in the sponge *Suberites domuncula*. J. Biol. Chem. 278(35):32810-32817. doi:10.1074/jbc.M304116200

Schröder HC, Wang X, Tremel W, Ushijima H, Müller WE (2008) Biofabrication of biosilica-glass by living organisms. Nat. Prod. Rep. 25(3):455-474. doi:10.1039/b612515h

Schröder M, Kaufman RJ (2005) The mammalian unfolded protein response, Annu. Rev. Biochem. 74:739-789. doi:10.1146/annurev.biochem.73.011303.074134

Schultz J, Milpetz F, Bork P, Ponting CP (1998) SMART, a simple modular architecture research tool: identification of signaling domains. Proc. Natl. Acad. Sci. USA. 95(11):5857-64. doi:10.1073/pnas.95.11.5857

Senft D, Ronai ZA (2015) UPR, autophagy, and mitochondria crosstalk underlies the ER stress response. Trends Biochem. Sci. 40(3):141-148. doi:10.1016/j.tibs.2015.01.002.

Sereno D, Müller WEG, Bausen M, Elkhooly TA, Markl JS, Wiens M (2017) An evolutionary perspective on the role of mesencephalic astrocyte-derived neurotrophic factor (MANF): At the crossroads of poriferan innate immune and apoptotic pathways. Biochem. Biophys. Rep. 11:161-173. doi:10.1016/j.bbrep.2017.02.009

Shalini S, Dorstyn L, Dawar S, Kumar S (2015) Old, new and emerging functions of caspases. Cell Death Differ. 22(4):526-539. doi:10.1038/cdd.2014.216

Shen J, Snapp EL, Lippincott-Schwartz J, Prywes R (2005) Stable binding of ATF6 to BiP in the endoplasmic reticulum stress response. Mol. Cell. Biol. 25(3):921-932. doi:10.1128/MCB.25.3.921-932.2005

Shen Y, Sun A, Wang Y, Cha D, Wang H, Wang F, Feng L, Fang S, Shen Y (2012) Upregulation of mesencephalic astrocyte-derived neurotrophic factor in glial cells is associated with ischemia-induced glial activation. J. Neuroinflammation. 9:254. doi:10.1186/1742-2094-9-254

Shimano M, Ouchi N, Walsh K (2012) Cardiokines: recent progress in elucidating the cardiac secretome. Circulation. 26(21):e327-332. doi:10.1161/CIRCULATIONAHA.112.150656

Shridhar R, Shridhar V, Rivard S, Siegfried JM, Pietraszkiewicz H, Ensley J, Pauley R, Grignon D, Sakr W, Miller OJ, Smith DI (1996) Mutations in the arginine-rich protein gene, in lung, breast, and prostate cancers, and in squamous cell carcinoma of the head and neck. Cancer Res. 56(24):5576-5578.

Sidrauski C, Walter P (1997) The transmembrane kinase Ire1p is a site-specific endonuclease that initiates mRNA splicing in the unfolded protein response. Cell 19;90(6):1031-1039. doi:http://dx.doi.org/10.1016/S0092-8674(00)80369-4

Siegl A, Kamke J, Hochmuth T, Piel J, Richter M, Liang C, Dandekar T, Hentschel U (2011) Single-cell genomics reveals the lifestyle of Poribacteria, a candidate phylum symbiotically associated with marine sponges. ISME J. 5(1):61-70. doi:10.1038/ismej.2010.95

Sievers F, Wilm A, Dineen DG, Gibson TJ, Karplus K, Li W, Lopez R, McWilliam H, Remmert M, Söding J, Thompson JD, Higgins DG (2011) Fast, scalable generation of high-quality protein multiple sequence alignments using

Clustal Omega. Mol. Syst. Biol. 7:539 doi:10.1038/msb.2011.75
Simion P, Philippe H, Baurain D, Jager M, Richter DJ, Di Franco A, Roure B, Satoh N, Quéinnec, E, Ereskovsky A, Lapébie P, Corre E, Delsuc F, King N, Wörheide G, Manuel M (2017). A large and consistent phylogenomic dataset supports sponges as the sister group to all other animals. Curr. Biol. 27:958-967. doi:https://doi.org/10.1016/j.cub.2017.02.031

Skilleter GA, Russell BD, Degnan BM, Garson MJ (2005) Living in a potentially toxic environment: comparisons of endofauna in two congeneric sponges from the great barrier reef. Mar. Ecol. Prog. Ser. 304:67-75. doi:10.3354/meps304067

Slaby BM, Hackl T, Horn H, Bayer K, Hentschel U (2017) Metagenomic binning of a marine sponge microbiome reveals unity in defense but metabolic specialization. ISME J. 11(11):2465-2478. doi:10.1038/ismej.2017.101

Smith CL, Varoqueaux F, Kittelmann M, Azzam RN, Cooper B, Winters CA, Eitel M, Fasshauer D, Reese TS (2014) Novel cell types, neurosecretory cells, and body plan of the early-diverging metazoan *Trichoplax adhaerens*. Curr. Biol. 24(14):1565-1572. doi:10.1016/j.cub.2014.05.046

Smith JA (2018) Regulation of cytokine production by the unfolded protein response; implications for infection and autoimmunity. Front. Immunol. 9:422. doi:10.3389/fimmu.2018.00422

Smith MH, Ploegh HL, Weissman JS (2011) Road to ruin: targeting proteins for degradation in the endoplasmic reticulum. Science 334(6059):1086-1090. doi:10.1126/science.1209235

Song IS, Kim HK, Jeong SH, Lee SR, Kim N, Rhee BD, Ko KS, Han J (2011) Mitochondrial peroxiredoxin III is a potential target for cancer therapy. Int. J. Mol. Sci. 12(10):7163-7185. doi:10.3390/ijms12107163

Soto C (2003) Unfolding the role of protein misfolding in neurodegenerative diseases. Nat. Rev. Neurosci. 4:49-60. doi:10.1038/nrn1007

Sperling EA, Peterson KJ, Pisani D (2009) Phylogenetic-signal dissection of nuclear housekeeping genes supports the paraphyly of sponges and the monophyly of Eumetazoa. Mol. Biol. Evol. 26(10):2261-2274. doi:10.1093/molbev/msp148

Srivastava M, Simakov O, Chapman J, Fahey B, Gauthier ME, Mitros T, Richards GS, Conaco C, Dacre M, Hellsten U, Larroux C, Putnam NH, Stanke M, Adamska M, Darling A, Degnan SM, Oakley TH, Plachetzki DC, Zhai Y, Adamski M, Calcino A, Cummins SF, Goodstein DM, Harris C, Jackson DJ, Leys SP, Shu S, Woodcroft BJ, Vervoort M, Kosik KS, Manning G, Degnan BM, Rokhsar DS (2010) The *Amphimedon queenslandica* genome and the evolution of animal complexity. Nature 466(7307):720-726. doi:10.1038/nature09201

Stothard P (2000) The sequence manipulation suite: JavaScript programs for analyzing and formatting protein and DNA sequences. Biotechniques 28(6):1102-1104. doi:https://doi.org/10.7939/R3FQ9QK0V

Stratoulias V, Heino TI (2015a) MANF silencing, immunity induction or autophagy trigger an unusual cell type in metamorphosing drosophila brain. Cell. Mol. Life Sci. 72(10):1989-2004. doi:10.1007/s00018-014-1789-7

Stratoulias V, Heino TI (2015b) Analysis of the conserved neurotrophic factor MANF in the Drosophila adult brain. Gene Expr. Patterns. 18(1-2):8-15. doi:10.1016/j.gep.2015.04.002

Suhaili SH, Karimian H, Stellato M, Lee TH, Aguilar MI (2017) Mitochondrial outer membrane permeabilization: a focus on the role of mitochondrial membrane structural organization. Biophys. Rev. 9(4):443-457. doi:10.1007/s12551-017-0308-0

Sun H, Jiang M, Fu X, Cai Q, Zhang J, Yin Y, Guo J, Yu L, Jiang Y, Liu Y, Feng L, Nie Z, Fang J, Jin L (2017) Mesencephalic astrocyte-derived neurotrophic factor reduces cell apoptosis via upregulating HSP70 in SHSY-5Y cells. Transl. Neurodegener. 22:6-12. doi:10.1186/s40035-017-0082-8

Sun ZP, Gong L, Huang SH, Geng Z, Cheng L, Chen ZY (2011) Intracellular trafficking and secretion of cerebral dopamine neurotrophic factor in neurosecretory cells. J. Neurochem. 117(1):121-32. doi:10.1111/j.1471-4159.2011.07179.x

Tadimalla A, Belmont PJ, Thuerauf DJ, Glassy MS, Martindale JJ, Gude N, Sussman MA, Glembotski CC (2008) Mesencephalic astrocyte-derived neurotrophic factor is an ischemia-inducible secreted endoplasmic reticulum stress response protein in the heart. Circ. Res.103(11):1249-1258. doi:10.1161/CIRCRESAHA.108.180679

Talavera G, Castresana J (2007) Improvement of phylogenies after removing divergent and ambiguously aligned blocks from protein sequence alignments. Syst. Biol. 56(4):564-577. doi:10.1080/10635150701472164

Talchai C, Xuan S, Lin HV, Sussel L, Accili D (2012) Pancreatic β cell dedifferentiation as a mechanism of diabetic β cell failure. Cell 150(6):1223-1234. doi:10.1016/j.cell.2012.07.029

Tao J, Petrova K, Ron D, Sha B (2010) Crystal structure of P58(IPK) TPR fragment reveals the mechanism for its molecular chaperone activity in UPR. J. Mol. Biol. 397(5):1307-1315. doi:10.1016/j.jmb.2010.02.028

Tattoli I, Sorbara MT, Vuckovic D, Ling A, Soares F, Carneiro LA, Yang C, Emili A, Philpott DJ, Girardin SE (2012) Amino acid starvation induced by invasive bacterial pathogens triggers an innate host defense program. Cell Host Microbe 14;11(6):563-575. doi:10.1016/j.chom.2012.04.012

Taylor MW, Radax R, Steger D, Wagner M (2007) Sponge-associated microorganisms: evolution, ecology, and biotechnological potential. Microbiol. Mol. Biol. Rev. 71(2):295-347. doi:10.1128/MMBR.00040-06

Teske BF, Wek SA, Bunpo P, Cundiff JK, McClintick JN, Anthony TG, Wek RC (2011) The eIF2 kinase PERK and the integrated stress response facilitate activation of ATF6 during endoplasmic reticulum stress. Mol. Biol. Cell. 22:4390-4405. doi:10.1091/mbc.E11-06-0510

Thakur NL, Hentschel U, Krasko A, Pabel CT; Anil AC, Müller WEG (2003) Antibacterial activity of the sponge *Suberites domuncula* and its primmorphs: Potential basis for epibacterial chemical defense. Aquat. Microb. Ecol. 31:77-83. doi:10.3354/ame031077

Thakur NL, Perović-Ottstadt S, Batel R, Korzhev M, B. Diehl-Seifert B, Müller IM, Müller WEG (2005) Innate immune defense of the sponge *Suberites domuncula* against gram-positive bacteria: induction of lysozyme and AdaPTin. Mar. Biol. 146: 271. doi: https://doi.org/10.1007/s00227-004-1438-z

Theis KR, Dheilly NM, Klassen JL, Brucker RM, Baines JF, Bosch TC, Cryan JF, Gilbert SF, Goodnight CJ, Lloyd EA, Sapp J, Vandenkoornhuyse P, Zilber-Rosenberg I, Rosenberg E, Bordenstein SR (2016) Getting the hologenome concept Right: an eco-evolutionary framework for hosts and their microbiomes. mSystems. 1(2):e00028-16

Thomas T, Moitinho-Silva L, Lurgi M, Björk JR, Easson C, Astudillo-García C, Olson JB, Erwin PM, López-Legentil S, Luter H, Chaves-Fonnegra A, Costa R, Schupp PJ, Steindler L, Erpenbeck D, Gilbert J, Knight R, Ackermann G, Victor Lopez J, Taylor MW, Thacker RW, Montoya JM, Hentschel U, Webster NS (2016) Diversity, structure and convergent evolution of the global sponge microbiome. Nat. Commun. 7:11870. doi:10.1038/ncomms11870

Thomas T, Rusch D, DeMaere MZ, Yung PY, Lewis M, Halpern A, Heidelberg KB, Egan S, Steinberg PD, Kjelleberg S (2010) Functional genomic signatures of sponge bacteria reveal unique and shared features of symbiosis. ISME J. 4(12):1557-1567. doi:10.1038/ismej.2010.74

Todd DJ, Lee AH, Glimcher LH (2008) The endoplasmic reticulum stress response in immunity and autoimmunity. Nat. Rev. Immunol. 8(9):663-674. doi:10.1038/nri2359

Towbin H, Staehelin T, Gordon J (1979) Electrophoretic transfer of proteins from polyacrylamide gels to nitrocellulose sheets: procedure and some applications. Proc. Natl. Acad. Sci. USA 76:4350-4354

Travers KJ, Patil CK, Wodicka L, Lockhart DJ, Weissman JS, Walter P (2000) Functional and genomic analyses reveal an essential coordination between the unfolded protein response and ER-associated degradation. Cell 101(3):249-258. doi:http://dx.doi.org/10.1016/S0092-8674(00)80835-1

Tseng KY, Anttila JE, Khodosevich K, Tuominen RK, Lindahl M, Domanskyi A, Airavaara M (2017b) MANF promotes differentiation and migration of neural progenitor cells with potential neural regenerative effects in stroke. Mol. Ther. pii:S1525-0016(17):30435-5. doi:10.1016/j.ymthe.2017.09.019

Tseng KY, Danilova T, Domanskyi A, Saarma M, Lindahl M, Airavaara M (2017a) MANF is essential for neurite extension and neuronal migration in the developing cortex. eNeuro. 29;4(5):ENEURO.0214-17. doi:10.1523/ENEURO.0214-17.2017

Ueda N, Richards GS, Degnan BM, Kranz A, Adamska M, Croll RP, Degnan SM (2016) An ancient role for nitric oxide in regulating the animal pelagobenthic life cycle: evidence from a marine sponge. Sci. Rep. 22(6):37546. doi:10.1038/srep37546

Untergasser A, Cutcutache I, Koressaar T, Ye J, Faircloth BC, Remm M, Rozen SG (2012) Primer3-new capabilities and interfaces. Nucleic Acids Res. 40(15): e115. doi:https://doi.org/10.1093/nar/gks596

Upton JP, Wang L, Han D, Wang ES, Huskey NE, Lim L, Truitt M, McManus MT, Ruggero D, Goga A, Papa FR, Oakes SA (2012) IRE1α cleaves select microRNAs during ER stress to derepress translation of proapoptotic caspase-2. Science. 338(6108):818-822. doi:10.1126/science.1226191

Urano F, Wang X, Bertolotti A, Zhang Y, Chung P, Harding HP, Ron D (2000) Coupling of stress in the ER to activation of JNK protein kinases by transmembrane protein kinase IRE1. Science 287(5453):664-666. doi:10.1126/science.287.5453.664

Uriz MJ, Agell G, Blanquer A, Turon X, Casamayor EO (2012) Endosymbiotic calcifying bacteria: a new cue to the origin of calcification in metazoa? Evolution 66(10):2993-2999. doi:10.1111/j.1558-5646.2012.01676.x

Urra H, Dufey E, Lisbona F, Rojas-Rivera D, Hetz C (2013) When ER stress reaches a dead end. Biochim. Biophys. Acta 1833(12):3507-3517. doi:10.1016/j.bbamcr.2013.07.024

Urra H, Hetz C (2017) Fine-tuning PERK signaling to control cell fate under stress. Nat. Struct. Mol. Biol. 24(10):789-790. doi:10.1038/nsmb.3478

Vacelet J, Boury-Esnault N (1995) Carnivorous sponges. Nature 373:333-335. doi:10.1038/373333a0

Vacelet J, Donadey C (1977) Electron microscope study of the association between some sponges and bacteria. J. Exp. Mar. Biol. Ecol. 30:301-314. doi:http://dx.doi.org/10.1016/0022-0981(77)90038-7

van der Burg CA, Prentis PJ, Surm JM, Pavasovic A (2016) Insights into the innate immunome of actiniarians using a comparative genomic approach. BMC

Genomics 17(1):850. doi:10.1186/s12864-016-3204-2

van Soest RW, Boury-Esnault N, Vacelet J, Dohrmann M, Erpenbeck D, De Voogd NJ, Santodomingo N, Vanhoorne B, Kelly M, Hooper JN (2012) Global diversity of sponges (Porifera). PLoS One. 7(4):e35105. doi:10.1371/jornal.pone.0035105

Venderova K, Park DS (2012) Programmed cell death in Parkinson's disease. Cold Spring. Harb. Perspect. Med. 1;2(8):a009365. doi:10.1101/cshperspect.a009365

Verhagen AM, Ekert PG, Pakusch M, Silke J, Connolly LM, Reid GE, Moritz RL, Simpson RJ, Vaux DL (2000) Identification of DIABLO, a mammalian protein that promotes apoptosis by binding to and antagonizing IAP proteins. Cell 102(1):43-53. doi:https://doi.org/10.1016/S0092-8674(00)00009-X

Verhoeve JTP, Dufour SC (2018) Microbiomes of the Arctic carnivourous sponges *Chondrocladia grandis* and *Cladorhiza oxeata* suggest a specific, but differential involvement of bacterial associates. Arctic Science 4(2):186-204. doi:10.1139/as-2017-0015

Vilar M, Mira H (2016) Regulation of neurogenesis by neurotrophins during adulthood: expected and unexpected roles. Front. Neurosci. 9(10):26. doi:10.3389/fnins.2016.00026

Vivier E, Medzhitov R (2016) Editorial overview: Innate immunity. Curr. Opin. Immunol. 38:v-vii. doi:10.1016/j.coi.2015.12.005

Voeltz GK, Rolls MM, Rapoport TA (2002) Structural organization of the endoplasmic reticulum. EMBO Rep. 3(10):944-950. doi:10.1093/embo-reports/kvf202

Vogel S (1977) Current-induced flow through living sponges in nature. Proc. Natl. Acad. Sci. USA 74(5):2069-2071.

Vogel S, Raulf N, Bregenhorn S, Biniossek ML, Maurer U, Czabotar P, Borner C (2012) Cytosolic Bax: does it require binding proteins to keep its pro-apoptotic activity in check? J. Biol. Chem. 287(12):9112-9127. doi:10.1074/jbc.M111.248906

Voutilainen MH, Arumäe U, Airavaara M, Saarma M (2015) Therapeutic potential of the endoplasmic reticulum located and secreted CDNF/MANF family of neurotrophic factors in Parkinson's disease. FEBS Lett. 589(24 PtA):3739-3748. doi:10.1016/j.febslet.2015.09.031

Voutilainen MH, Bäck S, Peränen J, Lindholm P, Raasmaja A, Männistö PT, Saarma M, Tuominen RK (2011) Chronic infusion of CDNF prevents 6-OHDA-induced deficits in a rat model of Parkinson's disease. Exp. Neurol. 228(1):99-108. doi:10.1016/j.expneurol.2010.12.013

Voutilainen MH, Bäck S, Pörsti E, Toppinen L, Lindgren L, Lindholm P, Peränen J, Saarma M, Tuominen RK (2009) Mesencephalic astrocyte-derived neurotrophic factor is neurorestorative in rat model of Parkinson's disease. J. Neurosci. 29(30):9651-9659. doi:10.1523/JNEUROSCI.0833-09.2009

Walkowicz L, Kijak E, Krzeptowski W, Górska-Andrzejak J, Stratoulias V, Woznicka O, Chwastek E, Heino TI, Pyza EM (2017) Downregulation of DmMANF in glial cells results in neurodegeneration and affects sleep and lifespan in *Drosophila melanogaster*. Front. Neurosci. 11:610. doi:10.3389/fnins.2017.00610

Walpole GFW, Grinstein S, Westman J (2018) The role of lipids in host-pathogen interactions. IUBMB Life. 70(5):384-392. doi:10.1002/iub.1737

Walter P, Ron D (2011) The unfolded protein response: from stress pathway to homeostatic regulation. Science. 334(6059):1081-1086. doi:10.1126/science.1209038

Wang D, Hou C, Cao Y, Cheng Q, Zhang K, Li H, Feng L, Shen Y (2018) XBP1 activation enhances MANF expressionvia binding to endoplasmic reticulum stress response elementes within MANF promoter region in hepatitis B. Int J. Biochem. Cell Biol. 99:140-146. doi:10.1016/j.biocel.2018.04.007

Wang H, Ke Z, Alimov A, Xu M, Frank JA, Fang S, Luo J (2014b) Spatiotemporal expression of MANF in the developing rat brain. PLoS ONE 9(2):e90433. doi:10.1371/journal.pone.0090433

Wang H, Wang X, Ke ZJ, Comer AL, Xu M, Frank JA, Zhang Z, Shi X, Luo J (2015b) Tunicamycin-induced unfolded protein response in the developing mouse brain. Toxicol. Appl. Pharmacol. 15;283(3):157-167. doi:10.1016/j.taap.2014.12.019

Wang J, Cheng Q, Wang X, Zu B, Xu J, Xu Y, Zuo X, Shen Y, Wang J, Shen Y (2014a) Deficiency of IRE1 and PERK signal pathways in systemic lupus erythematosus. Am. J. Med. Sci. 348(6):465-473. doi:10.1097/MAJ. 0000000000000328

Wang M, Wey S, Zhang Y, Ye R, Lee AS (2009) Role of the unfolded protein response regulator GRP78/BiP in development, cancer, and neurological disorders. Antioxid. Redox Signal. 11:2307-2316. doi:10.1089/ARS.2009.2485

Wang W, Dai H, Zhang Y, Chandrasekar R, Luo L, Hiromasa Y, Sheng C, Peng G, Chen S, Tomich JM, Reese J, Edwards O, Kang L, Reeck G, Cui F (2015a) Armet is an effector protein mediating aphid-plant interactions. FASEB J. 29(5):2032-2045. doi:10.1096/fj.14-266023.

Wang X, Quinn PJ (2010) Endotoxins: lipopolysaccharides of gram-negative bacteria. In: Subcell. Biochem. vol 53. Eds: Wang X, Quinn PJ. Springer doi:10.1007/978-90-481-9078-2_1

Wang XY, Song MM, Bi SX, Shen YJ, Shen YX, Yu YQ (2016) MRI Dynamically evaluates the therapeutic effect of recombinant human MANF on ischemia/reperfusion injury in rats. Int. J. Mol. Sci. 5;17(9):E1476. doi:10.3390/ijms17091476

Webb B, Sali A (2016) Comparative protein structure Modeling using MODELLER. Curr. Protoc. Protein Sci. 86(1):2.9.1-2.9.37. doi:10.1002/cpps.20

Weber K, Osborn M (1969) The reliability of molecular weights determinations by dodecyl sulfatepolyacrylamide gel electrophoresis. J. Biol. Chem. 244:4406-4412.

Webster NS, Negri AP, Webb RI, Hill RT (2002) A spongin-boring α-proteobacterium is the etiological agent of disease in the Great Barrier Reef sponge *Rhopaloeides odorabile*. Mar. Ecol. Prog. Ser. 232:305-309. doi:10.3354/meps232305

Webster NS, Thomas T (2016) The sponge hologenome. MBio.7(2):e00135-16. doi:10.1128/mBio.00135-16

Wehrl M, Steinert M, Hentschel U (2007) Bacterial uptake by the marine sponge *Aplysina aerophoba*. Microb. Ecol. 53(2):355-65. doi:10.1007/s00248-006-9090-4

Wei HM, Lin LC, Wang CF, Lee YJ, Chen YT, Liao YD (2016) Antimicrobial properties of an immunomodulator - 15 kDa human granulysin. PLoS One. 11(6):e0156321. doi:10.1371/journal.pone.0156321

Weir GC, Bonner-Weir S (2013) Islet β cell mass in diabetes and how it relates to function, birth, and death. Ann. NY Acad. Sci. 1281:92-105. doi:10.1111/nyas.12031

Wenger Y, Buzgariu W, Galliot B (2016) Loss of neurogenesis in Hydra leads to compensatory regulation of neurogenic and neurotransmission genes in epithelial cells. Philos. Trans. R. Soc. Lond. B. Biol. Sci. 371(1685):20150040. doi:10.1098/rstb.2015.0040

Westphal D, Dewson G, Czabotar PE, Kluck RM (2011) Molecular biology of Bax and Bak activation and action. Biochim. Biophys. Acta. 1813(4):521-531. doi:10.1016/j.bbamcr.2010.12.019

Westphal D, Kluck RM, Dewson G (2014) Building blocks of the apoptotic pore: how Bax and Bak are activated and oligomerize during apoptosis. Cell Death Differ. 21(2):196-205. doi:10.1038/cdd.2013.139

Whitmer KMH (2018) Model systems for exploring the evolutionary origins of the nervous system. In: Marine organisms as model systems in biology and medicine. Results and problems in cell differentiation 65. Eds: Kloc M, Jacek JZ. Springer. doi:10.1007/978-3-319-92486-1

Wiens M, Belikov SI, Kaluzhnaya OV, Schroder HC, Hamer B, Perović-Ottstadt S Borejko A, Luthringer B, Müller IM, Müller WE (2006) Axial (apical-basal) expression of pro-apoptotic and pro-survival genes in the lake Baikal demosponge *Lubomirskia baicalensis*. DNA Cell Biol. 25:152-164. doi:10.1089/dna.2006.25.152

Wiens M, Diehl-Seifert B, Müller WEG (2001) Sponge Bcl-2 homologous protein (BHP2-GC) confers selected stress resistance to human HEK-293 cells. Cell Death Diff. 8: 887-898. doi:10.1038/sj.cdd.4400906.

Wiens M, Korzev M, Perović-Ottstadt S, Luthringer B, Brandt D, Klein S, Müller WE (2007) Toll-like receptor are part of the innate immune defense system of sponges (Demospongiae: Porifera). Mol. Biol. Evol. 24:792-804. doi:10.1093/molbev/msl208

Wiens M, Korzhev M, Krasko A, Thakur NL, Perović-Ottstadt S, Breter HJ, Ushijima H, Diehl-Seifert B, Müller IM, Müller WE (2005) Innate immune defense of the sponge *Suberites domuncula* against bacteria involves a MyD88-dependent signaling pathway. Induction of a perforin-like molecule. J. Biol. Chem. 280(30):27949-27959. doi:10.1074/jbc.M504049200

Wiens M, Koziol C, Batel R, Müller WE (1998) Phenylalanine hydroxylase from the sponge *Geodia cydonium*: implication for allorecognition and evolution of aromatic amino acid hydroxylases. Dev. Comp. Immunol. 22(5-6):469-478. doi:https://doi.org/10.1016/S0145-305X(98)00034-2

Wiens M, Krasko A, Blumbach B, Müller IM, Müller WE (2000a) Increased expression of the potential proapoptotic molecule DD2 and increased synthesis of leukotriene B4 during allograft rejection in a marine sponge. Cell Death Differ. 7(5):461-469. doi:10.1038/sj.cdd.4400671

Wiens M, Krasko A, Müller CI, Müller WEG (2000b) Molecular evolution of apoptotic pathways: cloning of key domains from sponges (Bcl-2 homology domains and death domains) and their phylogenetic relationships. J. Mol. Evol. 50:520-531. doi:10.1007/s002390010055

Wiens M, Krasko A, Perović S, Müller WE (2003b) Caspase-mediated apoptosis in sponges: cloning and function of the phylogenetic oldest apoptotic proteases from Metazoa. Biochim. Biophys. Acta. 1593(2-3):179-189. doi:https://doi.org/10.1016/S0167-4889(02)00388-9

Wiens M, Kuusksalu A, Kelve M, Müller WE (1999) Origin of the interferon-inducible (2'-5') oligoadenylate synthetases: cloning of the (2'-5') oligoadenylate synthetase from the marine sponge *Geodia cydonium*. FEBS Lett. 462(1-2):12-8. doi:https://doi.org/10.1016/S0014-5793(99)01478-7

Wiens M, Luckas B, Brümmer F, Shokry M, Ammar A, Steffen R, Batel R, Diehl-Seifert B, Schröder HC; Müller WEG. (2003a) Okadaic acid: a potential defense molecule for the sponge *Suberites domuncula.* Mar. Biol. 142(2): 213-

223. https://doi.org/10.1007/s00227-002-0886-6

Wiens M, Müller WEG (2006) Cell death in Porifera: molecular players in the game of apoptotic cell death in living fossils. Can. J. Zool. 84:307-321. doi:http://dx.doi. org/10.1139/z05-165

Wiens M, Perovic-Ottstadt S, Müller IM, Müller WEG (2004) Allograft rejection in the mixed cell reaction system of the demosponge *Suberites domuncula* is controlled by differential expression of apoptotic genes. Immunogenetics 56:597-610. doi:10.1007/s00251-004-0718-6

Wiens M, Schröder HC, Korzhev M, Wang XH, Batel R, Müller WE (2011) Inducible ASABF-type antimicrobial peptide from the sponge *Suberites domuncula*: microbicidal and hemolytic activity in vitro and toxic effect on molluscs in vivo. Mar. Drugs. 9(10):1969-1994. doi:10.3390/md9101969

Wilkinson CR (1978a) Microbial associations in sponges. I. Ecology, physiology and microbial populations of coral reef sponges. Mar. Biol. 49:161. doi:https://doi.org/10.1007/BF00387115

Wilkinson CR (1978b) Microbial associations in sponges. III. Ultrastructure of the *in situ* associations in coral reef sponges. Mar. Biol. 49:177 doi:https://doi.org/10.1007/BF00387117

Wilkinson, CR, Garrone R, Vacelet J (1984) Marine sponges discriminate between food bacteria and bacterial symbionts: electron microscope radioautography and *in situ* evidence. Proc. R. Soc. Lond. B. 220:519-528. doi:10.1098/rspb.1984.0018

Wilson KH (2009) The genome sequence of the protostome *Daphnia pulex* encodes respective orthologues of a neurotrophin, a Trk and a p75NTR: Evolution of neurotrophin signaling components and related proteins in the bilateria. BMC Evol. Biol. 9:243. doi:10.1186/1471-2148-9-243

Wilson MC, Mori T, Rückert C, Uria AR, Helf MJ, Takada K, Gernert C, Steffens UA, Heycke N, Schmitt S, Rinke C, Helfrich EJ, Brachmann AO, Gurgui C, Wakimoto T, Kracht M, Crüsemann M, Hentschel U, Abe I, Matsunaga S, Kalinowski J, Takeyama H, Piel J (2014) An environmental bacterial taxon with a large and distinct metabolic repertoire. Nature 506(7486):58-62. doi:10.1038/nature12959

Woollacott RM (1993) Structure and swimming behavior of the Larva of *Haliclona tubifera* (Porifera: Demospongiae). J. Morphol. 218:301-321. doi:10.1002/jmor.1052180306

Wörheide G, Dohrmann M, Erpenbeck D, Larroux C, Maldonado M, Voigt O, Borchiellini C, Lavrov DV (2012) Deep phylogeny and evolution of sponges (phylum Porifera). Adv. Mar. Biol. 61:1-78. doi:10.1016/B978-0-12-3877871.00007-6

Wu T, Zhang F, Yang Q, Zhang Y, Liu Q, Jiang W, Cao H, Li D, Xie S, Tong N, He J (2017) Circulating mesencephalic astrocyte-derived neurotrophic factor is increased in newly diagnosed prediabetic and diabetic patients, and is associated with insulin resistance. Endocr. J. 64(4):403-410. doi:10.1507/endocrj.EJ16-0472

Xu W, Gao L, Li T, Zheng J, Shao A, Zhang J (2018) Mesencephalic astrocyte derived neurotrophic factor (MANF) protects against neuronal apoptosis via activation of Akt/MDM2/p53 signaling pathway in a rat model of intracerebral hemorrhage. Front. Mol. Neurosci. 11:176. doi:10.3389/fnmol.2018.00176

Yamamoto K, Sato T, Matsui T, Sato M, Okada T, Yoshida H, Harada A, Mori K (2007) Transcriptional induction of mammalian ER quality control proteins is mediated by single or combined action of ATF6α and XBP1. Dev. Cell. 13(3):365-376. doi:10.1016/j.devcel.2007.07.018

Yamazaki H, Hiramatsu N, Hayakawa K, Tagawa Y, Okamura M, Ogata R, Huang T, Nakajima S, Yao J, Paton AW, Paton JC, Kitamura M (2009) Activation of the Akt-NF-kappaB pathway by subtilase cytotoxin through the ATF6 branch of the unfolded protein response. J. Immunol. 183(2):1480-1487. doi:10.4049/ jimmunol.0900017

Yang S, Huang S, Gaertig MA, Li XJ, Li S (2014b) Age-dependent decrease in chaperone activity impairs MANF expression, leading to Purkinje cell degeneration in inducible SCA17 mice. Neuron.81(2):349-365. doi:10.1016/j.neuron.2013.12.002

Yang S, Yang H, Chang R, Yin P, Yang Y, Yang W, Huang S, Gaertig MA, Li S, Li XJ (2017) MANF regulates hypothalamic control of food intake and body weight. Nat. Commun. 8(1):579. doi:10.1038/s41467-017-00750-x

Yang W, Shen Y, Chen Y, Chen L, Wang L, Wang H, Xu S, Fang S, Fu Y, Yu Y, Shen Y (2014a) Mesencephalic astrocyte-derived neurotrophic factor prevents neuron loss via inhibiting ischemia-induced apoptosis. J. Neurol. Sci. 15;344(1-2):129-138. doi:10.1016/j.jns.2014.06.042.

Ye J, Rawson RB, Komuro R, Chen X, Davé UP, Prywes R, Brown MS, Goldstein JL (2000) ER stress induces cleavage of membrane-bound ATF6 by the same proteases that process SREBPs. Mol. Cell. 6(6):1355-1364. doi:https://doi.org/16/S1097-2765(00)00133-7

Yoshida H, Matsui T, Yamamoto A, Okada T, Mori K (2001) XBP1 mRNA is induced by ATF6 and spliced by IRE1 in response to ER stress to produce a highly active transcription factor. Cell 107:881-891. doi:http://dx.doi.org/10.1016/S0092-8674(01)00611-0

Yu YQ, Liu LC, Wang FC, Liang Y, Cha DQ, Zhang JJ, Shen YJ, Wang HP, Fang S, Shen YX (2010) Induction profile of MANF/ARMET by cerebral ischemia and its implication for neuron protection. J. Cereb. Blood Flow Metab. 30(1):79-91. doi:10.1038/jcbfm.2009.181

Yue X, Hariri DJ, Caballero B, Zhang S, Bartlett MJ, Kaut O, Mount DW, Wüllner U, Sherman SJ, Falk T (2014) Comparative study of the neurotrophic effects elicited by VEGF-B and GDNF in preclinical *in vivo* models of Parkinson's disease. Neuroscience 258:385-400. doi:10.1016/j. neuroscience.2013.11.038

Yuen B, Bayes JM, Degnan SM (2014) The characterization of sponge NLRs provides insight into the origin and evolution of this innate immune gene family in animals. Mol. Biol. Evol. 31(1):106-120. doi:10.1093/molbev/mst174

Zeng T, Peng L, Chao C, Fu B, Wang G, Wang Y, Zhu Z, Wang G (2015) IRE1 α-TRAF2-ASK1 complex-mediated endoplasmic reticulum stress and mitochondrial dysfunction contribute to CXC195-induced apoptosis in human bladder carcinoma T24 cells. Biochem. Biophys. Res. Commun. 460:530-536. doi:10.1016/j.bbrc.2015.03.064

Zhang J, Cai Q, Jiang M, Liu Y, Gu H, Guo J, Sun H, Fang J, Jin L (2017a) Mesencephalic astrocyte-derived neurotrophic factor alleviated 6-OHDA-induced cell damage via ROS-AMPK/mTOR mediated autophagic inhibition. Exp. Gerontol. 89:45-56. doi:10.1016/j.exger.2017.01.010

Zhang J, Tong W, Sun H, Jiang M, Shen Y, Liu Y, Gu H, Guo J, Fang J, Jin L (2017b) Nrf2-mediated neuroprotection by MANF against 6-OHDA-induced cell damage via PI3K/AKT/GSK3β pathway. Exp. Gerontol. 100:77-86. doi:10. 1016/j.exger.2017.10.021

Zhang L, Wang K, Lei Y, Li Q, Nice EC, Huang C (2015) Redox signaling: potential arbitrator of autophagy and apoptosis in therapeutic response. Free Radic. Biol. Med. 89:452-465. doi:10.1016/j.freeradbiomed.2015.08.030

Zhang Z, Shen Y, Luo H, Zhang F, Jing L, Wu Y, Xia X, Song Y, Li W, Jin L (2018) MANF protects dopamine neurons and locomotion defects from a human α-synuclein induced Parkinson's disease model in *C. elegans* by regulating ER stress and autophagy pathways. Exp. Neurol. 308:59-71. doi:10.1016/j.expneurol.2018.06.016

Zhao H, Liu Y, Cheng L, Liu B, Zhang W, Guo YJ, Nie L (2013) Mesencephalic astrocyte-derived neurotrophic factor inhibits oxygen-glucose deprivation-induced cell damage and inflammation by suppressing endoplasmic reticulum stress in rat primary astrocytes. J. Mol. Neurosci. 51(3):671-678. doi:10.1007/s12031-013-0042-4

Zhou W, Chang L, Fang Y, Du Z, Li Y, Song Y, Hao F, Lv L, Wu Y (2016) Cerebral dopamine neurotrophic factor alleviates $A\beta_{25–35}$-induced endoplasmic reticulum stress and early synaptotoxicity in rat hippocampal cells. Neurosci. Lett. 633:40-46. doi:10.1016/j.neulet.2016.09.008

Zhu B, Pennack JA, McQuilton P, Forero MG, Mizuguchi K, Sutcliffe B, Gu CJ, Fenton JC, Hidalgo A (2008) Drosophila neurotrophins reveal a common mechanism for nervous system formation. PLoS Biol. 18;6(11):e284.

doi:10.1371/journal.pbio.0060284

Zhu W, Li J, Liu Y, Xie K, Wang L, Fang J (2016) Mesencephalic astrocyte-derived neurotrophic factor attenuates inflammatory responses in lipopolysaccharide-induced neural stem cells by regulating NF-κB and phosphorylation of p38-MAPKs pathways. Immunopharmacol. Immunotoxicol. 38(3):205-213. doi:10.3109/08923973.2016.1168433

Zmasek CM, Godzik A (2013) Evolution of the animal apoptosis network. Cold Spring Harb. Perspect. Biol. 5(3):a008649. doi:10.1101/cshperspect.a008649

J. ABBREVIATIONS

∞	Infinite
°C	Grad Celsius
µl	Microliter
µm	Micrometer
µM	Micromolar
µg	Microgram

A

A. mellifera	*Apis mellifera*
A. mississippiensis	*Alligator mississippiensis*
A. quenslandica	*Amphimedon quenslandica*
A. suum	*Ascaris suum*
aa	Amino acid
AdaPTin 1	Perforin-like molecule adaptor gene
AF	Aggregation factor
ANOVA	One-way analysis of variance
AP	Alkaline phosphatase
Apaf1	Apoptotic protease activating factor 1
AR	Aggregation receptor
ARMET	Arginine-rich, mutated in early stage tumors
ASABF	*Ascaris suum* antibacterial factor
ATF4	Activating transcription factor 4
ATF6	Activating transcription factor 6
ATF6f	Activating transcription factor 6 fragment

B

BAK	BCL-2 antagonist killer
BAX	BCL-2-associated X protein
BCL-2	B-cell lymphoma 2
BFA	Brefeldin A
Bid	BH3 interacting domain death agonist
BiP	Immunoglobulin heavy chain-binding protein
BSA	Bovine serum albumin
bZIP	Basic leucin zipper transcription factor

C

C. briggsae	*Caenorhabditis briggsae*
C. elegans	*Caenorhabditis elegans*
C. rogercresseyi	*Caligus rogercresseyi*
cDNA	Complementary desoxyribonucleic acid (DNA)
CDNF	Conserved dopamine neurotrophic factor
CHOP	CCAAT/enhancer-binding protein homologous protein
cm	Centimeter
cm^2	Square centimeter
CNPY2	Canopy homolog 2

COPII	Coat protein II
CRELD2	Cysteine-rich with EGF-like domains 2
Cyt-c	Cytochrome C

D

D. melanogaster, Dm	*Drosophila melanogaster*
DmMANF	*Drosophila melanogaster* mesencephalic astrocyte-derived neurotrophic factor
D. rerio	*Danio rerio*
D. virilis	*Drosophila virilis*
Da	Dalton(s)
DAPI	4',6-diamidino-2-phenylindole
dd H_2O	Double-distilled water
DEPC	Diethyl pyrocarbonate
DEPC H_2O	Diethyl pyrocarbonate treated water
DIABLO	IAP-binding protein with a low pI
DISC	Death inducing signaling complex
DM	Diabetes mellitus
DMEM	Dulbecco´s modified Eagle´s medium
DMSO	Dimethyl sulphoxide
DNA	desoxyribonucleic acid
DNAase	Desoxyribonuclease
DNAase-free	Desoxyribonuclease free
dNTPs	Deoxynucleoside triphosphates
DPBS	Dulbecco's phosphate buffered saline
DTT	Dithiothreitol

E

E. coli	*Escherichia coli*
EDTA	Ethylenediaminetetraacetic acid
EIF2α	Eukaryotic translation-initiation factor 2α
ER	Endoplasmic reticulum
ERAD	Endoplasmic reticulum (ER) associated degradation
ERSE	Endoplasmic reticulum (ER) stress response elements
et al	et alii
EtBr	Ethidium bromide

F

FADD	FAS-associated death domain
FAS	First apoptosis signal receptor
FBS	Fetal bovine serum
FlAsH-EDT_2	Fluorescein arsenical hairpin binder-ethanedithiol
fmol	Femtomol

G

g	Gramme
g/l	Gramme per liter
GABA	Gamma-amino butyric acid

GADD34	DNA damage-inducible protein
GF-AFC	Glycylphenylalanyl-aminofluorocoumarin
GLS	Golgi-localization sequence
GSK3β	Glycogen synthase kinase 3 beta

H

H. sapiens	*Homo sapiens*
H_2O	Water
hARP	Human arginine-rich protein
HEK	Human embryonic kidney cells
HEK_{SDMANF}	HEK *Suberites domuncula* mesencephalic astrocyte-derived neurotrophic factor stable transfected cell line
HIS	Histidine
HIStag	Histidine tag
hrs	Hours

I

IFN-γ	Interferon gamma
iGluR	Glutamate receptor
IHC	Immunohistochemistry
IL-1β	Interleukin 1 beta
ILR-1	Interleukin receptor 1
IMAC	Immobilization on metal affinity chromatography
IPTG	Isopropyl-β-D-thiogalactoside
IRAK 1/4	Interleukin receptor-associated kinase 1/4
IRE1	Inositol-requiring transmembrane kinase/endonuclease 1
IRF	Interferon regulatory factor

J

JNK	JUN N-terminal kinase

K

kb	Kilobase(s)
kDa	KiloDalton(s)

L

L. salmonis	*Lepeophtheirus salmonis*
LPS	Lipopolysaccharides

M

M	Molar (mol/L)
M-PER	Mammalian protein extraction reagent
M. musculus	*Mus musculus*
MANF	Mesencephalic astrocyte-derived neurotrophic factor
min	Minute (s)
ml	Milliter

mM	Milimolar
MOMP	Mitochondrial outer member permeabilization
MOPS	3-(N-Morpholino) propanesulfonic acid
MPT	Mitochondrial permeability transition
mRNA	Messenger ribonucleic acid (RNA)
MyD88	Myeloid differentiation primary response 8

N

NCBI	National center for biotechnology information
NF-κB	Nuclear factor-kappa B
ng	Nanograms
Ni-NTA	Nickel-nitrilotriacetic acid
NJ	Neighbor-joining
NLR	(NOD)-Like receptor
NLRP3	NLR pirin domain 3
nm	Nanometers
NO	Nitric oxide
NOD1	Nucleotide-binding oligomerization domain protein 1
NOD2	Nucleotide-binding oligomerization domain protein 2
Nrf2	Nuclear factor erythroid 2-related factor
NS	Nephrotic syndrome
NTF/NTFs	Neurotrophic factor /neurotrophic factors

O

OD	Optic density
OD_{660}	Optic density at 660 nm
ORF/ORFs	Open reading frame/ open reading frames

P

P. troglodytes	*Pan troglodytes*
P38-MAPKs	P38-mitogen-activated protein kinases
pAbs	Polyclonal antibodies
PAGE	Polyacrylamide gel electrophoresis
PAMPs	Pathogen-associated molecules
PBS	Phosphate buffered saline
PCD	Programmed cell death
PCR	Polymerase chain reaction
PERK	Protein kinase RNA-like ER kinase
PFA	Paraformaldehyde
Pfam	Protein family
pH	Potentia hydrogenii
PI	Propidium iodide
PI3K	Phosphatidylinositol 3-kinase
pmol	Picomol
PRRs	Pattern recognition receptors
PUMA	P53 up-regulated modulator of apoptosis
PVDF	Polyvinylidene difluoride

R

RFU	Relative fluorescence unit
RIDD	IRE1α-dependent decay
RNA	Ribonucleic acid
RNase	Ribonuclease
ROS	Reactive oxygen species
rpm	Revolutions per minute
RT	Room temperature

S

s	Second(s)
S. domuncula	*Suberites domuncula*
S. salar	*Salmo salar*
S.O.C medium	Super optimal broth with catabolite repression medium
S1P	Site-1 protease
S2P	Site-2 protease
SAP	SAF-A/B, Acinus, PIAS
SDMANF	*Suberites domuncula* mesencephalic astrocyte-derived neurotrophic factor
SDS	Sodium dodecyl sulphate
SDTLR	*Suberites domuncula* Toll–like receptor
Ser/Thr	Serine/threonine
SLE	Systemic lupus erythematosus
SMAC	Second mitochondria-derived activator of caspases
SP	Signal peptide
ss	Single–stranded (ssDNA/ssRNA)
Suberites	*Suberites domuncula*

T

T. pseudonana	*Thalassiosira pseudonana*
Taq	*Thermus aquaticus*
TBE	Tris-borate-EDTA
tBid	Truncated Bid (BH3 interacting domain death agonist)
TBS	Tris-buffered saline
TBST	Tris-buffered saline Tween-20
TCA	Trichloroacetic acid
TCEP	Tris (2-carboxyethyl) phosphine
TE	Tris-EDTA
TG	Thapsigargin
TLR	Toll–like receptor (s)
TM	Tunicamycin
Tm	Melting temperature
TNF	Tumor necrosis factor
TNF-α	Tumor necrosis factor α
TRAF2	Tumour-necrosis factor (TNF)-receptor-associated factor 2)

U

UPR	Unfolded protein response
UPREs	Unfolded protein response elements
UV	Ultraviolet

V

v	Volts
v/v	Volume per volume, volume per volume

W

w/v	Weight/volume, weight per volume
wt	Wild-type

X

X. laevis	*Xenopus laevis*
XBP1	X-box binding protein 1
XIAP	X-linked inhibitor of apoptosis

K. LIST OF FIGURES AND TABLES

1. Figures

2. Tables

N. ERKLÄRUNG

Hiermit erkläre ich, die vorliegende Arbeit selbständig und nur mit Hilfe der angegebenen Personen und Mittel (Literatur, Apparaturen, Material) angefertigt zu haben. Bei den von mir durchgeführten Untersuchungen habe ich die Grundsätze guter wissenschaftlicher Praxis, wie sie in der Satzung der Johannes Gutenberg-Universität Mainz niedergelegt sind, eingehalten.

_____ _____

Ort, Datum Dayane Sereno Baêta Rodrigues

O. APPENDICES

1. Funding

The present doctoral thesis has been developed with funding by the European Research Council (ERC Advanced Investigator Grant) [redacted], the Deutsche Forschungsgemeinschaft DFG [redacted] and Coordination of Superior Level Staff Improvement (CAPES) in a cooperation program with Deutscher Akademischer Austauschdienst (DAAD).

2. Attached publication

Sereno D, Müller WEG, Bausen M, Elkhooly TA, Markl JS, Wiens M (2017) An evolutionary perspective on the role of mesencephalic astrocyte-derived neurotrophic factor (MANF): At the crossroads of poriferan innate immune and apoptotic pathways. Biochem. Biophys. Rep. 11:161-173.
doi:10.1016/j.bbrep.2017.0